CHAPTER 23

An analytical solution for solitary porosity waves: dynamic permeability and fluidization of nonlinear viscous and viscoplastic rock

JAMES A. D. CONNOLLY[1] AND YURY Y. PODLADCHIKOV[2]

[1] *Department of Earth Sciences, Swiss Federal Institute of Technology, Zurich, Switzerland;* [2] *Earth Sciences Department, University of Lausanne, Lausanne, Switzerland*

ABSTRACT

Porosity waves are a mechanism by which fluid generated by devolatilization and melting, or trapped during sedimentation, may be expelled from ductile rocks. The waves correspond to a steady-state solution to the coupled hydraulic and rheologic equations that govern the flow of the fluid through the matrix and matrix deformation. This chapter presents an intuitive analytical formulation of this solution in one dimension that is general with respect to the constitutive relations used to define the viscous matrix rheology and permeability. This generality allows for the effects of nonlinear viscous matrix rheology and disaggregation. The solution combines the porosity dependence of the rheology and permeability in a single hydromechanical potential as a function of material properties and wave velocity. With the ansatz that there is a local balance between fluid production and transport, the solution permits the prediction of dynamic variations in permeability and pressure necessary to accommodate fluid production. The solution is used to construct a phase diagram that defines the conditions for smooth pervasive flow, wave-propagated flow, and matrix fluidization (disaggregation). The viscous porosity wave mechanism requires negative effective pressure to open the porosity in the leading half of a wave. In nature, negative effective pressure may induce hydrofracture, resulting in a viscoplastic compaction rheology. The tube-like porosity waves that form in a matrix with this rheology channelize fluid expulsion and are predicted by geometric argumentation from the one-dimensional viscous solitary wave solution.

Key words: analytic solution, dynamic permeability, fluidization, lower crust, nonlinear viscous, porosity waves

INTRODUCTION

Many geological processes involve the expulsion of pervasively distributed fluids, as in the case of fluids trapped during sedimentation or fluids generated by partial melting and metamorphic devolatilization. Given the high elastic strength characteristic of rocks, efficient fluid expulsion requires irreversible deformation by time-dependent (viscous) or time-independent (plastic) mechanisms (Neuzil 2003; Gueguen *et al.* 2004). Models for ductile plastic compaction (cataclasis) reproduce the near-surface porosity profiles of sedimentary basins (Shi & Wang 1986; Audet & Fowler 1992), but creep is regarded as essential to deeper compaction processes (McKenzie 1987; Birchwood & Turcotte 1994; Fowler & Yang 1999). For such processes, permeability is a dynamic property that is determined by the interaction between rheology and the inherent gravitational instability of the intermingling of rock and fluids with different densities. This interaction may give rise to a hydrologic regime in which flow is accomplished by self-propagating domains of fluid-filled porosity (Fowler 1984; Richter & McKenzie 1984; Scott & Stevenson 1984). These domains, or porosity waves, correspond to steady-state solutions, that is, solutions in which the waves propagate with unchanging form, of the equations governing fluid flow through a viscous matrix. The intent of this study is to develop and explore an intuitive analytical solution for these waves that is general with respect to the constitutive laws chosen to characterize the viscous rheology and permeability of the rock matrix.

There are numerous formulations of the equations governing compaction of a two-phase viscous system consisting of a porous rock matrix saturated with a less viscous interstitial fluid in the geological literature (McKenzie 1984; Scott & Stevenson 1984; Bercovici *et al.* 2001). These formulations differ primarily in the choices of constitutive relations and independent variables. Analytical solutions for solitary waves that develop according

Crustal Permeability, First Edition. Edited by Tom Gleeson and Steven E. Ingebritsen.

Companion Websites: www.wiley.com/go/gleeson/crustalpermeability/
http://crustalpermeability.weebly.com/

to these formulations have been published (Barcilon & Richter 1986; Rabinowicz *et al.* 2002; Richard *et al.* 2012), but assume linear viscous behavior. This limitation is potentially important in the context of fluid flow in the lower crust because the viscous response of crustal rocks is expected to be nonlinear (Kohlstedt *et al.* 1995; Ranalli 1995). A nonlinear viscous formulation is of broad interest because it defines the length scale on which lower crustal fluid flow patterns may deviate from gravitationally controlled flow. The compaction length is also important in that it defines the spatial scale for porosity. Thus, although porosity conjures up an image of grain-scale structures, it may apply to substantially larger features, such as fractures, provided these features are hydraulically connected and small in comparison with the compaction length.

Shortly after the recognition of porosity waves as a potential fluid transport mechanism in geologic systems, it was shown that the planar, sill-like, waves predicted from one-dimensional (1D) formulations of the governing equations were unstable with respect to spherical waves in two-dimensional (2D) and three-dimensional (3D) space (Scott & Stevenson 1986; Barcilon & Lovera 1989; Wiggins & Spiegelman 1995). Despite this result, the present analysis is restricted to the 1D case because it provides a lower limit on the efficacy of compaction-driven fluid expulsion and because the characteristics of the 1D waves converge rapidly with those of 3D waves for the geologically interesting case of large amplitude waves (Connolly & Podladchikov 2007). With this restriction, there are three compaction-driven flow regimes that may arise as a consequence of a perturbation to the flux of an initial regime of steady flow through a matrix with uniform porosity (Fig. 23.1). If the perturbation is small, the steady-state solution is a periodic wave that degrades to a uniform increased porosity once the perturbation is eliminated. For larger perturbations, the steady state is a solitary wave. Once nucleated, the solitary wave is nondissipative and independent of its source. Thus, the solitary wave solution defines a steady-state regime in which flow is accomplished by self-propagating waves. Because the solitary wave amplitude is proportional to the intensity of perturbation, large perturbations may cause the matrix to disaggregate to a fluidized suspension. The analytic solution outlined here is used to define the conditions for these regimes.

The solitary wave regime is one where the fluid flows through a coherent solid matrix, whereas in the fluidized regime the solid is suspended within, and carried by, the fluid, as in a granitic magma so that the suspension behaves as a single phase that is transported through dikes or as diapirs (Vigneresse *et al.* 1996). Although peripheral to the scope of this study, the generation of granitic melts by partial melting of the lower crust is a prominent example of fluidization in ductile rock. Unless melting is so extensive that it forms a magmatic suspension directly, a segregation mechanism is required to amplify melt fractions to the level required for transport by dikes or diapirs. Given the common occurrence of oriented vein-like segregations (e.g., Brown 2010), attention in the compaction literature has focused on the role of shear-enhanced melt segregation (Stevenson 1989; Holtzman *et al.* 2003; Rabinowicz & Vigneresse 2004). While melt segregation is not explored in this study, the mechanism of fluidization discussed here is distinct in that low melt fractions can be amplified to a suspension even under isostatic conditions. Such a mechanism may be relevant in the formation of large-scale diatexite migmatites, which record a wholesale evolution from unmelted source rock to granitic magma (Sawyer 1998; Milord *et al.* 2001).

The mechanism responsible for porosity waves in a viscous matrix is implicit in the conventional view of the mechanics responsible for compaction profiles in active sedimentary basins (Hunt 1990; Japsen *et al.* 2011) and the partially molten region beneath mid-ocean ridges (Forsyth *et al.* 1998). In both of these settings, which span the physical conditions of the lower crust, compaction is thought to maintain near-eustatic porosity–depth profiles in rocks that are moving relative to the Earth's surface. In the case of sedimentary basins, the rock matrix moves downward relative to surface due to burial, whereas at mid-ocean ridges, the rock matrix rises toward the surface as a consequence of mantle upwelling. The distinction between these scenarios and that of a porosity wave is no more than a matter of reference frame, in that in the former porosity is eustatic and the rock matrix moves, while in the latter, the rock matrix is largely stationary and the porosity moves. Indeed, mechanical models that explain eustatic porosity in sedimentary basins (Fowler & Yang 1999; Connolly & Podladchikov 2000) and at mid-ocean ridges (Katz 2008) differ trivially from the simple viscous formulation employed here. Specifically, for sedimentary basins a viscoplastic rheology is introduced to account for near-surface compaction, and for mid-ocean ridges, the model is modified to account for fluid production. The existence of porosity waves in a viscous matrix has also been demonstrated experimentally by mechanical analog (Olson & Christensen 1986; Scott *et al.* 1986; Helfrich & Whitehead 1990). Thus, suggestions that porosity waves act as agents for compartmentalization and fluid migration in sedimentary basins (McKenzie 1987; Connolly & Podladchikov 2000; Appold & Nunn 2002) and the lower crust (Suetnova *et al.* 1994; Connolly 1997; Gliko *et al.* 1999; Tian & Ague 2014) are less exotic than they might seem at first sight. We make no attempt to make the case for the role of porosity waves in the lower crust in this study; rather, the reader is referred to the aforementioned works and recent reviews (Connolly & Podladchikov 2013; Ague 2014) that consider the relevance of the model and the hydraulic properties of the crust in greater detail.

In addition to neglecting 3D effects, the viscous solitary wave solution neglects the potential roles of plasticity (e.g., brittle failure), elasticity (e.g., fluid compressibility and poroelasticity), and thermal activation. To a first approximation, many of these effects can be inferred from the 1D viscous model as addressed in the "Discussion" Section of this chapter. Elastic effects are the exception. The poroelastic limit, relevant to fluid flow in the upper crust, admits a solitary porosity wave solution that is manifest by fluid pressure surges (Rice 1992). This solitary

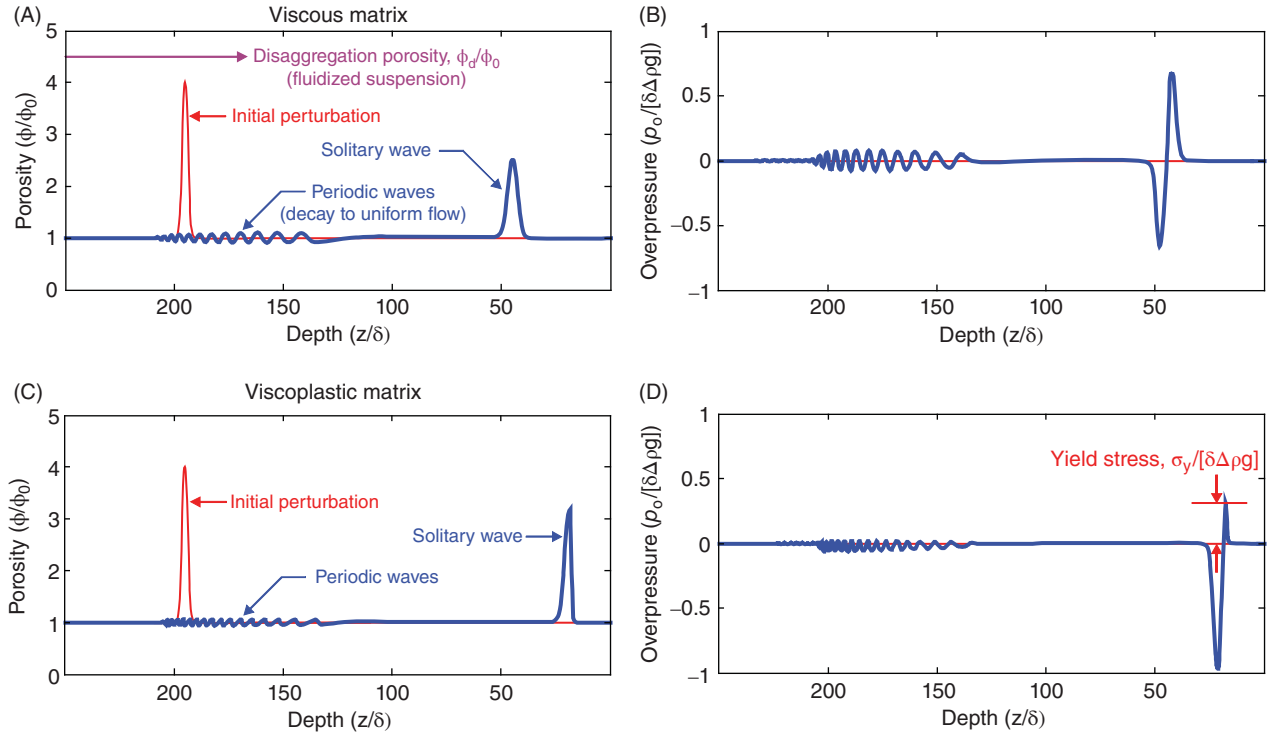

Fig. 23.1. Numerically simulated porosity wave evolution from a region of increased porosity within an otherwise uniform flow regime through viscous and viscoplastic porous media. (A) Porosity versus depth for the viscous case. The first wave to initiate from the flow perturbation (i.e., the region of elevated porosity) is a solitary wave that propagates above the background porosity in the same direction as fluid flow through the unperturbed matrix. The solitary wave is nondissipative in the steady-state limit; thus, it propagates infinite distance with essentially unchanging form. Due to transient effects, a periodic wave train initiates behind the solitary wave; the periodic wave train propagates both in and against the direction of fluid flow through the unperturbed matrix. The wave train corresponds to a periodic steady state in which the porosity oscillates about the background level. Porosity wave velocities are proportional to amplitude; thus, with time the solitary wave becomes isolated from the periodic wave train, which has no significant excess volume and degrades to the original uniform flow regime as it spreads. A narrow region of increased porosity was chosen for the initial conditions to emphasize the periodic solution. This choice leads to solitary waves that have lower porosity than the source region. Wider source regions tend to generate waves with porosities that are higher than in the source region; if these porosities exceed the disaggregation porosity (indicated schematically), the matrix disaggregates to a fluidized suspension. This range of porosity wave behavior can also be induced by perturbing the background fluid flux, as might occur as a consequence of devolatilization (melting). (B) Fluid overpressure (negative effective pressure) versus depth for the viscous case, the porosity dependence of the matrix permeability causes fluid pressure anomalies that are responsible for dilating and compacting the porosity during the passage of a wave. Although fluid flow from low to high overpressure may seem to contradict Darcy's law, if the overpressures are converted to hydraulic head, it is apparent that the direction of fluid flow in porosity waves is consistent with Darcy's law. (C) Porosity and (D) overpressure profiles for a viscoplastic scenario in which plasticity is manifest by hydrofracture when overpressure exceeds the brittle yield stress. This rheology affects wave symmetry, but does not fundamentally change porosity wave behavior because the rate of fluid expulsion remains limited by viscous compaction. In the numerical simulation, the effect of the viscoplastic rheology on the periodic waves with overpressures below the yield stress is an artifact of the reduced effective shear viscosity used to simulate brittle failure. Porosity (ϕ), depth (z), overpressure (p_o), and time are scaled relative to the background porosity (ϕ_0), viscous compaction length (δ), characteristic pressure ($\delta|\Delta\rho g|$), and the speed of fluid flow through the unperturbed matrix ($(|v_0|)$ discussed later in the text. The 1D volume of the initial perturbation is the same ($8.862\ \delta\phi_0$) in both simulations, and the transient profiles (blue curves) are for the same model time ($50\ \delta/|v_0|$). The numerical simulations were obtained by finite difference methods for the small porosity formulation (Appendix) with $m_\sigma = 1$, $n_\phi = 3$, and $n_\sigma = 1$. (*See color plate section for the color representation of this figure.*)

solution, which is consistent with a variety of upper crustal phenomena (Revil & Cathles 2002; Miller *et al.* 2004; Joshi *et al.* 2012), contrasts with the viscous case in that it is dissipative and does not require supra-lithostatic fluid pressures. Viscoelastic compaction formulations show that there is a continuum of periodic wave solutions between the viscous and elastic solitary wave limits (Connolly & Podladchikov 1998; Chauveau & Kaminski 2008). However, in numerical simulations, thermal activation of the viscous rheology leads to a rapid variation between a lower crustal regime in which viscoelastic porosity wave solutions show no appreciable elastic character (Connolly 1997) and an upper crustal regime lacking any significant viscous character (Connolly & Podladchikov 1998). These results are taken as justification for the neglect of elastic phenomena in the present treatment of lower crustal fluid expulsion. In this regard, it is important to distinguish fluid expulsion from fluid flow as, particularly in the noncompacting limit, thermoelastic expansivity of the fluid may create pressure gradients responsible for fluid circulation (Hanson 1997; Nabelek 2009; Staude *et al.* 2009).

MATHEMATICAL FORMULATION

Darcian flow of an incompressible fluid through a viscous matrix composed of incompressible solid grains is considered here largely following the formulation of Scott & Stevenson (1984). Although the solid and fluid components are incompressible, the matrix is compressible because fluid may be expelled from the pore volume. Conservation of solid and fluid mass requires

$$\frac{\partial(1-\phi)}{\partial t} + \nabla\cdot((1-\phi)\mathbf{v}_s) = 0 \tag{23.1}$$

and

$$\frac{\partial\phi}{\partial t} + \nabla\cdot(\phi\mathbf{v}_f) = 0, \tag{23.2}$$

where ϕ is porosity and subscripts *f* and *s* distinguish the velocities, $\mathbf{v}$, of the fluid and solid (see Table 23.1 for notation). From Darcy's law, the force balance between the solid matrix and fluid is

$$\phi(\mathbf{v}_f - \mathbf{v}_s) = -\frac{k}{\eta_f}(\nabla p_f - \rho_f g\mathbf{u}_z), \tag{23.3}$$

where k is the hydraulic permeability of the solid matrix, an unspecified function of porosity; ρ_f and η_f are the density and shear viscosity of the fluid, respectively; and $\mathbf{u}_z$ is a downward-directed unit vector. Identifying the mean stress $\overline{\sigma}$ as the vertical load

$$\overline{\sigma} = \int_0^z [(1-\phi)\rho_s + \phi\rho_f]g\mathbf{u}_z dz. \tag{23.4}$$

Thus, in terms of the fluid overpressure

$$p_o = p_f - \overline{\sigma}, \tag{23.5}$$

(i.e., negative effective pressure) Eq. 23.3 is

$$\phi(\mathbf{v}_f - \mathbf{v}_s) = -\frac{k}{\eta_f}(\nabla p_o + (1-\phi)\Delta\rho g\mathbf{u}_z), \tag{23.6}$$

where $\Delta\rho = \rho_s - \rho_f$. The divergence of the total volumetric flux of matter is the sum of Eqs 23.1 and 23.2:

$$\nabla\cdot(\mathbf{v}_s + \phi(\mathbf{v}_f - \mathbf{v}_s)) = 0, \tag{23.7}$$

and substituting Eq. 23.6 into Eq. 23.7 gives

$$\nabla\cdot\left(\mathbf{v}_s - \frac{k}{\eta_f}(\nabla p_o + (1-\phi)\Delta\rho g\mathbf{u}_z)\right) = 0. \tag{23.8}$$

It is assumed that the bulk viscosity of a pure phase is infinite, an assumption necessary to assure that the individual phases do not have time-dependent compressibility (Nye

Table 23.1 Frequently used symbols

Symbol	Meaning
A; A_ϕ	Viscous flow coefficient, Eq. 23.9; wave amplitude, ϕ_{max}/ϕ_0
a_ϕ	Permeability function geometric factor, Eq. 23.17
a_σ	Compaction rate function geometric factor, Eq. 23.19
b_ϕ	Permeability function solidity exponent, Eq. 23. 17
f_ϕ	Compaction rate function, Eq. 23.19
f_1; f_2	Hydraulic function, Eq. 23.36; rheological function porosity dependence, Eq. 23.37
H; ΔH	Hydraulic potential, Eqs 23.39, 23.54, 23.62, and 23.76; $H(\phi) - H(\phi_0)$
k; k_0	Permeability, Eq. 23.17; background value
m_σ	Compaction rate function porosity exponent, Eq. 23.19
n_ϕ	Permeability function porosity exponent, Eq. 23.17
n_σ	Viscous flow law stress exponent, Eq. 23.9
p_o; p_f; p	Fluid overpressure, $p_f - p$; fluid pressure; total pressure ($\overline{\sigma}$)
q; q_0	Fluid flux; background value
$\overline{q}_e$; q_s	Time-averaged excess flux, Eq. 23.61; 1D fluid production rate
Q; Q_p	Fluid transport rate for a spherical viscous wave, Eq. 23.63; 3D fluid production rate
Q_p	Fluid transport rate for a 3D viscoplastic wave, Eq. 23.65
V_e	1D wave excess volume, Eq. 23.60
v_0, v_ϕ	1D Darcy fluid velocity at $\phi = \phi_0$, $p_o = 0$, Eq. 23.20; 1D wave velocity, Eqs 23.55 and 23.57,
v_ϕ^{crit}	1D solitary wave critical velocity, Eq. 23.43
$\mathbf{v}$	3D velocity
z	Depth coordinate, positive downward
δ	Viscous compaction length scale, Eq. 23.51
$\Delta\rho$; $\Delta\sigma$	$\rho_s - \rho_f$; differential stress
η_s; η_f	Solid shear viscosity; fluid shear viscosity
λ, λ_p	Viscous wavelength; viscoplastic wavelength
ϕ; ϕ_0; ϕ_d	Hydraulically connected porosity; background value; value at disaggregation
ϕ_1; ϕ_{max}	Focal point porosity, a real root of $f_1 = 0$; maximum wave porosity
ρ_s; ρ_f	Solid density; fluid density
$\overline{\sigma}$; σ_y	Mean stress (p); failure stress
τ	Compaction timescale, $\delta/\lvert v_0\rvert$
∇, $\nabla\cdot$	Gradient, divergence
$f\lvert_{x=x_0}$	Value of a function f at $x = x_0$

1953); therefore, viscous compaction must be accomplished by grain-scale shear deformation that eliminates porosity. For solid grains that deform according to a power-law constitutive relation,

$$\dot{\varepsilon} = A|\Delta\sigma|^{n_\sigma - 1}\Delta\sigma, \tag{23.9}$$

where $\dot{\varepsilon}$ is the uniaxial strain rate in response to differential stress $\Delta\sigma$, n_σ is the stress exponent, and A is the coefficient of viscous flow; matrix rheology is then introduced through Terzaghi's effective stress principle as

$$\nabla \cdot v_s = f_\phi A|p_o^{n_\sigma - 1}|p_o. \tag{23.10}$$

where f_ϕ includes an unspecified porosity dependence and a geometric factor that relates the uniaxial strain rate of the solid to the bulk strain rate of the matrix. In the limit $n_\sigma \to 1$, the shear viscosity of the solid is $\eta_s = 1/(3A)$, and the bulk viscosity of the solid matrix is η_s/f_ϕ The divergence of the solid velocity is identical to the bulk strain rate of the matrix and related to the compaction rate by

$$\dot{\phi} \equiv -\frac{1}{\phi}\frac{\mathrm{d}\phi}{\mathrm{d}t} = \nabla \cdot v_s \frac{1-\phi}{\phi}. \tag{23.11}$$

The power-law form of Eq. 23.9 precludes certain less common viscous constitutive relations; for example, the exponential form appropriate for low temperature plasticity (Kameyama *et al.* 1999), a completely general derivation, follows if the term $A|p_o^{n_\sigma - 1}|$ in Eq. 23.10 is replaced by a generic function of the magnitude of the overpressure.

Equations 23.1, 23.8, and 23.10 form a closed system of equations in the unknown quantities (ϕ), p_o, and v_s. To avoid the unnecessary complication associated with the use of vector notation for a 1D problem, in the remainder of this analysis vector quantities are represented by signed scalars and the gradient and divergence operators are replaced by $\partial/\partial z$.

The 1D steady state

For analytical purposes, the existence of a 1D solitary porosity wave solution is assumed in which the wave propagates with unchanging form and velocity through a matrix with an initial fluid-filled porosity ϕ_0 at zero overpressure. In a reference frame that travels with the wave, integration of Eq. 23.1 gives the solid velocity as

$$v_s = v_\infty \frac{1-\phi_0}{1-\phi}, \tag{23.12}$$

where $v_\infty(1-\phi_0)$ is the solid flux at infinite distance from the wave. After substitution of Eq. 23.12, the integrated form of Eq. 23.8 can be rearranged to

$$\frac{\partial p_o}{\partial z} = \left(q_t - v_\infty \frac{1-\phi_0}{1-\phi}\right)\frac{\eta_f}{k} - (1-\phi)\Delta\rho g, \tag{23.13}$$

where $q_t = \phi v_f + (1-\phi)v_s$ is the constant, total, volumetric flux of matter through the column, which evaluates in the limit $\phi \to \phi_0$ and $p_o \to 0$ as

$$q_t = v_\infty - (1-\phi_0)\frac{k_0}{\eta_f}\Delta\rho g, \tag{23.14}$$

where k_0 is the permeability at ϕ_0. Using Eq. 23.14, Eq. 23.13 is rewritten

$$\frac{\partial p_o}{\partial z} = v_\infty \frac{\eta_f}{k}\frac{\phi-\phi_0}{1-\phi} - \Delta\rho g\left(1-\phi-(1-\phi_0)\frac{k_0}{k}\right). \tag{23.15}$$

Likewise, after substitution of Eq. 23.12, Eq. 23.10 can be rearranged to

$$\frac{\partial \phi}{\partial z} = \frac{(1-\phi)^2}{1-\phi_0}\frac{f_\phi}{v_\infty}A|p_o|^{n_\sigma - 1}p_o. \tag{23.16}$$

For a given wave velocity, Eqs 23.15 and 23.16 form a closed system of two partial differential equations in two unknown functions (ϕ and p_o) of depth.

Constitutive relations and scales

Although general forms are retained where possible, to place the analysis in context, it is useful to specify possible constitutive relations for permeability and the porosity dependence, f_ϕ of the rheological constitutive relation (Eq. 23.10). To describe the variation in permeability due to compaction, the theoretical Carman–Kozeny porosity–permeability relationship (Carman 1939) is generalized as

$$k = a_\phi \frac{\phi^{n_\phi}}{(1-\phi)^{b_\phi}}, \tag{23.17}$$

where a_ϕ is a grain-size-dependent material constant and the formal values of b_ϕ and n_ϕ, 2 and 3, respectively, imply that the first-order control on the porosity dependence of the permeability at small porosity is determined by n_ϕ. From analysis of *in situ* rock permeability, Neuzil (1994) shows that pore geometry and grain size give rise to variations in permeability that span eight orders of magnitude, but that porosity dependence is approximately cubic. A cubic dependence is predicted from theory irrespective of whether flow is intergranular or fracture controlled (Norton & Knapp 1977; Gavrilenko & Gueguen 1993). Accordingly, a cubic dependence, that is, $n_\phi = 3$, is considered to be most relevant. Higher exponents are observed in rocks where the degree of hydraulic connectivity varies strongly with porosity (Zhu *et al.* 1995, 1999). The solidity (i.e., $1-\phi$) exponent b_ϕ is constrained by considering the settling of a single grain through a static fluid. In this case, both the effective pressure and its gradient vanish, and substitution of Eq. 23.17 into Eq. 23.6 yields the settling velocity

$$v_s = \frac{a_\phi}{\eta_f}\frac{\phi^{n_\phi - 1}}{(1-\phi)^{b_\phi - 1}}\Delta\rho g, \tag{23.18}$$

which is an increasing function for all allowed values of porosity only if $1 \leq b_\phi < n_\phi$ and finite at $\phi \to 1$, as required by Stoke's law, only if $b_\phi = 1$.

The porosity dependence f_ϕ of the rheological equation (Eq. 23.10) must satisfy two physical constraints. In the limit $\phi \to 0$, f_ϕ must similarly vanish so that effective bulk viscosity becomes infinite to assure that the pure solid does not compact; and in the limit $\phi \to \phi_d$, f_ϕ must be infinite to assure that the solid and fluid pressure fields converge when the matrix has no cohesive strength, that is, when the matrix is fluidized. In detail, this transition is likely to be complex and material dependent, but theoretical and experimental considerations suggest that the transition occurs at $\phi_d \sim 20\%$ (Arzi 1978; Auer *et al.* 1981; Ashby 1988; Vigneresse *et al.* 1996). To account for these limits, the expressions of Wilkinson & Ashby (1975), derived explicitly for compaction by dislocation creep, are generalized here as

$$f_\phi = a_\sigma \phi^{m_\sigma}(1-\phi)/(1-\phi^{1/n_\sigma})^{n_\sigma}(\phi_d/|\phi_d - \phi|)^{n_\sigma - 1/2}, \qquad (23.19)$$

where formally $m_\sigma = 1$ and, for spherical pores, $a_\sigma = n_\sigma^{-n_\sigma}(3/2)^{n_\sigma+1}$. For diffusion-controlled compaction, a_σ is strongly dependent on grain size and the exponent m_a varies between 1/2 and 5/6 (Ashby 1988). In practice, the numerous compaction formulations in the geological literature differ primarily in the choice of m_σ. For simplicity, early studies neglected the porosity dependence ($m_\sigma = 0$; McKenzie 1984; Barcilon & Richter 1986), whereas most recent formulations (Sumita *et al.* 1996; Connolly 1997; Bercovici *et al.* 2001) take $m_\sigma = 1$.

Many of the material properties relevant to geological compaction vary over orders of magnitude and/or are extraordinarily uncertain (Neuzil 2003); for this reason, no attempt is made to parameterize the relations used here. Rather, results are given relative to the background porosity, Darcian fluid velocity through the unperturbed matrix

$$v_0 = -\frac{k_0}{\eta_f \phi_0}(1-\phi_0)\Delta\rho g \qquad (23.20)$$

or its speed $c_0 = |v_0|$, and the compaction length scale

$$\delta = \sqrt[n_\sigma+1]{\left(\frac{2}{3}\right)^{n_\sigma+1}\frac{k_0 n_\sigma^{n_\sigma}}{A\eta_f \phi_0^{m_\sigma}}|\Delta\rho g|^{1-n_\sigma}} \qquad (23.21)$$

suggested by nondimensionalization of Eqs 23.15, 23.16 and 23.19 in the small porosity limit (Appendix), a limit that has the consequence that the solutions are independent of the absolute porosity. The scales for pressure, time, and fluid flux are then $p_o = \delta|\Delta\rho g|$, $\tau = \delta/|v_0|$, and $q_0 = \phi_0 v_0$, respectively. Parameter ranges relevant to lower crustal fluid flow are reviewed elsewhere (Connolly & Podladchikov 2013; Ague 2014).

For a linear viscous matrix with shear viscosity $\eta_s = 1/(3A)$, Eq. 23.21 simplifies to

$$\delta = \sqrt{\frac{4}{3}\frac{\eta_s}{\phi_0^{m_\sigma}}\frac{k_0}{\eta_f}}, \qquad (23.22)$$

which, accounting for differences in the formulation of the bulk viscosity of the matrix, is identical to the viscous compaction length of McKenzie (1984). In the linear viscous case with $m_\sigma = 1$, δ is the length scale over which the bulk strain rate would change by a factor of e, the base of the natural logarithm, for the characteristic overpressure gradient $\Delta\rho g$. It is, therefore, the length scale over which compaction processes would generate an e-fold variation in porosity. For the present formulation, the analytical significance of δ is less clear, but it emerges that δ remains a reasonable estimate of the length scale for an e-fold variation in porosity.

ANALYTICAL SOLUTION FOR THE 1D STEADY STATE

The steady-state wave solutions to the compaction Eqs 23.13 and 23.16 are best understood by analogy with the solutions to the equations of motion of an initially stationary ball on a frictionless 1D curved surface in response to gravitational acceleration. To exploit this analogy, the solution for an oscillating ball (Fig. 23.2) is recapitulated here.

The oscillating ball

The equations of motion for the ball are its acceleration due to gravity

$$\frac{\partial v}{\partial t} = -\frac{\partial h}{\partial x}g, \qquad (23.23)$$

and the definition of velocity

$$\frac{\partial x}{\partial t} = v, \qquad (23.24)$$

where x is the horizontal position of the ball, v is its velocity, and h is a shape function that describes the height of the surface as a function of x. Combining Eqs 23.23 and 23.24 to eliminate time

$$\frac{\partial v}{\partial x} = -\frac{g}{v}\frac{\partial h}{\partial x} \qquad (23.25)$$

and rearranging Eq. 23.25 yields

$$0 = v\mathrm{d}v + g\frac{\partial h}{\partial x}\mathrm{d}x. \qquad (23.26)$$

The indefinite integral of Eq. 23.26 defines a property

$$u \equiv \frac{v^2}{2} + gh, \qquad (23.27)$$

the energy per unit mass, which is conserved by the ball. The solutions to Eqs 23.23 and 23.24 correspond to contours of u as a function of v and x, where, through Eq. 23.27 at $v = 0$, the initial height of the ball (Fig. 23.2A) defines the contour of interest for a particular problem (Fig. 23.2B). Closed contours (e.g., the red contour in Fig. 23.2B) correspond to a wave solution in which the ball oscillates between its initial position, x_i and

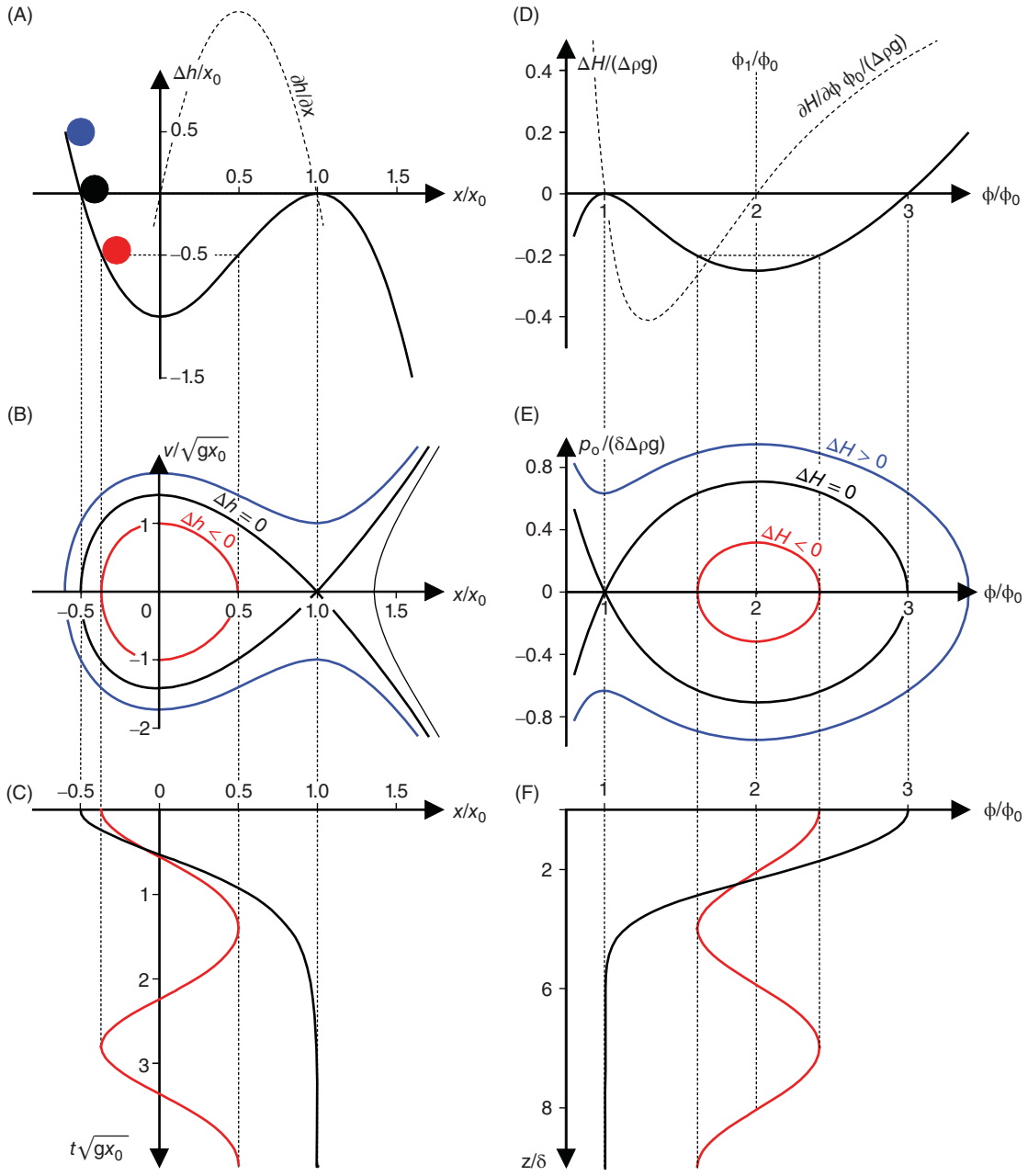

Fig. 23.2. Analogy of porosity waves with the oscillatory movement of a ball on a frictionless surface of variable height with a local maximum (i.e., a saddle point). In the analogy, the porosity wave properties H, ϕ, p_o, and z map to h, x, v, and t of the oscillating ball. If the ball is placed on the surface (e.g., the red ball in A) at a height below and to the left of the local maximum, the ball oscillates between points of equal height. In this case, the velocity–position trajectory of the ball defines a closed path around the focal point at $x = v = 0$ (e.g., the red curve in B) and its velocity–time (or position–time) trajectory defines a periodic wave train (e.g., the red curve in C). The location of the focal point ($x/x_0 = 0$) for the waves is dependent only on the shape of the surface, whereas the wave frequency is controlled by the gravitational acceleration. The solitary wave solution for the oscillating ball corresponds to the case that a ball (i.e., the black ball in A) is placed on the surface at the height of the saddle point. In this case, the ball would have no kinetic energy if it reached the saddle point; however, because the ball decelerates as it approaches the saddle point, the wave solution has an infinite period. If the ball is released from a height above the saddle point (i.e., the blue ball in A), it rolls continuously away from its initial position and there is no wave solution to the governing equations. The analogy of the oscillating ball to porosity wave solution is imperfect only in that the shape of function, or hydraulic potential, H of the porosity wave is dependent on wave velocity (Fig. 23.3), which is related to the intensity of the perturbation responsible for generating waves. For the velocity specified for H as illustrated in (D), the only wave solution capable of stably connecting the background porosity to a region of increased porosity is the solitary wave (i.e., the black trajectories in E and F); the periodic solutions (e.g., the red trajectories E and F) correspond to waves in which the porosity would oscillate about the focal point ($\phi/\phi_0 = 2$) between a porosity that is less than the maximum porosity of the solitary wave and greater than the background porosity. The solitary wave shape function illustrated in (D) is from the small porosity formulation of the compaction equations (Appendix) with $m_\sigma = 0$, $n_\phi = 3$, and $v_\phi/v_0 = 7$. (*See color plate section for the color representation of this figure.*)

a position of equal height at which its kinetic energy vanishes, and open contours (e.g., the blue contour in Fig. 23.2B) correspond to an aperiodic (i.e., non-wave) solution in which the ball rolls indefinitely away from its initial position. Because u is a monotonic function of v and is directly proportional to h, the focus of any closed contour must lie along the $v=0$ axis and correspond to an extremum in h, that is, a real root *of* $\partial h/\partial x = 0$. From physical considerations, it is evident that the solution is only stable if this root is a minimum, that is, $\partial^2 h/\partial x^2 > 0$. A well-known implication of this solution is that shape function h entirely determines both the amplitude and stability of oscillation, while the gravitational constant controls the velocity of the ball and, therefore, the period of oscillation.

For a ball placed at position x_i with $v_i = 0$, its velocity as it accelerates from its initial position can be computed by rearranging the definite integral of Eq. 23.26 as

$$v = \sqrt{-2g\Delta h}, \tag{23.28}$$

where $\Delta h = h - h_i$ and h_i is height of the ball at x_i. The time dependence of the solution is then recovered by substitution of Eq. 23.28 into Eq. 23.24 and inverting the result to obtain

$$t = \frac{1}{\sqrt{2g}} \int_{x_i}^{x} \frac{dx}{\sqrt{\Delta h}}. \tag{23.29}$$

For oscillatory solutions, Eq. 23.29 gives the time dependence of the solution for half the period of the oscillation. Thus, the oscillatory solution corresponds to a periodic wave (e.g., the red curve in Fig. 23.2C) in position (or velocity) as a function of time.

To quantify the preceding discussion, consider an arbitrarily chosen shape function such that

$$\frac{\partial h}{\partial x} = \frac{6}{x_0^2} x(x_0 - x), \tag{23.30}$$

which integrates to $h = x^2(3x_0 - 2x)/x_0^2$. The roots of Eq. 23.30 define the local extrema of h; thus, the surface has extrema at the structural root $x=0$, at which $h=0$, and the general root $x=x_0$, at which $h=h_0=x_0$. Restricting attention to the case $x_0 < 0$, for which the general root is a maximum, the structural root $x=0$ is the focus of all possible wave solutions and the general root x_0 defines the maximum value of x_i for which these solutions are possible (Fig. 23.2A). The minimum value of x_i, that is, $-x_0/2$, at which a wave solution is possible is obtained by solving $h=h_0$ for $x_i < x_0$. The closed contour of u as a function of position and velocity that demarcates the boundary between periodic and aperiodic solutions corresponds to a solitary solution. The existence of such a solution requires that h has at least two extrema. In the present example, the solution corresponds to the portion of the contour of u that emanates from the saddle point located by the structural root x_0 at $v=0$ (the black contour in Fig. 23.2B at $x/x_0 < 1$). In distinction to the periodic solutions, for the solitary wave solution, after the ball is released it does not return to its initial position, but rather comes to rest at the saddle point (at $x/x_0 = 1$), where its height is identical to its initial height. The physical reason for this behavior is that both the acceleration of the ball and its kinetic energy vanish at the saddle point. This trajectory (the black curve in Fig. 23.2C) is half the solitary wave solution; the complete solution would be obtained if the motion of the ball initiated from the saddle point. The absence of both kinetic energy and acceleration at the saddle point strictly precludes the occurrence of the complete solitary solution; however, the negative curvature of the surface at the saddle point has the consequence that a ball placed at the saddle point would be unstable with respect to infinitesimally small perturbations.

There are two types of solitary solution distinguished on the basis of whether the period of the solution is finite or infinite. The origin of these solutions can be understood by a thought experiment in which the initial conditions are chosen to coincide exactly with the conditions at which the trajectory of the solitary solution crosses the $v=0$ axis, that is, in the present example at $x/x_0 = -1/2$ (Fig. 23.2A). As the ball has no kinetic energy and is at height $h=h_0$, the ball has exactly the energy necessary to reach the saddle point x_0, but because the acceleration of the ball becomes vanishingly small as the saddle point is approached, the time required for the ball to reach the saddle point may be infinite. In the present example, it can be verified by the analytic integration of Eq. 23.29 that the time required for the ball to reach the saddle point is infinite; this result can be deduced more generally by observing that it is only necessary to consider the motion of the ball in the immediate vicinity of the saddle point. Accordingly, taking the first non-zero term of a Taylor series expansion of Eq. 23.28 about x_0

$$v \approx \pm(x - x_0)\sqrt{-g\left.\frac{\partial^2 h}{\partial x^2}\right|_{x=x_0}}. \tag{23.31}$$

Equation 23.29 then evaluates as

$$t \approx \frac{\ln(X)}{\sqrt{-g\left.\frac{\partial^2 h}{\partial x^2}\right|_{x=x_0}}}, \tag{23.32}$$

where $X = x - x_0$ is the distance from the saddle point and noting that $\partial^2 h/\partial x^2|_{x=x_0} < 0$ is a necessary condition for x_0 to be a saddle point, it follows that $t \to \infty$ as $X \to 0$. Thus, solitary solutions to Eqs 23.23 and 23.24 are of infinite period regardless of the details of the shape function. Rearranging Eq. 23.32 to express the distance of the ball from the saddle point as a function of time

$$X \approx e^{t/\tau}, \tag{23.33}$$

where $\tau = 1\Big/\sqrt{-g\partial^2 h/\partial x^2|_{x=x_0}}$ provides a natural timescale for the motion of the ball.

Wave solutions to the compaction equations

To make the analogy between the wave solutions of the compaction equations and the oscillating ball apparent, Eqs 23.15 and 23.16 are abbreviated as

$$\frac{\partial p_o}{\partial z} = f_1 \tag{23.34}$$

and

$$\frac{\partial \phi}{\partial z} = f_2 \frac{A}{v_\phi} |p_o|^{n_\sigma - 1} p_o, \tag{23.35}$$

where $v_\phi = -v_\infty$ is the velocity of a wave relative to a fixed point in the unperturbed matrix and f_1 and f_2 are

$$f_1 = -v_\phi \frac{\eta_f}{k} \frac{\phi - \phi_0}{1 - \phi} - \Delta\rho g \left[1 - \phi - (1 - \phi_0) \frac{k_0}{k} \right] \tag{23.36}$$

and

$$f_2 = \frac{(1 - \phi)^2}{1 - \phi_0} f_\phi. \tag{23.37}$$

Combining Eqs 23.34 and 23.35 to eliminate z, and rearranging, yields

$$0 = |p_o|^{n_\sigma - 1} p_o \mathrm{d}p_o - \frac{v_\phi}{A} \frac{f_1}{f_2} \mathrm{d}\phi, \tag{23.38}$$

which must be satisfied by the ϕ–p_c trajectory of any steady-state solution to Eqs 23.15 and 23.16. Defining a function H such that

$$H \equiv -\int \frac{f_1}{f_2} \mathrm{d}\phi \tag{23.39}$$

or $\partial H / \partial \phi = -f_1 / f_2$, Eq. 23.38 is rewritten as

$$0 = |p_o|^{n_\sigma - 1} p_o \mathrm{d}p_o + \frac{v_\phi}{A} \frac{\partial H}{\partial \phi} \mathrm{d}\phi. \tag{23.40}$$

Comparison of Eqs 23.40 and 23.26 reveals that wave solutions to the compaction equations, at constant phase velocity, are a mathematical analog to the equations of motion for the oscillating ball, wherein the compaction variables [ϕ, p_o, z] map to [x, v, t]; the shape function H can be thought of as a hydromechanical potential that corresponds to the height h of the ball, and the factor v_ϕ / A has the same role as the gravitational constant g. Integration of Eq. 23.40 defines a property

$$U \equiv \frac{|p_o|^{n_\sigma - 1} p_o^2}{n_\sigma + 1} + \frac{v_\phi}{A} H \tag{23.41}$$

akin to the mass normalized energy u for the oscillating ball, which is conserved by porosity waves. Closed contours of U define the wave solutions to the compaction equations as a function of p_o and ϕ for a given velocity. As in the case of the oscillating ball, closed contours define periodic solutions where the porosity oscillates between two values, characterized by equal H, at which p_o vanishes (e.g., the red contour in Fig. 23.2E). The periodic solutions are bounded by the contour that defines the solitary solution (black contour, Fig. 23.2E). Similarly, analogous to the oscillating ball solution, because U is directly proportional to H and increases with both negative and positive overpressure, the focus of any closed contour must lie along the $p_o = 0$ axis and correspond to an extremum in H, for example, the real root, ϕ_1, of $\partial H / \partial \phi = 0$. The porosity dependence (f_2) of the rheologic equation (Eq. 23.35) must be finite and positive if the matrix is coherent; consequently, the roots of $\partial H / \partial \phi = 0$ are independent of the rheologic constitutive relationship and identical to the roots of the hydraulic equation (Eq. 23.34), that is, the porosities that satisfy $f_1 = 0$. Although the number of roots cannot be determined without specifying the porosity–permeability relationship, the formulation of Eq. 23.15 is such that ϕ_o is always a root, analogous to x_0 in Eq. 23.30. Consequently, if

$$\left. \frac{\partial^2 H}{\partial \phi^2} \right|_{\phi = \phi_0} = \frac{\Delta\rho g}{f_2|_{\phi = \phi_0}} \left(\frac{1 - \phi_0}{k_0} \left. \frac{\partial k}{\partial \phi} \right|_{\phi = \phi_0} - 1 + \frac{v_\phi}{\phi_0 v_0} \right) \tag{23.42}$$

is greater than zero, then ϕ_0 is a stable level of porosity and small flow perturbations to a uniform flow regime will lead to periodic oscillations in the porosity about ϕ_0 (Fig. 23.3A). In contrast, if H is a maximum at ϕ_0, then ϕ_0 is a saddle point and solitary wave solutions are possible (Fig. 23.3B). Equating Eq. 23.42 to zero and solving for v_ϕ yields the critical velocity at which the background porosity ϕ_0 switches from focal to saddle point

$$v_\phi^{crit} = v_0 \phi_0 \left(1 - \frac{(1 - \phi_0)}{k_0} \left. \frac{\partial k}{\partial \phi} \right|_{\phi = \phi_0} \right) \tag{23.43}$$

such that ϕ_0 is a saddle point for waves with $v_\phi / v_0 > v_\phi^{crit} / v_0$, which is thus a necessary condition for the existence of the solitary wave solution. Although Eq. 23.43 appears to admit the possibility of solitary waves that propagate against the direction of buoyancy-driven fluid flow through the unperturbed matrix, substituting the explicit function for permeability given by Eq. 23.17 in Eq. 23.43 yields

$$v_\phi^{crit} / v_0 = [n_\phi (1 - \phi_0) + (b_\phi - 1) \phi_0], \tag{23.44}$$

which is positive for any plausible choice of n_ϕ and b_ϕ, as discussed earlier.

Provided a solitary wave solution exists, that is, $v_\phi / v_0 > v_\phi^{crit} / v_0$ and $H(\phi_d) > H(\phi_0)$ (as in Fig. 23.3B), then solving $\Delta H = H(\phi) - H(\phi_0) = 0$ yields the maximum porosity of the wave ϕ_{max}. As the overpressure vanishes at ϕ_{max}, the dependences of p_o and z on ϕ are obtained in exactly the same manner as the dependence of v and t on x for the oscillating ball (Eqs 23.28 and 23.29). Thus, from the definite integral of Eq. 23.40

$$p_o = \pm \sqrt[n_\sigma + 1]{(n_\sigma - 1) \frac{v_\phi}{A} \Delta H} \tag{23.45}$$

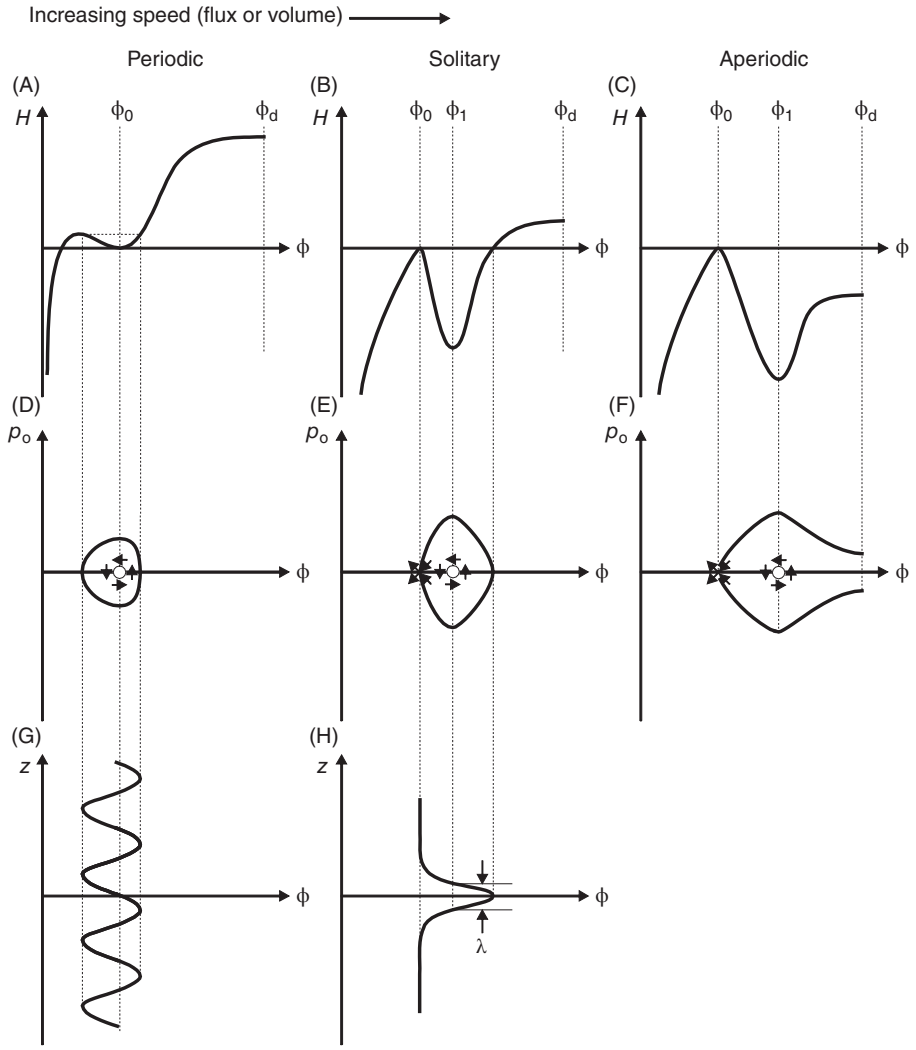

Fig. 23.3. Shape functions, phase portraits, and porosity wave patterns as a function of phase velocity illustrating the periodic, solitary, and aperiodic (fluidized) compaction-driven flow regimes. In general, phase velocity can be taken as a measure of the intensity of a flow perturbation. At low velocities (A, D, G), the background porosity ϕ_0 is the focal point of a periodic solution. At intermediate velocities (B, E, H), the focal point, that is, the minimum in H, shifts to $\phi_1 > \phi_0$; the potential H recovers to $H(\phi_0)$ at a porosity intermediate between ϕ_1 and the disaggregation porosity ϕ_d; and the relevant solution is a solitary wave. At still higher velocities (C, F), $H(\phi_d) < H(\phi_0)$ so there is no steady-state wave solution as there is no closed path in $p_o - \phi$ space connecting ϕ_0 to an elevated level of porosity; and the perturbation causes the matrix to disaggregate.

and inverting the result of substitution of Eq. 23.45 into Eq. 23.35,

$$z = \pm \sqrt[n_\sigma+1]{\frac{v_\phi}{A}} \int_{\phi_{max}}^{\phi} \frac{d\phi}{p_o^{n_\sigma} f_2}, \tag{23.46}$$

where z is the depth relative to the wave center at which $\phi = \phi_{max}$ and $p_o = 0$. Any porosity of the solitary solution is associated with both positive and negative values of p_o and z, corresponding to the upper and lower halves of the wave. For this reason, the sign of factors in expressions for p_o and z has no significance; rather than explicitly indicating this with magnitude notation in Eqs 23.45 and 23.46, and subsequent equations, it is to be understood that any negative term is to be replaced by its absolute value.

Nonlinear rheology creates a distinction between the solitary solution of the compaction equations and that of the oscillating ball in that it is possible to obtain a solitary porosity wave of finite wavelength. This behavior is demonstrated by linearizing Eq. 23.46 about ϕ_0 to obtain

$$z \approx \pm \left(\frac{v_\phi}{A f_2|_{\phi=\phi_0}} \left(\frac{n_\sigma + 1}{2} \left. \frac{\partial f_1}{\partial \phi} \right|_{\phi=\phi_0} \right)^{-n_\sigma} \right)^{\frac{1}{n_\sigma+1}} \int_{\Phi}^{0} \Phi^{-\frac{2n_\sigma}{n_\sigma+1}} d\Phi, \tag{23.47}$$

where $\Phi = \phi - \phi_0$. The bifurcation between finite- and infinite-wavelength solutions is determined entirely by the stress exponent in Eq. 23.47, such that finite solutions can exist only for $n_\sigma < 1$, and is independent of the details of the hydraulic potential. As $n_\sigma \geq 1$ is characteristic of viscous behavior in rocks, it is expected that solitary porosity waves only develop in viscous rocks with finite initial porosity. Finite-wavelength solitary waves propagate, by definition, through a matrix with no initial porosity. It has been shown elsewhere that finite-wavelength solutions exist for viscoelastic compaction rheology (Connolly & Podladchikov 1998); the present analysis raises the possibility that shear-thickening viscous mechanisms ($n_\sigma < 1$) could also operate at the zero porosity limit in natural systems.

Just as the linearized equation for time in the oscillating ball problem (Eq. 23.33) provides a natural timescale for the movement of the ball near x_0, the linearized equation for depth in the solution of the compaction equations provides a characteristic length scale for variations in porosity near ϕ_0. By rewriting the integral in Eq. 23.47 in terms of $d\ln\Phi$, and differentiating, this length scale is

$$\delta' \sim \frac{\partial z}{\partial \ln \Phi} \approx \left(\Phi^{1-n_\sigma} \frac{v_\phi}{A f_2|_{\phi=\phi_0}} \left(\frac{n_\sigma + 1}{2} \left. \frac{\partial f_1}{\partial \phi} \right|_{\phi=\phi_0} \right)^{-n_\sigma} \right)^{\frac{1}{n_\sigma+1}}, \tag{23.48}$$

the depth interval over which porosity decays from $e\phi_0$ to ϕ_0 within a solitary wave. The derivative on the right-hand side of Eq. 23.48

$$\left. \frac{\partial f_1}{\partial \phi} \right|_{\phi=\phi_0} = \frac{\Delta\rho g}{\phi_0} \left(\frac{v_\phi^{\text{crit}}}{v_0} - \frac{v_\phi}{v_0} \right) \approx -\frac{\Delta\rho g}{\phi_0} \frac{v_\phi}{v_0} \tag{23.49}$$

is zero at $v_\phi = v_\phi^{\text{crit}}$, but decreases monotonically in v_ϕ; thus, the approximate form is valid for large speeds. Adopting this approximation, substituting $\Phi = (e-1)\,\phi_0$ in Eq. 23.48, and expanding f_2 at ϕ_0 as $a_\sigma f_\phi|_{\phi=\phi_0}(1-\phi_0)$ yields

$$\delta' = \frac{\partial z}{\partial \ln \Phi} \approx \left(\frac{\nu_\phi [\phi_0 (e-1)]^{1-n_\sigma}}{A a_\sigma f_\phi|_{\phi=\phi_0} (1-\phi_0)} \left[\frac{n_\sigma + 1}{2} \frac{\Delta\rho g}{\phi_0} \frac{\nu_\phi}{\nu_0} \right]^{-n_\sigma} \right)^{\frac{1}{n_\sigma+1}}, \tag{23.50}$$

effectively a lower bound on the wavelength of the solitary solution. Using the constitutive relations and scales given by Eqs 23.17, 23.19 and 23.20, and estimating wave speed as the magnitude of v_ϕ^{crit} ($\sim n_\phi |v_0|$, Eq. 23.44), then in the small porosity limit

$$\delta' = \sqrt[n_\sigma+1]{n_\sigma^{n_\sigma} \left(\frac{2}{3} \right)^{n_\sigma+1} \frac{a_\phi \phi_0^{n_\sigma - m_\sigma}}{A \eta_f} |\Delta\rho g|^{1-n_\sigma}} \sqrt[n_\sigma+1]{\left(\frac{2}{n_\sigma+1} \right)^{n_\sigma} (n_\phi [e-1])^{1-n_\sigma}}, \tag{23.51}$$

where the first factor is the scale δ obtained by dimensional analysis (Eq. 23.21) and the second factor is unity for the linear viscous case and close to, but less than, one for the nonlinear case with typical values of n_ϕ and n_σ. This result confirms that δ is a reasonable estimate of the compaction length scale and suggests, unsurprisingly, that increasing the nonlinear character of the viscous rheology generally leads to stronger spatial variations in porosity. In view of the minor difference between δ and δ', δ is preferred here because of its simplicity.

Solitary wave properties in the small porosity limit

To illustrate the features of solitary waves explicitly, the solution is considered in conjunction with the constitutive relations given by Eqs 23.17 and 23.19 in the small porosity limit ($1 - \phi \to 1$, $\phi_d - \phi \to \phi_d$). Equations 23.34 and 23.35 are then

$$\frac{\partial p_o}{\partial z} = \Delta\rho g \left(\frac{v_\phi}{v_0} \frac{[(\phi/\phi_0) - 1] + 1}{[\phi/\phi_0]^{n_\phi}} - 1 \right) \tag{23.52}$$

and

$$\frac{\partial \phi}{\partial z} = A a_\sigma \frac{\phi^{m_\sigma}}{v_\phi} |p_o|^{n_\sigma - 1} p_o, \tag{23.53}$$

respectively. Using these forms, the wave hydraulic potential H can be arranged as the sum of two integrals

$$H = \frac{\Delta\rho g}{\phi_0^{m_\sigma} a_\sigma} \int \left(\frac{\phi_0}{\phi} \right)^{m_\sigma} - \left(\frac{\phi_0}{\phi} \right)^{n_\phi + m_\sigma} d\phi + \frac{\Delta\rho g}{\phi_0^{m_\sigma} a_\sigma} \frac{v_\phi}{v_0} \int \left(\frac{\phi_0}{\phi} \right)^{n_\phi + m_\sigma} - \left(\frac{\phi_0}{\phi} \right)^{n_\phi + m_\sigma - 1} d\phi, \tag{23.54}$$

where both integrands are zero at $\phi = \phi_0$, and for $\phi > \phi_0$, $n_\phi > 1$, and $m_\sigma \geq 0$, the first integrand is positive and the second integrand negative. Furthermore, for conditions at which the solitary solution is possible, that is, $v_\phi/v_0 > v_\phi^{\text{crit}}/v_0$, H is a maximum at $\phi = \phi_0$, and H must have a minimum at the ϕ_1, the focal point where $\partial p_o/\partial z$ (Eq. 23.52) vanishes and the magnitude of the overpressure is a maximum (Fig. 23.3B). At $\phi > \phi_1$, H recovers to the background value $H(\phi_0)$ at the maximum porosity of the wave $\phi_{\max}$. It follows from the form of Eq. 23.54 that for a fixed choice of exponents, the rate at which H recovers to the background value $H(\phi_0)$ at $\phi > \phi_1$ decreases with wave speed. Thus, wave amplitude must increase with wave speed (Fig. 23.4A). For specified v_ϕ the leading term of the first integrand will dominate the rate at which H recovers to $H(\phi_0)$ at $\phi > \phi_1$. Consequently, increasing m_a increases amplitude (cf. solid black and cyan curves, Fig. 23.4A); this result is intuitive because increasing the nonlinearity of the effective bulk viscosity leads to a weakening of the matrix with increasing porosity. A less intuitive consequence of Eq. 23.54 is that increasing the nonlinearity of the porosity–permeability relationship, that is, increasing n_ϕ decreases wave amplitude (cf. orange and black curves, Fig. 23.4A). This occurs because at $\phi > \phi_1$ the rate at which the sum of the integrands decays with porosity increases with n_ϕ.

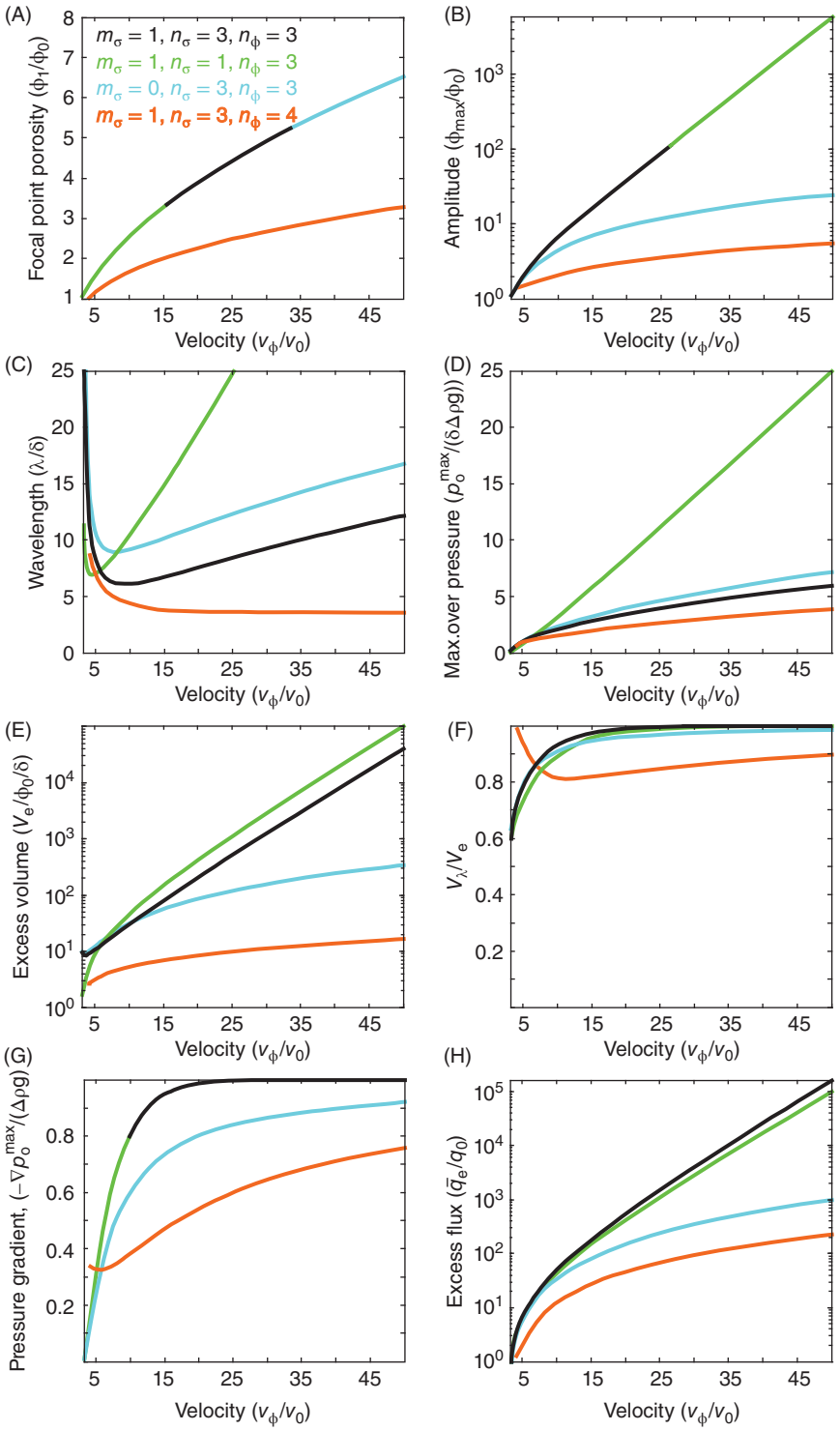

Fig. 23.4. Porosity wave properties in the small porosity limit ($\phi \ll \phi_d$) as a function of relative wave velocity for choices of the porosity exponents in the constitutive relations as indicated by color coding. Typical values for the exponents characterizing the porosity dependences of the permeability and effective bulk viscosity are $n_\phi = 3$ and $m_\sigma \leq 1$; a stress exponent $n_\sigma = 3$ is characteristic of dislocation creep, the viscous deformation mechanism commonly assumed for the lower crust (Ranalli 1995). The minimum relative velocity considered for each choice of exponents is $v_\phi/v_0 = n_\phi + 0.2$, slightly above the critical value $v_\phi/v_0 = n_\phi$, for the existence of the solitary solution (Eq. 23.44). Continuous curves drawn in different colors indicate that the properties are identical for the corresponding exponent choices. Focal point porosity (A) and amplitude (B). Focal point porosity, ϕ_1, is dependent only on n_ϕ, and the divergence of amplitude from ϕ_1 shows that the effect of increasing the nonlinearity (i.e., m_σ) of the effective bulk viscosity is to increase amplitude. In contrast, increasing nonlinearity of the porosity–permeability relationship decreases amplitude, which is independent of n_σ. (C) Wavelength, λ, is the distance separating the overpressure extrema within a wave (Fig. 23.3H). (D) Maximum fluid overpressure, the maximum underpressure (i.e., effective stress) is $-p_o^{max}$, both extrema occur at ϕ_1 (Fig. 23.3E). (E) Excess volume (Eq. 23.60) correlates with amplitude except at low wave speed, whereupon it decreases with speed in solutions for high n_σ/n_ϕ. That the excess volume for the nonlinear viscous cases ($n_\sigma = 3$) becomes larger than that for the linear viscous case ($n_\sigma = 1$) at low speeds ($v_\phi/v_0 \sim 6$) indicates a shifting of the porosity toward the tails of the nonlinear viscous solution. (F) Fraction of the volume that occurs within $\pm\lambda/2$ of ϕ_{max}. (G) Maximum $-p_0$ gradient, which occurs at ϕ_{max}, unity corresponds to a hydrostatic fluid pressure gradient. (H) Average excess fluid flux associated with wave passage. (*See color plate section for the color representation of this figure.*)

The relationship between wave velocity and amplitude ($A_\phi = \phi_{max}/\phi_0$) for $m_\sigma \neq 1$ obtained by solving $\Delta H = 0$ is

$$v_\phi = v_0 \frac{n_\phi + m_\sigma - 2}{1 - m_\sigma} \frac{([m_\sigma - 1][A_\phi^{-n_\phi} - 1] - n_\phi)A_\phi^{1-m_\sigma} + n_\phi}{A_\phi^{1-n_\phi-m_\sigma}([n_\phi + m_\sigma - 1][A_\phi - 1] + 1) - 1}, \tag{23.55}$$

which for the specific case $n_\phi = 3$ and $m_a = 0$ reduces to the linear relationship $v_\phi = v_0(2A_\phi + 1)$ obtained by Scott & Stevenson (1984, Barcilon & Richter 1986). The integrated form of Eq. 23.54 for general values of m_a is singular at $m_a = 1$, the value typically assumed in compaction literature. For this less general, but more widely used, case

$$H = \frac{\Delta\rho g}{a_\sigma}\left(\frac{1 - v_\phi/v_0}{n_\phi(\phi/\phi_0)^{n_\phi}} + \frac{v_\phi/v_0(\phi/\phi_0)^{1-n_\phi}}{n_\phi - 1} + \ln(\phi/\phi_0)\right), \tag{23.56}$$

$$v_\phi = v_0(n_\phi - 1)\frac{A_\phi^{n_\phi}(\ln A_\phi^{n_\phi} + 1) - 1}{1 + (A_\phi - 1)n_\phi - A_\phi^{n_\phi}}, \tag{23.57}$$

which similarly reduces to Scott & Stevenson's (1984) result for $n_\phi = 3$. Although Eq. 23.57 cannot be solved analytically for amplitude, it is apparent that in the small porosity limit, amplitude is not a function of n_σ. Evaluation of the integral in Eq. 23.46 gives the two values of pressure at any porosity within a solitary wave (Fig. 23.3E) as

$$p_o = \pm\delta\Delta\rho g(n_\sigma + 1)\left(\frac{1}{2^{n_\sigma}n_\phi}\frac{v_\phi}{v_0}\right)^{\frac{1}{n_\sigma+1}} \left(\frac{v_\phi/v_0 - 1}{(\phi/\phi_0)^{n_\phi}} - \ln(\phi/\phi_0)^{n_\phi} + 1 - \frac{v_\phi}{v_0}\frac{\left(1 - \frac{n_\phi}{(\phi/\phi_0)^{n_\phi} - 1}\right)}{n_\phi - 1}\right)^{\frac{1}{n_\sigma+1}}. \tag{23.58}$$

The corresponding integral for depth

$$z = \pm\delta\left(\frac{n_\phi}{2}\right)^{\frac{n_\sigma}{n_\sigma+1}}\left(\frac{v_\phi}{v_0}\right)^{\frac{1}{n_\sigma+1}}\int_{\phi_{max}}^{\phi}\frac{1}{\phi} \left(\left[1 - \frac{v_\phi}{v_0}\right]\left[\frac{\phi_0}{\phi}\right]^{n_\phi} + \ln\frac{\phi}{\phi_0} - 1 - \frac{v_\phi}{v_0}\frac{\left[1 - \left(\frac{\phi_0}{\phi}\right)\right]^{n_\phi - 1}}{n_\phi - 1}\right)^{-\frac{n_\sigma}{n_\sigma+1}} d\phi \tag{23.59}$$

must, in general, be evaluated numerically (a Fortran computer program for this purpose is available from the author).

Because the matrix recovers to the background porosity asymptotically in a steady-state solitary wave (for $n_\sigma \geq 1$), the true wavelength is infinite (cf. Eq. 23.47). For practical purposes, it is desirable to define an effective wavelength, which defines the extent of the wave that includes the bulk of the anomalous porosity. To this end, the wavelength λ is taken to be the interval between the points of minimum and maximum overpressure (Figs 23.3H and 23.4C). The ratio of the excess volume, that is, the total volume of fluid associated with the passage of a wave (Fig. 23.4E),

$$V_c = \int_{-\infty}^{\infty}(\phi - \phi_0)dz \tag{23.60}$$

to that obtained by integrating over $\pm\lambda/2$ shows that even at low speeds, >80% of the porosity of a wave occurs within the interval $\pm\lambda/2$ about the center of wave (Fig. 23.4F).

The effect of nonlinear viscous rheology is best understood in terms of the overpressure at the focal point porosity ϕ_1 (Fig. 23.4D). The magnitude of the overpressure gradient is limited by the hydrostatic pressure gradient for the fluid phase, a limit that is approached rapidly with increasing velocity at the center of a porosity wave (black–green curve, Fig. 23.4G); thus, at the velocity at which the maximum pressures of the linear and nonlinear viscous solutions are equal (~5.9 v_0, black and green curves, Fig. 23.4D), the dilational strain rate must fall more rapidly in the nonlinear case between ϕ_1 and ϕ_{max}, and as both ϕ_1 and ϕ_{max} are independent of n_σ, this must lead to a relatively flat-topped porosity distribution in which a greater proportion of the porosity lies within the interval $\pm\lambda/2$ about ϕ_{max}. Conversely, as speeds fall below that at which the overpressures at the focal point porosities of the solutions are equal, a greater proportion of the porosity shifts to the tails of the porosity distribution for the nonlinear case, leading to broad, poorly defined waves. This behavior is confirmed by linearization of the integral for the second moment of the solitary wave porosity distribution, which shows that in the limit $A_\phi \to 1$ or, equivalently, $v_\phi \to v_\phi^{crit}$, the moment becomes infinite if $n_\sigma \geq 3$ and explains the minima in V_c as a function of velocity for nonlinear viscous matrix rheology (black and cyan curves, Fig. 23.4E). The existence of the minima is of little practical consequence, because it occurs at velocities at which wavelengths are so long that the solitary waves would be indistinguishable from uniform fluid flow. Increasing n_ϕ counters this effect so that for $n_\sigma = 3$ and $n_\phi = 4$, waves are well formed at all velocities (orange curve, Fig. 23.4E). The instantaneous excess fluid flux, that is, the flux in excess of the background value $q_0 = v_0\phi_0$ within a wave is $q_c = v_\phi(\phi - \phi_0)$, and time-averaged fluid flux associated with wave passage (Fig. 23.4H) is estimated as

$$\overline{q}_c = \frac{v_\phi}{\lambda}V_c. \tag{23.61}$$

In the limit $v_\phi \to v_\phi^{crit}$, $\lambda \to \infty$; therefore, $\overline{q}_c/q_0$ must fall monotonically to zero with velocity, implying that there is a solitary wave solution for any value of $\overline{q}_c/q_0 > 0$.

Dynamic permeability in response to external forcing

There is no fundamental principle that dictates a balance between fluid production and transport in geological

environments, but for the range of conditions investigated by numerical simulations of metamorphic compaction-driven fluid flow, this balance does develop locally (Connolly 1997, 2010). Assuming such a balance in conjunction with the solitary porosity wave solution provides a means of predicting the dynamic variations in permeability that develop from an initially steady hydrologic regime in response to metamorphic fluid production (Connolly & Podladchikov 2013). This model amounts to no more than assuming that the time-averaged permeability of a compacting system is that necessary to accommodate fluid flux associated with an external forcing (Ingebritsen & Manning 1999). The information gained by implementing the solitary wave solution in this context is insight into the instantaneous variations in porosity and pressure that develop in response to the forcing.

In a 1D compacting system, a requirement for a balance between wave-propagated fluid transport and fluid production is that the magnitude of the time-averaged flux associated with the passage of a wave (Eq. 23.61) must be greater than or equal to the vertically integrated production q_s, because a wave with $|\overline{q}_c| < q_s$ would be unable to separate from its source. If $|\overline{q}_c| > q_s$, then the waves must be separated by a depth interval of $\Delta z = \lambda(|\overline{q}_c/q_s| - 1)$. In numerical simulations, the transient dynamics of wave separation are such that $|\overline{q}_c/q_s|$ is typically <1 (Connolly 1997). This result suggests that the properties of waves expected in metamorphic environments can be predicted by equating $\overline{q}_c$ to q_s and exploiting the monotonic relationship between $\overline{q}_c$ and v_ϕ (Figs 23.4H and 23.5). In earlier works (Connolly & Podladchikov 2013), it was asserted incorrectly that solitary wave solutions do not exist for $\overline{q}_c/q_0 > 2$; in fact, solitary solutions exist for all $\overline{q}_c/q_0 > 0$, but, as remarked previously, waves that develop at small excess flux magnitudes have such long wavelengths that it is unlikely they would be distinguishable from uniform fluid flow in natural environments.

While the scenario outlined here seems the most relevant to fluid flow in ductile portions of the Earth's crust, it is conceivable that fluid production may occur so rapidly, that is, on a timescale $\ll \delta/|v_0|$, that compaction mechanisms cannot accommodate fluid production. The effect of such an imbalance may be to produce a region of increased porosity bounded by unreacted and, presumably, compacted rocks. In this scenario, the response of the system is dependent on the vertical extent, Δz, of the region of increased porosity. If the extent is small ($\Delta z \sim \delta$), then a single solitary wave will evolve from the source region in such a way to carry the excess volume of the source region (as in Fig. 23.1A). The minimum in excess volume as

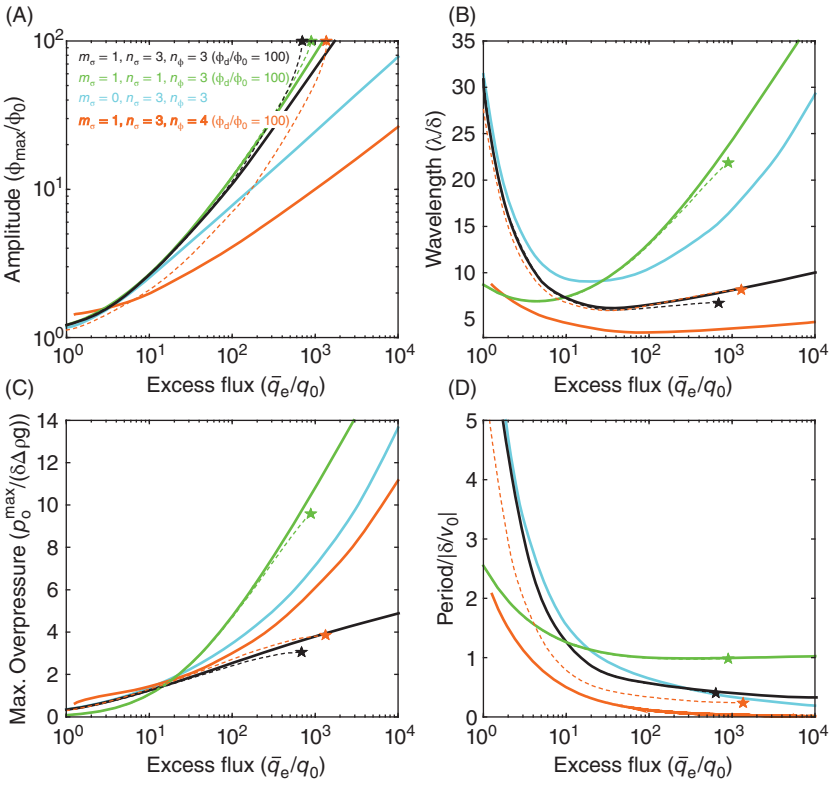

Fig. 23.5. Porosity wave properties as a function of the average excess fluid flux associated with wave passage for the exponent choices indicated by the legend and color coding. Solid curves are for the small porosity limit ($\phi \ll \phi_d$) as in Figure 23.4; dashed curves show the influence of a disaggregation in the intermediate porosity limit ($\phi_d \gg 1 - \phi$) for the specific case that $\phi_d/\phi_0 = 100$, discussed in the text (Fig. 23.3B). Star symbol at the end of dashed curves indicates the disaggregation condition. Properties of waves likely to be generated in natural settings in response to fluid production can be estimated by equating vertically integrated fluid production to the average excess flux. (*See color plate section for the color representation of this figure.*)

a function of velocity for strongly nonlinear viscous rheology gives rise to potential ambiguity for such initial conditions, because the same excess volume may be accommodated in a wave with either low or high velocity. It is speculated here that the high-velocity solution dominates. If the extent of the reacted porosity is large ($\Delta z \gg \delta$), then the multiple waves that evolve from the region can be expected to carry the excess flux $q_c \approx q_2 - q_0$ where q_2 is the flux through the increased porosity ϕ_2 at $p_o = 0$. Spiegelman (1993) demonstrated that waves that nucleate at the boundary between an infinite source and unreacted rocks are periodic waves in which porosity oscillates about the focal point ϕ_1 of the solitary solution (e.g., the red curve in Fig. 23.2E,F). However, for large porosity contrasts, that is, $\phi_1 \gg \phi_0$, the distinction is unimportant.

Example #1: 1D VISCOUS WAVE

To illustrate the application of the 1D viscous solitary wave solution, consider an initial state characterized by $\delta \sim 100$ m, $\phi_0 \sim 10^{-4}$, $\Delta\rho g \sim 10^3$ kg m^{-3}, $v_0 \sim -10^{-9}$ m s^{-1} ($q_0 = v_0\phi_0 = -10^{-13}$ m s^{-1}), as might be appropriate for dehydration in the lower crust at amphibolite facies conditions (i.e., temperatures of 773–923 K, Connolly & Podladchikov 2013). Taking $n_\sigma = n_\phi = 3$ and $m_\sigma = 1$ as the most probable values for the constitutive exponents, a fluid production rate of $q_s = 10^{-11}$ m s^{-1} will generate solitary waves with (black curves, Fig. 23.5) $\phi_{max} = 10.0\ \phi_0 = 1.0 \times 10^{-3}$, $\lambda = 6.3\ \delta = 630$ m, $p_o^{max} = 2.4\ \delta\Delta\rho g = 0.24$ MPa, and a period of 1.0 $\delta/|v_0| = 1.6 \times 10^3$ years. From the period (0.50 $\lambda/|v_0|$), or the relationship between flux and velocity (Fig. 23.4H), $v_\phi = -\lambda/\text{period} = -0.39$ m year^{-1} (12.2 v_0) and the maximum overpressure gradient is $\nabla p_o = -0.84\ \Delta\rho g$ (Fig. 23.4E), that is, the fluid pressure gradient within the wave is nearly hydrostatic (cf. Eq. 23.5). Holding all other parameters constant, the effect of changing from power-law viscous ($n_\sigma = 3$) to linear viscous ($n_\sigma = 1$, green curves in Figs 23.4 and 23.5) matrix rheology is to double the speed, amplitude, and maximum overpressure of the waves. This effect reflects that at $v_\phi/v_0 > 5.9$ (the crossing of the green and black curves in Fig. 23.4E), the nonlinear wave has a greater excess volume; thus, slow waves in the nonlinear viscous case are capable of accommodating the same flux as faster waves in the linear viscous case.

Disaggregation and the compaction-driven flow regimes

Wave amplitude grows monotonically with speed in the small porosity approximation because the $1-\phi$ and $\phi_d - \phi$ terms in Eqs 23.15–23.17 and 23.19 that limit the possible values of the porosity are neglected; thus, the formulation has no upper bound on porosity. Given that a granular matrix is expected to disaggregate at $\phi_d \sim 20\%$ (Arzi 1978; Auer *et al.* 1981; Ashby 1988; Vigneresse *et al.* 1996), the $\phi_d - \phi$ term is likely to dominate wave behavior before the dampening effects of the $1-\phi$ terms become significant. Elsewhere, it has been shown that for constitutive relations that do not account for disaggregation, the $1-\phi$ terms are unimportant at absolute porosities of ~25% for typical choices of the exponents n_σ, n_ϕ, b_ϕ, and m_σ (Connolly & Podladchikov 2000; a Fortran computer program that solves the large porosity formulation is available upon request). Accordingly, the effect of disaggregation is assessed here by an intermediate porosity approximation in which the $\phi_d - \phi$ term of Eq. 23.19 is retained, but porosity terms of order 1 (i.e., $1-\phi$ and $1-\phi^{1/n_\sigma}$) are dropped to obtain

$$H = \frac{\Delta\rho g}{\phi_0^{m_\sigma} \zeta_\sigma} \int \frac{\left[\left(\frac{\phi_0}{\phi}\right)^{m_\sigma} - \left(\frac{\phi_0}{\phi}\right)^{n_\phi + m_\sigma} + \frac{v_\phi}{v_0}\left(\left[\frac{\phi_0}{\phi}\right]^{n_\phi + m_\sigma} - \left[\frac{\phi_0}{\phi}\right]^{n_\phi + m_\sigma - 1}\right)\right]}{\left[\frac{\phi_d}{|\phi_d - \phi|}\right]^{n_\sigma - 1/2}} d\phi \tag{23.62}$$

for the properties of waves with porosities approaching ϕ_d. As the denominator of the integrand in Eq. 23.62 becomes infinite at $\phi = \phi_d$, H must have a maximum at ϕ_d and if $H(\phi_d) < H(\phi_0)$ (Fig. 23.3C), then there is no closed contour of the function U that connects the background porosity to an increased level of porosity (Eq. 23.41, Fig. 23.3F) and no solitary solution is possible. Because the integrand of Eq. 23.62 is simply the combined integrands of Eq. 23.54, scaled by the disaggregation term, the effects of varying the exponents n_ϕ, n_σ, and m_σ are readily separated. Specifically, lowering n_σ or raising n_ϕ or m_σ increases $H(\phi_d)$ relative to $H(\phi_0)$, extending the range of solitary wave velocities that the matrix can sustain without disaggregating (Fig. 23.6A). In contrast to the small porosity limit where H, and therefore wave amplitude, is independent of the stress exponent n_σ, in the intermediate porosity limit, although the focal point porosity ϕ_1, and therefore p_o^{max} (Fig. 23.6C), remains independent of n_σ, the relation between amplitude and velocity is dependent on n_σ. For $n_\sigma = n_\phi = 3$, this dependence is prominent for $\phi/\phi_d > 0.1$ (black curves, Fig. 23.6A) and is even more pronounced with increasing nonlinearity in the porosity–permeability relationship (orange curves, Fig. 23.6A). Because the effect of the disaggregation term is to weaken the matrix with increasing porosity, its effect is to sharpen the porosity distribution within solitary waves, akin to the result of increasing m_σ, leading to an increase in excess volume compared with models that do not account for disaggregation.

By solving for the solitary wave velocity at which $H(\phi_d) = H(\phi_0)$ and computing the corresponding value of $\overline{q}_c$ (Eq. 23.61), it is possible to estimate the range of fluid production rates that can be sustained without causing the solid matrix to become fluidized. For example, taking $n_\phi = 3$ and $\phi_d/\phi_0 = 100$, fluid production rates of 700–900 $|q_0|$ are adequate to induce fluidization (Fig. 23.7); for comparison, to cause fluidization by, albeit unstable, uniform flow, the required fluid production rates are $|q_0|(\phi_d/\phi_0)^{n_\phi}$, that is, $10^6\ |q_0|$. Thus, porosity waves have the potential to strongly enhance weak flow perturbations. In terms of fluxes, the lower limit of the solitary wave regime corresponds to $\overline{q}_c = 0$; thus, the periodic regime can only be induced by a negative vertically integrated fluid production rate such as would result from the consumption of fluids by retrograde hydration reactions. Alternatively, for waves induced

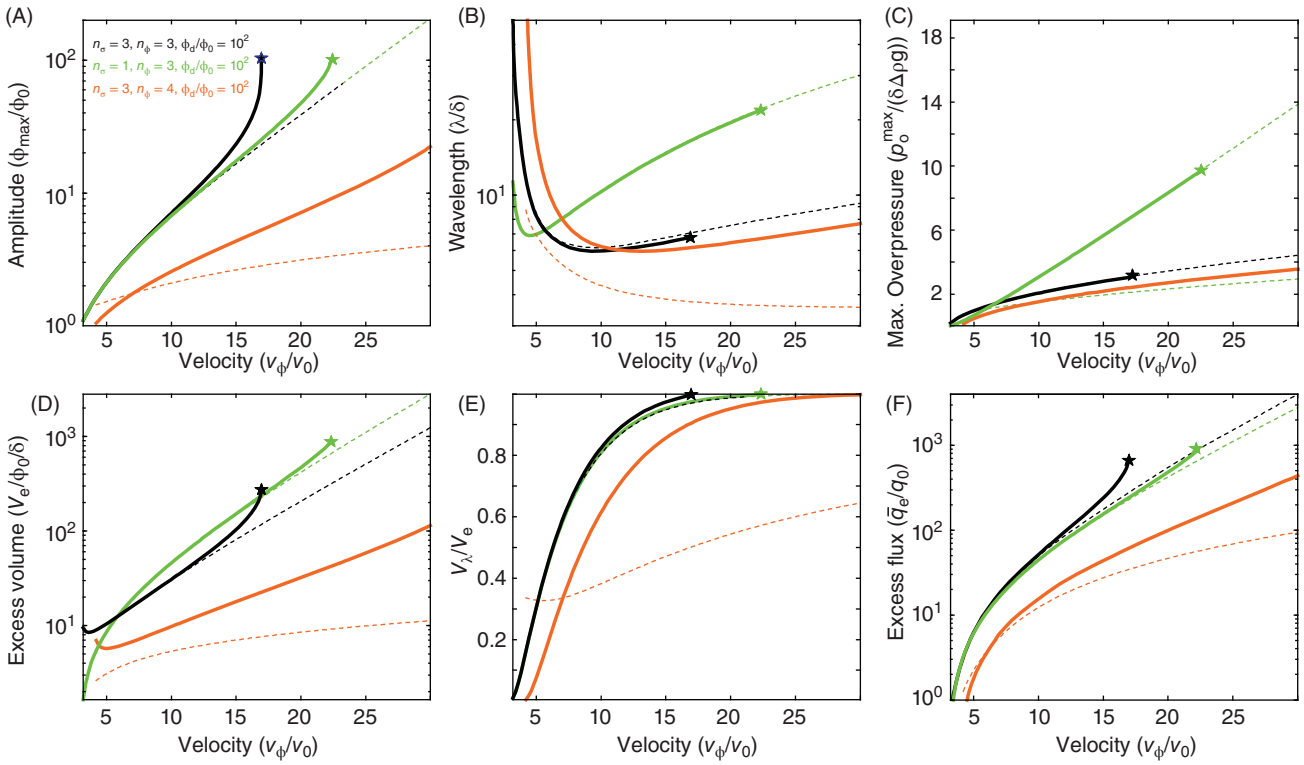

Fig. 23.6. Porosity wave properties in the intermediate porosity limit ($\phi_d \ll 1 - \phi$) as a function of velocity for a disaggregation porosity ϕ_d a hundred times greater than ϕ_0. All examples are for $m_\sigma = 1$ with other exponents of the formulation as indicated by the legend and color coding. The star symbol indicates the disaggregation condition. Dashed curves show the corresponding properties for the small porosity limit as in Figure 23.4. The solutions show that the effect of disaggregation is strongly dependent on both n_ϕ and n_σ; for $n_\phi = 3$, the disaggregation effect becomes significant if ϕ_{max} is within an order of magnitude of ϕ_d and is amplified by increasing n_σ. Properties for these solutions are shown as a function of $\overline{q}_e$ in Figure 23.5. (*See color plate section for the color representation of this figure.*)

by a perturbation defined in terms of an excess volume (e.g., Fig. 23.1), the periodic solution requires negative excess volume, that is, an obstruction (Spiegelman 1993) to a region of uniform flow. The appearance of periodic waves in numerical simulations (e.g., Fig. 23.1A or Connolly 1997) reflects the dynamics of solitary wave separation, in which over-compaction of the matrix obstructs the background flow.

DISCUSSION

This study has explored the behavior of the solitary porosity wave solution to the compaction equations in 1D viscous media. The solution provides a simple means of estimating the scales of pressure and porosity (or permeability) variations as a function of fluid production rates and constitutive relations. Although porosity waves have been posited as a mechanism for fluid flow in the lower crust (Suetnova *et al.* 1994; Connolly 1997; Gliko *et al.* 1999; Ague 2014; Tian & Ague 2014), their expression in nature would be complicated by a number of factors. These factors, which include geometry, lithological heterogeneity, tectonic stress, and rheological variations, have been reviewed elsewhere (Connolly & Podladchikov 2004, 2013). Here, some aspects of this earlier review, which are particularly relevant to potential applications of the 1D solitary wave solution, are recapitulated in the context of a conceptual model for compaction-driven fluid flow in the lower crust (Fig. 23.8).

Linear or nonlinear viscous rheology?

Even if the viscous deformation mechanism is nonlinear, in rocks undergoing simultaneous compaction and shear deformation, it does not necessarily follow that effective viscous rheology for the compaction process is nonlinear. Both compaction and macroscopic shear deformation are accomplished by microscopic shear. Thus, if a rock is simultaneously subject to both modes of deformation, then they must be accommodated by the same microscopic mechanism. This mechanism is determined by the largest of the stresses responsible for deformation, $|\Delta\sigma|$ or $|p_o|$, with the result that if the stresses are of different magnitude, the viscous response to the inferior stress is approximately linear and determined by effective viscosity resulting from the deformation induced by the superior stress. Regardless of magnitude, far-field tectonic stress facilitates compaction by lowering the effective viscosity of the solid matrix (Tumarkina *et al.* 2011).

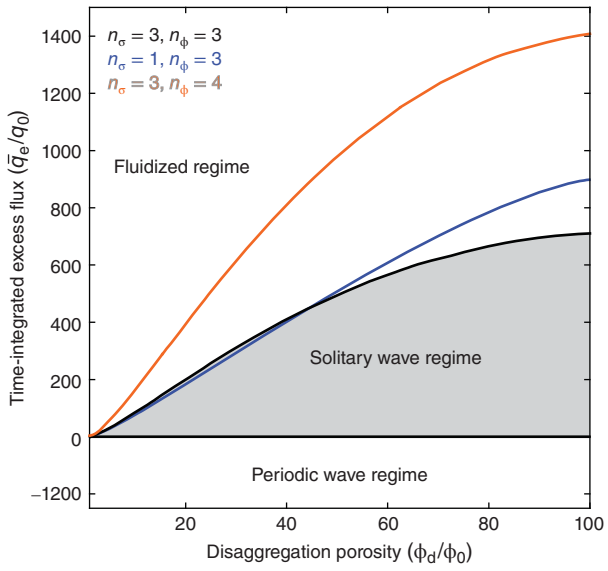

Fig. 23.7. Phase diagram depicting the hydrologic regimes predicted by the intermediate porosity limit solitary wave solution as a function of the disaggregation porosity and excess flux. The regime that develops in response to fluid production can be predicted by equating the magnitude of the excess flux carried by the waves to the vertically integrated fluid production $\bar{q}_s$. The boundary between the solitary wave and fluidized regime is dependent on the exponents m_σ, n_σ, and n_ϕ; it is shown for $m_\phi = 1$, with other exponents as indicated by the inset and color coding. Solitary waves become progressively more diffuse and indistinguishable from uniform flow as $\bar{q}_e/q_0 \to 0$. Periodic wave trains develop in response to negative fluid production, for example, the consumption of fluids by hydration reactions, or an obstruction to the background porosity (Spiegelman 1993). In nature, such periodic wave trains would decay to uniform flow. (*See color plate section for the color representation of this figure.*)

3D geometry and nonviscous rheology

As remarked earlier, the 1D solitary wave solution is unstable with respect to spherical solitary waves in three dimensions (Wiggins & Spiegelman 1995). However, as wave speeds increase, the overpressure gradient in solitary waves rapidly approaches the limit (i.e., $-[1-\phi]\Delta\rho g$) imposed by the fluid hydrostat (Fig. 23.4G). At this condition, the velocity and porosity distribution along the vertical axis of the 1D and 3D waves are essentially identical, and the excess volume of the 3D wave can be estimated by applying spherical symmetry to porosity distribution of the 1D wave (Connolly & Podladchikov 2007). Transient models of multidimensional waves suggest that they collect fluid from a source region of area $\sim\pi\lambda^2$ (Wiggins & Spiegelman 1995). Thus, the properties of the 3D waves that would initiate in response to fluid production can be predicted by equating the product of vertically integrated fluid production rate and the source area, $Q_s = \pi\lambda^2 q_s$ with the volumetric transport rate

$$Q = \frac{v_\phi}{\lambda}\int_0^\infty 4\pi r^2(\phi - \phi_0)\mathrm{d}r, \qquad (23.63)$$

where the integral is the 3D excess fluid volume associated with the wave and is approximated by using the 1D solitary wave solution for the radial porosity distribution. In practice, because λ varies as a function of q_s, solving $Q_s = Q$, is an iterative problem.

Example #2: 3D VISCOUS WAVE

To illustrate the consequences of 3D geometry, consider the same parameters as in Example #1. Taking the 1D wavelength, $\lambda = 6.3\ \delta$, as an initial estimate for the 3D solution, the required fluid transport rate is $Q/|q_0\delta^2| = q_s\pi\lambda^2/|q_0\delta^2| = 100\ \pi\ 6.3^2 = 1.25\times10^4$. For this value of Q, $v_\phi/v_0 = 29$ (black curve, Fig. 23.10) and $\lambda/\delta = 9.1$ (black curve, Fig. 23.4C). Using this revised estimate of wavelength, $Q/|q_0\delta^2| = 2.6\times10^4$, which in turn yields new velocity and wavelength estimates of $v_\phi/v_0 = 37.6$ and $\lambda/\delta = 11.0$. After three iterations, successive refinement of the estimates for fluid transport rate, velocity, and wavelength by this method yields $Q = 37.9\times10^{-5}$ m^3 s^{-1}, $\lambda = 11.0\ \delta = 1100$ m, $v_\phi = 41.4$ $v_0 = -1.31$ m year^{-1}, $p_o^{max} = 5.35\ \delta\Delta\rho g = 5.35$ MPa, and $\phi_{max} = 1390$ $\phi_0 = 0.139$ for the 3D wave. This result demonstrates that increased spatial focusing of fluid flow caused by 3D effects has the capacity to generate both the large porosities necessary to cause disaggregation and/or the overpressures necessary to induce brittle (plastic) failure.

Thermal activation

Thermal activation will, generally, lead to an upward increase in the effective shear viscosity of the lower crust on a length scale l_A that is dependent on the activation energy of the viscous mechanism and the geothermal gradient, but typically ~1 km (Connolly & Podladchikov 2013). Consequently, all other factors being equal, the compaction length scale δ will increase upward through the crust as $\sqrt[n_\sigma+1]{\exp(z/l_A)}$, that is, by a factor of ~10 over a vertical interval distance of 6–8 l_A. This variation has consequences for the relevance of the steady-state solution, which assumes a constant effective shear viscosity. Provided $\delta < l_A$, the variation in shear viscosity due to thermal activation is weak on the porosity wave length-scale. In this case, quasi-steady-state waves that closely approximate the steady-state solution can be expected to develop. The evolution of such quasi-steady-state waves can be anticipated from the steady-state solution given that the waves are likely to conserve excess volume (Fig. 23.4E, Connolly & Podladchikov 2013). As δ becomes comparable to l_A, multidimensional waves flatten to sill-like structures. Although these structures superficially resemble the 1D steady-state solitary wave solution, their vertical dimension is dictated by l_A and they slow exponentially as they propagate upward (Connolly 1997; Connolly & Podladchikov 1998). This behavior suggests that if porosity waves develop on a geologically relevant length scale at depth within the crust, then, in the absence of other deformation mechanisms, they will tend to stagnate below the brittle–ductile transition (Fig. 23.8).

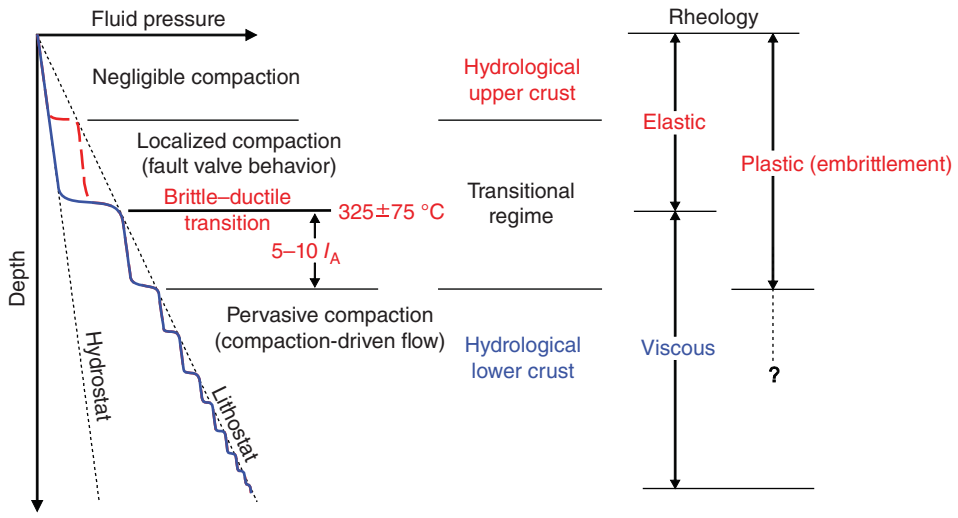

Fig. 23.8. Conceptual model of the hydrologic regimes that would result from superimposing thermally activated compaction on crustal column with heterogeneous permeability (Connolly & Podladchikov 2013). In the upper crustal regime, faulting maintains such high permeabilities that negligible deviation from hydrostatic fluid pressure is adequate to drive fluid circulation (Zoback & Townend 2001). This regime is limited at depth by the conditions at which localized compaction becomes an effective mechanism for sealing fault-generated permeability (Gratier *et al.* 2003; Tenthorey & Cox 2006). At greater depth, pervasive compaction and/or metamorphic fluid production may generate transient fluid overpressure that is periodically relieved by faulting (Sibson 1992). At the brittle–ductile transition (i.e., the base of the seismogenic zone), it is improbable that pervasive compaction can keep pace with metamorphic fluid production; thus, the transitional hydrologic regime is likely to persist over an interval that extends ~10 l_A below the brittle–ductile transition, where l_A is the characteristic length scale for variation in the ductile rheology (typically ~1 km, Connolly & Podladchikov 2013). Beneath the transitional regime, pervasive compaction is capable of generating hydraulic seals, and fluid, if present, is at near-lithostatic pressure. Within this lowermost regime, fluid flow is truly compaction driven. In the absence of fluid production, the tendency of both time and depth is to decrease the wavelength of the fluid pressure compartments, resulting in a near-steady state. Barring the possibility of a subcrustal fluid source, the flux in this near-steady regime must decrease with depth. Thus, the magnitude of the perturbation caused by fluid production to the lower crustal regime is dependent on its depth. In the deepest portion of the crust, the rheology is viscous as assumed in the formulation presented here. Upward strengthening of the viscous rheology would cause porosity waves to provoke elastic and plastic deformation mechanisms at shallower levels. Because viscous porosity waves are associated with negative effective pressure anomalies, $\sim\lambda\Delta\rho g/2$, the first deviation from viscous behavior is likely to be viscoplastic. Viscoplastic rheology causes fluid flow to be focused into tube-like channels (Connolly & Podladchikov 2007; Connolly 2010). At still shallower depths, viscous compaction becomes entirely ineffective, leading to a viscoelastic transition. In numerical models, such a viscoelastic transition causes lower crustal solitary porosity waves to dissipate as porosity–pressure surges in the upper crust (Connolly & Podladchikov 1998). (*See color plate section for the color representation of this figure.*)

Example #3: THERMAL ACTIVATION

Consider a 1D solitary porosity wave with initial properties $\delta_i \sim 100$ m, $\lambda = 630$ m, $p_o^{max} = 0.24$ MPa, and $v_\phi = 12.2\ v_0$, as in Example #1, which propagates upward through a cooling, but otherwise uniform crust, characterized by $l_A \sim 1$ km. The initial dimensionless excess volume $(V_e/\delta_i/\phi_0)$ of the wave is 41.4 (black curve, Fig. 23.4H). After the wave rises 5 km, the local compaction length increases to $\delta = \delta_i \sqrt[n_\sigma+1]{\exp(\Delta z/l_A)} = 350$ m. If the wave conserves its dimensional excess volume (v_e), then the dimensionless excess volume $V_e/\delta/\phi_0$ must decrease to 11.9. For this new dimensionless excess volume, the wave velocity is $v_\phi/v_0 = 5.6$ (Fig. 23.4H), and its wavelength and maximum overpressure increase to 2200 m (Fig. 23.4C) and 0.40 MPa (Fig. 23.4D), respectively. As this wavelength is greater than l_A, the steady-state solution most likely overestimates both velocity and wavelength (Connolly & Podladchikov 1998).

Viscoplastic rheology

In the viscous limit, a solitary wave is associated with a maximum fluid overpressure of $\sim\lambda\Delta\rho g/2$ that grows as the wave propagates upward into cooler rocks. As rocks have little tensile strength (e.g., Gueguen *et al.* 2004), it is probable that such fluid overpressures would induce hydrofracture and/or other plastic dilational mechanisms. Brittle deformation associated with active metamorphism (Etheridge *et al.* 1984; Simpson 1998) is broadly consistent with the notions that embrittlement occurs at high fluid pressure and on spatial scales $\ll\delta$. In this scenario, the effect of plastic weakening can be simulated by reducing the coefficient of viscous flow by a factor of $R^{n_\sigma+1}$ for $p_o > 0$. The *ad hoc* factor R can be adjusted to match the presumed yield stress, σ_y, of the plastic mechanism. In 1D numerical models that use this approximation, asymmetrical, steady-state solitary waves develop in which a small overpressured region is fed by a much larger underpressured region (Fig. 23.1C–D). In the small porosity limit, such solutions are permitted because the hydraulic potential H (Eq. 23.54), which determines the shape of the viscous solitary wave, is independent of A and n_σ. Thus, both the upper and lower portions of the viscoplastic solitary wave are given by the viscous solitary wave solution with the sole modification that the compaction length scale in the overpressured region is

$$\delta_p = \delta R. \qquad (23.64)$$

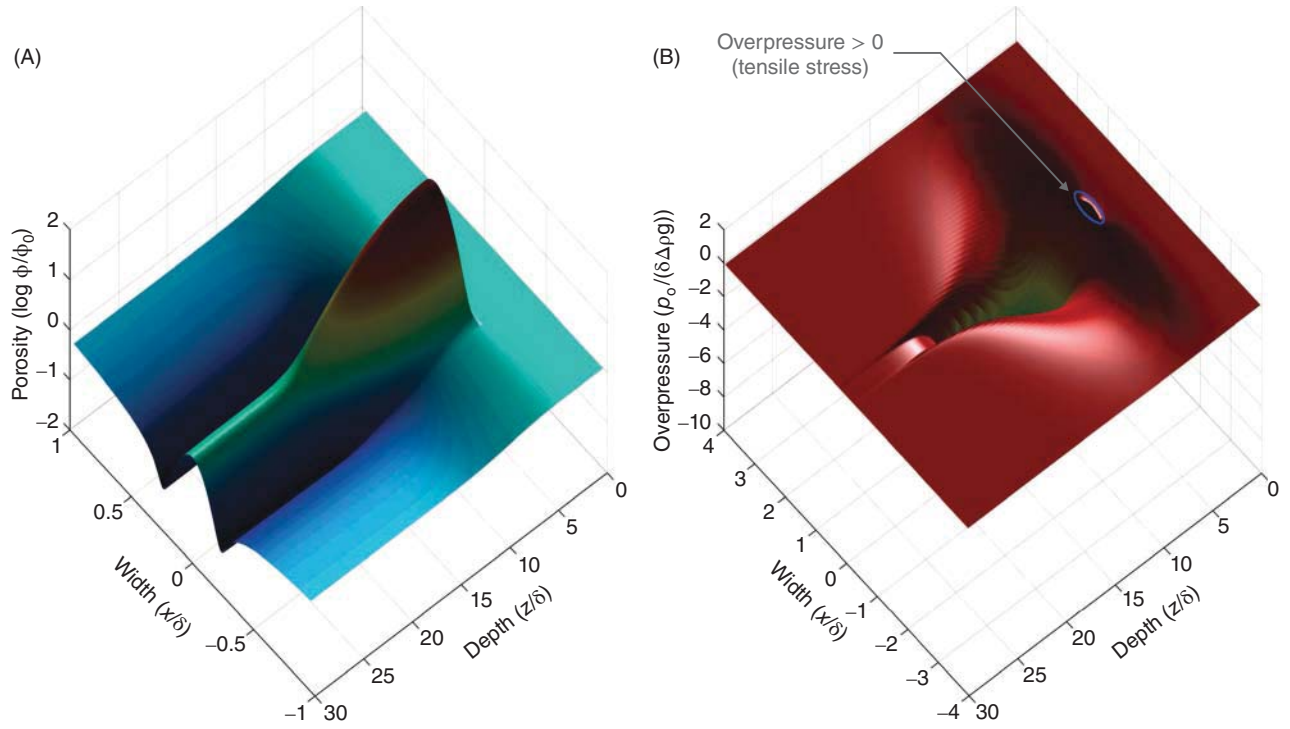

Fig. 23.9. Two-dimensional numerical simulation of a solitary porosity wave in a viscoplastic matrix. (A) Porosity; (B) fluid overpressure. The axial porosity and overpressure profiles of the wave are identical to the 1D case (Fig. 23.1C,D), but in the 2D case, the asymmetric overpressure distribution causes compaction of the background porosity on either side of the wave, leaving a tube-like channel that localizes subsequent fluid flow; the logarithmic scale for porosity emphasizes this effect. Numerical simulations (B. J. P. Kaus, personal communication 2005) have confirmed that 3D solitary waves in a viscoplastic matrix have radial symmetry orthogonal to the direction of propagation as in the viscous limit (Wiggins & Spiegelman 1995); thus, the 2D wave shown here corresponds to the axial section of a 3D wave. (*See color plate section for the color representation of this figure.*)

As the effect of weakening is to reduce the timescale during decompaction to $\tau_p = \delta R/|v_0|$, it is unsurprising that in three dimensions the overpressured region develops the spherical porosity distribution of the viscous solution on the length scale δ_p, which then recovers in the underpressured region to ϕ_0 on the length scale δ, giving rise to a wave shape similar to that of a cigar aligned in the direction of flow with the lit end upward (Connolly & Podladchikov 2007). In contrast to the 1D case, the asymmetry of the pressure distribution for such a wave obviates a true steady state. Specifically, numerical simulations (Fig. 23.9) show that the underpressured lower portion of the wave drains more fluid from surrounding matrix than is expelled into the matrix by the overpressured upper portion with the result that viscoplastic solitary waves grow with time. The imbalance in fluxes has the consequence that waves leave a tube-like channel, with porosities slightly ϕ_0, in their wake. This channel localizes subsequent fluid flow because it is surrounded by an interval of compacted matrix radius δ.

Although the 3D viscoplastic solitary wave solution is not steady state, at any point in time its properties are well represented by a geometric transformation of the viscous steady-state solution. Neglecting the small fraction of the excess volume associated with the overpressured portion of the wave, the porosity distribution of the viscoplastic wave approximates the lower half of a prolate ellipsoid with semi-major axis $\lambda_p = \lambda/2$ and semi-minor axis of $R\lambda/2$, where λ is the wavelength of a viscous wave with the same velocity as the viscoplastic wave (Fig. 23.4C). As the velocity–amplitude relation (Fig. 23.4B) is, for $v_\phi/v_0 > \sim 2n_\phi$, essentially independent of the dimension of the solution, the fluid transport rate for the viscoplastic case is

$$Q_p = \frac{Q}{2} R^2, \tag{23.65}$$

where Q is the transport rate for the spherical viscous solitary wave (Eq. 23.63). In contrast to the 3D viscous case, where fluid is collected from an area proportional to λ, in the viscoplastic case, the horizontal radius of the wave is small in comparison with δ (Connolly & Podladchikov 2007; Connolly 2010). Thus, 3D viscoplastic waves collect fluid from a source area of $\sim\pi(\delta/2)^2$ regardless of the vertically integrated fluid production rate q_s. Consequently, for a given q_s, the initial velocity of a viscoplastic wave can be estimated by equating the fluid production likely to be collected by the wave, $q_s\pi(\delta/2)^2$, with Q_p. Using Eq. 23.65, the fluid transport rate of the viscous solution with the same velocity–amplitude relation as

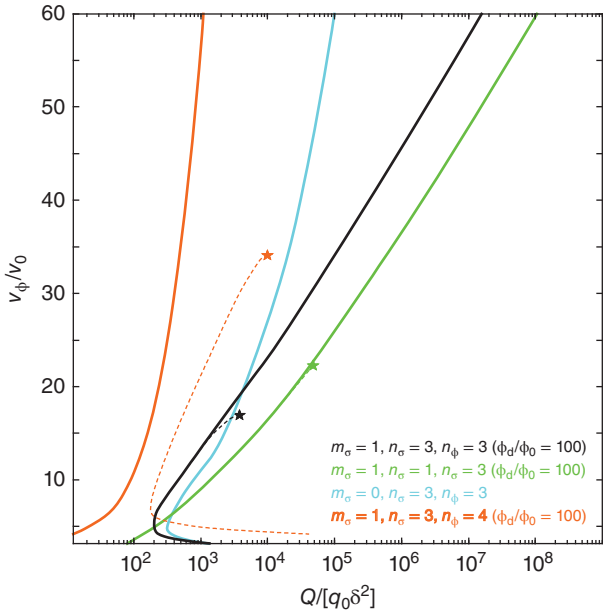

Fig. 23.10. Wave velocity as a function of volumetric fluid transport rate (Q) by spherically symmetrical 3D porosity waves (Wiggins & Spiegelman 1995) for exponent choices as indicated by the legend. For velocities at which the fluid pressure gradient (Fig. 23.4G) is nearly hydrostatic, the properties of the 1D and 3D solution are essentially identical; thus, at these conditions, the velocity can be used to predict 3D wave properties from the 1D solution (Fig. 23.4, and Examples #2 and #3). Where velocity is not a monotonic function of Q, it is probable that the high-velocity (short-wavelength) solution dominates. (*See color plate section for the color representation of this figure.*)

the viscoplastic wave is then

$$Q = \frac{\pi}{2} q_s \left(\frac{\delta}{R}\right)^2. \tag{23.66}$$

From this value of Q the relation between Q and v_ϕ for the 3D viscous solution (Fig. 23.10) yields the velocity of the viscoplastic wave. The remaining properties of the wave are then recovered from the 1D viscous solution as a function of this velocity with the modifications: $\lambda_p = \lambda/2$, $p_o^{\min} = -p_o^{\max}$, and the maximum overpressure, ostensibly σ_y, is $-Rp_o^{\min}$.

It is possible to derive rigorous expressions for the effective viscosity resulting from various types of plastic yielding and the corresponding 1D solitary wave solutions (Yarushina 2009), but the viscoplastic solution for brittle yielding is well represented by the simple model presented here (Eq. 23.65) if the parameter R is adjusted to match σ_y. In particular, that viscoplastic matrix rheology causes solitary waves to grow with time and channelize fluid flow is likely to be a robust prediction. Unfortunately, the nonsteady character of the 3D solution simulated by the simple model creates an unrealistic situation in which the implied brittle yield strength grows with time. Although a multidimensional transient model with true brittle yielding remains to be investigated, in such a model $p_o^{\max}$ is constrained by σ_y, while the volume of the overpressured portion at σ_y can be expected to increase with time. Such effects could substantially alter the results of the geometric model (i.e., Eq. 23.65) used to estimate the fluid transport rate here.

Example #4: 3D VISCOPLASTIC WAVE

To quantitatively illustrate the consequences of the foregoing model for viscoplastic waves, consider parameters as in Example #1, but with $R = 0.1$. The fluid transport rate of the corresponding 3D viscous wave (Eq. 23.66) is $Q/|q_0\delta^2| = (q_s/|q_0|)\pi/(2R^2) = 1.57 \times 10^4$. From the relationship between Q and v_ϕ (Fig. 23.10), $v_\phi = 25.3$ $v_0 = -0.79\,\text{m year}^{-1}$, and for this velocity (Fig. 23.4), $\phi_{max} = 94.5$ $\phi_0 = 9.45 \times 10^{-3}$, $\lambda_p = \lambda/2 = 4.24$ $\delta = 424\text{vm}$, and $p_o^{\min} = -p_o^{\max} = -3.99$ $\delta\Delta\rho g = -3.99\,\text{MPa}$. From the model geometry, the actual fluid transport rate (Eq. 23.65) $Q_p = 1.57 \times 10^4$ $(R^2/2)$ $|q_0\delta^2| = 2.48\,\text{m}^3\,\text{year}^{-1}$; the maximum fluid overpressure $\sigma_y = -Rp_o^{\min} = 0.399\,\text{MPa}$; the radius of the wave and the channel left in its wake is $\lambda_p = \lambda/2 = 4.24$ $\delta = 424\,\text{m}$; and the channels would have a spacing $\sim\delta = 100\,\text{m}$.

Viscoelastic rheology

The omnipresent elastic response of the rock matrix (or pore fluid) becomes significant as the effective bulk viscosity of the matrix increases. Such an increase is to be expected as the crust strengthens upward toward the brittle–ductile transition and also locally in response to decreases in porosity. In general, steady-state solutions for Maxwell viscoelastic porous media take the form of heteroclinic shock waves that connect two distinct levels (ϕ_0 and ϕ_1 in the present formulation) of porosity (Rice 1992; Connolly & Podladchikov 1998). These can be understood in terms of the oscillating ball analogy to viscous solution (Fig. 23.2) in that elasticity acts similarly to friction on the motion of the ball, which dampens the oscillations of the ball so that it comes to rest at the focal point. Fluid compressibility and poroelasticity have opposite effects (Connolly & Podladchikov 1998): in a system composed of a viscous, inelastic, matrix and a compressible fluid the focal point porosity ϕ_1 is at the leading edge of the shock and the background porosity ϕ_0 is in its wake, whereas in a system composed of a viscoelastic matrix and a incompressible fluid the background porosity ϕ_0 is at the leading edge of the shock and the focal point porosity ϕ_1 is in its wake. Thus, the relative magnitude of the fluid and matrix elastic compressibilities controls whether the elevated porosity ϕ_1 is at the leading edge or in the wake of the viscoelastic. Most applications of elastic and viscoelastic porosity wave solutions in the geological literature (Rice 1992; Revil & Cathles 2002; Miller *et al.* 2004; Chaveau & Kaminski 2008; Joshi *et al.* 2012) assume negligible fluid compressibility. The heteroclinic character of viscoelastic solutions has the peculiar implication that the nondissipative elastic rheology leads to dissipative porosity shock waves. In transient models, a viscoelastic transition caused by upward strengthening provokes a rapid transition from lower crustal solitary waves, which are well approximated by the viscous limit, to porosity fluid pressure surges in the upper crust (Connolly & Podladchikov

1998). Even if both solid and fluid constituents are considered to be incompressible, surface tension as incorporated in the formulation of Bercovici *et al.* (2001) has the effect of generating a Kelvin viscoelastic compaction rheology. The Kelvin limit may be of relevance at the small porosities thought to be characteristic of the lower crust (Connolly & Podladchikov 2013; Ague 2014) at which surface tension may inhibit compaction.

CONCLUDING REMARKS

There is no smoking gun as evidence for the existence of porosity waves as a mechanism for fluid flow in the lower crust. The porosity wave model is the mathematical consequence of a set of physical assumptions that are generally thought to apply to lower crustal processes. Most prominent among these assumptions are that lower crustal rocks compact by viscous creep and that fluid flow is described by Darcy's law. The virtue of the porosity wave model is that it represents a physically consistent steady state and provides a simple means of anticipating the hydrodynamic response of the lower crust to perturbations such as fluid production. The formulation developed here has small ($\phi \ll \phi_d$) and intermediate ($\phi_d \ll 1-\phi$) porosity approximations that are dependent only on relative porosity (ϕ/ϕ_0); material properties or, alternatively, scales (ϕ_0, $|v_0|$, and δ); two exponents (m_σ and n_ϕ) that characterize the porosity dependence of the effective bulk viscosity and permeability of the rock matrix; and an exponent (n_σ) that characterizes the stress dependence of effect shear viscosity of the rock matrix. In particular, the role of the stress exponent n_σ has not been considered in previous studies. The most surprising feature resulting from this nonlinearity is that it appears to admit a finite-wavelength solitary solution for shear-thickening ($n_\sigma < 1$) viscous mechanisms. Finite-wavelength solitary porosity waves are of interest because they permit deformation-propagated fluid flow through an initially impermeable matrix (Connolly & Podladchikov 1998). For the shear-thinning ($n_\sigma > 1$) viscous mechanisms thought to be characteristic of the lower crust (Kohlstedt *et al.* 1995; Ranalli 1995), the stress exponent does not fundamentally change the behavior described for the linear viscous case (Fowler 1984; Richter & McKenzie 1984; Scott & Stevenson 1984). However, somewhat counterintuitively, at low velocities ($v_\phi/v_0 < \sim 6$) nonlinearity results in poorly defined waves in which a greater proportion of the porosity lies in the tails of the waves compared to the porosity distribution of the linear viscous case. At higher velocities, this trend reverses so that a greater proportion of the fluid occurs near the center of mass of a wave in the nonlinear case. Disaggregation effects and increasing the nonlinearity of the effective bulk viscosity also lead to more sharply defined porosity distributions.

The ansatz that porosity waves evolve to accommodate the vertically integrated fluid production rate q_s in natural systems has the trivial consequence that in the 1D limit the effective permeability resulting from the porosity wave mechanism, $k_{\text{effective}} \approx k_0 \overline{q}_c / q_0$, is $\sim k_0 q_s / |q_0|$, where k_0 and q_0 are the background permeability and fluid flux, respectively, and $\overline{q}_c$ is time-averaged flux carried by a wave (Fig. 23.4H). Local variations in permeability are significantly larger, for example, in the 1D quantitative example considered here (Example #1), the maximum local permeability $k_0[\phi_{\max}/\phi_0]^{n_\phi}$ is an order of magnitude greater than the effective permeability and three orders of magnitude greater than k_0. Spatial effects associated with 3D porosity waves lead to substantially higher effective permeability. In the quantitative example of the 3D viscous case (Example #2), $k_{\text{effective}} \approx k_0 Q / |q_0 \pi (\lambda/2)^2| = 3990\, k_0$, and for the viscoplastic case (Example #4), $k_{\text{effective}} \approx k_0 Q_p / |q_0 \pi (R\lambda_p)^2| = 139 k_0$. These results are dependent on highly uncertain, but plausible, values for q_s and the scales ϕ_0, $|v_0|$, and δ (Connolly & Podladchikov 2013). In general, q_s can be estimated from the knowledge of the lithology of interest and the geodynamic scenario responsible for fluid production. The background porosity ϕ_0 and fluid velocity v_0 are roughly constrained from relatively well-known physical properties and theoretical considerations, leaving the compaction length scale δ as the greatest source of uncertainty in that it combines the hydraulic and rheological properties of the combined fluid–rock system. At present, it seems that the spatial scales of compaction-driven flow phenomena offer the most accurate means of estimating the compaction length in natural environments.

ACKNOWLEDGMENTS

This chapter was improved by reviews from Jay Ague and Martin Appold and by the editorial direction of Tom Gleeson, Steve Ingebritsen, and Craig Manning. The original version of this chapter was written while the author was a guest of the Centre of Advanced Studies at the Norwegian Academy of Science and Letters for the "Dynamics of Fluid Rock Systems" project led by Bjorn Jamtveit between 2000 and 2001.

APPENDIX: NONDIMENSIONALIZATION

For typical constitutive relations, the compaction equations admit a dimensionless form in the small porosity limit ($1-\phi \to 1$, $\phi_d - \phi \to \phi_d$) that is independent of the absolute porosity (Scott & Stevenson 1984). In this limit, the constitutive relations given by Eqs 23.17 and 23.19 are

$$k = a_\phi \phi^{n_\phi} \tag{23.67}$$

$$f_\phi = n_\sigma^{-n_\sigma} (3/2)^{n_\sigma + 1} \phi^{m_\sigma}. \tag{23.68}$$

Using these relations, and substituting $v_\phi = -v_\infty$, the dimensional forms of Eqs 23.15 and 23.16 simplify to

$$\frac{\partial p_o}{\partial z} = -v_\phi \frac{\eta_f}{k}(\phi - \phi_0) - \Delta\rho g \left(1 - \left[\frac{\phi_0}{\phi}\right]^{n_\phi}\right) \tag{23.69}$$

and

$$\frac{\partial \phi}{\partial z} = -\left(\frac{3}{2}\right)^{n_\sigma+1} \frac{\phi^{m_\sigma}}{n_\sigma^{n_\sigma} v_\phi} A |p_o|^{n_\sigma-1} p_o. \tag{23.70}$$

Taking the small porosity limit for the Darcy velocity through the unperturbed matrix

$$v_0 = -\frac{\alpha_\phi \phi_0^{n_\phi-1}}{\eta_f} \Delta\rho g, \tag{23.71}$$

ϕ_0, $|\Delta\rho g|$, and δ as characteristic scales for velocity, porosity, pressure gradient, and length, respectively, the nondimensional wave velocity, porosity, overpressure, hydraulic potential, and depth are $v'_\phi = v_\phi / v_0$, $\phi' = \phi/\phi_0$, $p'_o = p_o/(\delta|\Delta\rho g|)$, $H' = H\phi_0^{m_\sigma-1}/|\Delta\rho g|$, and $z' = z/\delta$. Inverting these relations to express the dimensional variables in terms of the scales and nondimensional variables, the nondimensional forms of Eqs 23.69 and 23.70 are

$$\frac{\partial p'_o}{\partial z'} = [1 + v'_\phi(\phi' - 1)]/\phi'^{n_\phi} - 1 \tag{23.72}$$

and

$$\frac{\partial \phi'}{\partial z'} = \left(\frac{3}{2}\delta\right)^{n_\sigma+1} \frac{\alpha_\phi \phi_0^{n_\phi-m_\sigma}}{n_\sigma^{n_\sigma} |\Delta\rho g|^{n_\sigma-1}} A \frac{\phi'^{m_\sigma} |p'_o|^{n_\sigma-1} p'_o}{v'_\phi}. \tag{23.73}$$

Defining the compaction length scale as

$$\delta \equiv \sqrt[n_\sigma+1]{\frac{n_\sigma^{n_\sigma} \alpha_\phi \phi_0^{n_\phi-m_\sigma}}{A\eta_f |\Delta\rho g|^{n_\sigma-1}} \left(\frac{2}{3}\right)^{n_\sigma+1}}, \tag{23.74}$$

Eq 23.73 reduces to

$$\frac{\partial \phi'}{\partial z'} = \frac{\phi'^{m_\sigma} |p'_o|^{n_\sigma-1} p'_o}{v'_\phi}. \tag{23.75}$$

The dimensionless hydraulic potential is then

$$H' = \int \frac{1 - [1 + v'_\phi(\phi' - 1)]/\phi'^{n_\phi}}{\phi'^{m_\sigma}} d\phi'. \tag{23.76}$$

The hydraulic potential and solitary wave solution in Figure 23.2D–F are computed from Eqs 23.72, 23.75 and 23.76 with $m_\sigma = 0$, $n_\phi = 3$, and $v'_\phi = 7$.

References

Abelin H, Neretnieks I, Tunbrant S, Moreno L (1985) Migration in a single fracture: Experimental results and evaluation. Final report, Stripa Project, SKB, Stockholm.

Acocella V, Gudmundsson A, Funiciello R (2000) Interaction and linkage of extension fractures and normal faults: examples from the rift zone of Iceland. *Journal of Structural Geology,* **22**, 1233–1246.

Adamides NG (1990) Hydrothermal circulation and ore deposition in the Troodos ophiolite, Cyprus. In: *Ophiolites: Oceanic Crustal Analogues* (eds Malpas J, Moores EM, Panayiotou A, Xenophontos C), pp. 685–704, Geological Survey Department, Nicosia, Cyprus.

Adams AL, Germaine JT, Flemings PB, Day-Stirrat RJ (2013) Stress induced permeability anisotropy of resedimented Boston Blue Clay. *Water Resources Research,* **49**, doi:10.1002/wrcr .20470.

Adler PM (1997) Fracture deformation and influence on permeability. *Physical Review*, **56**, 3167–3184.

Ague JJ (2014) Fluid flow in the deep crust. In: *Treatise on Geochemistry*, 2nd edn (eds Holland HD, Turekian KK), pp. 203–247. Elsevier, Oxford.

Ahlbom K, Andersson J-E, Nordqvist R, Ljunggren C, Tiren S, Voss C (1991) Fjallveden study site – Scope of activities and main results. *Swedish Nuclear Fuel Waste Management Company (SKB) Technical Report*, **SKB-TR-91-52**.

Aki K, Richards PG (2002) *Quantitative Seismology*, 2nd edn University Science Books, Sausalito.

Akinfiev NN, Diamond LW (2009) A simple predictive model of quartz solubility in water-salt-C02 systems at temperatures up to 1000°C and pressures up to 1000 MPa. *Geochimica Cosmochimica Acta*, **76**, 1597–1608.

Allen DM, Grasby SE, Voormeij DA (2006) Determining the circulation depth of thermal springs in the southern Rocky Mountain Trench, south-eastern British Columbia, Canada using geothermometry and borehole temperature logs. *Hydrogeology Journal*, **14**, 159–172.

Allen SK, Cox SC, Owens IF (2011) Rock avalanches and other landslides in the central Southern Alps of New Zealand: a regional study considering possible climate change impacts. *Landslides*, **8**, 33–48.

Alley WM, Healy RW, LaBaugh JW, Reilly TE (2002) Flow and storage in groundwater systems. *Science,* **296**, 1985–1990.

Allis RG, Henley RW, Carman AF (1979) The thermal regime beneath the Southern Alps. In: *The Origin of the Southern Alps* (eds Walcott RI, Cresswell MM), *Bulletin of the Royal Society of New Zealand*, **18**, 79–85.

Allis RG, Shi Y (1995) New insights to temperature and pressure beneath the central Southern Alps, New Zealand. *New Zealand Journal of Geology and Geophysics*, **38**, 585–592.

Al-Tabbaa A, Wood DM (1987) Some measurements of the permeability of kaolin. *Geotechnique,* **37**, 499–514.

Alt-Epping P, Diamond LW, Häring MO (2013) Prediction of water-rock interaction and porosity evolution in a granitoid-hosted enhanced geothermal system, using constraints from the 5 km Basel-1 well. *Applied Geochemistry*, **38**, 121–133.

Alves MA, Oliveira PJ, Pinho FT (2003) A convergent and universally bounded interpolation scheme for the treatment of advection. *International Journal for Numerical Methods in Fluids,* **41**, 47–75.

Amann-Hildenbrand A, Bertier P, Busch A, Krooss BM (2013) Experimental investigation of the sealing capacity of generic clay-rich caprocks. *International Journal of Greenhouse Gas Control,* **19**, 620–641.

Ames LL, McGarrah JE, Walker BA (1983) Sorption of trace constituents from aqueous solutions onto secondary minerals, I, Uranium. *Clays and Clay Minerals,* **31**, 321–334.

Anderholm SK (2001) Mountain-front recharge along the east side of the Albuquerque Basin, Central New Mexico. *U.S. Geological Survey Water-Resources Investestigations Report*, **00–4010**.

Anderson A, Blackwell D, Chickering C, Boyd T, Home R, Mackenzie M, Moore J, Nickull D, Richard S, Shevenell L (2013) National Geothermal Data System (NGDS) geothermal data domain: assessment of geothermal community data needs. *Proceedings of the Stanford Geothermal Workshop, 2013, Stanford University, California, paper SGP-TR-198*, http://www.geothermal-energy.org/pdf/IGAstandard/SGW/2013/Anderson.pdf (accessed 04 May 2016).

Anderson EM (1951) *The Dynamics of Faulting*. Oliver & Boyd, Edinburgh.

Anderson MP (2005) Heat as a ground water tracer. *Ground Water*, **43**, 951–968.

Anderson RN, Zoback MD, Hickman SH, Newmark RL (1985) Permeability versus depth in the upper oceanic crust: in situ measurements in DSDP hole 504B, eastern equatorial Pacific. *Journal of Geophysical Research*, **90**, 3659–3669.

Anderson-Sprecher R (1994) Model comparisons and R^2. *The American Statistician,* **48**, 113–117.

Crustal Permeability, First Edition. Edited by Tom Gleeson and Steven E. Ingebritsen.

Companion Websites: www.wiley.com/go/gleeson/crustalpermeability/
http://crustalpermeability.weebly.com/

Ankit K, Nestler B, Selzer M, Reichardt M (2013) Phase-field study of grain boundary tracking behavior in crack-seal microstructures. *Contributions to Mineralogy and Petrology*, **166**, 1709–1723.

Anonymous (1988) Granulometrische analyse Asten 02. Technical report, Rijks Geologische Dienst, Haarlem.

Antonioli A, Piccininni D, Chiaraluce L, Cocco M (2005) Fluid flow and seismicity pattern: evidence from the 1997 Umbria-March (central Italy) seismic sequence. *Geophysical Research Letters,* **32**, doi:10.1029/2004GL022256.

Aplin AC, Fleet AJ, MacQuaker JHS (1999) Muds and mudstones: physical and fluid flow properties. *Geological Society of London Special Publication*, **158**, 1–8.

Appold MS, Garven G, Boles JR, Eichhubl P (2007) Numerical modeling of the origin of calcite mineralization in the Refugio-Carneros fault, Santa Barbara Basin, California. *Geofluids*, **7**, 79–95.

Appold MS, Nunn JA (2002) Numerical models of petroleum migration via buoyancy-driven porosity waves in viscously deformable sediments. *Geofluids*, **2**, 233–247.

Aquilina L, Genter A, Elsass P, Pribnow D (2000) Evolution of fluid circulation in the Rhine graben: constraints from the chemistry of present fluids. In: *Hydrogeology of Crystalline Rocks* (eds Stober I, Bucher K), pp. 177–203. Kluwer Academic Publishers, Dordrecht.

Araneda OA, Morales RF, Rojas EG, Henríquez JO, Molina RE (2007) Rock preconditioning application in virgin caving condition in a panel caving mine, CODELCO Chile El Teniente Division. In: *Proceedings International Symposium, Deep and High Stress Mining*, pp. 111–120. Australian Centre for Geomechanics, Perth, Australia.

Arch J, Maltman A (1990) Anisotropic permeability and tortuosity in deformed wet sediments. *Journal of Geophysical Research*, **95**, 9035–9045.

Arehart GB, Coolbaugh MF, Poulson SR (2003) Evidence for a magmatic source of heat for the Steamboat Springs geothermal system using trace elements and gas geochemistry. *Geothermal Resources Council Transactions,* **27**, 269–274.

Armand G (2000) Contribution à la caractérisation en laboratoire et à la modélisation constitutive du comportement mécanique des joints rocheux. PhD thesis, Université Joseph Fourier, Grenoble, France.

Armbruster T, Kohler T, Meisel T, Nagler TF (1996) The zeolite, fluorite, quartz assemblage of the fissure at Gibelsbach, Fiesch (Valais, Switzerland): crystal chemistry, REE patterns, and genetic speculations. *Schweizerische Mineralogische und Petrographische Mitteilungen*, **76**, 131–146.

Arzi AA (1978) Critical phenomena in rheology of partially melted rocks. *Tectonophysics*, **44**, 173–184.

Ashby MF (1988) The modeling of hot isostatic pressing. In: *Proceedings HIP: Hot Isostatic Pressing – Theories and Applications* (ed Garvare T), pp. 29–40, Centek, Lulea, Sweden.

Asmerom Y, Polyak V, Burns S (2010) Variable winter moisture in the southwestern United States linked to rapid glacial climate shifts. *Nature Geoscience*, **3**, 114–117.

ASTM International (2004) *Standard Test Methods for Measurement of Hydraulic Conductivity of Saturated Porous Materials Using a Flexible Wall Permeameter*, *D5084–03*. ASTM International, West Conshoshocken, PA.

ASTM International (2006) *Standard Test Method for One-dimensional Consolidation Properties of Saturated Cohesive Soils Using Controlled-Strain Loading*, *D4186–06*. ASTM International, West Conshoshocken, PA.

Audet DM, Fowler AC (1992) A mathematical model for compaction in sedimentary basins. *Geophysical Journal International*, **110**, 577–590.

Auer F, Berckhemer H, Oehlschlegel G (1981) Steady-state creep of fine-grain granite at partial melting. *Journal of Geophysics-Zeitschrift Tur Geophysik*, **49**, 89–92.

Aydin A, Schultz R (1990) Effect of mechanical interaction on the development of strike-slip faults with echelon patterns. *Journal of Structural Geology,* **12**, 123–129.

Bächler D (2003) Coupled thermal-hydraulic-chemical modelling at the Soultz-sous-Forêts HDR reservoir (France). PhD thesis, ETH Zurich, No. 15044.

Bäckblom G, Martin CD (1999) Recent experiments in hard rock to study the excavation response: implication of the performance of a nuclear waste geological repository. *Tunneling and Underground Space Technology*, **14**, 377–394.

Baertschi P, Silverman SR (1951) The determination of relative abundances of the oxygen isotopes in silicate rocks. *Geochimica et Cosmochimica Acta*, **1**, 317–328.

Baghbanan A, Jing L (2008) Stress effects on permeability in fractured rock masses with correlated fracture length and aperture. *International Journal of Rock Mechanics and Mining Sciences*, **45**, 1320–1334.

Baker ET, German CR (2004) On the global distribution of hydrothermal vent fields. In: *Mid-Ocean Ridges: Hydrothermal Interactions between the Lithosphere and Oceans* (eds German CR, Lin J, Parson LM), pp. 245–266. American Geophysical Union, Washington, DC.

Baker ET, Massoth GJ, Feely RA (1987) Cataclysmic hydrothermal venting on the Juan de Fuca Ridge. *Nature,* **329**, 149–151.

Balashov VN, Yardley BWD (1998) Modeling metamorphic fluid flow with reaction-compaction-permeability feedbacks. *American Journal of Science*, **298**, 441–470.

Baldridge WS, Keller GR, Haak V, Wendlandt E, Jiracek GR, Olsen KH (1995) The Rio Grande Rift. In: *Continental Rifts: Evolution, Structure, Tectonics* (ed Olsen KH), *Developments in Geotectonics,* **25**, 233–265, Elsevier, Amsterdam.

Bandis S, Lumsden AC, Barton NR (1983) Fundamentals of rock joint deformation. *International Journal of Rock Mechanics and Mining Sciences*, **20**, 249–268.

Bandstra JL, Buss HL, Campen RK, Liermann LJ, Noore J, Hausrath EM, Navarre-Sitchler AK, Jang J-H, Brantley SL, 2008, Compilation of mineral dissolution rates. In: *Kinetics of Water-Rock Interaction* (eds Brantley SL, Kubicki JD, White AF), pp. 737–824, Springer Verlag, New York.

Banerjee NR, Gillis KM (2001) Hydrothermal alteration in a modern suprasubduction zone: the Tonga forearc crust. *Journal of Geophysical Research*, **106**, 21737–21750.

Banerjee NR, Gillis KM, Muehlenbachs K (2000) Discovery of epidosites in a modern oceanic setting, the Tonga forearc. *Geology*, **28**, 151–154.

Bangs NL, Shipley TH, Moore JC, Moore GF (1999) Fluid accumulation and channeling along the northern Barbados Ridge decollement thrust. *Journal of Geophysical Research*, **104**, 20399–20414

Banwart SA, Chorover J, Gaillardet J, Sparks D, White T, Anderson S, Aufdenkampe A, Bernasconi S, Brantley SL, Chadwick O, Dietrich WE, Duffy C, Goldhaber M, Lehnert K, Nikolaidis NP, Ragnarsdottir KV (2013) *Sustaining Earth's Critical Zone Basic Science and Interdisciplinary Solutions for Global Challenges*. University of Sheffield, Sheffield.

Baragar WRA, Lambert MB, Baglow N, Gibson IL (1990) The sheeted dike zone in the Troodos ophiolite. In: *Ophiolites: Oceanic Crustal Analogues* (eds Malpas J, Moores EM, Panayiotou A, Xenophontos C), pp. 37–52. Geological Survey Department, Nicosia, Cyprus.

Barcilon V, Lovera OM (1989) Solitary waves in magma dynamics. *Journal of Fluid Mechanics*, **204**, 121–133.

Barcilon V, Richter FM (1986) Nonlinear-waves in compacting media. *Journal of Fluid Mechanics*, **164**, 429–448.

Bargar KE (1988) Secondary mineralogy of core from geothermal drill hole CTGH-1, Cascade Range, Oregon. In: Geology and geothermal resources of the Breitenbush-Austin Hot Springs area, Clackamas and Marion Counties (ed Sherrod DR), pp. 39–45. *State of Oregon Department of Geology and Mineral Industries Open-File Report*, **O-88-5**.

Bargar KE, Keith TEC (1999) Hydrothermal mineralogy of core from geothermal drill holes at Newberry volcano, Oregon. *U.S. Geological Survey Professional Paper*, **1578**.

Barnes I, Downes CJ, Hulston JR (1978) Warm springs, South Island, New Zealand, and their potential to yield laumontite. *American Journal of Science*, **278**, 1412–1427.

Barroll MW, Reiter M (1990) Analysis of the Socorro hydrogeothermal system: central New Mexico. *Journal of Geophysical Research*, **95**, 21949–21963.

Bart M, Shao JF, Lydzba D, Haji-Sotoudeh M (2004) Coupled hydromechanical modeling of rock fractures under normal stress. *Canadian Geotechnical Journal*, **41**, 686–697.

Barton N (1982) *Modelling Rock Joint behaviour from in situ Block Tests: Implication for Nuclear Waste Repository Design*. Office of Nuclear Waste Isolation, Columbus, Ohio, ONWI-308.

Barton N (2007) Thermal over-closure of joints and rock masses and implications for HLW repositories. *Proceedings of the 11th Congress of the International Society for Rock Mechanics*, Lisbon, Portugal, 9–13 June 2007.

Barton N, Bandis S, Bakhtar K (1985) Strength, deformation and conductivity coupling of rock joints. *International Journal of Rock Mechanics and Mining Sciences*, **22**, 121–140.

Barton N, Choubey V (1977) The shear strength of rock joints in theory and practice. *Rock Mechanics*, **10**, 1–54.

Bateman R, Ayer JA, Dubé B (2008) The Timmins-Porcupine gold camp, Ontario: anatomy of an Archean greenstone belt and ontogeny of gold mineralization. *Economic Geology*, **103**, 1285–1308.

Batjes NH (1996) Total carbon and nitrogen in the soils of the world. *European Journal of Soil Science*, **47**, 151–163.

Batzle M, Wang Z (1992) Seismic properties of pore fluids. *Geophysics*, **57**, 1396–1408.

Bauer F (1987) Die Kristallinen Gesteine aus der Bohrlochvertiefung Urach 3 und ihre fluiden Einschlüsse: eine Interpretation der hydrothermalen Überprägung anhand der Fluid-Daten aus EinschluBmessungen. Dissertation at Universitat (T.H.) Fridericiana Karlsruhe.

Bauer HH, Vaccaro JJ (1990) Estimates of ground-water recharge to the Columbia Plateau regional aquifer system, Washington, Oregon, and Idaho, for pre development and current land-use conditions. *U.S. Geological Survey Water-Resources Investigations Report*, **88–4108**, http://pubs.er.usgs.gov/usgspubs/wri/wri884108 (accessed 04 May 2016).

Bear J (1972) *Dynamics of Fluids in Porous Media*. American Elsevier, New York.

Bear J (1979) *Hydraulics of Groundwater*. McGraw-Hill, New York.

Bear LM (1963) *The Mineral Resources and Mining Industry of Cyprus*. Geological Survey Department, Nicosia, Cyprus.

Beavan RJ, Denys P, Denham M, Hager B, Herring T, Molnar P (2010a) Distribution of present-day vertical deformation across the Southern Alps, New Zealand, from 10 years of GPS data. *Geophysical Research Letters*, **37**, LI6305.

Beavan RJ, Ellis SM, Wallace LM, Denys P (2007) Kinematic constraints from GPS on oblique convergence of the Pacific and Australian Plates, central South Island, New Zealand. In: *A Continental Plate Boundary: Tectonics at South Island, New Zealand* (eds Okaya DA, Stern TA, Davey FJ), *American Geophysical Union Geophysical Monograph*, **175**, pp. 75–94, AGU.

Beavan RJ, Fielding E, Motagh M, Samsonov S, Donnelly N (2011) Fault location and slip distribution of the 22 February 2011 M_w6.2 Christchurch, New Zealand, earthquake from geodetic data. *Seismological Research Letters*, **82**, 789–799.

Beavan RJ, Samsonov S, Denys P, Sutherland R, Palmer NG, Denham M (2010b) Oblique slip on the Puysegur subduction interface in the 2009 July M_w7.8 Dusky Sound earthquake from GPS and InSAR observations: implications for the tectonics of southwestern New Zealand. *Geophysical Journal International*, **183**, 1265–1286.

Beavan RJ, Samsonov S, Motagh M, Wallace L, Ellis S, Palmer NG (2010c) The Darfield (Canterbury) earthquake: geodetic observations and preliminary source model. *Bulletin of the New Zealand Society for Earthquake Engineering*, **43**, 228–235.

Becker JA, Bickle MJ, Galy A, Holland TJB (2008) Himalayan metamorphic $C0_2$ fluxes: quantitative constraints from hydrothermal springs. *Earth and Planetary Science Letters*, **265**, 616–629.

Becker K (1990) A guide to formation testing using ODP drillstring packers. *Ocean Drilling Program Technical Note*, **14**, College Station, Texas.

Becker K, Davis EE (2004) In situ determinations of the permeability of the igneous oceanic crust. In: *Hydrogeology of the Oceanic Lithosphere* (eds Davis E, Elderfield H), pp. 189–224. Cambridge University Press, Cambridge, UK.

Beeler NM, Hickman SH (2004), Stress-induced, time-dependent fracture closure at hydrothermal conditions. *Journal of Geophysical Research*, **109**, B02211, doi:10.1029/2002JB001782.

Bekins BA, Dreiss SJ (1992) A simplified analysis of parameters controlling dewatering in accretionary prisms. *Earth and Planetary Science Letters*, **109**, 275–287.

Bekins B, Matmon D, Screaton EJ, Brown KM (2011) Reanalysis of in situ permeability measurements in the Barbados decollement. *Geofluids*, **11**, 57–70.

Bekins B, McCaffrey AM, Dreiss SJ (1994) Influence of kinetics on the smectite to illite transition in the Barbados accretionary prism. *Journal of Geophysical Research*, **99**, 18147–18158.

Bekins B, McCaffrey AM, Dreiss SJ (1995) Episodic and constant flow models for the origin of low-chloride waters in a modern accretionary complex. *Water Resources Research*, **31**, 3205–3215.

Bekins BA, Screaton EJ (2007) Pore pressure and fluid flow in the northern Barbados accretionary complex. In: *The Seismogenic Zone of Subduction Thrust Faults* (ed Dixon T), pp. 148–170, Columbia University Press, New York.

Belanger DW, Freeze GA, Lolcama JL, Pickens JF (1989) Interpretation of hydraulic testing in crystalline rock at the Leuggern borehole. In: Technical Report 87-19 (ed Nagra), SKB, Baden, Switzerland, http://www.nagra.ch/data/documents/database/dokumente/%24default/Default%20Folder/Publikationen/NTBs%201987-1988/d_ntb87-19.pdf (accessed 04 May 2016).

Belcher WR (2004) Death Valley regional ground-water flow system, Nevada and California—Hydrogeologic framework and transient ground-water flow model. *US Geological Survey Scientific Investigations Report*, **1171**, 408.

Bendall B, Hogarth R, Holl H, McMahon A, Larking A, Reid P (2014) Australian experience in EGS permeability enhancement – A review of 3 case studies. *Proceedings, Thirty-Ninth Workshop on Geothermal Reservoir Engineering, Stanford University, Stanford, California*.

Benjelloun ZH (1993) *Étude Experimentale et Modelisation du Comportement Hydromécanique des Joints Rocheux*. PhD thesis, Université Joseph Fourier, Grenoble, France.

Bennett RH, Fischer KM, Lavoie DL, Bryant WR, Rezak R (1989) Porometry and fabric of marine clay and carbonate sediments: determinants of permeability. *Marine Geology*, **89**, 127–152.

Bense V, Gleeson T, Loveless S, Bour O, Scibek J (2013) Fault zone hydrogeology. *Earth-Science Reviews*, **127**, 171–192.

Benson SM, Cole DR (2008) CO_2 sequestration in deep sedimentary formations. *Elements*, **4**, 325–331.

Berckhemer H, Rauen A, Winter H, Kern H (1997) Petrophysical properties of the 9-km-deep crustal section at KTB. *Journal of Geophysical Research*, **102**, 18337–18361.

Bercovici D, Ricard Y, Schubert G (2001) A two-phase model for compaction and damage, 1, General theory. *Journal of Geophysical Research*, **106**, 8887–8906.

Bergamaschi L, and Putti M (1999) Mixed finite elements and Newton-type linearizations for the solution of Richards' equation. *International Journal of Numerical Methods in Engineering*, **45**, 1026–1045.

Berkowitz B (2002) Characterizing flow and transport in fractured geological media: a review. *Advances in Water Resources*, **25**, 861–884.

Bernabe Y (1987) A wide range permeameter for use in rock physics. *International Journal of Rock Mechanics and Mining Sciences*, **24**, 309–315.

Berner EK, Berner RA (1996) *Global Environment: Water, Air, and Geochemical Cycles*. Prentice-Hall, Upper-Saddle River, NJ.

Berner RA (1978) Rate control of mineral dissolution under Earth surface conditions. *American Journal of Science*, **278**, 1235–1252.

Berner RA (2004) *The Phanerozoic Carbon Cycle: $C0_2$ and 0_2*. Oxford University Press, New York.

Berryman JG (2003) Dynamic permeability in poroelasticity. *Stanford Exploration Project*, **113**, 443–453.

Berryman KR, Cochran UA, Clark KJ, Biasi GP, Langridge RM, Villamor P (2012) Major earthquakes occur regularly on an isolated plate boundary fault. *Science*, **336**, 1690–1693.

Bertrand EA, Caldwell TG, Hill GJ, Wallin EL, Bennie SL, Cozens N, Onacha SA, Ryan GA, Walter C, Zaino A, Wameyo P (2012) Magnetotelluric imaging of upper-crustal convection plumes beneath the Taupo Volcanic Zone, New Zealand. *Geophysical Research Letters*, **39**, L02304.

Bettison-Varga L, Schiffman P, Janecky DR (1995) Fluid-rock interaction in the hydrothermal upflow zone of the Solea graben, Troodos ophiolite, Cyprus. *Geological Society of America Special Papers*, **296**, 81–111.

Bettison-Varga L, Varga RJ, Schiffman P. (1992) Relation between ore-forming hydrothermal systems and extensional deformation in the Solea graben spreading center, Troodos ophiolite, Cyprus. *Geology*, **20**, 987–990.

Bhatnagar PL, Gross EP, Krook M (1954) A model for collision processes in gases, I, Small amplitude processes in charged and neutral one-component systems. *Physical Review Letters*, **94**, 511–525.

Bickle MJ, Teagle DAH (1992) Strontium alteration in the Troodos ophiolite – Implications for fluid fluxes and geochemical transport in mid-ocean ridge hydrothermal systems. *Earth and Planetary Science Letters*, **113**, 219–237.

Bickle MJ, Teagle DAH, Beynon J, Chapman HJ (1998) The structure and controls on fluid-rock interactions in ocean ridge hydrothermal systems: constraints from the Troodos ophiolite. In: *Modern Ocean Floor Processes and the Geological Record*, **148** (eds Mills RA, Harrison K), pp. 127–152. Geological Society of London, London.

Biot MA (1941) General theory of three-dimensional consolidation. *Journal of Applied Physics*, **12**, 155–164.

Biot MA (1956a) Theory of propagation of elastic waves in a fluid-saturated porous solid, I, Low-frequency range. *Journal of the Acoustical Society of America*, **28**, 168–178.

Biot MA (1956b) Theory of propagation of elastic waves in a fluid-saturated porous solid, II, Higher frequency range. *Journal of the Acoustical Society of America*, **28**, 179–191.

Biot MA (1962) Generalized theory of acoustic propagation in porous dissipative media. *Journal of the Acoustical Society of America*, **34**, 1254–1264.

Birchwood RA, Turcotte DL (1994) A unified approach to geopressuring, low-permeability zone formation, and secondary porosity generation in sedimentary basins. *Journal of Geophysical Research*, **99**, 20051–20058.

Bittleston SH, Ferguson J, Frigaard IA (2002) Mud removal and cement placement during primary cementing of an oil well - Laminar non-Newtonian displacements in an eccentric annular Hele-Shaw cell. *Journal of Engineering Mathematics*, **43**, 229–253.

Bjørlykke K (1999) Principal aspects of compaction and fluid flow in mudstones. *Geological Society of London Special Publication*, **158**, 73–78.

Bjornsson G, Bodvarsson G (1990) A survey of geothermal reservoir properties. *Geothermics,* **19**, 17–27.

Blackwell DD (1983) Heat flow in the northern Basin and Range province. In *The Role of Heat in the Development of Energy and Mineral Resources in the Northern Basin and Range Province*, *Geothermal Resources Council Special Report*, **13**, 81–93.

Blackwell DD (1994) A summary of deep thermal data from the Cascade Range and analysis of the "rain curtain" effect. *Oregon Department of Geology and Mineral Industries Open-File Report*, **O-94-07**, 75–131.

Blanc G, Doussan C, Thomas C, Boulegue J (1991) Non-steady state diffusion and advection model of transient concentration-depth profiles from the Barbados accretionary complex. *Oceanologica Acta*, **16**, 363–372.

Blankennagel RK, Weir JE Jr (1973) Geohydrology of the eastern part of Pahute Mesa, Nevada Test Site, Nye County, Nevada. *US Geological Survey Professional Paper*, **712-B**.

Blümling P, Bernier F, Lebon P, Martin D (2007) The excavation damaged zone in clay formations time-dependent behaviour and influence on performance assessment. *Physics and Chemistry of the Earth*, **32**, 588–599.

Boano F, Harvey JW, Marion A, Packman AI, Revelli R, Ridolfi L, Wörman A (2014) Hyporheic flow and transport processes: mechanisms, models, and biogeochemical implications. *Reviews of Geophysics*, **52**, 603–679, doi:10.1002/2012RG000417.

Bodnar RJ, Azbej T, Becker SP, Cannatelli C, Fall A, Severs MJ (2013) Whole earth geohydrologic cycle, from the clouds to the core: the distribution of water in the dynamic Earth system. *The Geological Society of America Special Paper*, **500**, 431–461.

Bodnar RJ, Cannatelli C, De Vivo B, Lima A, Belkin HE, Milia A (2007) Quantitative model for magma degassing and ground deformation (bradyseism) at Campi Flegrei, Italy: implications for future eruptions. *Geology*, **35**, 791–794.

Bodnar RJ, Lecumberri-Sanchez P, Moncada D, Steele-Maclnnis M (2014) Fluid inclusions in hydrothermal ore deposits. In: *Treatise on Geochemistry*, 2nd edn (eds Holland HD, Turekian KK), pp. 119–142, Elsevier, Oxford.

Boese C, Jacobs K, Smith EGC, Stern TA, Townend J (2014) Background and delayed-triggered swarms in the central Southern Alps, South Island, New Zealand. *Geochemistry, Geophysics, Geosystems*, **15**, 945–964.

Boese CM, Stern TA, Townend J, Bourguignon S, Sheehan A, Smith EGC (2013) Sub-crustal earthquakes within the Australia-Pacific plate boundary zone beneath the Southern Alps, New Zealand. *Earth and Planetary Science Letters*, **376**, 212–219.

Boese C, Townend J, Smith EGC, Stern TA (2012) Microseismicity and stress in the vicinity of the Alpine Fault, central Southern Alps, New Zealand. *Journal of Geophysical Research*, **117**, B02302, doi:10.1029/2011JB008460.

Boles JR, Eichhubl P, Garven G, Chen J (2004) Evolution of a hydrocarbon migration pathway along basin-bounding faults: evidence from fault cement. *American Association of Petroleum Geologists Bulletin*, **88**, 947–970.

Boles JR, Grivetti M (2000) Calcite cementation along the Refugio/Carneros Fault, coastal California: a link between deformation, fluid movement and fluid-rock interaction at a basin margin. *Journal of Geochemical Exploration*, **69–70**, 313–316.

Bolton AJ, Maltman AJ, Clennell MB (1999) Nonlinear stress-dependence of permeability: a mechanism for episodic fluid flow in accretionary wedges. *Geology*, **27**, 239–242.

Borchardt R, Emmermann R (1993) Vein minerals in KTB rocks. *KTB Report,* **2**, 481–488.

Borchardt R, Zulauf G, Emmermann R, Hoefs J, Simon K (1990) Abfolge und Bildungsbedingungen von Sekundarmineralien in der KTB-Vorbohrung. *KTB Report*, **90-4**, 76–88.

Borthwick J, Harmon RS (1982) A note regarding CIF_3 as an alternative to BrF_5 for oxygen isotope analysis. *Geochimica et Cosmochimica Acta*, **46**, 1665–1668.

Boulon MJ (1995) A 3-D direct shear device for testing the mechanical behaviour and the hydraulic conductivity of rock joints. *Proceedings of the MJFR-2 Conference*, Vienna, Austria, Balkema, Rotterdam, 407–413.

Boulon MJ, Selvadurai APS, Benjelloun H, Feuga B (1993) Influence of rock joint degradation on hydraulic conductivity. *International Journal of Rock Mechanics and Mining Sciences,* **30**, 1311–1317.

Boulton C, Moore DE, Lockner DA, Toy VG, Townend J, Sutherland R (2014) Frictional properties of exhumed fault gouges in DFDP-1 cores, Alpine Fault, New Zealand. *Geophysical Research Letters*, **41**, 356–362.

Bourbie T, Zinszner B (1985) Hydraulic and acoustic properties as a function of porosity in Fontainebleau Sandstone. *Journal of Geophysical Research*, **90**, 11524–11532.

Bourlange S, Henry P (2007) Numerical model of fluid pressure solitary wave propagation along the decollement of an accretionary wedge: application to the Nankai wedge. *Geofluids,* **7**, 323–334.

Bourlange S, Henry P, Moore JC, Mikada H, Klaus A (2003) Fracture porosity in the décollement zone of Nankai accretionary wedge using logging while drilling resistivity data. *Earth and Planetary Science Letters*, **209**, 103–112.

Boutt DF, Saffer D, Doan M, Lin W, Ito T, Kano Y, Flemings P, McNeill LC, Byrne T, Hayman NW, Moe KT (2012) Scale dependence of in situ permeability measurements in the Nankai accretionary prism: the role of fractures. *Geophysical Research Letters*, **39**, L07302.

Bowman JR, Willlett SD, Cook SJ (1994) Oxygen isotopic transport and exchange during fluid flow: one-dimensional models and applications. *American Journal of Science*, **294**, 1–55.

Boyer F, Guazzelli E, Pouliquen O (2011) Unifying suspension and granular rheology. *Physical Review Letters*, **107**, 188301.

Brace WF (1980) Permeability of crystalline and argillaceous rocks. *International Journal of Rock Mechanics and Mining Sciences*, **17**, 241–251.

Brace WF (1984) Permeability of crystalline rocks: new in situ measurements. *Journal of Geophysical Research*, **89**, 4327–4330.

Brace WF, Walsh JB, Frangos WT (1968) Permeability of granite under high pressure. *Journal of Geophysical Research*, **73**, 2225–2236.

Bradley BA, Cubrinovski M (2011) Near-source strong ground motions observed in the 22 February 2011 Christchurch earthquake. *Seismological Research Letters*, **82**, 853–865.

Brandon MT, Vance JA (1992) Tectonic evolution of the Cenozoic Olympic subduction complex, Washington state, as deduced from fission track ages for detrital zircons. *American Journal of Science*, **292**, 565–636.

Brantley SL (2004) Reaction kinetics of primary rock-forming minerals under ambient conditions. In: *Surface and Ground Water, Weathering, and Soils* (eds Drever JI, Holland HD, Turekian KK), pp. 73–117, Treatise on Geochemistry, Elsevier, Amsterdam.

Brantley SL, Chen Y (1995) Chemical weathering rates of pyroxenes and amphiboles. *Mineralogical Society of America Reviews in Mineralogy and Geochemistry*, **31**, 119–172.

Brantley SL, Kubicki JD, White AF (2008) *Kinetics of Water-Rock Interaction*. Springer Verlag, New York.

Brantley SL, Megonigal JP, Scatena FN, Balogh-Brunstad Z, Barnes RT, Bruns MA, Van Cappellen P, Dontsova K, Hartnett HE, Hartshorn AS, Heimsath A, Herndon E, Jin L, Keller CK, Leake JR, Mcdowell WH, Meinzer FC, Mozdzer TJ, Petsch S, Pett-Ridge J, Pregitzer KS, Raymond PA, Riebe CS, Shumaker K, Sutton-Grier A, Walter R, Yoo K (2011) Twelve testable hypotheses on the geobiology of weathering. *Geobiology*, **9**, 140–165.

Brantley SL, Mellott N (2000) Surface area and porosity of primary silicate minerals. *American Mineralogist*, **85**, 1767–1783.

Bray CJ, Karig DE (1985) Porosity of sediments in accretionary prisms and some implications for dewatering processes. *Journal of Geophysical Research*, **90**, 768–778.

Bredehoeft JD (1967) Response of well-aquifer systems to Earth tides. *Journal of Geophysical Research*, **72**, 3075–3087.

Bredehoeft JD (1997) Fault permeability near Yucca Mountain. *Water Resources Research*, **33**, 2459–2463.

Bredehoeft JD, Papadopulos IS (1965) Rates of vertical ground water flow estimated from the Earth's thermal profile. *Water Resources Research*, **1**, 325–328.

Bredehoeft JD, Papadopulos SS (1980) A method for determining the hydraulic properties of tight formations. *Water Resources Research*, **16**, 223–238.

Brodsky EE, Karakostas V, Kanamori H (2000) A new observation of dynamically triggered regional seismicity: earthquakes in Greece following the August, 1999 Izmit, Turkey earthquake. *Geophysical Research Letters*, **27**, 27410–27414.

Brodsky EE, Roeloffs E, Woodcock D, Gall I, Manga M (2003) A mechanism for sustained groundwater pressure changes induced by distant earthquakes. *Journal of Geophysical Research*, **108**, doi:10.1029/2002JB002321.

Brown ET, Hoek E (1978) Trends in relationships between measured in-situ stresses and depth. *International Journal of Rock Mechanics and Mining Sciences*, **15**, 211–215.

Brown KL (1986) Gold deposition from geothermal discharges in New Zealand. *Economic Geology*, **81**, 979–983.

Brown KM (1995) The variation of the hydraulic conductivity structure of an overpressured thrust zone with effective stress. In: *Proceedings of the Ocean Drilling Program, Scientific Results*, **146** (eds Carson B, Westbrook GK, Musgrave RJ, Suess E), pp. 281–289, Texas A & M University, Ocean Drilling Program, College Station, TX.

Brown KM, Bekins BA, Clennell B, Dewhurst D, Westbrook GK (1994) Heterogeneous hydrofracture development and accretionary fault dynamics. *Geology*, **22**, 259–262.

Brown KM, Saffer DM, Bekins BA (2001) Smectite diagenesis, pore-water freshening, and fluid flow at the toe of the Nankai wedge. *Earth and Planetary Science Letters*, **194**, 97–109.

Brown KM, Tryon MD, DeShon HR, Dorman LM, Schwartz SY (2005) Correlated transient fluid pulsing and seismic tremor in the Costa Rica subduction zone. *Earth and Planetary Science Letters*, **238**, 189–203.

Brown M (2010) The spatial and temporal patterning of the deep crust and implications for the process of melt extraction. *Philosophical Transactions of the Royal Society of London, Series A, Mathematical, Physical and Engineering Sciences*, **368**, 11–51.

Brown SR (1987a) A note on the description of surface roughness using fractal dimension. *Geophysical Research Letters,* **14**, 1095–1098.

Brown SR (1987b) Fluid flow thorough rock joints: the effect of surface roughness. *Journal of Geophysical Research,* **92**, 1337–1347.

Brown SR (1989) Transport of fluid and electric current through a single fracture. *Journal of Geophysical Research*, **94**, 9429–9438.

Brown SR, Scholz CH (1985) Closure of random elastic surfaces in contact. *Journal of Geophysical Research*, **90**, 5531–5545.

Brown SR, Scholz CH (1986) Closure of rock joints. *Journal of Geophysical Research*, **91**, 4939–4948.

Brown SR, Stockman HW, Reeves SJ (1995) Applicability of Reynolds equation for modeling fluid flow between rough surfaces. *Geophysical Research Letters,* **22**, 2537–2540.

Browne PRL, Courtney SS, Wood CP (1989) Formation rates of calc-silicate minerals deposited inside drillhole casing, Ngatamariki geothermal field, New Zealand. *American Mineralogist*, **74**, 759–763.

Brückmann W, Moran K, MacKillop AK (1997) Permeability and consolidation characteristics from Hole 949B, northern Barbados Ridge. In: *Proceedings of the Ocean Drilling Program, Scientific Results*, **156** (eds Shipley TH, Ogawa Y, Blum P, Bahr JM), pp. 109–114, Ocean Drilling Program, College Station, TX.

Bruel D (2007) Using the migration of the induced seismicity as a constraint for fractured Hot Dry Rock reservoir modelling. *International Journal of Rock Mechanics and Mining Sciences*, **44**, 1106–1117.

Brunner P, Kinzelbach W (2005) Sustainable groundwater management. In: *Encyclopedia of Hydrological Sciences* (ed Anderson MG), Part 13. Wiley, New York.

Brush DJ, Thomson NR (2003) Fluid flow in synthetic rough-walled fractures: Navier-Stokes, Stokes, and local cubic law assumptions. *Water Resources Research,* **39**, doi:10.1029/2002WR001346.

Bryant WR (2002) Permeability of clays, silty-clays and clayey-silts. *Gulf Coast Association of Geological Societies Transactions*, **52**, 1069–1077.

Bryant WR, Hottman WE, Trabant PK (1974) Permeability of unconsolidated and consolidated marine sediments, Gulf of Mexico. *AAPG Bulletin*, **58**, 2207.

Bucher K, Stober I (2010) Fluids in the upper continental crust. *Geofluids,* **10**, 241–253.

Bucher K, Stober I, Seelig U (2012) Water deep inside the mountains: unique water samples from the Gotthard rail base tunnel, Switzerland. *Chemical Geology,* **334**, 240–253.

Bucher K, Zhang L, Stober I (2009) A hot spring in granite of the western Tianshan, China. *Applied Geochemistry*, **24**, 402–410.

Bucher-Nurminen K (1981) The formation of metasomatic reaction veins in dolomitic marble roof pendants in the Bergell intrusion (Province Sondrio, Northern Italy). *American Journal of Science*, **281**, 1197–1222.

Bucher-Nurminen K (1989) Reaction veins in marbles formed by a fracture-reaction-seal mechanism. *European Journal of Mineralogy*, **1**, 701–714.

Baumgartner LP, Valley JV (2001) Stable isotope transport and contact metamorphic fluid flow. In: *Stable Isotope Geochemistry* (eds Valley JW, Cole DR), *Reviews in Mineralology*, **43**, 415–467, University of Wisconsin, Madison, WI.

Baumgartner LP, Gerdes ML, Person MA, Roselle, GT (1997) Porosity and permeability of carbonate rocks during contact metamorphism. In: *Fluid Flow and Transport in Rocks: Mechanisms and Effects* (eds Jamveit B, Yardley BWD), Chapman & Hall, London, 83–98.

Bunger AP, Jeffrey RG, Kear JP, Zhang XP, Morgan M (2011) Experimental investigation of the interaction among closely spaced hydraulic fractures. In: 45th US Rock Mechanics/Geomechanics Symposium, June 26–29, 2011, San Francisco, California.

Burchfiel BC, Royden LH, van der Hilst RD, Hager BH (2008) A geological and geophysical context for the Wenchuan earthquake of 12 May 2008, Sichuan, People's Republic of China. *GSA Today*, **18**, 4–11.

Burgmann R, Pollard DD (1994) Strain accommodation about strike-slip fault discontinuities in granitic rock under brittle-to-ductile conditions. *Journal of Structural Geology*, **16**, 1655–1674.

Burns ER, Morgan DS, Lee KK, Haynes JV, Conlon TD (2012a) Evaluation of long-term water-level declines in basalt aquifers near Mosier, Oregon. *U.S. Geological Survey Scientific Investigations Report*, **2012–5002**, http://pubs.er.usgs.gov/publication/sir20125002 (accessed 04 May 2016).

Burns ER, Morgan DS, Peavler RS, Kahle SC (2011) Three-dimensional model of the geologic framework for the Columbia Plateau Regional Aquifer System, Idaho, Oregon, and Washington. *U.S. Geological Survey Scientific Investigations Report*, **2010–5246**, http://pubs.er.usgs.gov/publication/sir20105246 (accessed 04 May 2016).

Burns ER, Snyder DT, Haynes JV, Waibel MS (2012b) Groundwater status and trends for the Columbia Plateau Regional Aquifer System, Washington, Oregon, and Idaho. *U.S. Geological Survey Scientific Investigations Report*, **2012–5261**, http://pubs.er.usgs.gov/publication/sir20125261 (accessed 04 May 2016).

Burns E, Williams CF, Ingebritsen SE, Voss CI, Spane FA, DeAngelo J (2015) Understanding heat and groundwater flow through continental flood basalt provinces: insights gained from alternative models of permeability/depth relationships for the Columbia Plateau, USA. *Geofluids,* **15**, 120–138.

Butler GA, Cauffman TL, Lolcama JL, Longsine DE, McNeish JA (1989) Interpretation of hydraulic testing at the Weiach borehole. In: *SKB Technical Report*, **87-20** (ed SKB), Nagra, Baden, Switzerland, http://www.nagra.ch/data/documents/database/dokumente/$default/Default%20Folder/Publikationen/NTBs%201987-1988/e_ntb87-20.pdf (accessed 04 May 2016).

Butler JJ Jr (1998) *The Design, Performance, and Analysis of Slug Tests*. Lewis Publishers, New York.

Byerlee J (1978) Friction of rocks. *Pure and Applied Geophysics*, **116**, 615–626.

Caine JS, Evans JP, Forster CB (1996) Fault zone architecture and permeability structure. *Geology*, **24**, 1025–1028.

Candela T, Renard F, Klinger Y, Mair K, Schmittbuhl J, Brodsky EE (2012) Roughness of fault surfaces over nine decades of length scales. *Journal of Geophysical Research,* **117**, B08409, doi:10.1029/2011JB009041.

Canfield DE, Kump LR (2013) Carbon cycle makeover. *Science*, **339**, 533–534.

Cann JR, Gillis KM (2004) Hydrothermal insights from the Troodos ophiolite, Cyprus. In: *Hydrogeology of the Oceanic Lithosphere* (eds Davis E, Elderfield H), pp. 274–310. Cambridge University Press, Cambridge.

Cann JR, McCaig AM, Yardley BWD (2015) Rapid generation of reaction permeability in the roots of black smoker systems, Troodos ophiolite, Cyprus. *Geofluids,* **15**, 179–192.

Cann JR, Strens MR (1989) Modeling periodic megaplume emission by black smoker systems. *Journal of Geophysical Research*, **94**, 12227–12237.

Cappa F (2006) Role of fluids in the hydromechanical behavior of heterogeneous fractured rocks: *in situ* characterization and numerical modelling. *Bulletin of Engineering Geology and the Environment*, **65**, 321–337.

Cappa F, Guglielmi Y, Gaffet S, Lancon H, Lamarque I (2006a) Use of in situ fiber optic sensors to characterize highly heterogeneous elastic displacement fields in fractured rocks. *International Journal of Rock Mechanics and Mining Sciences*, **43**, 647–654.

Cappa F, Guglielmi Y, Rutqvist J, Tsang C-F, Thoraval A (2006b) Hydromechanical modeling of pulse tests that measure both fluid pressure and fracture-normal displacement at the Coaraze Laboratory site, France. *International Journal of Rock Mechanics and Mining Sciences*, **43**, 1062–1082.

Cappa F, Rutqvist J (2011) Modeling of coupled deformation and permeability evolution during fault reactivation induced by deep underground injection of CO_2. *International Journal of Greenhouse Gas Control*, **5**, 336–346.

Cappa F, Rutqvist J, Yamamoto K (2009) Modeling crustal deformation and rupture processes related to upwelling of deep $C0_2$-rich fluids during the 1965–1967 Matsushiro earthquake swarm in Japan. *Journal of Geophysical Research,* **114**, 1–20.

Cardwell WJ, Parsons R (1945) Average permeabilities of heterogeneous oil sands. *American Institute of Mining and Metallurgical Engineers Technical Publication,* **1852**, 1–9.

Carman PC (1937) Fluid flow through granular beds. *Transactions Institution of Chemical Engineers,* **15**, 150–166.

Carman PC (1939) Permeability of saturated sands, soils and clays. *Journal of Agricultural Science*, **29**, 262–273.

Carman PC (1956) *Flow of Gases Through Porous Media*. Academic Press, New York.

Carrigan CR, King GCP, Barr GE, Bixler NE (1991) Potential for water-table excursions induced by seismic events at Yucca Mountain, Nevada. *Geology*, **19**, 1157–1160.

Carslaw HS, Jaeger JC (1959) *Conduction of Heat in Solids*, 2nd edn Oxford University Press, London.

Carson B, Screaton EJ (1998) Fluid flow in accretionary prisms: evidence for focused, time-variable discharge. *Reviews of Geophysics*, **36**, 329–351.

Carson B, Seke E, Paskevich V, Holmes ML (1994) Fluid expulsion sites on the Cascadia accretionary prism: mapping diagenetic deposits with processed GLORIA imagery. *Journal of Geophysical Research*, **99**, 11959–11969.

Cassar C, Nicolas M, Pouliquen O (2005) Submarine granular flows down inclined planes. *Physics of Fluids*, **17**, 103301.

Catalli F, Meier M-A, Wiemer S (2013) The role of Coulomb stress changes for injection-induced seismicity: the Basel enhanced geothermal system. *Geophysical Research Letters*, **40**, doi:10.1029/2012GL054147.

Cathles LM (1977) An analysis of the cooling of intrusives by ground-water convection which includes boiling. *Economic Geology*, **72**, 804–826.

Cathles LM (1993) A capless 350°C flow zone model to explain megaplumes, salinity variations, and high-temperature veins in ridge axis hydrothermal systems. *Economic Geology*, **88**, 1977–1988.

Cathles LM, Adams JJ (2005) Fluid flow and petroleum and mineral resources in the upper (<20 km) continental crust. *Economic Geology 100th Anniversary Volume*, 77–110.

Cathles LM, Erendi HJ, Barrie T (1997) How long can a hydrothermal system be sustained by a single intrusive event? *Economic Geology*, **92**, 766–771.

Cattaneo CR (1958) Sur une forme de l'equation de la chaleur eliminant le paradoxe d'une propagation instantanee. *Comptes Rendus*, **247**, 431–433.

Cattin R, Chamot-Rooke N, Pubellier M, Rabaute A, Delescluse M, Vigny C, Fleitout L, Dubernet P (2009) Stress change and effective friction coefficient along the Sumatra-Andaman-Sagaing fault system after the 26 December 2004 (M_w = 9.2) and the 28 March 2005 (M_w = 8.7) earthquakes. *Geochemistry, Geophysics, Geosystems*, **10**, Q03011.

Cederbom CE, van der Beek P, Schlunegger F, Sinclair HD, Oncken O (2011) Rapid extensive erosion of the North Alpine foreland basin at 5-4 Ma. *Basin Research*, **23**, 528–550.

Chabora E, Zemach E, Spielman P, Drakos P, Hickman S, Lutz S, Boyle K, Falconer A, Robertson-Tait A, Davatzes NC, Rose P, Majer E, Jarpe S (2012) Hydraulic stimulation of well 27-15, Desert Peak Geothermal Field, Nevada USA. *Proceedings Thirty-Seventh Workshop on Geothermal Reservoir Engineering*, Stanford University.

Chan L-H, Kastner M (2000) Lithium isotopic compositions of pore fluids and sediments in the Costa Rica subduction zone: implications for fluid processes and sediment contribution to the arc volcanoes. *Earth and Planetary Science Letters*, **183**, 275–290.

Chan T, Christiansson R, Boulton GS, Ericsson LO, Hartikainen J, Jensen MR, Mas Ivars D, Stanchcell FW, Vistrand P, Wallroth T (2005) DECOVALEX III BMT 3/BENCHPAR WP4: the thermo-hydro-mechanical responses to a glacial cycle and their potential implications for deep geological disposal of nuclear fuel waste in a fractured crystalline rock mass. *International Journal of Rock Mechanics and Mining Sciences,* **42**, 805–827.

Chapuis RP (2012) Predicting the saturated hydraulic conductivity of soils: a review. *Bulletin of Engineering Geology and the Environment*, **71**, 401–434.

Chapuis RP, Aubertin M (2003) On the use of the Kozeny Carman equation to predict the hydraulic conductivity of soils. *Canadian Geotechnical Journal,* **628**, 616–628.

Chauveau B, Kaminski E (2008) Porous compaction in transient creep regime and implications for melt, petroleum, and CO_2 circulation. *Journal of Geophysical Research*, **113**, B09406.

Chebotarev II (1955) Metamorphism of natural waters in the crust of weathering, 1. *Geochimica et Cosmochimica Acta*, **8**, 22–48.

Chen X, Shearer PM, Abercrombie RE (2012) Spatial migration of earthquakes within seismic clusters in Southern California: evidence for fluid diffusion. *Journal of Geophysical Research*, **117**, B04301, doi:10.1029/2011JB008973.

Chen Y, Brantley SL (1998) Diopside and anthophyllite dissolution at 25 degrees and 90 degrees C and acid pH. *Chemical Geology*, **147**, 233–248.

Chen Z, Narayan SP, Yang Z, Rahman SS (2000) An experimental investigation of hydraulic behavior of fractures and joints in granitic rock, *International Journal of Rock Mechanics and Mining Sciences,* **37**, 1061–1071.

Chester FM, Evans JP, Biegel RL (1993) Internal structure and weakening mechanisms of the San Andreas fault. *Journal of Geophysical Research*, **98**, 771–786.

Chia Y, Chiu JJ, Chiang Y-H, Lee T-P, Liu C-W (2008) Spatial and temporal changes of groundwater level induced by thrust faulting. *Pure and Applied Geophysics*, **165**, 5–16.

Chia Y, Wang Y-S, Chiu JJ, Liu C-W (2001) Changes of groundwater level due to the 1999 Chi-Chi earthquake in the Choshui River alluvial fan in Taiwan. *Bulletin of the Seismological Society of America*, **91**, 1062–1068.

Chiodini G, Frondini F, Marini L (1995) Theoretical geothermometers and P_{CO2} indicators for aqueous solutions coming from hydrothermal systems of medium-low temperature hosted in carbonate-evaporite rocks. Application to the thermal springs of the Etruscan Swell, Italy. *Applied Geochemistry*, **10**, 337–346.

Christian GD, Dasgupta P, Schug K. (2014) *Analytical Chemistry*. John Wiley and Sons, Inc., Hoboken, NJ.

Claesson L, Skelton A, Graham C, Morth CM (2007) The timescale and mechanisms of fault sealing and water-rock interaction after an earthquake. *Geofluids*, **7**, 427–440.

Clauser C (1992) Permeability of crystalline rocks. *Eos Transactions American Geophysical Union*, **73**, 233, 237–238.

Clavier C, Coates G, Dumanoir J (1984) Theoretical and experimental bases for the dual-water model for interpretation of shaly sands. *SPE Journal*, **24**, 153–168.

Clift P, Vannucchi P (2004) Controls on tectonic accretion versus erosion in subduction zones: implications for the origin and recycling of the continental crust. *Reviews of Geophysics*, **42**, RG2001.

Cline JS, Bodnar RJ (1991) Can economic porphyry copper mineralization be generated by a typical calc-alkaline melt? *Journal of Geophysical Research*, **96**, 8113–8126.

Cloke PL, Kesler SE (1979) Halite trend in hydrothermal solutions. *Economic Geology*, **74**, 1823–1831.

Cloos M (1984) Landward-dipping reflectors in accretionary wedges: active dewatering conduits? *Geology*, **12**, 519–522.

Clowes RM, Brandon MT, Green AG, Yorath CJ, Brown AS, Kanasewich ER, Spencer C (1987) LITHOPROBE - southern Vancouver Island: Cenozoic subduction complex imaged by deep seismic reflections. *Canadian Journal of Earth Sciences*, **24**, 31–51.

Coggon RM, Teagle DAH, Smith-Duque CE, Alt JC, Cooper MJ (2010) Reconstructing past seawater Mg/Ca and Sr/Ca from mid-ocean ridge flank carbonates. *Science*, **327**, 1114–1117.

Committee on Fracture Characterization and Fluid Flow (1996) *Rock Fractures and Fluid Flow*. National Academy Press, Washington, DC.

Conin M, Bourlange S, Henry P, Boiselet A, Gaillot P (2013) Distribution of resistive and conductive structures in Nankai accretionary wedge reveals contrasting stress paths. *Tectonophysics*, **611**, 181–191.

Connell J (2000) Generation and destruction of porosity during the hydrothermal alteration of the sheeted dike complex in the Troodos ophiolite, Cyprus. MSc (Geochemistry) thesis, University of Leeds.

Connolly JAD (1997) Devolatilization-generated fluid pressure and deformation-propagated fluid flow during prograde regional metamorphism. *Journal of Geophysical Research*, **102**, 18149–18173.

Connolly JAD (2010) The mechanics of metamorphic fluid expulsion. *Elements*, **6**, 165–172.

Connolly JAD, Podladchikov YY (1998) Compaction-driven fluid flow in viscoelastic rock. *Geodinamica Acta*, **11**, 55–84.

Connolly JAD, Podladchikov YY (2000) Temperature-dependent viscoelastic compaction and compartmentalization in sedimentary basins. *Tectonophysics*, **324**, 137–168.

Connolly JAD, Podladchikov YY (2004) Fluid flow in compressive tectonic settings: implications for mid-crustal seismic reflectors and downward fluid migration. *Journal of Geophysical Research*, **109**, B04201.

Connolly JAD, Podladchikov YY (2007) Decompaction weakening and channeling instability in ductile porous media: implications for asthenospheric melt segregation. *Journal of Geophysical Research*, **112**, B10205, doi:10.1029/2005JB004213.

Connolly JAD, Podladchikov YY (2013) A hydromechanical model for lower crustal fluid flow. In: *Metasomatism and the Chemical Transformation of Rock* (eds Harlov DE, Austrheim H), pp. 599–658. Springer, Berlin.

Connolly JAD, Podladchikov YY (2015) An analytical solution for solitary porosity waves: implications for dynamic permeability and fluidization of nonlinear viscous and viscoplastic rock. *Geofluids*, **15**, 269–292.

Connolly P, Cosgrove J (1999) Prediction of static and dynamic fluid pathways within and around dilational jogs. *Geological Society of London Special Publications*, **155**, 105–121.

Constantinou G, Govett GJS (1972) Genesis of sulphide deposits, ochre and umber of Cyprus. *Transactions of the Institution of Mining and Metallurgy*, **81**, B34–B46.

Constantinou G, Govett GJS (1973) Metallogensis associated with the Troodos ophiolite. *Economic Geology*, **68**, 843–858.

Coogan LA (2008) Reconciling temperatures of metamorphism, fluid fluxes and heat transport in the upper crust at intermediate to fast-spreading mid-ocean ridges. *Geochemistry, Geophysics, Geosystems*, **9**, doi:10.1029/2007/GC001787.

Coogan LA (2009) Altered oceanic crust as an inorganic record of palaeoseawater Sr concentration. *Geochemistry, Geophysics, Geosystems*, **10**, doi:10.1029/2008/GC002341.

Cook HE, Corboy J (2004) Great Basin Paleozoic carbonate platform – Facies, facies transitions, depositional models, platform architecture, sequence stratigraphy, and predictive mineral hosts models. *US Geological Survey Open-File Report*, **2004-1078**.

Cook NGW (1992) Natural joints in rock: mechanical, hydraulic and seismic behaviour and properties under normal stress. *International Journal of Rock Mechanics and Mining Sciences*, **29**, 198–223.

Coolbaugh MF, Arehart GB, Faulds JE, Garside LJ (2005) Geothermal systems in the Great Basin, western United States: modern analogues to the roles of magmatism, structure, and regional tectonics in the formation of gold deposits. In: *Geological Society of Nevada Symposium 2005: Window to the World* (eds Rhoden HN, Steininger RC, Vikre PG), pp. 1063–1082. Nevada Geological Society, Reno, NV.

Cooper HH, Bredehoeft JD, Papadopulos IS, Bennett RR (1965) The response of well-aquifer systems to seismic waves. *Journal of Geophysical Research*, **70**, 3915–3926.

Cooper HH, Jacob CE (1946) A generalized graphical method for evaluating formation constants and summarizing well-field history. *Transactions American Geophysical Union*, **27**, 526–534.

Coumou D, Driesner T, Geiger S, Paluszny A, Heinrich CA (2009a) High-resolution three-dimensional simulations of mid-ocean ridge hydrothermal systems. *Journal of Geophysical Research*, **114**, B07104.

Coumou D, Driesner T, Heinrich CA (2008) The structure and dynamics of mid-ocean ridge hydrothermal systems. *Science*, **321**, 1825–1828.

Coumou D, Driesner T, Weis P, Heinrich CA (2009b) Phase separation, brine formation, and salinity variation at Black Smoker hydrothermal systems. *Journal of Geophysical Research*, **114**, B03212.

Cousins WJ, McVerry GH (2010) Overview of strong-motion data from the Darfield earthquake. *Bulletin of the New Zealand Society for Earthquake Engineering*, **43**, 222–227.

Cowie PA, Scholz CH (1992) Displacement-length scaling relationship for faults: data synthesis and discussion, *Journal of Structural Geology*, **14**, 1149–1156.

Cox SC, Barrell DJA (2007) Geology of the Aoraki area: scale 1:250,000. *Institute of Geological & Nuclear Sciences 1:250,000 Geological Map*, **15**.

Cox SC, Craw D, Chamberlain CP (1997) Structure and fluid migration in a late Cenozoic duplex system forming the main divide in the central Southern Alps, New Zealand. *New Zealand Journal of Geology and Geophysics*, **40**, 359–373.

Cox SC, Menzies C, Sutherland R, Denys P, Chamberlain C, Teagle D (2015) Changes in hot spring temperature and hydrogeology of the Alpine Fault hanging wall, New Zealand, induced by South Island earthquakes. *Geofluids*, **15**, 216–239.

Cox SC, Rutter HK, Sims A, Manga M, Wier JJ, Ezzy T, White PA, Horton TW, Scott D (2012a) Hydrological effects of the M_w7.1 Darfield (Canterbury) earthquake, 4 September 2010,

New Zealand. *New Zealand Journal of Geology and Geophysics*, **55**, 231–247.

Cox SC, Song SH, White PA, Davidson P, Strong DT (2010) The Canterbury and other earthquakes: far field effects on groundwater. In: Water: The Blue Gold. *Proceedings of the New Zealand Hydrological Society Conference 2010,* 7–10 December, University of Otago, Dunedin, 175–176.

Cox SC, Stirling MW, Herman F, Gerstenberger M, Ristau J (2012b) Potentially active faults in the rapidly eroding landscape adjacent to the Alpine Fault, central Southern Alps, New Zealand. *Tectonics*, **31**, TC2011.

Cox SC, Sutherland R (2007) Regional geological framework of South Island, New Zealand, and its significance for understanding the active plate boundary. In: *A Continental Plate Boundary: Tectonics at South Island, New Zealand* (eds Okaya DA, Stern TA, Davey FJ). *American Geophysical Union Geophysical Monograph*, **175**, 19–46, AGU.

Cox SF (2005) Coupling between deformation, fluid pressures, and fluid flow in ore-producing hydrothermal systems at depth in the crust. *Economic Geology,* **100**th Anniversary Volume, 39–75.

Cox SF (2010) The application of failure mode diagrams for exploring the roles of fluid pressure and stress states in controlling styles of fracture-controlled permeability enhancement in faults and shear zones. *Geofluids*, **10**, 217–233.

Cox SF, Knackstedt MA, Braun J (2001) Principles of structural control on permeability and fluid flow in hydrothermal systems. *Reviews in Economic Geology*, **14**, 1–24.

Craig H, Lupton JE (1981) Helium and mantle volatiles in the ocean and the oceanic crust. In: *The Sea*, Vol. 7 (ed Emiliani E), pp. 391–428, Wiley Interscience, New York.

Craig RF (2004) *Craig's Soil Mechanics*, 7th edn Spon, London.

Crane K (1987) Structural evolution of the East Pacific Rise axis from 13°10′N to 10°35′N: interpretations from SeaMARC I data. *Tectonophysics*, **136**, 65–92.

Crawford BR, Faulkner DR, Rutter EH (2008) Strength, porosity, and permeability development during hydrostatic and shear loading of synthetic quartz-clay fault gouge. *Journal of Geophysical Research*, **113**, B03207, doi:10.1029/2006JB004634.

Curewitz D, Karson J (1994) Structural settings of hydrothermal outflow: fracture permeability maintained by fault propagation and interaction. *Journal of Volcanology and Geothermal Research*, **79**, 149–168.

Curtis CD, Lipshie SR, Oertel G, Pearson MJ (1980) Clay orientation in some Upper Carboniferous mudrocks, its relationship to quartz content and some inferences about fissility, porosity and compactional history. *Sedimentology*, **27**, 333–339.

Cutillo PA, Screaton EJ, Ge S (2003) Three-dimensional numerical simulation of fluid flow and heat transport within the Barbados Ridge accretionary complex. *Journal of Geophysical Research*, **108**, doi:10.1029/2002JB002240.

Daigle H, Dugan B (2011) Permeability anisotropy and fabric development: a mechanistic explanation. *Water Resources Research*, **47**, W12517, doi:10.1029/2011WR011110.

Daigle H, Dugan B (2014) Data report: permeability, consolidation, stress state, and pore system characteristics of sediments from Sites C0011, C0012, and C0018 of the Nankai Trough. In: *Proceedings of the Integrated Ocean Drilling Program*, **333**, (eds Henry P, Kanamatsu T, Moe K, and the Expedition 333 Scientists), 1–23.

Daigle H, Screaton E (2015a) Evolution of sediment permeability during burial and subduction. *Geofluids,* **15**, 84–105.

Daigle H, Screaton EJ (2015b) Predicting the permeability of sediments entering subduction zones. *Geophysical Research Letters*, **42**, 5219–5226.

Daigle H, Thomas B, Rowe H, Nieto M (2014) Nuclear magnetic resonance characterization of shallow marine sediments from the Nankai Trough, Integrated Ocean Drilling Program Expedition 333. *Journal of Geophysical Research*, **119**, 2631–2650.

Danielopol DL, Griebler C, Gunatilaka A, Notenboom J (2003) Present state and future prospects for groundwater ecosystems. *Environmental Conservation,* **30**, 104–130.

Davis D, Suppe J, Dahlen FA (1983) Mechanics of fold-and-thrust belts and accretionary wedges. *Journal of Geophysical Research*, **88**, 1153–1172.

Davis EE, Becker K, Wang K, Carson B (1995) Long-term observations of pressure and temperature in Hole 892B, Cascadia accretionary prism. In: *Proceedings of the Ocean Drilling Program, Scientific Results*, **146**, (eds Carson B, Westbrook GK, Musgrave RJ, Suess E), 299–311, ODP.

Davis EE, Heesemann M, Wang K (2011) Evidence for episodic aseismic slip across the subduction seismogenic zone off Costa Rica: CORK borehole pressure observations at the subduction prism toe. *Earth and Planetary Science Letters*, **306**, 299–305.

Day GA (1987) Source of recharge to the Beowawe geothermal system, Nevada. MS thesis, University of Nevada-Reno.

Day-Stirrat RJ, Aplin AC, Srodoh J, van der Pluijm BA (2008) Diagenetic reorientation of phyllosilicate minerals in Paleogene mudstones of the Podhale Basin, southern Poland. *Clays and Clay Minerals*, **56**, 100–111.

Day-Stirrat RJ, Dutton SP, Milliken KL, Loucks RG, Aplin AC, Hillier S, van der Pluijm BA (2010) Fabric anisotropy induced by primary depositional variations in the silt:clay ratio in two fined-grained slope fan complexes: Texas Gulf Coast and northern North Sea. *Sedimentary Geology*, **226**, 42–53.

De Borst, R (1987) Integration of plasticity equations for singular yield functions. *Computers & Structures*, **26**, 823–829.

de Dreuzy JR, de Boiry P, Pichot G, Davy P (2010) Use of power averaging for quantifying the influence of structure organization on permeability upscaling in on-lattice networks under mean parallel flow. *Water Resources Research*, **46**, doi:10.1029/2009WR008769.

Deichmann N, Ernst J (2009) Earthquake focal mechanisms of the induced seismicity in 2006 and 2007 below Basel (Switzerland). *Swiss Journal of Geosciences*, **102**, 457–466.

Deichmann N, Giardini D (2009) Earthquakes induced by the stimulation of an Enhanced Geothermal System below Basel (Switzerland). *Seismological Research Letters*, **80**, 784–798.

Delepine N, Cuenot N, Rothert E, Parotidis M, Rentsch S, Shapiro SA (2004) Characterization of fluid transport properties of the Hot Dry Rock reservoir Soultz-2000 using induced microseismicity. *Journal of Geophysics and Engineering*, **1**, 77–83.

DeMets C, Gordon RG, Argus DF (2010) Geologically current plate motions. *Geophysical Journal International*, **181**, 1–80.

Deming D (1993) Regional permeability estimates from investigations of coupled heat and groundwater flow, North Slope Alaska. *Journal of Geophysical Research,* **98**, 16271–16286.

Deming D, Craganu C, Lee Y (2002) Self-sealing in sedimentary basins. *Journal of Geophysical Research*, **107**, doi:10.1029/2001JB000504.

Dempsey D, Kelkar S, Lewis K, Hickman S, Davatzes N, Moos D, Zemach E (2013) Modeling shear stimulation of the EGS well Desert Peak 27-15 using a coupled thermal-hydrological-mechanical simulator. *47th US Rock Mechanics/Geomechanics Symposium*, American Rock Mechanics Association.

Derode B, Cappa F, Guglielmi Y, Rutqvist J (2013) Coupled seismo-hydromechanical monitoring of inelastic effects on injection-induced fracture permeability. *International Journal of Rock Mechanics and Mining Sciences,* **61**, 266–274.

Detournay E, Cheng AH-D (1993) Fundamentals of poroelasticity. In: *Comprehensive Rock Engineering: Principles, Practice and Projects, Vol. II, Analysis and Design Method* (ed Fairhurst C), pp. 113–171. Pergamon Press, Oxford.

Detrick RS, Buhl P, Mutter J, Orcutt J, Madsen J, Brocher T (1987) Multi-channel seismic imaging of a crustal magma chamber along the East Pacific Rise. *Nature*, **326**, 35–41.

Detwiler RL (2008) Experimental observations of deformation caused by mineral dissolution in variable-aperture fractures. *Journal of Geophysical Research*, **113**, B08202.

Detwiler RL, Pringle SE, Glass RJ (1999) Measurement of fracture aperture fields using transmitted light: an evaluation of measurement errors and their influence on simulations of flow and transport through a single fracture. *Water Resources Research*, **35**, 2605–2617.

Dewhurst DN, Aplin AC, Sarda JP (1999a) Influence of clay fraction on pore-scale properties and hydraulic conductivity of experimentally compacted mudstones. *Journal of Geophysical Research*, **104**, 29261–29274.

Dewhurst DN, Aplin AC, Sarda JP, Yang Y (1998) Compaction-driven evolution of porosity and permeability in natural mudstones: an experimental study. *Journal of Geophysical Research*, **103**, 651–661.

Dewhurst DN, Brown KM, Clennell MB, Westbrook GK (1996) A comparison of the fabric and permeability anisotropy of consolidated and sheared silty clay. *Engineering Geology*, **42**, 253–267.

Dewhurst DN, Yang Y, Aplin AC (1999b) Permeability and fluid flow in natural mudstones. *Geological Society of London Special Publication*, **158**, 23–43.

Dieterich JH (1992) Earthquake nucleation on faults with rate-and state-dependent friction. *Tectonophysics*, **211**, 115–134.

Dietrich HG (1982) Geological results of the Urach 3 Borehole and the correlation with other boreholes. In: *The Urach Geothermal Project* (ed Haenel R), pp. 49–58. Schweizerbart'sche Verlagsbuchhandlung, Stuttgart.

Di Federico V (1997) Estimates of equivalent aperture for non-Newtonian flow in a rough-walled fracture. *International Journal of Rock Mechanics and Mining Sciences,* **34**, 1133–1137.

Di Iorio D, Lavelle JW, Rona PA, Bemis K, Xu G, Germanovich LN, Lowell RP, Gene G (2012) Measurements and models of heat flux and plumes from hydrothermal discharges near the deep seafloor. *Oceanography*, **25**, 168–179.

Dilles JH (1987) The petrology of the Yerington Batholith, Nevada: evidence for the evolution of porphyry copper ore fluids. *Economic Geology*, **82**, 1750–1789.

Dingman SL (2002) *Physical Hydrology,* 2nd edn Waveland Press, Long Grove, IL.

Dixon TH, Moore JC (2007) The seismogenic zone of subduction thrust faults: introduction. In: *The Seismogenic Zone of Subduction Thrust Faults* (eds Dixon TH, Moore JC), pp. 42–85. Columbia University Press, New York.

Dobrovolsky IP, Zubkov SI, Miachkin VI (1979) Estimation of the size of earthquake preparation zones. *Pure and Applied Geophysics*, **117**, 1025–1044.

Doe TW, Korbin GE (1987) A comparison of hydraulic fracturing and hydraulic jacking stress measurements. *Proceedings of 28th U.S. Rock Mechanics Symposium*, Tucson, 283–90.

Domenico PA, Swartz FW (1990) *Physical and Chemical Hydrogeology*. John Wiley & Sons, New York.

Doyen PM (1988) Permeability, conductivity, and pore geometry of sandstone. *Journal of Geophysical Research*, **93**, 7729–7740.

Dowrick DJ (1996) The modified Mercalli earthquake intensity scale; revisions arising from recent studies of New Zealand earthquakes. *Bulletin of the New Zealand National Society for Earthquake Engineering*, **29**, 92–106.

Driesner T (2007) The system $H_2$0-NaCl, Part II, Correlations for molar volume, enthalpy, and isobaric heat capacity from 0 to 1000 degrees C, 1 to 5000 bar, and 0 to 1 X-NaCl. *Geochimica et Cosmochimica Acta*, **71**, 4902–4919.

Driesner T (2010) The interplay of permeability and fluid properties as a first-order control of heat transport, venting temperatures and venting salinities at mid-ocean ridge hydrothermal systems. *Geofluids*, **10**, 132–141.

Driesner T, Geiger S (2007) Numerical simulation of multiphase fluid flow in hydrothermal systems. In: *Fluid-Fluid Interactions*, Vol. 65 (eds Liebscher A, Heinrich CA), pp. 187–212, Mineralogical Society of America, Chantilly, VA.

Driesner T, Heinrich CA (2007) The system $H_2$0-NaCl, Part I, Correlation formulae for phase relations in temperature-pressure -composition space from 0 to 1000 degrees C, 0 to 5000 bar, and 0 to 1 X-NaCl. *Geochimica et Cosmochimica Acta*, **71**, 4880–4901.

Drost BW, Whiteman KJ, Gonthier JB (1990) Geologic framework of the Columbia Plateau Aquifer System, Washington, Oregon, and Idaho. *U.S. Geological Survey Water-Resources Investigations Report*, **87-4238**, http://pubs.er.usgs.gov/usgspubs/wri/wri874238 (accessed 06 May 2016).

du Pont SC, Gondret P, Perrin B, Rabaud M, (2003) Granular avalanches in fluids. *Physical Review Letters*, **90**, 044301.

Duba AG, Durham WB, Handin JW, Wang HF (eds) (1990) The brittle-ductile transition in rocks – The Heard volume. *American Geophysical Union Geophysical Monograph*, **56**.

Dugan B, Daigle H (2011) Data report: Permeability, compressibility, stress state, and grain size of shallow sediments from Sites C0004, C0006, C0007, and C0008 of the Nankai accretionary complex. In Kinoshita M, Tobin H, Ashi J, Kimura G, Lallemant S, Screaton EJ, Curewitz D, Masago H, Moe KT, and the Expedition 314/315/316 Scientists, *Proceedings of the Integrated Ocean Drilling Program,* **314/315/316**,1–11.

Dugan B, Sheahan TC (2012) Offshore sediment overpressures of passive margins: mechanisms, measurement, and models. *Reviews of Geophysics*, **50**, RG3001.

Dugan B, Zhao X (2013) Data report: Permeability of sediments from Sites C0011 and C0012, NanTroSEIZE, Stage 2, Subduction inputs. In Saito S, Underwood MB, Kubo Y, and the Expedition 322 Scientists, *Proceedings of the Integrated Ocean Drilling Program*, **322**, 1–14.

Dunbar N (2005) Quaternary volcanism in New Mexico. *New Mexico Museum of Natural History and Science Bulletin*, **28**, 95–106.

Durham WB (1997) Laboratory observations of the hydraulic behavior of a permeable fracture from 3800 m depth in the KTB pilot hole. *Journal of Geophysical Research*, **102**, 18405–18416.

Durham WB, Bonner BP (1994) Self-propping and fluid flow in slightly offset joints at high effective pressures. *Journal of Geophysical Research*, **99**, 9391–9399.

Durham WB, Bourcier WL, Burton EA (2001) Direct observation of reactive flow in a single fracture. *Water Resources Research,* **37**, doi:10.1029/2000WR900228.

Durney DW, Ramsay JG (1973) Incremental strains measured by syntectonic crystal growths. In: *Gravity and Tectonics* (eds DeJong KA, Scholten R), pp. 67–96. Wiley, New York.

Dussan EB, Sharma Y (1992) Analysis of the pressure response of a single-probe formation tester. *SPE Formation Evaluation*, **7**, 151–156.

Dusseault M, McLennan J (2011) Massive multistage hydraulic fracturing: where are we? In: 45th US Rock Mechanics/Geomechanics Symposium, June 26–29, 2011, San Francisco, California.

Dziak RP, Chadwick WW, Christopher GG, Embley RW (2003) Hydrothermal temperature changes at the southern Juan de Fuca Ridge associated with MW 6.2 Blanco Transform earthquake. *Geology*, **31**, 119–122.

Earnest E, Boutt D (2014) Investigating the role of hydromechanical coupling on flow and transport in shallow, fractured rock aquifers. *Hydrogeology Journal*, **22**, 1473–1491.

Eaton D, van der Baan M, Birkelo B, Tary J-B (2014) Scaling relations and spectral characteristics of tensile microseisms: evidence for opening/closing cracks during hydraulic fracturing. *Geophysical Journal International*, **196**, 1844–1857.

Edmunds WM, Savage D (1991) Geochemical characteristics of groundwater in granites and related crystalline rocks. In: *Applied Groundwater Hydrology, a British Perspective* (eds Downing RA, Wilkinson WB), pp. 199–216. Clarendon Press, Oxford.

Edwards S, Hudson-Edwards K, Cann J, Malpas J, Xenophontos C (2010) *Classic Geology in Europe, 7, Cyprus*. Terra Publishing, Harpenden, UK.

Eggleston C, Rojstaczer S (1998) Identification of large-scale hydraulic conductivity trends and the influence of trends on contaminant transport. *Water Resources Research*, **34**, 2155–2168.

Ehrenberg SN, Nadeau PH (2005) Sandstone vs. carbonate petroleum reservoirs: a global perspective on porosity-depth and porosity-permeability relationships. *AAPG Bulletin*, **89**, 435–445.

Ekinci MK (2012) Permeability, clay mineralogy, and microfabric of fine grained sediments from the Nankai Trough and Shikoku Basin, offshore southwest Japan. MS thesis, University of Missouri.

Ekinci MK, Likos WJ, Underwood MB, Guo J (2011) Data report: Permeability of mud(stone) samples from IODP Sites C0006 and C0007, Nankai Trough Seismogenic Zone Experiment. In Kinoshita M, Tobin H, Ashi J, Kimura G, Lallemant S, Screaton EJ, Curewitz D, Masago H, Moe KT, and the Expedition 314/315/316 Scientists, *Proceedings of the Integrated Ocean Drilling Program*, **314/315/316**, 1–40.

Elders WA, Frioleifsson GO, Zierenberg RA, Pope EC, Mortensen AK, Guomundsson A, Lowenstern JB, Marks NE, Owens L, Bird DK, Reed M, Olsen NJ, Schiffman P (2011) Origin of a rhyolite that intruded a geothermal well while drilling at the Krafla volcano, Iceland. *Geology*, **39**, 231–234.

Elkhoury JE, Brodsky EE, Agnew DC (2006) Seismic waves increase permeability. *Nature*, **441**, 1135–1138.

Elkhoury JE, Niemeijer A, Brodsky EE, Marone C (2011) Laboratory observations of permeability enhancement by fluid pressure oscillation of in situ fractured rock. *Journal of Geophysical Research*, **116**, B02311, doi:10.1029/2010JB007759.

Elliot GM, Brown ET, Boodt PI, Hudson JA (1985) Hydrochemical behaviour of joints in the Carmenelis granite SW England. *Proceedings of the International Symposium on Fundamentals of Rock Joints,* Bjorkliden, Sweden, A. A. Balkema, Rotterdam, 249–258.

Ellis AJ, Mahon WAJ (1964) Natural hydrothermal systems and experimental hot water/rock interactions. *Geochimica et Cosmochimica Acta*, **28**, 1323–1357.

Ellis AJ, Mahon WAJ (1967) Natural hydrothermal systems and experimental hot water/rock interactions, Part II. *Geochimica et Cosmochimica Acta*, **31**, 519–538.

Ellis S, Beavan J, Eberhart-Phillips D, Stöckhert B (2006) Simplified models of the Alpine Fault seismic cycle: stress transfer in the mid-crust. *Geophysical Journal International*, **166**, 386–402.

Ellsworth WL (2013) Injection-induced earthquakes. *Science*, **341**, 142.

Elsworth D, Goodman RE (1986) Characterization of rock fissure hydraulic conductivity using idealized wall roughness profiles. *International Journal of Rock Mechanics and Mining Sciences*, **23**, 233–243.

Ely DM, Burns ER, Morgan DS, Vaccaro JJ (2014) Numerical simulation of groundwater flow in the Columbia Plateau Regional Aquifer System, Idaho, Oregon, and Washington. *U.S. Geological Survey Scientific Investigations Report*, **2014–5127**.

Emter D, Wenzel HG, Zürn W (1999) Das Observatorium Schiltach. *DGG Mitteilungen*, **3**, 1–15.

Engvik A., Ihlen PM, Austrheim A. (2014) Characterisation of Na-metasomatism in the Sveconorwegian Bamble sector of south Norway. *Geoscience Frontiers*, **5**, 659–672.

Erzinger J, Stober I (2005) Introduction to special issue: long-term fluid production in the KTB pilot hole, Germany. *Geofluids*, **5**, 1–7.

Esaki T, Du S, Mitani Y, Ikusada K, Jing L (1999) Development of a shear-flow test apparatus and determination of coupled properties for a single rock joint. *International Journal of Rock Mechanics and Mining Sciences,* **36**, 641–650.

Etheridge MA, Wall VJ, Cox SF, Vernon RH (1984) High fluid pressures during regional metamorphism and deformation – Implications for mass-transport and deformation mechanisms. *Journal of Geophysical Research*, **89**, 4344–4358.

Evans JP, Forster CB, Goddard JV (1997) Permeability of fault-related rocks, and implications for hydraulic structure of fault zones. *Journal of Structural Geology*, **19**, 1393–1404.

Evans K, Wyatt F (1984) Water table effects on the measurement of earth strain. *Tectonophysics*, **108**, 323–337.

Evans KF (2005) Permeability creation and damage due to massive fluid injections into granite at 3.5 km at Soultz, 2, Critical stress and fracture strength. *Journal of Geophysical Research*, **110**, B04204, doi:10.1029/2004JB003169.

Evans KF, Genter A, Sausse J (2005) Permeability creation and damage due to massive fluid injections into granite at 3.5 km at Soultz, 1, Borehole observations. *Journal of Geophysical Research*, **110**, B04203, doi:10.1029/2004JB003168.

Fairhurst C (2013) Fractures and fracturing: hydraulic fracturing in jointed rock. In: *Effective and Sustainable Hydraulic Fracturing* (eds Bunger A, McLennan J, Jeffrey R), pp. 47–79, InTech, Rijeka, Croatia.

Fairley JP, Ingebritsen SE, Podgorney RK (2010) Challenges for numerical modeling of enhanced geothermal systems. *Ground Water*, **48**, 482–483.

Fan Y, Richard S, Bristol RS, Peters SE, Ingebritsen SE, Moosdorf N, Packman A, Gleeson T, Zaslavsky I, Peckham S, Murdoch L, Fienen M, Cardiff M, Tarboton D, Jones N, Hooper R, Arrigo J, Gochis D, Olson J, Wolock D (2015) DigitalCrust – A 4D data system of material properties for transforming research on crustal fluid flow. *Geofluids*, **15**, 372–379.

Fardin PC (2003) The effect of scale on the morphology, mechanics and transmissivity of single rock fractures, structural non-stationarity on the surface roughness and the shear strength of rock fractures. PhD thesis, Royal Institute of Technology (KTH), Stockholm, Sweden.

Faulder DD, Johnson SD, Benoit WR (1997) Flow and permeability structure of the Beowawe, Nevada hydrothermal system. Proceedings, Twenty-Second Workshop on Geothermal Research and Engineering, Stanford, California, *Stanford Geothermal Program Technical Report*, **SGP-TR-155**, 63–73.

Faulds JE, Hinz NH, Coolbaugh MF, Cashman PH, Kratt C, Dering G, Edwards J, Mayhew B, McLachlan H (2011) Assessment of favorable structural settings of geothermal systems in the Great Basin, western USA. *Geothermal Research Council Transactions*, **35**, 777–783.

Faulkner DR, Jackson CAL, Lunn RJ, Schlische RW, Shipton ZK, Wibberley CAJ, Withjack MO (2010) A review of recent developments concerning structure, mechanics and fluid flow properties of fault zones. *Journal of Structural Geology*, **32**, 1557–1575.

Faulkner DR, Rutter EH (2001) Can the maintenance of overpressured fluids in large strike-slip fault zones explain their apparent weakness? *Geology*, **29**, 503–506.

Faust CR, Mercer JW (1979) Geothermal reservoir simulation, 1, Mathematical models for liquid- and vapor-dominated hydrothermal systems. *Water Resources Research*, **15**, 23–29.

Favara R, Grassa F, Inguaggiato S, Valenza M (2001) Hydrogeochemistry and stable isotopes of thermal springs: earthquake-related chemical changes along Belice Fault (western Sicily). *Applied Geochemistry*, **16**, 1–17.

Ferguson CA, Osburn GR, McIntosh WC (2012) Oligocene calderas in the San Mateo Mountains, Mogollon-Datil volcanic field, New Mexico. *New Mexico Geological Society Guidebook*, **63**, 74–77.

Ferris JG (1951) Cyclic fluctuations of water level as a basis for determining aquifer transmissivity. *International Association of Hydrological Sciences (IAHS)*, **33**, 148–155.

Ferry JM (1987) Metamorphic hydrology at 13-km depth and 400–500°C. *American Mineralogist*, **72**, 39–58.

Ferry JM (1994) Overview of the petrologic record of fluid flow during regional metamorphism in northern New England. *American Journal of Science*, **294**, 905–988.

Fetter CW (1994) *Applied Hydrogeology*, 3rd edn Prentice Hall, Englewood Cliffs, NJ.

Filgris MN (2001) Römische Baderuine Badenweiler. Historische Wurzeln des Kurortes neu prasentiert. *Denkmalsplege in Baden-Wurttemberg*, **4**, 166–175.

Finnegan S, Peters SE, Fischer WW (2011) Late Ordovician-Early Silurian selective extinction patterns in Laurentia and their relationship to climate change. In: *Ordovician of the World* (eds Gutiérrez-Marco JC, Rábano I, Garcia-Bellido D), pp. 155–159. C*uadernos del Museo Geominera*, **14**, Madrid, Spain.

Fisher AT, Hounslow MW (1990) Transient fluid flow through the toe of the Barbados accretionary complex: constraints from Ocean Drilling Program Leg 110, heat flow studies and simple models. *Journal of Geophysical Research*, **95**, 8845–8858.

Fisher AT, Zwart G (1997) Packer experiments along the décollement of the Barbados accretionary complex: measurements of in situ permeability. In: *Proceedings of the Ocean Drilling Program, Scientific Results*, **156**, (eds Shipley TH, Ogawa Y, Blum P, Bahr JM), pp. 199–218, Ocean Drilling Program, College Station, TX.

Fisher AT, Zwart G, the Ocean Drilling Program Leg 156 Scientific Party (1996) Relation between permeability and effective stress along a plate boundary fault. Barbados accretionary complex. *Geology*, **24**, 307–310.

Fitts TG, Brown KM (1999) Stress-induced smectite dehydration: ramifications for patterns of freshening and fluid expulsion in the N. Barbados accretionary wedge. *Earth and Planetary Science Letters*, **172**, 179–197.

Fogg G, Senger RL (1985) Automatic generation of flow nets with conventional ground-water modeling algorithms. *Groundwater*, **23**, 336–344.

Fogg GE, LaBolle EM (2006) Motivation of synthesis, with an example on groundwater quality sustainability. *Water Resources Research*, **42**, W03S05.

Folk RL (1966) A review of grain-size parameters. *Sedimentology*, **6**, 73–93.

Fonneland-Jorgensen H, Furnes H, Muehlenbachs K, Dilek Y (2005) Hydrothermal alteration and tectonic evolution of an intermediate- to fast-spreading back-arc oceanic crust: late Ordovician Solund-Stavfjord ophiolite, western Norway. *Island Arc*, **14**, 517–541.

Fontaine FJ, Wilcock WSD, Foustoukos DE, Butterfield DA (2009) A Si-Cl geothermobarometer for the reaction zone of

high-temperature, basaltic-hosted midocean ridge hydrothermal systems. *Geochemistry, Geophysics, Geosystems*, **10**, Q05009.

Ford A, Blenkinsop TG, McLellan JG (2009) Factors affecting fluid flow in strike-slip fault systems: coupled deformation and fluid flow modeling with application to the western Mount Isa inlier, Australia. *Geofluids*, **9**, 2–23.

Fornari DJ, Shank T, Von Damm KL, Gregg TKP, Lilley M, Levai G, Bray A, Haymon RM, Perfit MR, Lutz R (1998) Time-series temperature measurements at high-temperature hydrothermal vents, East Pacific Rise 9°49'-51'N: evidence for monitoring a crustal cracking event. *Earth and Planetary Science Letters*, **160**, 419–431.

Forster C, Smith L (1988a) Groundwater flow systems in mountainous terrain, 1, Numerical modeling technique. *Water Resources Research*, **24**, 999–1010.

Forster C, Smith L (1988b) Groundwater flow systems in mountainous terrain, 2, Controlling factors. *Water Resources Research*, **24**, 1011–1023.

Forster C, Smith L (1989) The influence of groundwater flow on thermal regimes in mountainous terrain: a model study. *Journal of Geophysical Research*, **94**, 9439–9451.

Forsyth DW, Scheirer DS, Webb SC, Dorman LM, Orcutt JA, Harding AJ, Blackman DK, Morgan JP, Detrick RS, Shen Y, Wolfe CJ, Canales JP, Toomey DR, Sheehan AF, Solomon SC, Wilcock WSD, Team MS (1998) Imaging the deep seismic structure beneath a mid-ocean ridge: the MELT experiment. *Science*, **280**, 1215–1218.

Fossen H, Schultz RA, Runhovde E, Rotevatn A, Buckley SJ (2010) Fault linkage and graben stopovers in the Canyonlands (Utah) and the North Sea Viking Graben, with implications for hydrocarbon migration and accumulation. *American Association of Petroleum Geologists Bulletin*, **94**, 597–613.

Foster SSD, Chilton PJ (2003) Groundwater: the processes and global significance of aquifer degradation. *Philosophical Transactions of the Royal Society of London. Series B, Biological Sciences*, **358**, 1957–1972.

Fournier RO (1979) A revised equation for the Na/K geothermometer. *Geothermal Resources Council Transactions*, **3**, 221–224.

Fournier RO (1981) Application of water geochemistry to geothermal exploration and reservoir engineering. In: *Geothermal Systems: Principles and Case Histories* (eds Ryback L, Muffler LJP), pp. 109–143. John Wiley and Sons, New York.

Fournier RO (1989) Lectures on geochemical interpretation of hydrothermal waters. *UNU Geothermal Training Programme, Reykjavik Iceland*, **10**.

Fournier RO (1991) The transition from hydrostatic to greater than hydrostatic fluid pressure in presently active continental hydrothermal systems in crystalline rock. *Geophysical Research Letters*, **18**, 955–958.

Fournier RO (1999) Hydrothermal processes related to movement of fluid from plastic into brittle rock in the magmatic-epithermal environment. *Economic Geology*, **94**, 1193–1211.

Fournier RO, Potter RW II (1982) A revised and expanded (quartz) geothermometer. *Geothermal Resources Council Bulletin*, **11**, 3–12.

Fowler AC (1984) A mathematical model of magma transport in the asthenosphere. *Geophysical and Astrophysical Fluid Dynamics*, **33**, 155–190.

Fowler AC, Yang X (1999) Pressure solution and viscous compaction in sedimentary basins. *Journal of Geophysical Research*, **104**, 12989–12997.

Francheteau J, Armijo R, Cheminee JL, Hekinian R, Lonsdale P, Blum N (1992) Dike complex of the East Pacific Rise exposed in the walls of Hess Deep and the structure of the upper oceanic crust. *Earth and Planetary Science Letters*, **111**, 109–121.

Frape SK, Fritz P (1987) Geochemical trends for groundwaters from the Canadian shield. In: *Saline Water and Gases in Crystalline Rocks* (eds Fritz P, Frape SK), pp. 19–38. *Geological Association of Canada Special Paper*, **33**, The Runge Press Limited, Ottawa, ON.

Freeze RA, Cherry JA (1979) *Groundwater*. Prentice-Hall, Englewood Cliffs, NJ.

Fridleifsson GO, Elders WA (2005) The Iceland Deep Drilling Project: a search for deep unconventional geothermal resources. *Geothermics*, **34**, 269–285.

Friedrich AM, Lee J, Wernicke BP, Sieh K (2004) Geologic context of geodetic data across a Basin and Range normal fault, Crescent Valley, Nevada. *Tectonics*, **23**, 1–24.

Frisch U, d'Humieres D, Hasslacher B, Lallemand P, Pomeau Y, Rivet J-P (1987) Lattice gas hydrodynamics in two and three dimensions. *Complex Systems*, **1**, 649–707.

Frisch U, Hasslacher B, Pomeau Y (1986) Lattice-gas automata for the Navier-Stokes equation. *Physical Review Letters*, **56**, 1505–1508.

Fritz DE, Farmer GL, Verplanck EP (2006) Application of Sr isotopes in secondary silicate minerals to paleogroundwater hydrology: an example from K-metasomatized rocks in the western US. *Chemical Geology*, **235**, 276–285.

Frohlich C, Ellsworth W, Brown WA, Brunt M, Luetgert J, MacDonald T, Walter S (2014) The 17 May 2012 M4.8 earthquake near Timpson, East Texas: an event possibly triggered by fluid injection. *Journal of Geophysical Research*, **119**, 581–593.

Frost BR, Bucher K (1994) Is water responsible for geophysical anomalies in the deep continental crust? A petrological perspective. *Tectonophysics*, **231**, 293–309.

Fry B, Bannister SC, Beavan RJ, Bland L, Bradley BA, Cox SC, Cousins WJ, Gale NH, Hancox GT, Holden C, Jongens R, Power WL, Prasetya G, Reyners ME, Ristau J, Robinson R, Samsonov S, Wilson KJ, team G (2010) The M_w7.6 Dusky Sound earthquake of 2009: preliminary report. *Bulletin of the New Zealand Society for Earthquake Engineering*, **43**, 24–40.

Fuis GS, Moore TE, Plafker G, Brocher TM, Fisher MA, Mooney WD, Nokleberg WJ, Page RA, Beaudoin BC, Christensen NI, Levander AR, Lutter WJ, Saltus RW, Ruppert NA (2008) Trans-Alaska crustal transect and continental evolution involving subduction underplating and synchronous foreland thrusting. *Geology*, **36**, 267–270.

Furlong KP, Hanson RB, Bowers JR (1991) Modeling thermal regimes. *Reviews in Mineralogy*, **26**, 437–505.

Fusseis F, Handy MR (2008) Micromechanisms of shear zone propagation at the brittle-viscous transition. *Journal of Structural Geology*, **30**, 1242–1253.

Fusseis F, Handy, MR, Schrank C (2006) Networking of shear zones at the brittle-to-viscous transition (Cap de Creus, NE Spain). *Journal of Structural Geology*, **28**, 1228–1243.

Fyfe WS, Price NJ, Thompson AB (1978) *Fluids in the Earth's Crust*. Elsevier Scientific, New York.

Gale J (1990) Hydraulic behaviour of rock joints. *Conference on Rock Joints, Proceedings of the ISRM,* 351–362.

Gale JE, Wilson CR, Witherspoon PA, Wilson CR (1982) Swedish-American cooperative program on radioactive waste storage in mined caverns in crystalline rock. In: *SKB Technical Report*, **49** (ed Swedish Nuclear Fuel Supply Co & Lawrence Berkeley Laboratory), National Technical Information Service, U.S. Department of Commerce, Springfield, VA, http://esd.lbl.gov/files/publications/stripa_reports/Technical_Project_Report_No_49.pdf (accessed 06 May 2016).

Galet RM (2011) Thermo-hydro-mechanical study of deformable porous media with double porosity in local thermal non-equilibrium. PhD thesis, University of New South Wales.

Gallahan WE, Duncan RA (1994) Spatial and temporal variability in crystallisation of celadonites within the Troodos ophiolite, Cyprus: implications for low-temperature alteration of the oceanic crust. *Journal of Geophysical Research*, **99**, 3147–3161.

Galvan B, Miller SA (2013) A full GPU simulation of evolving fracture networks in a heterogeneous poro-elasto-plastic medium with effective-stress-dependent permeability. In: *GPU Solutions to Multi-scale Problems in Science and Engineering* (eds Yuen DA, Wong L, Chi X, Johnsson L, Ge W, Shi Y), pp. 305–319, Springer, Berlin, Heidelberg.

Gamage K, Bekins B, Screaton E (2005) Data report: Permeabilities of eastern equatorial Pacific and Peru margin sediments. *Proceedings of the Ocean Drilling Program, Scientific Results,* **201**, 1–18.

Gamage K, Screaton E (2003) Data report: Permeabilities of Nankai accretionary prism sediments. *Proceeding of the Ocean Drilling Program, Scientific Results,* **190/196**, 1–21.

Gamage K, Screaton E (2006) Characterization of excess pore pressures at the toe of the Nankai accretionary complex, Ocean Drilling Program Sites 1173, 1174, and 808: results of one-dimensional modeling. *Journal of Geophysical Research*, **111**, B04103.

Gamage K, Screaton E, Bekins B, Aiello I (2011) Permeability-porosity relationships of subduction zone sediments. *Marine Geology*, **279**, 19–36.

Gangi AF (1978) Variation of whole and fractured porous rock permeability with confining pressure. *International Journal of Rock Mechanics and Mining Sciences*, **15**, 249–257.

Ganguly J (2002) Diffusion kinetics in minerals: principles and applications to tectono-metamorphic processes. *EMU Notes in Mineralogy*, **4**, 271–309.

Garg SK, Pritchett JW (1977) On pressure-work, viscous dissipation and the energy balance relation for geothermal reservoirs. *Advances in Water Resources*, **1**, 41–47.

Garg SK, Pritchett JW, Wannamaker PE, Combs J (2007) Characterization of geothermal reservoirs with electrical surveys: Beowawe geothermal field. *Geothermics*, **36**, 487–517.

Garrels RM, Howard PF (1959) Reactions of feldspar and mica with water at low temperature and pressure. *Clays and Clay Minerals*, **6**, 68–88.

Garven G, Bull SW, Large RR (2001) Hydrothermal fluid flow models of stratiform ore genesis in the McArthur Basin, Northern Territory, Australia. *Geofluids*, **1**, 289–311.

Garza RAP, Titley SR, Pimentel FB (2001) Geology of the Escondida porphyry copper deposit, Antofagasta region, Chile. *Economic Geology*, **96**, 307–324.

Gassiat C, Gleeson T, Luijendijk E (2013) The location of old groundwater in hydrogeologic basins and layered aquifer systems. *Geophysical Research Letters*, **40**, 3042–3047.

Gavrilenko P, Gueguen Y (1993) Fluid overpressures and pressure solution in the crust. *Tectonophysics*, **21**, 91–110.

Ge S (1997) A governing equation for fluid flow in rock fractures. *Water Resources Research,* **33**, 53–61.

Ge S, Stover SC (2000) Hydrodynamic response to strike- and dip-slip faulting in a half-space. *Journal of Geophysical Research*, **105**, 25513–25524.

Genser J, Cloetingh SAPL, Neubauer F (2007) Late orogenic rebound and oblique Alpine convergence: new constraints from subsidence analysis of the Austrian Molasse basin. *Global and Planetary Change,* **58**, 214–223.

Genter A, Evans K, Cuenot N, Fritsch D (2010) Contribution of the exploration of deep crystalline fractured reservoir of Soultz to the knowledge of enhanced geothermal systems (EGS). *Comptes Rendus Geoscience*, **342**, 502–516.

Geological Survey of Japan (2013) Volcanoes of Japan. Retrieved January 10, 2014, from https://gbank.gsj.jp/volcano/.

GeoNet (2014) Earthquake strong motion data and processing. http://info.geonet.org.nz/display/appdata/Strong-Motion+Data, accessed 15 February 2014.

Gerdes M, Baumgartner L, Person M (1995) Permeability heterogeneity in metamorphic rocks: implications from stochastic modeling. *Geology*, **23**, 945–948.

German CR, Lin J (2004) The thermal structure of the oceanic crust, ridge-spreading and hydrothermal circulation: how well do we understand their inter-connections? In: *Mid-Ocean Ridges: Hydrothermal Interactions between the Lithosphere and Oceans* (eds German CR, Lin J, Parson LM), *AGU Geophysical Monograph Series*, **148**, 1–18.

Giacomini A, Buzzi O, Ferrero AM, Migliazza M, Giani GP (2007) Numerical study of flow anisotropy within a single natural rock joint. *International Journal of Rock Mechanics and Mining Sciences*, **45**, 47–58.

Gieskes JM, Vrolijk P, Blanc G (1990) Hydrogeochemistry, ODP Leg 110: an overview. In: *Proceedings of the Ocean Drilling Program, Scientific Results*, **110**, (eds Moore JC, Mascle A, Leg 110 Scientific Party), pp. 395–408, Ocean Drilling Program, College Station, TX.

Giger SB, Tenthorey E, Cox SF, Fitz Gerald JD (2007) Permeability evolution in quartz fault gouges under hydrothermal conditions. *Journal of Geophysical Research*, **112**, doi:10.1029/2006JB004828.

Giggenbach WF (1986) Graphical techniques for the evaluation of water/rock equilibrium conditions by use of Na, K, Mg and Ca contents of discharge waters. *Proceedings of the Eighth New Zealand Geothermal Workshop*, Auckland, New Zealand, 37–43.

Giggenbach WF (1988) Geothermal solute equilibria: derivation of Na-K-Mg-Ca geoindicators. *Geochimica Cosmochimica Acta*, **52**, 2749–2765.

Giggenbach WF (1991) Chemical techniques in geothermal exploration. *UNITAR/UNDP Guidebook: Application of Geochemistry in Resources Development*, 119–144.

Giggenbach WF, Sano Y, Wakita H (1993) Isotopic composition of helium, and CO_2 and CH_4 contents in gases produced along the New Zealand part of a convergent plate boundary. *Geochimica et Cosmochimica Acta*, **57**, 3427–3455.

Gilmer A, Mauldin R, Keller G (1986) A gravity study of the Jornado del Muerto and Palomas Basins. *New Mexico Geological Society Guidebook*, **37**, 131–134.

Gingerich SB, Voss CI (2005) Three-dimensional variable-density flow simulation of a coastal aquifer in southern Oahu, Hawaii, USA. *Hydrogeology Journal*, **13**, 436–450.

Giordano M (2009) Global groundwater? Issues and solutions. *Annual Review of Environment and Resources,* **34**, 153–178.

Gischig VS, Wiemer S (2013) A stochastic model for induced seismicity based on non-linear pressure diffusion and irreversible permeability enhancement. *Geophysical Journal International*, **194**, 1229–1249.

Gledhill KR, Ristau J, Reyners ME, Fry B, Holden C (2011) The Darfield (Canterbury, New Zealand) M_w7.1 earthquake of September 2010: a preliminary seismological report. *Seismological Research Letters*, **82**, 378–386.

Gleeson SA, Yardley BWD, Munz IA (2003) Infiltration of basinal fluids into high-grade basement, South Norway: sources and behaviour of waters and brines. *Geofluids*, **3**, 33–48.

Gleeson T, Alley WM, Allen DM, Sophocleous MA, Zhou Y, Taniguchi M, Van der Steen J (2012a) Towards sustainable groundwater use: setting long-term goals, backcasting, and managing adaptively. *Ground Water,* **50**, 19–26.

Gleeson T, Moosdorf N, Hartmann J, van Beek LPH (2014) A glimpse beneath Earth's surface: GLobal HYdrogeology MaPS (GLHYMPS) of permeability and porosity. *Geophysical Research Letters*, **41**, 3891–3898.

Gleeson T, Smith L, Moosdorf N, Hartmann J, Dürr H, Manning A, Beek L, Jellinek A (2011) Mapping permeability over the surface of the Earth. *Geophysical Research Letters*, **38**, doi:10.1029/2010GL045565.

Gleeson T, Van der Steen J, Sophocleous MA, Taniguchi M, Alley WM, Allen DM, Zhou Y (2010) Groundwater sustainability strategies. *Nature Geoscience,* **3**, 378–379.

Gleeson T, Wada Y, Bierkens MFP, van Beek LPH (2012b) Water balance of global aquifers revealed by groundwater footprint. *Nature,* **488**, 197–200.

Gliko AO, Singh RN, Swathi PS (1999) Physical approach to the problem of origin of charnockitic rocks of southern India: mechanisms of crustal heating and transfer of carbon dioxide. *Russian Journal of Earth Sciences*, **1**, 409–421.

Goertz-Allmann BP, Goertz A, Wiemer S (2011) Stress drop variations of induced earthquakes at the Basel geothermal site. *Geophysical Research Letters*, **38**, doi:10.1029/2011GL047498.

Gómez-Hernández JJ, Gorelick SM (1989) Effective groundwater model parameter values: influence of spatial variability of hydraulic conductivity, leakance, and recharge. *Water Resources Research*, **25**, 405–419.

Goodman, R (1976) *Methods of Geological Engineering in Discontinuous Rocks*. West Publishing, Eagan, MN.

Gorokhovich Y, Fleeger G (2007) Pymatuning earthquake in Pennsylvania and Late Minoan crisis on Crete. *Water Science & Technology: Water Supply*, **7**, 245–251.

Graham DW, Christie DM, Harpp KS, Lupton JE (1993) Mantle-plume helium in submarine basalts from the Galapagos Platform. *Science*, **262**, 2023–2026.

Gratier JP, Favreau P, Renard F (2003) Modeling fluid transfer along California faults when integrating pressure solution crack sealing and compaction processes. *Journal of Geophysical Research*, **108**, B02104, doi:10.1029/2001JB000380.

Griffiths FJ, Joshi RC (1989) Change in pore size distribution due to consolidation of clays. *Géotechnique*, **39**, 159–167.

Gruen G, Weis P, Driesner T, Heinrich CA, de Ronde CEJ (2014) Hydrodynamic modeling of magmatic–hydrothermal activity at submarine arc volcanoes, with implications for ore formation. *Earth and Planetary Science Letters*, **404**, 307–318.

Gueguen Y, Dormieux L, Bouteca M (2004) Fundamentals of poromechanics. In: *Mechanics of Fluid-Saturated Rocks* (eds Gueguen Y, Bouteca M), pp. 55–79. Elsevier Academic Press, Burlington, MA.

Guglielmi Y, Cappa F, Lane H, Janowczyk JB, Rutqvist J, Tsang C-F, Wang JSY (2014) ISRM suggested method for step-rate injection method for fracture in-situ properties (SIMFIP): using a 3-component borehole deformation sensor. *Rock Mechanics and Rock Engineering*, **47**, 303–311.

Gulley AK, Ward NFD, Cox SC, Kaipio JP (2013) Groundwater responses to the recent Canterbury earthquakes: a comparison. *Journal of Hydrology*, **504**, 171–181.

Guo J, Underwood MB (2014) Data report: Consolidation characteristics of sediments from Sites C0011, C0012, and C0018, IODP Expeditions 322 and 333, NanTroSEIZE Stage 2. In: Saito S, Underwood MB, Kubo Y, and the Expedition 322 Scientists, *Proceedings of the Integrated Ocean Drilling Program*, **322**.

Gürbüz A (2010) Geometric characteristics of pull-apart basins. *Lithosphere*, **2**, 199–206.

Gustafson LB, Hunt JP (1975) Porphyry copper deposit at El Salvador, Chile. *Economic Geology*, **70**, 857–912.

Haar L, Gallagher JS, Kell GS (1984) *NBS/NRC Steam Tables: Thermodynamic and Transport Properties and Computer Programs for Vapor and Liquid States of Water in SI Units*. Hemisphere Publishing, New York.

Hacker BR (2008) H_2O subduction beyond arcs. *Geochemistry, Geophysics, Geosystems*, **9**, Q03001.

Häfner F, Lauterbach M, Bamberg HF (1985) Physikalische Eigenschaften von Grund- und mineralisiertem Wasser, von Erdöl und Erdgas. *Wissenschaftlich-Technischer Informationsdienst*, **26**, 18–27.

Hagemann SG, Groves DI, Ridley JR, Vearncombe JR (1992) The Archean lode gold deposits at Wiluna, Western Australia: high-level, brittle-style mineralization in a strike-slip regime. *Economic Geology*, **87**, 1022–1053.

Haimson BC (1975) The state of stress in the Earth's crust. *Reviews of Geophysics*, **13**, 350–352.

Haines SH, van der Pluijm BA, Ikari MJ, Saffer DM, Marone C (2009) Clay fabric intensity in natural and artificial fault gouges: implications for brittle fault zone processes and sedimentary basin clay fabric evolution. *Journal of Geophysical Research*, **114**, B05406.

Hakami E, Larsson E (1996) Aperture measurement and flow experiments on a single natural fracture. *International Journal of Rock Mechanics and Mining Sciences*, **33**, 395–404.

Halevy I, Peters SE, Fischer WW (2012) Sulfate burial constraints on the Phanerozoic sulfur cycle. *Science*, **337**, 331–334.

Hammerschmidt SB, Davis EE, Hupers A, Kopf A (2013) Limitation of fluid flow at the Nankai Trough megasplay fault zone. *Geo-Marine Letters*, **33**, 405–408.

Hancox GT, Cox SC, Turnbull IM, Crozier MJ (2003) Reconnaissance studies of landslides and other ground damage caused by the M_w7.2 Fiordland earthquake of 22 August 2003. *Institute of Geological & Nuclear Sciences Science Report*, **2003/30**.

Hanks TC, Kanamori H (1979) A moment magnitude scale. *Journal of Geophysical Research,* **84**, 2348–2350.

Hannisdal B, Peters SE (2011) Phanerozoic earth system evolution and marine biodiversity. *Science*, **334**, 1121–1124.

Hans J, Boulon MJ (2003) A new device for investigating the hydro-mechanical properties of rock joints. *International Journal for Numerical and Analytical Methods in Geomechanics*, **27**, 513–548.

Hansen AJ, Vaccaro JJ, Bauer HH (1994) Ground-water flow simulation of the Columbia Plateau Regional Aquifer System, Washington, Oregon, and Idaho. *U.S. Geological Survey Water-Resources Investigations Report*, **91–4187**, http://pubs.er.usgs.gov/usgspubs/wri/wri914187 accessed 06 May 2016.

Hanson RB (1992) Effects of fluid production on fluid-flow during regional and contact metamorphism. *Journal of Metamorphic Geology*, **10**, 87–97.

Hanson RB (1995) The hydrodynamics of contact metamorphism. *Geological Society of America Bulletin*, **107**, 595–611.

Hanson RB (1997) Hydrodynamics of regional metamorphism due to continental collision. *Economic Geology*, **92**, 880–891.

Hao KX, Si H, Fujiwara H, Owaze T (2009) Coseismic surface-ruptures and crustal deformations of the 2008 Wenchuan earthquake M_w7.9, China. *Geophysical Research Letters*, **36**, L11303.

Hardebeck JL (2012) Fluid-driven seismicity response of the Rinconada fault near Paso Robles, California, to the 2003 M6.5 San Simeon earthquake. *Bulletin of the Seismological Society of America*, **102**, 377–390.

Harder H (1959) Contribution to the geochemistry of boron, part II, Boron in sediments. *Nachrichten der Akademie der Wissenschaften in Göttingen, II, Mathematisch-Physikalische Klasse*, **6**, 123–183.

Hardin E, Barton N, Voegele M, Board M, Lingle R, Pratt H, Ubbes W (1982) Measuring the thermomechanical and transport properties of a rockmass using the heated block test. *Proceedings of the 23th U.S. Symposium on Rock Mechanics*, University of California, Berkeley, California, August 25–27, 1982, 802–13.

Hardy JR Jr (1991) *Laboratory Tests Conducted on Barre Granite: Compressive Strength, Flexural Strength, Modulus of Rupture, Adsorption and Bulk Specific Gravity and Petrographic Analysis*. Department of Mining Engineering, Pennsylvania State University, PA.

Häring MO, Schanz U, Ladner F, Dyer BC (2008) Characterisation of the Basel 1 enhanced geothermal system. *Geothermics*, **37**, 469–495.

Harlow FH, Ellison MA, Reid JH (1964) The particle-in-cell computing method for fluid dynamics. *Methods in Computational Physics*, **3**, 319–343.

Harper GD, Bowman JR, Kuhns R (1988) A field, chemical and stable isotope study of subseafloor metamorphism of the Josphine ophiolite, California-Oregon. *Journal of Geophysical Research*, **93**, 4625–4656.

Harris C (1989) Oxygen-isotope zonation of agates from Karoo volcanics of the Skeleton Coast, Namibia. *American Mineralogist*, **74**, 476–481.

Harrison R, Cather S (2004) The hot springs fault systems of south-central New Mexico—evidence for northward translation of the Colorado Plateau during the Laramide orogeny. *New Mexico Bureau of Geology and Mineral Resources Bulletin*, **160**, 161–180.

Harrison R, Lozinsky R, Eggleston T, McIntosh W (1993) Geologic map of the Truth or Consequences 30×60 minute quadrangle. *New Mexico Bureau of Mines and Mineral Resources Open-File Report*, **390**, scale 1:100 000.

Harvey C, Gorelick SM (2000) Rate-limited mass transfer or macrodispersion: which dominates plume evolution at the macrodispersion experiment (MADE) site? *Water Resources Research*, **36**, 637–650.

Hasegawa A, Nakajima J, Uchida N, Okada T, Zhao D, Matsuzawa T, Umino N (2009) Plate subduction, and generation of earthquakes and magmas in Japan as inferred from seismic observations: an overview. *Gondwana Research*, **16**, 370–400.

Hasegawa A, Umino N, Takagi A (1978) Double-planed structure of the deep seismic zone in the northeastern Japan arc. *Tectonophysics*, **47**, 43–58.

Hasegawa A, Yoshida K, Asano Y, Okada T, Iinuma T, Ito Y (2012) Change in stress field after the 2011 great Tohoku-Oki earthquake. *Earth and Planetary Science Letters*, **355–356**, 231–243.

Hasegawa A, Yoshida K, Okada T (2011) Nearly complete stress drop in the 2011 M_w9.0 off the Pacific coast of Tohoku earthquake. *Earth, Planets and Space*, **63**, 703–707.

Hatherton T, Leopard AE (1964) The densities of New Zealand rocks. *New Zealand Journal of Geology and Geophysics*, **7**, 605–625.

Haw MD (2004) Jamming, two-fluid behavior, and "self-filtration" in concentrated particulate suspensions. *Physical Review Letters*, **92**, 342–360.

Hayba DO, Ingebritsen SE (1994) The computer model HYDROTHERM, a three-dimensional finite-difference model to simulate ground-water flow and heat transport in the temperature range of 0 to 1,200°C. *U.S. Geological Survey Water-Resources Investigations Report*, **94–4045**.

Hayba DO, Ingebritsen SE (1997) Multiphase groundwater flow near cooling plutons. *Journal of Geophysical Research*, **102**, 12235–12252.

Haymon RM (1996) The response of ridge-crest hydrothermal systems to segmented, episodic magma supply. *Geological Society of London Special Publication*, **118**, 157–168.

Headquarters for Earthquake Research Promotion (2008) Evaluation of the Aizu-Bonchi Toen and Seien faults (in Japanese). Retrieved from http://www.jishin.go.jp/main/chousa, accessed 06 May 2016.

Hedenquist JW, Arribas A, Reynolds TJ (1998) Evolution of an intrusion-centered hydrothermal system: Far Southeast-Lepanto porphyry and epithermal Cu-Au deposits, Philippines. *Economic Geology*, **93**, 373–404.

Hedenquist JW, Lowenstern JB (1994) The role of magmas in the formation of hydrothermal ore-deposits. *Nature*, **370**, 519–527.

Heederik JP (1988) Geothermische Reserves Centrale Slenk, Nederland: Exploratie en evaluatie. Technical report, TNO, Utrecht.

Heimgartner M, Louie JN, Scott JB, Thelen W, Lopez CT, Coolbaugh M (2006) The crustal thickness of the great basin: using seismic refraction to assess regional geothermal potential. *Geothermal Resources Council Transactions*, **30**, 83–86.

Heinrich CA (2006) How fast does gold trickle out of volcanoes? *Science*, **314**, 263–264.

Heinrich CA, Candela PA (2014) Fluids and ore formation in the earth's crust. In: *Treatise on Geochemistry*, 2nd edn (eds Holland HD, Turekian KK), pp. 1–28, Elsevier, Oxford.

Heinrich W, Hoffbauer R, Hubberten HW (1995) Contrasting fluid-flow patterns at the Bufa del Diente contact aureole, northeast Mexico – Evidence from stable isotopes. *Contributions to Mineralogy and Petrology*, **119**, 362–376.

Helfferich F (1966) Ion exchange kinetics. *Ion Exchange*, **1**, 65–100.

Helfrich KR, Whitehead JA (1990) Solitary waves on conduits of buoyant fluid in a more viscous-fluid. *Geophysical and Astrophysical Fluid Dynamics*, **51**, 35–52.

Hendriks B, Andriessen P, Huigen Y, Leighton C, Redfield T, Murrell G, Gallagher K, Nielsen SB (2007) A fission track data compilation for Fennoscandia. *Norsk Geolqgisk Tidsskrift*, **87**, 143–155.

Henley RW, Ellis AJ (1983) Geothermal systems ancient and modern – A geochemical review. *Earth-Science Reviews*, **19**, 1- 50.

Henry P (2000) Fluid flow at the toe of the Barbados accretionary wedge constrained by thermal, chemical, and hydrogeologic observations and models. *Journal of Geophysical Research*, **105**, 25855–25872.

Henry P, Foucher J-P, Le Pichon X, Sibuet M, Kobayashi K, Tarits P, Chamot-Rooke N, Furuta T, Schultheiss P (1992) Interpretation of temperature measurements from the Kaiko-Nankai cruise: modeling of fluid flow in clam colonies. *Earth and Planetary Science Letters*, **109**, 355–371.

Henry P, Lallemant S, Nakamura K, Tsunogai U, Mazzotti S, Kobayashi K (2002) Surface venting at the toe of the Nankai wedge and implications for flow paths. *Marine Geology*, **187**, 119–143.

Henry P, Le Pichon X (1991) Fluid flow along a décollement layer: a model applied to the 16°N section of the Barbados accretionary wedge. *Journal of Geophysical Research*, **96**, 6507–6528.

Hensen C, Wallmann K, Schmidt M, Ranero C, Suess E (2004) Fluid expulsion related to mud extrusion off Costa Rica – A window to the subducting slab. *Geology*, **32**, 201–204

Herdianita NR, Rodgers KA, Browne PRL (2000) Routine instrumental procedures to characterise the mineralogy of modern and ancient silica sinters. *Geothermics*, **29**, 65–81.

Herman F, Cox SC, Kamp PJJ (2009) Low-temperature thermochronology and thermokinematic modelling of deformation, exhumation, and development of topography in the central Southern Alps, New Zealand. *Tectonics*, **28**, TC5011.

Herman F, Seward D, Valla PG, Carter A, Kohn B, Willett SD, Ehlers TA (2013) Worldwide acceleration of mountain erosion under a cooling climate. *Nature*, **504**, 423–426.

Hersum TG, Marsh BD (2006) Igneous microstructures from kinetic models of crystallization. *Journal of Volcanology and Geothermal Research*, **154**, 34–47.

Hezarkhani A, Williams-Jones AE (1998) Controls of alteration and mineralization in the Sungun porphyry copper deposit, Iran: evidence from fluid inclusions and stable isotopes. *Economic Geology*, **93**, 651–670.

Hezarkhani A, Williams-Jones AE, Gammons CH (1999) Factors controlling copper solubility and chalcopyrite deposition in the Sungun porphyry copper deposit, Iran. *Mineralium Deposita*, **34**, 770–783.

Hickey KA, Barker SLL, Dipple GM, Arehart GB, Donelick RA (2014) The brevity of hydrothermal fluid flow revealed by thermal halos around giant gold deposits: implications for Carlin-type gold systems. *Economic Geology*, **109**, 1461–1487.

Hickman S, Davatzes N (2010) In-situ stress and fracture characterization for planning of an EGS stimulation in the Desert Peak Geothermal Field, Nevada. *Proceedings Thirty-Fifth Workshop on Geothermal Reservoir Engineering*, Stanford University.

Hicks DD, Hill J, Shankar U (1996) Variation of suspended sediment yields around New Zealand: the relative importance of rainfall and geology. *International Association of Hydrological Sciences Publication*, **236**, 149–156.

Hiederer R, Kochy M (2011) Global soil organic carbon estimates and the harmonized world soil database. *European Commission Joint Research Center Scientific and Technical Report*, **EUR 25225 EN**, http://eusoils.jrc.ec.europa.eu/esdb_archive/eusoils_docs/other/EUR25225.pdf accessed 06 May 2016.

Higuera FJ, Jimenez J (1989) Boltzmann approach to lattice gas simulations. *Europhysics Letters*, **9**, 663.

Hildenbrand A, Schlomer S, Krooss BM (2002) Gas breakthrough experiments on fine-grained sedimentary rocks. *Geofluids*, **2**, 3–23.

Hildenbrand A, Schlömer S, Krooss BM, Littke R (2004) Gas breakthrough experiments on pelitic rocks: comparative study with N_2, CO_2 and CH_4. *Geofluids*, **4**, 61–80.

Hill DP (1977) A model for earthquake swarms. *Journal of Geophysical Research*, **82**, 1347–1352.

Hill DP, Prejean S (2005) Magmatic unrest beneath Mammoth Mountain, California. *Journal of Volcanology and Geothermal Research*, **146**, 257–283.

Hill DP, Reasenberg PA, Michael A, Arabaz WJ, Beroza G, Brumbaugh D, Brune JN, Castro R, Davis S, dePolo D, Ellsworth WL, Gomberg J, Harmsen S, House L, Jackson SM, Johnston MJS, Jones L, Keller R, Malone S, Mungaia L, Nava S, Pechmann JC, Sanford A, Simpson RW, Smith RB, Stark M, Stickney M, Vidal S, Walter S, Wong V, Zollweg J (1993) Seismicity remotely triggered by the magnitude 7.3 Landers, California, earthquake. *Science*, **260**, 1617–1623.

Hinz N, Siler D, Faulds J (2012) 3D Geologic mapping-structural studies of geothermal systems in the Basin and Range, *Digital Mapping Techniques 2012 Proceedings*, http://ngmdb.usgs.gov/Info/dmt/DMT12presentations.html, accessed 06 May 2016.

Hinzen K-G (2003) Stress field in the northern Rhine area, central Europe, from earthquake fault plane solutions. *Tectonophysics*, **377**, 325–356.

Hiramatsu Y, Honma H, Saiga A, Furumoto M, Ooida T (2005) Seismological evidence on characteristic time of crack healing in the shallow crust. *Geophysical Research Letters*, **32**, doi:10.1029/2005GL022657.

Hirose F, Miyaoka K, Hayashimoto N, Yamazaki T, Nakamura M (2011) Outline of the 2011 off the Pacific coast of Tohoku earthquake (M_w9.0)—Seismicity: foreshocks, mainshock, aftershocks, and induced activity. *Earth, Planets and Space*, **63**, 513–518.

Hitzman MW, many others (Committee on Induced Seismicity Potential in Energy Technologies) (2012) *Induced Seismicity Potential in Energy Technologies*. National Academy Press, Washington, DC.

Hobday C, Worthington MH (2012) Field measurements of normal and shear fracture compliance. *Geophysical Prospecting*, **60**, 488–499.

Hofstra AH, Cline JS (2000) Characteristics and models for Carlin-type gold deposits. *Reviews in Economic Geology*, **13**, 163–220.

Holdich RG (2002) *Fundamentals of Particle Technology*. Midland Information Technology and Publishing, Loughborough.

Holland HD (2005) Sea level, sediments and the composition of seawater. *American Journal of Science*, **305**, 220–239.

Holness MB (2003) Growth and albitization of K-feldspar in crystalline rocks in the shallow crust: a tracer for fluid circulation during exhumation? *Geofluids*, **3**, 89–102.

Holtzman BK, Groebner NJ, Zimmerman ME, Ginsberg SB, Kohlstedt DL (2003) Stress-driven melt segregation in partially molten rocks. *Geochemistry Geophysics Geosystems*, **4**, doi:10.1029/2001GC000258.

Hooft EEE, Detrick RS (1993) The role of density in the accumulation of basaltic melts at mid-ocean ridges. *Geophysical Research Letters*, **20**, 423–426.

Hori S, Hasegawa A (1991) Location of a mid-crustal magma body beneath Mt. Moriyoshi, northern Akita Prefecture, as estimated from reflected S×S phases. *Zisin (Journal of the Seismological Society of Japan 2nd series)*, **44**, 39–48.

Horne RN (1996) *Modern Well Test Analysis, A Computer Aided Approach,* 2nd edn Petroway Inc., Palo Alto, CA.

Horsrud P, Sønstebø EF, Bøe R (1998) Mechanical and petrophysical properties of North Sea shales. *International Journal of Rock Mechanics and Mining Sciences*, **35**, 1009–1020.

Horton DG (1991) Secondary minerals in Columbia River Basalt, Pasco basin, Washington, Rep. WHC-SA-1352-FP, Pacific Northwest National Laboratory, Richland, WA.

Howald T, Person M, Campbell A, Lueth V, Hofstra A, Sweetkind D, Gable C, Banerjee A, Luijendijk E, Crossey L, Karlstrom K, Kelley S, Phillips F (2015) Evidence for long-time scale ($>10^3$ years) changes in hydrothermal activity induced by seismic events. *Geofluids*, **15**, 252–268.

Howarth JD, Fitzsimons SJ, Norris RJ, Jacobsen GE (2012) Lake sediments record cycles of sediment flux driven by large earthquakes on the Alpine fault, New Zealand. *Geology*, **40**, 1091–1094.

Hsieh PA, Bredehoeft JD (1981) A reservoir analysis of the Denver earthquakes: a case of induced seismicity. *Journal of Geophysical Research*, **86**, 903–920.

Hsieh PA, Bredehoeft JD, Rojstaczer SA (1988) Response of well aquifer systems to Earth tides: problem revisited. *Water Resources Research*, **24**, 468–472.

Hsieh PA, Tracy JV, Neuzil CE, Bredehoeft JD, Silliman SE (1981) A transient laboratory method for determining the hydraulic properties of 'tight' rocks, I, Theory. *International Journal of Rock Mechanics and Mining Sciences*, **18**, 245–252.

Hsiung SM, Chowdhury AH, Nataraja MS (2005) Numerical simulation of thermal-mechanical processes observed at the Drift-Scale Heater Test at Yucca Mountain, Nevada, USA. *International Journal of Rock Mechanics and Mining Sciences*, **42**, 652–666.

Hu DW, Zhu QZ, Zhou H, Shao JF (2010) A discrete approach for anisotropic plasticity and damage in semi-brittle rocks. *Computational Geotechnics*, **37**, 658–666.

Hu K, Issler D (2009) A comparison of core petrophysical data with well log parameters, Beaufort-Mackenzie Basin. *Geological Survey of Canada Open File*, **6042**.

Huang F, Jian C, Tang Y, Xu G, Deng Z, Chi G-C, Farrar CD (2004) Response changes of some wells in the mainland subsurface fluid monitoring network of China, due to the September 21 1999, M_s7.6 Chi-Chi earthquake. *Tectonophysics*, **390**, 217–234.

Huang R, Audétat A (2012) The titanium-in-quartz (TitaniQ) thermobarometer: a critical examination and re-calibration. *Geochimica et Cosmochimica Acta*, **84**, 75–89.

Hubbert MK (1940) The theory of ground-water motion. *The Journal of Geology*, **48**, 785–944.

Huber C, Chopard B, Manga M (2010) A lattice Boltzmann model for coupled diffusion. *Journal of Computational Physics*, **229**, 7956–7976.

Huber C, Parmigiani A, Chopard B, Manga M, Bachmann O (2008) Lattice Boltzmann model for melting with natural convection. *International Journal of Heat and Fluid Flow*, **29**, 1469–1480.

Huber C, Su Y (2015) A pore-scale investigation of the dynamic response of saturated porous media to transient stresses. *Geofluids*, **15**, 11–23.

Hudson JA, Bäckstrom A, Rutqvist J, Jing L (2008) DECOVALEX-THMC Project, Task B, Understanding and characterizing the excavation disturbed zone, Final Report (EDZ Guidance Document) characterizing and modelling the Excavation damaged Zone (EDZ) in crystalline rocks in the context of radioactive waste disposal. *SKI Report*, **43**.

Huenges E, Erzinger J, Kück J, Engeser B, Kessels W (1997) The permeable crust: geohydraulic properties down to 9101 m depth. *Journal of Geophysical Research*, **102**, 18255–18265.

Hulen JB, Lutz SJ (1999) Altered volcanic rocks as hydrologic seals on the geothermal system of Medicine Lake volcano, California. *Geothermal Resources Council Bulletin*, **7**, 217–222.

Humphris SE, Cann JR (2000) Constraints on the energy and chemical balances of the modern TAG and ancient Cyprus seafloor sulfide deposits. *Journal of Geophysical Research*, **105**, 28477–28488.

Hunt JM (1990) Generation and migration of petroleum from abnormally pressured fluid compartments. *American Association of Petroleum Geologists Bulletin*, **74**, 1–12.

Hüpers A, Kopf AJ (2012) Data report: Consolidation properties of silty claystones and sandstones sampled seaward of the Nankai Trough subduction zone, IODP Sites C0011 and C0012. In Saito S, Underwood MB, Kubo Y, and the Expedition 322 Scientists, *Proceedings of the Integrated Ocean Drilling Program*, **322**, 1–23.

Hurwitz S, Lowenstern JB, Heasler H (2007) Spatial and temporal geochemical trends in the hydrothermal system of Yellowstone National Park: inferences from river solute fluxes. *Journal of Volcanology and Geothermal Research*, **162**, 149–171.

Husen S, Taylor R, Smith RB, Healser H (2004a) Changes in geyser eruption behavior and remotely triggered seismicity in Yellowstone National Park produced by the 2002 M_w7.9 Denali fault earthquake, Alaska. *Geology*, **32**, 537–540.

Husen S, Wiemer S, Smith RB (2004b) Remotely triggered seismicity in the Yellowstone National Park region by the 2002 M_w7.9 Denali fault earthquake, Alaska. *Bulletin of the Seismological Society of America*, **94**, S317–S331.

Hutnak M, Hurwitz S, Ingebritsen SE, Hsieh PA (2009) Numerical models of caldera deformation: effects of multiphase and multicomponent hydrothermal fluid flow. *Journal of Geophysical Research*, **114**, B04411, doi:10.1029/2008JB006151.

Huuse M, Jackson CAL, Van Rensbergen P, Davies RJ, Flemings PB, Dixon RJ (2010) Subsurface sediment remobilization and fluid flow in sedimentary basins: an overview. *Basin Research*, **22**, 342–360.

IAPWS (1997) Release on the IAPWS industrial formulation 1997 for the thermodynamic properties of water and steam. The International Association for the Properties of Water and Steam, Lucerne, Switzerland.

Ichikawa Y, Selvadurai APS (2012) *Transport Phenomena in Porous Media: Aspects of Micro/Macro Behaviour*. Springer Verlag, Berlin.

Ienaga M, McNeill LC, Mikada H, Saito S, Goldberg D, Moore JC (2006) Borehole image analysis of the Nankai accretionary wedge, ODP Leg 196: structural and stress studies. *Tectonophysics*, **426**, 207–220.

Ikari MJ, Saffer DM (2012) Permeability contrasts between sheared and normally consolidated sediments in the Nankai accretionary prism. *Marine Geology*, **295–298**, 1–13.

Illies JH (1972) The Rhine graben rift system-plate tectonics and transform faulting. *Geophysical Surveys*, **1**, 27–60.

Ingebritsen SE, Geiger S, Hurwitz S, Driesner T (2010) Numerical simulation of magmatic hydrothermal systems. *Reviews of Geophysics*, **48**, RG1002.

Ingebritsen SE, Gleeson T (2015) Crustal permeability: introduction to the special issue. *Geofluids*, **15**, 1–10.

Ingebritsen SE, Manning CE (1999) Geological implications of a permeability-depth curve for the continental crust. *Geology*, **27**, 1107–1110.

Ingebritsen SE, Manning CE (2002) Diffuse fluid flux through orogenic belts: implications for the world ocean. *Proceedings of the National Academy of Sciences USA*, **99**, 9113–9116.

Ingebritsen SE, Manning CE (2010) Permeability of the continental crust: dynamic variations inferred from seismicity and metamorphism. *Geofluids*, **10**, 193–205.

Ingebritsen SE, Sanford W, Neuzil CE (2006) *Groundwater in Geologic Processes*, 2nd edn Cambridge University Press, Cambridge, UK.

Institute of Geophysics-CAS (China Earthquake Administration) (1976) *China Earthquake Catalog*. Center for Chinese Research Material, Washington, DC (in Chinese).

Ishibashi T, McGuire TP, Watanabe N, Tsuchiya N, Elsworth D (2013) Permeability evolution in carbonate fractures: competing roles of confining stress and fluid pH. *Water Resources Research*, **49**, 2828–2842, doi:10.1002/wrcr.20253.

Ishibashi T, Watanabe N, Hirano N, Okamoto A, Tsuchiya N (2012) GeoFlow: a novel model simulator for prediction of the 3-D channeling flow in a rock fracture network. *Water Resources Research*, **48**, W07601, doi:10.1029/2011WR011226.

Ishibashi T, Watanabe N, Hirano N, Okamoto A, Tsuchiya N (2015) Beyond-laboratory-scale prediction for channeling flows through subsurface rock fractures with heterogeneous aperture distributions revealed by laboratory evaluation. *Journal of Geophysical Research*, **120**, doi:10.1002/2014JB011555.

Itaba S, Koizumi N, Matsumoto N, Takahashi M, Sato T, Ohtani R, Kitagawa Y, Kuwahara Y, Ozawa K (2008) Groundwater level changes related to the ground shaking of the Noto Hanto Earthquake in 2007. *Earth, Planets and Space*, **60**, 1153–1159.

Itasca (2013) *UDEC 5.0 Universal Distinct Element Code*. Itasca Consulting Group Incorporated, Minneapolis, Minnesota.

Iwai K (1976) Fundamental studies of fluid flow through a single fracture. PhD thesis, University of California, Berkeley.

Iwatsuki T, Yoshida H (1999) Groundwater chemistry and fracture mineralogy in the basement granite rock in the Tono uranium mine area, Gifu Prefecture, Japan – Groundwater composition, Eh evolution analysis by fracture filling minerals. *Geochemical Journal*, **33**, 19–32.

Izawa E, Urashima Y, Ibaraki K, Suzuki R, Yokoyama T, Kawasaki K, Koga A, Taguchi S (1990) The Hishikari gold deposit – High-grade epithermal veins in Quaternary volcanics of southern Kyushu, Japan. *Journal of Geochemical Exploration*, **36**, 1–56.

Jaeger JC (1971) Friction of rocks and stability of rock slopes. *Geotechnique*, **21**, 97–134.

Jaeger JC, Cook NGW, Zimmerman RW (2007) *Fundamentals of Rock Mechanics*, 4th edn Blackwell, Maiden, MA.

Jafari MK, Pellet F, Boulon MJ, Amini Hosseini K (2004) Experimental study of mechanical behaviour of rock joints under cyclic loading. *Rock Mechanics and Rock Engineering*, **37**, 3–23.

Jakob A, Mazurek M, Heer W (2003) Solute transport in crystalline rocks at Aspo, II, Blind predictions, inverse modelling and lessons learnt from test STT1. *Journal of Contaminant Hydrology*, **6**, 175–190.

Jamtveit B, Putnis CV, Malthe-Sorenssen A (2009) Reaction induced fracturing during replacement processes. *Contributions to Mineralogy and Petrology*, **157**, 127–133.

Japan Beyond Brittle Project (2014) Japan Beyond Brittle Project. URL: http://jbbp.kankyo.tohoku.ac.jp/JBBP/outline.html accessed 06 May 2016.

Japsen P, Dysthe DK, Hartz EH, Stipp SLS, Yarushina VM, Jamtveit B (2011) A compaction front in North Sea chalk. *Journal of Geophysical Research*, **116**, B11208.

Jeffrey RG, Bunger A, Lecampion B, Zhang X, Chen ZR, van As A, Allison DP, de Beer W, Dudley JW, Siebrits E, Thiercelin M, Mainguy M (2009) Measuring hydraulic fracture growth in naturally fractured rock. SPE Annual Technical Conference and Exhibition, 4-7 October, New Orleans, Louisiana, http://dx.doi.org/10.2118/124919-MS, accessed 06 May 2016.

Jenner GA, Cawood PA, Rautenschlein M, White WM (1987) Composition of back-arc basin volcanics, Valu Fa Ridge, Lau Basin – Evidence for a slab-derived component in their mantle source. *Journal of Volcanology and Geothermal Research*, **32**, 209–222.

Jerram DA, Widdowson M (2005) The anatomy of continental flood basalt provinces: geological constraints on the processes and products of flood volcanism. *Lithos*, **79**, 385–405.

Jiang T, Peng Z, Wang W, Chen Q-F (2010a) Remotely triggered seismicity in continental China following the 2008 M_w7.9 Wenchuan earthquake. *Bulletin of the Seismological Society of America*, **100**, 2574–2589.

Jiang X-W, Wan L, Cardenas MB, Ge S, Wang X-S (2010b) Simultaneous rejuvenation and aging of groundwater in basins due to depth-decaying hydraulic conductivity and porosity. *Geophysical Research Letters*, **37**, L05403.

Jiang X-W, Wan L, Wang XS, Liang SH, Hu BX (2009) Estimation of fracture normal stiffness using a transmissivity-depth correction. *International Journal of Rock Mechanics and Mining Sciences*, **46**, 51–58.

Jiang X-W, Wang X-S, Wan L (2010c) Semi-empirical equations for the systematic decrease in permeability with depth in porous and fractured media. *Hydrogeology Journal*, **18**, 839–850.

Jing Z, Richards JW, Watanabe K, Hashida T (2000) A three-dimensional stochastic rock mechanics model of engineered geothermal systems in fractured crystalline rock. *Journal of Geophysical Research,* **105**, 23663–23679, doi:10.1029/2000JB900202.

John DA, Hofstra AH, Fleck RJ, Brummer JE, Saderholm EC (2003) Geologic setting and genesis of the mule canyon low-sulfidation epithermal gold-silver deposit, north-central Nevada. *Economic Geology*, **98**, 425–463.

John DA, Wrucke CT (2003) Geologic map of the Mule Canyon quadrangle, Lander County, Nevada. *Nevada Bureau of Mines and Geology Map*, **144**.

Johnson DL, Koplik J, Dashen R (1987) Theory of dynamic permeability and tortuosity in fluid-saturated porous media. *Journal of Fluid Mechanics*, **176**, 379–402.

Jones BL (1987) Conventional core analysis studies for TNO-DGV, Institute of Applied Geoscience on well Asten 2. Technical report, Redwood Corex, Sassenheim.

Jones JB, Mulholland PJ (eds) (2000) *Streams and Ground Waters*. Academic Press, San Diego.

Jones ME, Addis MA (1985) On changes in porosity and volume during burial of argillaceous sediments. *Marine and Petroleum Geology*, **2**, 247–253.

Jónsson S, Segall P, Pedersen R, Björnsson G (2003) Post-earthquake ground movements correlated to pore-pressure transients. *Nature*, **424**, 179–183.

Joshi A, Appold MS, Nunn JA (2012) Evaluation of solitary waves as a mechanism for oil transport in poroelastic media: a case study of the South Eugene Island field, Gulf of Mexico basin. *Marine and Petroleum Geology*, **37**, 53–69.

Jowitt SM, Jenkin GRT, Coogan LA, Naden J (2012) Quantifying the release of base metals from source rocks for volcanogenic massive sulfide deposits: effects of protolith composition and alteration mineralogy. *Journal of Geochemical Exploration*, **118**, 47–59.

Juhlin C, Sandstedt H (1989) Storage of nuclear waste in very deep boreholes: feasibility study and assessment of economic potential. In: *SKB Technical Report*, **89-39** (ed SKB), SKB, Stockholm, Sweden, http://www.skb.se/upload/publications/pdf/TR89-39webb.pdf accessed 06 May 2016.

Juhlin C, Wallroth T, Smellie J, Eliasson T, Ljunggren C, Leijon B, Beswick J (1998) The very deep hole concept – Geoscientific appraisal of conditions at great depth. *SKB Technical Report*, **98-05**.

Jung R (2013) EGS – Goodbye or Back to the Future. In: *Effective and Sustainable Hydraulic Fracturing* (eds Bunger A, McLennan J, Jeffrey R), pp. 95–121, InTech, Rijeka, Croatia.

Jupp T, Schultz A (2000) A thermodynamic explanation for black smoker temperatures. *Nature*, **403**, 880–883.

Juteau T, Manac'h O, Lécuyer C, Ramboz C (2000) The high-temperature reaction zone of the Oman ophiolite: new field data, micro thermometry of fluid inclusions, PIXE analyses and oxygen isotopic ratios. *Marine Geophysical Researches*, **21**, 351–385.

Kahle SC, Morgan DS, Welch WB, Ely DM, Hinlde SR, Vaccaro JJ, Orzol LL (2011) Hydrogeologic framework and hydrologic budget components of the Columbia Plateau Regional Aquifer System, Washington, Oregon, and Idaho. *U.S. Geological Survey Scientific Investigations Report*, **2011–5124**, http://pubs.er.usgs.gov/publication/sir20115124 accessed 06 May 2016.

Kahle SC, Olsen TD, Morgan DS (2009) Geologic setting and hydrogeologic units of the Columbia Plateau Regional Aquifer System, Washington, Oregon, and Idaho. *U.S. Geological Survey Scientific Investigations Map*, **3088**, http://pubs.er.usgs.gov/usgspubs/sim/sim3088 accessed 06 May 2016.

Kaieda H, Jones R, Moriya H, Sasaki S, Ushijima K (2005) Ogachi HDR reservoir evaluation by AE and geophysical methods, In: *Proceedings of World Geothermal Congress 2005*, 24–29 April, Antalya, Turkey.

Kaiser AE, Holden C, Beavan RJ, Beetham RD, Benites RA, Celentano A, Collet D, Cousins WJ, Cubrinovski M, Dellow GD, Denys P, Fielding E, Fry B, Gerstenberger MC, Langridge RM, Massey CI, Motagh M, Pondard N, McVerry GH, Ristau J, Stirling MW, Thomas J, Uma SR, Zhao JX (2012) The M_w6.2 Christchurch Earthquake of February 2011: preliminary report. *New Zealand Journal of Geology and Geophysics*, **55**, 67–90.

Kaiser P, Valley B, Dusseault M, Duff D (2013) Hydraulic fracturing mine back trials – Design rationale and project status, http://dx.doi.org/10.5772/56260 accessed 06 May 2016.

Kameyama M, Yuen DA, Karato SI (1999) Thermal-mechanical effects of low-temperature plasticity (the Peierls mechanism) on the deformation of a viscoelastic shear zone. *Earth and Planetary Science Letters*, **168**, 159–172.

Kanamori H, Anderson DL (1975) Theoretical basis of some empirical relations in seismology. *Bulletin of the Seismological Society of America*, **65**, 1073–1095.

Kano Y, Yanagidani T (2006) Broadband hydroseismograms observed by closed borehole wells in the Kamioka mine, central Japan: response of pore pressure to seismic waves from 0.05 to 2 Hz. *Journal of Geophysical Research*, **111**, B03410.

Karig DE (1990) Experimental and observational constraints on the mechanical behaviour in the toes of accretionary prisms. *Geological Society London Special Publication*, **54**, 383–398.

Karig DE, Lundberg N (1990) Deformation bands from the toe of the Nankai accretionary prism. *Journal of Geophysical Research*, **95**, 9099–9109.

Karingithi C (2009) Chemical geothermometers for geothermal exploration. *Short Course IV on Exploration for Geothermal Resources, organized by UNU-GTP, KenGen and GDC.*

Karnis A, Goldsmith HL, Mason SG (1966) Kinetics of flowing dispersions, I, Concentrated suspensions of rigid particles. *Journal of Colloid and Interface Science*, **22**, 531–553.

Kastner M, Elderfield H, Martin JB (1991) Fluids in convergent margins: what do we know about their composition, origin, role in diagenesis and importance for oceanic chemical fluxes? *Philosophical Transactions of the Royal Society Series A*, **335**, 243–259.

Kaszuba J, Yardley BWD, Andreani M (2013) Experimental perspectives of mineral dissolution and precipitation due to carbon dioxide-water-rock interactions. *Reviews in Mineralogy & Geochemistry,* **77**, 153–188.

Kato A, Igarashi T, Obara K, Sakai S, Takeda T, Saiga A, Iidaka T, Iwasaki T, Hirata N, Goto K, Miyamachi H, Matsushima T, Kubo A, Katao H, Yamanaka Y, Terakawa T, Nakamichi H, Okuda T, Horikawa S, Tsumura N, Umino N, Okada T, Kosuga M, Takahashi H, Yamada T (2013) Imaging the source regions of normal faulting sequences induced by the 2011 M9.0 Tohoku-Oki earthquake. *Geophysical Research Letters*, **40**, 273–278.

Katz RF (2008) Magma dynamics with the enthalpy method: benchmark solutions and magmatic focusing at mid-ocean ridges. *Journal of Petrology*, **49**, 2099–2121.

Kay MA, Main IG, Elphick SC, Ngwenya BT (2006) Fault gouge diagenesis at shallow burial depth: solution-precipitation reactions in well-sorted and poorly sorted powders of crushed sandstone. *Earth and Planetary Science Letters*, **243**, 607–614.

Keller GV, Grose LT, Murray JC, Skokan CK (1979) Results of an experimental drill hole at the summit ol Kilauea Volcano, Hawaii. *Journal of Volcanology and Geothermal Research*, **5**, 345–385.

Kelley DS, Carbotte SM, Caress DW, Clague DA, Delaney JR, Gill JB, Hadaway H, Holden JF, Hooft EEE, Kellogg JP, Lilley MD, Stoermer M, Toomey D, Weeldy R, Wilcock WSD (2012) Endeavour Segment of the Juan de Fuca Ridge: one of the most remarkable places on Earth. *Oceanography*, **25**, 44–61.

Kelley SA, Chapin CE (1997) Cooling histories of mountain ranges in the southern Rio Grande Rift based on apatite fission-track analysis – a reconnaissance survey. *New Mexico Geology*, **19**, 1–14.

Kempe S (1979) Carbon in the rock cycle. In: *The Global Carbon Cycle* (eds Bolin B, Degens ET, Kempe S, Ketner P), pp. 343–375. Scientific Committee on Problems of the Environment (SCOPE), Old Woking, UK.

Kemp SJ, Wagner D (2006) The mineralogy, geochemistry and surface area of mudrocks from the London Clay Formation of southern England. *British Geological Survey Physical Hazards Programme Internal Report*, **IR/06/060**, Nottingham, UK.

Kennedy BM, van Soest MC (2007) Flow of mantle fluids through the ductile lower crust: helium isotope trends. *Science*, **318**, 1433–1436.

Kennett JP (1982) *Marine Geology*. Prentice Hall, Englewood Cliffs, NJ.

Kern LR, Perkins TK, Wyant RE (1959) The mechanics of sand movement in fracturing. *Transactions of the American Institute of Mining and Metallurgical Engineers*, **216**, 403–405.

Kesler SE (1994) *Mineral Resources, Economics and the Environment*. Macmillan Publishing, New York.

Kestin J, Khalifa HE, Correia RJ (1981) Tables of the dynamic and kinematic viscosity of aqueous KCl solutions in the temperature range 25–l50°C and the pressure range 0.1–35 MPa. *Journal of Physical and Chemical Reference Data*, **10**, 57–70.

Khilar KC, Fogler HS (1998), *Migrations of Fines in Porous Media*. Kluwer Academic Publishers, Boston, Dordrecht.

Kidd RGW (1977) A model for the process of formation of the upper oceanic crust. *Geophysical Journal of the Royal Astronomical Society*, **50**, 149–183.

Kidd RGW, Cann JR (1974) Chilling statistics indicate an ocean-floor spreading origin for the Troodos complex, Cyprus. *Earth and Planetary Science Letters*, **24**, 151–155.

Kim ST, O'Neil JR (1997) Equilibrium and nonequilibrium oxygen isotope effects in synthetic carbonates. *Geochimica et Cosmochimica Acta*, **61**, 3461–3475.

Kim Y-S, Peacock DCP, Sanderson DJ (2004) Fault damage zones. *Journal of Structural Geology*, **26**, 503–517.

King C-Y, Azuma S, Igarashi G, Ohno M, Saito H, Wakita H (1999) Earthquake-related water level changes at 16 closely clustered wells in Tono, central Japan. *Journal of Geophysical Research*, **104**, 13073–13082.

King C-Y, Basler D, Presser TS, Evans CW, White LD, Minissale AD (1994a) In search of earthquake-related hydrologic and chemical changes along the Hayward fault. *Applied Geochemistry*, **9**, 83–91.

King GC, Stein RS, Lin J (1994b) Static stress changes and the triggering of earthquakes. *Bulletin of the Seismological Society of America*, **84**, 567–585.

Kinoshita M, Tobin H, Ashi J, Kimura G, Lallemant S, Screaton EJ, Curewitz D, Masago H, Moe KT, the Expedition 314/315/316 Scientists (2009) Proceedings of the Integrated Ocean Drilling Program, **314/315/316**.

Király L (1969) Anisotropy and heterogeneity within jointed limestone. *Eclogae Geologicae Helvetiae*, **62**, 613–619.

Kita I, Taguchi S, Matsubaya O (1985) Oxygen isotope fractionation between amorphous silica and water at 34–93°C. *Nature*, **314**, 83–84.

Kitagawa Y, Fujimoro K, Koizumi N (2007) Temporal change in permeability of the Nojima fault zone by repeated water injection experiments. *Tectonophysics*, **443**, 183–192.

Kitajima H, Chester FM, Biscontin G (2012) Mechanical and hydraulic properties of Nankai accretionary prism sediments: effect of stress path. *Geochemistry, Geophysics, Geosystems*, **13**, Q0AD27.

Kitajima H, Saffer DM (2012) Elevated pore pressure and anomalously low stress in regions of low frequency earthquakes along the Nankai Trough subduction megathrust. *Geophysical Research Letters*, **39**, L23301.

Kiyama T, Kita H, Ishijima Y, Yanagidani T, Akoi K, Sato T (1996) Permeability in anisotropic granite under hydrostatic compression and tri-axial compression including post-failure region. *Proceedings 2nd North American Rock Mechanics Symposium,* 1643-50.

Knoll MD (1996) A petrophysical basis for ground penetrating radar and very early time electromagnetics: Electrical properties of sand-clay mixtures. PhD thesis, The University of British Columbia.

Knoll MD, Knight R (1994) Relationships between dielectric and hydrogeologic properties of sand-clay mixtures. *Proceedings of the Fifth International Conference on Ground Penetrating Radar,* **1**, 12–16.

Kodaira S, Iidaka T, Kato A, Park JO, Iwasaki T, Kaneda Y (2004) High pore fluid pressure may cause silent slip in the Nankai trough. *Science*, **304**, 1295–1298.

Koerner A, Kissling E, Miller SA (2004) A model of deep crustal fluid flow following the $M_w = 8.0$ Antofagasta, Chile, earthquake. *Journal of Geophysical Research*, 109, doi:10.1029/2003JB002816.

Koh J, Rosnhan H, Rahman SS (2011) A numerical study on the long term thermo-poroelastic effects of cold water injection into naturally fractured geothermal reservoirs. *Computers and Geotechnics*, **38**, 669–682.

Kohl T, Megel T (2005), Coupled hydro-mechanical modelling of the GPK3 reservoir stimulation at the European EGS site, Soultz-sous-Forêts. *Proceedings of the Thirtieth Workshop on Geothermal Reservoir Engineering*, Stanford University, Stanford, California.

Kohlstedt DL, Evans B, Mackwell SJ (1995) Strength of the lithosphere – constraints imposed by laboratory experiments. *Journal of Geophysical Research,* **100**, 17587–17602.

Koiter WT (1953) Stress-strain relations, uniqueness and variational theorems for elastic-plastic materials with a singular yield surface. *Quarterly of Applied Mathematics*, **11**, 350–354.

Koizumi N, Lai WC, Kitagawa Y, Matsumoto N (2004) Comment on "Coseismic hydrological changes associated with dislocation of the September 21, 1999 Chichi earthquake, Taiwan" by Min Lee et al. *Geophysical Research Letters*, **31**, L13603, doi:10.1029/2004GL019897.

Kolditz O (1995) Modeling flow and heat transfer in fractured rocks – Conceptual model of a 3-D Deterministic fracture network. *Geothermics*, **24**, 451–470.

Koltermann CE, Gorelick SM (1995) Fractional packing model for hydraulic conductivity derived from sediment mixtures. *Water Resources Research*, **31**, 3283–3297.

Kondo H, Kimura G, Masago H, Ohmori-Ikehara K, Kitamura Y et al. (2005) Deformation and fluid flow of a major out-of-sequence thrust located at seismogenic depth in an accretionary complex: Nobeoka thrust in the Shimanto Belt, Kyushu, Japan. *Tectonics*, **24**, TC6008.

Konikow LF, Kendy E (2005) Groundwater depletion: a global problem. *Hydrogeology Journal,* **13**, 317–320.

Konzuk JS, Kueper BH (2004) Evaluation of cubic law based models describing single-phase flow through a rough-walled fracture. *Water Resources Research*, **40**, W02402.

Koons PO (1987) Some thermal and mechanical consequences of rapid uplift: an example from the Southern Alps, New Zealand. *Earth and Planetary Science Letters*, **86**, 307–319.

Koons PO (1989) The topographic evolution of collisional mountain belts: a numerical look at the Southern Alps, New Zealand. *American Journal of Science*, **289**, 1041–1069.

Koons PO (1994) Three-dimensional critical wedges: tectonics and topography in oblique collisional zones. *Journal of Geophysical Research*, **99**, 12301–12305.

Koons PO, Craw D (1991) Evolution of fluid driving forces and composition within collisional orogens. *Geophysical Research Letters*, **18**, 935–938.

Koons PO, Craw D, Cox SC, Upton P, Templeton AS, Chamberlain CP (1998) Fluid flow during active oblique convergence: a Southern Alps model from mechanical and geochemical observations. *Geology*, **26**, 159–162.

Koons PO, Norris RJ, Craw D, Cooper AF (2003) Influence of exhumation on the structural evolution of transpressional plate boundaries: an example from the Southern Alps, New Zealand. *Geology*, **31**, 3–6.

Kopf A, Strasser M, Monsees N, Underwood MB, Guo J (2011) Data report: Particle size analysis of sediments recovered during IODP Expeditions 315 and 316, Sites C0001–C0008, Nankai Trough forearc, off Japan. In Kinoshita M, Tobin H, Ashi J, Kimura G, Lallemant S, Screaton EJ, Curewitz D, Masago H, Moe KT, and the Expedition 314/315/316 Scientists, *Proceeding Integrated Ocean Drilling Program*, **314/315/316**, 1–19.

Kopp C, Fruehn J, Flueh ER, Reichert C, Kukowski N, Bialas J, Klaeschen D (2000) Structure of the Makran subduction zone from wide-angle and reflection seismic data. *Tectonophysics*, **329**, 171–191.

Korzhinskii DS (1959) *Physicochemical Basis of the Analysis of the Paragenesis of Minerals*. Consultants Bureau, New York.

Korzhinskii DS (1965) The theory of systems with perfectly mobile components and processes of mineral formation. *American Journal of Science,* **263**, 193–205.

Korzhinskii DS (1970) *Theory of Metasomatic Zoning*. Oxford University Press, Oxford.

Kosuga M, Watanabe K, Hashimoto K, Kasai H (2012) Seismicity in the northern part of Tohoku District induced by the 2011 off the Pacific Coast of Tohoku earthquake. *Zisin (Journal of the Seismological Society of Japan 2nd series)*, **65**, 69–83.

Kothe DB, Rider WJ (1995) A comparison of interface tracking methods. *Proceedings 26th American Institute of Aeronautics and Astronautics (AIAA) Computational Fluid Dynamics Conference*, 19–22 June, San Diego, California.

Kozeny J (1927) Ueber kapillare leitung des wassers im boden. *Sitzungsberichte Akademie der Wissenschaften Wien*, **136**, 271–306.

Krieger IM, Dougherty TJ (1959) A mechanism for non-Newtonian flow in suspensions of rigid spheres. *Transactions of the Society of Rheology*, **3**, 137–152.

Krusemann GP, de Ridder NA (1991) Analysis and evaluation of pumping test data. *International Institute for Land Reclamation and Improvement Publication*, **47**.

Kühn M (2004) *Reactive Flow Modeling of Hydrothermal Systems*. Springer, Berlin, Heidelberg, New York.

Kukkonen IK (1995) Thermal aspects of groundwater circulation in bedrock and its effect on crustal geothermal modelling in Finland, the central Fennoscandian Shield. *Tectonophysics*, **244**, 119–136.

Kumar S, Bodvarsson GS (1990) Fractal study and simulation of fracture roughness. *Geophysical Research Letters,* **17**, 701–704.

Kwon O, Kronenberg AK, Gangi AF, Johnson B, Herbert BE (2004) Permeability of illite-bearing shale, 1, Anisotropy and effects of clay content and loading. *Journal of Geophysical Research,* **109**, B10205.

Lachenbruch AH, Sass JH (1977) Heat flow in the United States and the thermal regime of the crust. *American Geophysical Union Geophysical Monograph Series*, **20**, 626–675.

Labaume P, Kastner M, Trave A, Henry P (1997a) Carbonate veins from the décollement zone at the toe of the northern Barbados accretionary prism: microstructure, mineralogy, geochemistry, and relations with prism structures and fluid regime. In: *Proceedings of the Ocean Drilling Program, Scientific Results*, **156**, (eds Shipley TH, Ogawa Y, Blum P, Bahr JM), pp. 79–96, Ocean Drilling Program, College Station, TX.

Labaume P, Maltman AJ, Bolton A, Tessier D, Ogawa Y, Takizawa S (1997b) Scaly fabrics in sheared clays from the décollement zone of the Barbados accretionary prism. In: *Proceedings of the Ocean Drilling Program, Scientific Results*, **156**, (eds Shipley TH, Ogawa Y, Blum P, Bahr JM), pp. 59–77, Ocean Drilling Program, College Station, TX.

Ladanyi B, Archambault G (1970) Simulation of shear behaviour of a jointed rock mass. *Proceedings 11th Symposium on Rock Mechanics,* American Institute of Mechanical Engineers, New York.

Lai G, Ge H, Xue L, Brodsky EE, Huang F, Wang W (2014) Tidal response variation and recovery following the Wenchuan earthquake from water level data of multiple wells in the near field. *Tectonophysics*, **619–620**, 115–122.

Lai WC, Koizumi N, Matsumoto N, Kitagawa Y, Lin CW, Shieh CL, Lee YP (2004) Effects of seismic ground motion and geological setting on the coseismic groundwater level changes caused by the 1999 Chi-Chi earthquake, Taiwan. *Earth, Planets, and Space*, **56**, 873–880.

Landtwing MR, Pettke T, Halter WE, Heinrich CA, Redmond PB, Einaudi MT, Kunze K (2005) Copper deposition during quartz dissolution by cooling magmatic-hydrothermal fluids: the Bingham porphyry. *Earth and Planetary Science Letters*, **235**, 229–243.

Lauer RM, Saffer DM (2012) Fluid budgets of subduction zone forearcs: the contribution of splay faults. *Geophysical Research Letters*, **39**, LI3604.

Lecampion B, Garagash D (2014) Confined flow of suspensions modeled by a frictional rheology. *Journal of Fluid Mechanics*, **759**, 199–235.

Lecumberri-Sanchez P, Steele-MacInnis M, Weis P, Driesner T, Bodnar RJ (2015) Salt precipitation in magmatic-hydrothermal systems associated with upper crustal plutons. *Geology*, **43**, G37163-1, doi:10.1130/G37163.1.

Lee HS, Cho TF (2002) Hydraulic characteristics of rough fractures in linear flow under normal and shear load. *Rock Mechanics and Rock Engineering*, **35**, 299–318.

Lee S-G, Kim T-K, Lee TJ (2011) Strontium isotope geochemistry and its geochemical implication from hot spring waters in South Korea. *Journal of Volcanology and Geothermal Research*, **208**, 12–22.

Leonard M (2010) Earthquake fault scaling: self-consistent relating of rupture length, width, average displacement, and moment release. *Bulletin of the Seismological Society of America*, **100**, 1971–1988.

Le Pichon X, Henry P, Lallemant S (1990) Water flow in the Barbados accretionary complex. *Journal of Geophysical Research*, **95**, 8945–8967.

Leroueil S, Bouclin G, Tavenas F, Bergeron L, La Rochelle P (1990) Permeability anisotropy of clays as a function of strain. *Canadian Geotechnical Journal*, **27**, 568–579.

Leroy P, Revil A (2004) A triple-layer model of the surface electrochemical properties of clay minerals. *Journal of Colloid and Interface Science,* **270**, 371–380.

Li L, Unsworth MJ, Booker JR, Wei W, Tan H, Jones AG (2003) Partial melt or aqueous fluid in the mid-crust of Southern Tibet? Constraints from INDEPTH magnetotelluric data. *Geophysical Journal International*, **153**, 289–304.

Li Y-G, Ellsworth WL, Thurber CH, Malin PE, Aid K (1997) Fault-zone guided waves from explosions in the San Andreas fault at Parkfield and Cienega Valley, California. *Bulletin of the Seismological Society of America*, **87**, 210–221.

Lilliefors HW (1967) On the Kolmogorov-Smirnov test for normality with mean and variance unknown. *Journal of the American Statistical Association*, **62**, 399–402.

Lin J, Stein RS (2004) Stress triggering in thrust and subduction earthquakes and stress interaction between the southern San Andreas and nearby thrust and strike-slip faults. *Journal of Geophysical Research*, **109**, B02303.

Lin W, Takahashi M, Nakamura T, Fujii Y (2008) Tensile strength and deformability of Inada Granite and their anisotropy: comparison between uniaxial tension test and Brazilian test. *Japanese Geotechnical Journal*, **3**, 165–173.

Lin WN, Daily W (1990) Hydrological properties of Topopah spring tuff under a thermal-gradient-laboratory results. *International Journal of Rock Mechanics and Mining Sciences,* **27**, 373–386.

Lindberg A, Siitari-Kauppi M (1998) Shear zone-related hydrothermal alteration in Proterozoic rocks in Finland. *9th International Symposium on Water-Rock Interaction*, **WRI-9**, 413-6.

Lister CRB (1974) On the penetration of water into hot rock. *Geophysical Journal International,* **39**, 465–509.

Litchfield NJ, Van DR, Sutherland R, Barnes PM, Cox SC, Norris RJ, Beavan RJ, Langridge RM, Villamor P, Berryman KR, Stirling MW, Nicol A, Nodder SD, Lamarche G, Barrell DJA, Pettinga JR, Little TA, Pondard N, Clark KJ (2013) A model of active faulting in New Zealand. *New Zealand Journal of Geology and Geophysics*, **57**, 32–56.

Little CTS, Cann JR, Herrington RJ, Morisseau M (1999) Late Cretaceous hydrothermal vent communities from the Troodos ophiolite, Cyprus. *Geology*, **27**, 1027–1030.

Little TA, Cox SC, Vry JK, Batt G (2005) Variations in exhumation level and uplift rate along the oblique-slip Alpine Fault, central Southern Alps, New Zealand. *Geological Society of America Bulletin*, **117**, 707–723.

Liu G, Zheng C, Gorelick SM (2007) Evaluation of the applicability of the dual-domain mass transfer model in porous media containing connected high-conductivity channels. *Water Resources Research*, **43**, W12407.

Liu H-H, Rutqvist J, Berryman JC (2009) On the relationship between stress and elastic strain for porous and fractured rock. *International Journal of Rock Mechanics and Mining Sciences*, **46**, 289–296.

Liu H-H, Wei M-Y, Rutqvist J (2013) Normal-stress dependence of fracture hydraulic properties including two-phase flow properties. *Hydrogeology Journal*, **21**, 371–382.

Liu LB, Roeloffs E, Zheng XY (1989) Seismically induced water level fluctuations in the Wali well, Beijing, China. *Journal of Geophysical Research*, **94**, 9453–9462.

Liu WQ, Manga M (2009) Changes in permeability caused by dynamic stresses in fractured sandstone. *Geophysical Research Letters*, **36**, L20307.

Liu WQ, Wang CH, Hwang LS (2010) Temporal variation of seepage water chemistry before and after the Hengchun M_s7.2 earthquake in south Taiwan. *Geoderma*, **155**, 107–114.

Liu Y, Rice JR (2007) Spontaneous and triggered aseismic deformation transients in a subduction fault model. *Journal of Geophysical Research*, **112**, B09404.

Long H, Flemings PB, Germaine JT, Saffer DM (2011) Consolidation and overpressure near the seafloor in the Ursa Basin, deepwater Gulf of Mexico. *Earth and Planetary Science Letters,* **305**, 11–20.

Long JCS, Remer JS, Wilson CR, Witherspoon PA (1982a) Porous media equivalents for networks of discontinuous fractures. *Water Resources Research,* **18**, 645–658.

Long JJ, Imber J (2011) Geological controls on fault relay zone scaling. *Journal of Structural Geology*, **33**, 1790–1800.

Long PE, Apted MJ, Spane FA, Kim K (1982b) Geologic, geochemical, rock mechanics, and hydrologic characteristics of candidate repository horizons. Session II-B, BWIP Technology Review, Proceedings of the 1982 National Waste Terminal Storage Program Information Meeting. U.S. Department of Energy, DOE/NWTS-30, pp. 29–36.

Lopez DL, Smith L (1995) Fluid flow in fault zones: analysis of the interplay of convective circulation and topographically driven groundwater flow. *Water Resources Research*, **31**, 1489–1503.

Loucks RG, Dodge MM, Galloway WE (1984) Regional controls of diagenesis and reservoir quality in Lower Tertiary sandstones along the Texas Gulf Coast. In: *Clastic Diagenesis* (eds McDonald DA, Surdam RC), *American Association of Petroleum Geologists Memoir*, **37**, pp. 15–46, AAPG.

Louis C (1969) A study of groundwater flow in jointed rock and its influence on the stability of rock masses. Technical Report 9, Rock Mechanics, Imperial College, London, United Kingdom.

Louis C (1974) Rock hydraulics. In: *Rock Mechanics* (ed Muller L), pp. 299–387. Springer, Vienna.

Louis C, Dessenne JL, Feuga B (1977) Interaction between water flow phenomena and the mechanical behavior of soil or rock masses. In: *Finite Elements in Geomechanics* (ed Gudehus G), pp. 479–511. John Wiley & Sons, New York.

Lowell RP (1991) Modeling continental and submarine hydrothermal systems. *Reviews of Geophysics*, **29**, 457–476.

Lowell RP, Germanovich LN (2004) Hydrothermal processes at mid-ocean ridges: results from scale analysis and single-pass models. In: *Mid-Ocean Ridges: Hydrothermal Interactions between the Lithosphere and Oceans*, **148** (eds German CR, Lin J, Parson LM), pp. 219–244. American Geophysical Union, Washington, DC.

Lowell RP, Van Cappellen P, Germanovich LN (1993) Silica precipitation in fractures and the evolution of permeability in hydrothermal upflow zones. *Science*, **260**, 192–194.

Lowenstein TK, Timofeeff MO, Brennan ST, Hardie LA (2001) Oscillations in Phanerozoic seawater chemistry: evidence from fluid inclusions. *Science*, **294**, 1086–1088.

Lozinsky RP (1987) Cross-section across the Jornado del Muerto, Engle, and Northern Palomas Basins, south-central New Mexico. *New Mexico Geology*, **9**, 55–57.

Lucier A, Zoback M (2008) Assessing the economic feasibility of regional deep saline aquifer CO_2 injection and storage: a geomechanics-based workflow applied to the Rose Run sandstone in eastern Ohio, USA. *International Journal of Greenhouse Gas Control*, **2**, 230–247.

Luijendijk E (2012) The role of fluid flow in the thermal history of sedimentary basins: inferences from thermochronology and numerical modeling in the Roer Valley Graben, southern Netherlands. PhD thesis, Vrije Universiteit, Amsterdam.

Luijendijk E, Gleeson T (2015) How well can we predict permeability in sedimentary basins? Deriving porosity-permeability algorithms for non-cemented sand and clay mixtures. *Geofluids*, **15**, 67–83.

Luijendijk E, Ter Voorde M, Van Balen RT, Verweij H, Simmelink E (2011) Thermal state of the Roer Valley Graben, part of the European Cenozoic Rift System. *Basin Research*, **23**, 65–82.

Luthi S, Souhaité P (1990) Fracture apertures from electrical borehole scans. *Geophysics*, **55**, 821–833.

Lynn BA, Campbell KA, Moore J, Brown PRL (2008) Origin and evolution of the Steamboat Springs siliceous sinter deposit, Nevada, U.S.A. *Sedimentary Geology*, **210**, 111–131.

Lyon MK, Leal LG (1998a) An experimental study of the motion of concentrated suspensions in two-dimensional channel flow, Part 1, Monodisperse systems. *Journal of Fluid Mechanics*, **363**, 25–56.

Lyon MK, Leal LG (1998b) An experimental study of the motion of concentrated suspensions in two-dimensional channel flow, Part 2, Bidisperse systems. *Journal of Fluid Mechanics*, **363**, 57–77.

Lyubetskaya T, Ague JJ (2009) Modeling the magnitudes and directions of regional metamorphic fluid flow in collisional orogens. *Journal of Petrology*, **50**, 1505–1531.

Mader HM, Llewellin EW, Mueller SP (2013) The rheology of two-phase magmas: a review and analysis. *Journal of Volcanology and Geothermal Research*, **257**, 135–158.

Maher K, Chamberlain CP (2014) Hydrologic regulation of chemical weathering and the geologic carbon cycle. *Science*, **343**, 1502–1504.

Mahesh P, Kundu B, Catherine JK, Gahalaut VK (2011) Anatomy of the 2009 Fiordland earthquake (M_w7.8), South Island, New Zealand. *Geoscience Frontiers*, **2**, 17–22.

Mahyari AT, Selvadurai APS (1998) Enhanced consolidation in brittle geomaterials susceptible to damage. *Mechanics of Cohesive Frictional Materials*, **3**, 291–303.

Mailloux B, Person M, Kelley S, Dunbar N, Cather S, Strayer L, Hudleston P (1999) Tectonic controls on the hydrogeology of the Rio Grande Rift, New Mexico. *Water Resources Research*, **35**, 2641–2659.

Makurat A, Barton N, Rad NS, Bandis S (1990a) Joint conductivity variation due to normal and shear deformation. In: *Proceedings of the International Symposium on Rock Joints*, Loen, Norway, 4–7 June 1990 (eds Barton N, Stephansson O), pp. 535–540. Balkema, Rotterdam.

Makurat A, Barton N, Tunbridge L, Vik G (1990b) The measurements of the mechanical and hydraulic properties of rock joints at different scale in the Stripa project. In: *Proceedings of the International Symposium on Rock Joints*, Loen, Norway, 4–7 June 1990 (eds Barton N, Stephansson O), pp. 541–548. Balkema, Rotterdam.

Mallon AJ, Swarbrick RE (2002) A compaction trend for non-reservoir North Sea chalk. *Marine and Petroleum Geology*, **19**, 527–539.

Mallon AJ, Swarbrick RE (2008) How should permeability be measured in fine-grained lithologies? Evidence from the chalk. *Geofluids*, **8**, 35–45.

Mallon AJ, Swarbrick RE, Katsube TJ (2005) Permeability of fine-grained rocks: new evidence from chalks. *Geology*, **33**, 21–24.

Maloney SM, Kaiser PK, Vorauer A (2006) A Re-assessment of in situ stresses in the Canadian Shield. In: *The 41st U.S. Symposium on Rock Mechanics* (ed Yale DP) pp. 1494–1503. American Rock Mechanics Association, Golden, Colorado.

Maltman A, Labaume P, Housen B (1997) Structural geology of the décollement at the toe of the Barbados accretionary prism. In: *Proceedings of the Ocean Drilling Program, Scientific Results*, **156** (eds Shipley TH, Ogawa Y, Blum P, Bahr JM), 279–292, Ocean Drilling Program, College Station, TX.

Manga M (1996) Hydrology of spring-dominated streams in the Oregon Cascades. *Water Resources Research*, **32**, 2435–2439.

Manga M (1997) A model for discharge in spring-dominated streams and implications for the transmissivity and recharge of quaternary volcanics in the Oregon Cascades. *Water Resources Research*, **33**, 1813–1822.

Manga M, Beresnev I, Brodsky EE, Elkhoury JE, Elsworth D, Ingebritsen SE, Mays DC, Wang C-Y (2012) Changes in permeability caused by transient stresses: field observations, experiments, and mechanisms. *Reviews of Geophysics*, **50**, RG2004.

Manga M, Brodsky E (2006) Seismic triggering of eruptions in the far field: volcanoes and geysers. *Annual Review of Earth and Planetary Sciences*, **34**, 263–291.

Manga M, Brodsky EE, Boone M (2003) Response of streamflow to multiple earthquakes. *Geophysical Research Letters*, **30**, 1214.

Manga M, Kirchner JW (2004) Interpreting the temperature of water at cold springs and the importance of gravitational potential energy. *Water Resources Research*, **40**, W05110, doi:10.1029/2003WR002905.

Manga M, Rowland JC (2009) Response of Alum Rock springs to the October 30, 2007 earthquake and implications for the origin of increased discharge after earthquakes. *Geofluids,* **9**, 237–250.

Manga M, Wang C-Y (2007) Earthquake hydrology. In: *Treatise on Geophysics* (ed Schubert GS), pp. 293–320. Elsevier, Amsterdam.

Manighetti I, Campillo M, Sammis C, Mai PM, King G (2005) Evidence for self-similar, triangular slip distributions on earthquakes: implications for earthquake and fault mechanics. *Journal of Geophysical Research*, **110**, doi:10.1029/2004JB003174.

Manning C, Ingebritsen SE (1999) Permeability of the continental crust: the implications of geothermal data and metamorphic systems. *Reviews of Geophysics*, **37**, 127–150.

March A (1932) Mathematische theorie der regelung nach der korngestelt bei affiner deformation. *Zeitschrift fur Kristallographie, Mineralogie und Petrographie*, **81**, 285–297.

Marchildon N, Dipple GM (1998) Irregular isograds, reaction instabilities, and the evolution of permeability during metamorphism. *Geology*, **26**, 15–18.

Mariner RH, Presser TS, Evans WC (1983) Geochemistry of active geothermal systems in the Northern Basin and Range Province. *Geothermal Resources Council Special Report*, **13**, 95–119.

Marion DP (1990) Acoustical, mechanical, and transport properties of sediments and granular materials. PhD thesis, Stanford University.

Markl G, Bucher K (1998) Composition of fluids in the lower crust inferred from metamorphic salt in lower crustal rocks. *Nature*, **391**, 781–783.

Marschall P, Horseman S, Gimmi T (2005) Characterisation of gas transport properties of the Opalinus Clay, a potential host rock formation for radioactive waste disposal. *Oil & Gas Science Technology - Revue d'IFP Energies Nouvelles*, **60**, 121–139.

Marshall TJ (1958) A relation between permeability and size distribution of pores. *Journal of Soil Science*, **9**, 1–8.

Martin CD, Chandler NA (1994) The progressive fracture of Lac du Bonnet Granite. *International Journal of Rock Mechanics and Mining Sciences*, **31**, 643–659.

Martino JB, Chandler NA (2004) Excavation-induced studies at the Underground Research Laboratory. *International Journal of Rock Mechanics and Mining Sciences*, **41**, 1413–1426.

Mascle A, Moore JC, ODP Leg 110 Scientific Party (1988) *Proceedings of the Ocean Drilling Program*, *Initial Reports (Pt. A)*, **110**.

Massart TJ, Selvadurai APS (2012) Stress-induced permeability evolution in quasi-brittle geomaterials. *Journal of Geophysical Research,* **117**, doi:10.1029/2012JB009251.

Massart TJ, Selvadurai APS (2014) Computational modelling of crack-induced permeability evolution in granite with dilatant cracks. *International Journal of Rock Mechanics and Mining Sciences*, **70**, 593–604.

Matmon D, Bekins BA (2006) Hydromechanics of a high taper angle, low-permeability prism: a case study from Peru. *Journal of Geophysical Research*, **111**, B07101.

Matsuki K, Chida Y, Sakaguchi K, Glover PWJ (2006) Size effect on aperture and permeability of a fracture as estimated in large synthetic fractures. *International Journal of Rock Mechanics and Mining Sciences,* **43**, 726–755.

Matthai SK, Geiger S, Roberts SG, Paluszny A, Belayneh M, Burri A, Mezentsev A, Lu H, Coumou D, Driesner T, Heinrich CA (2007) Numerical simulation of multi-phase fluid flow in structurally complex reservoirs. In: *Structurally Complex Reservoirs*, vol. **292** (eds Jolley SJ, Barr D, Walsh JJ, Knipe RJ), pp. 405–429. The Geological Society, London.

Matthews CS, Russell DG (1967) *Pressure Buildup and Flow Tests in Wells*. Society of Petroleum Engineers, Dallas, TX.

Maurer DK, Plume RW, Thomas JM, Johnson AK (1996) Water resources and effects of changes in ground-water use along the Carlin Trend, north-central Nevada. *U.S. Geological Survey Water-Resources Investigations Report*, **96–4134**.

Mavko G, Nur A (1997) The effect of a percolation threshold in the Kozeny-Carman relation. *Geophysics*, **62**, 1480–1482.

Mazurek M (2000) Geological and hydraulic properties of water-conducting features in crystalline rocks. In: *Hydrogeology of Crystalline Rocks* (eds Stober I, Bucher K), pp. 3–26. Kluwer Academic Publishers, Dordrecht.

Mazurek M, Hurford AJ, Leu W (2006) Unravelling the multi-stage burial history of the Swiss molasse basin: integration of apatite fission track, vitrinite reflectance and biomarker isomerisation analysis. *Basin Research*, **18**, 27–50.

Mazurek M, Jakob A, Bossart P (2003) Solute transport in crystalline rocks at Aspo, I, Geological basis and model calibration. *Journal of Contaminant Hydrology*, **61**, 157–174.

McCaig AM (1997) The geochemistry of volatile flow in shear zones. In: *Deformation-Enhanced Fluid Transport in the Earth's Crust and Mantle* (ed Holness MB) *Mineralogical Society Series*, **8**, pp. 227–266, Chapman & Hall, London.

McCarthy JF (1991) Analytical models of the effective permeability of sand-shale reservoirs. *Geophysical Journal International*, **105**, 513–527.

McCord JP, Moe H (1990) Interpretation of hydraulic testing at the Kaisten borehole. In: *Nagra Technical Report*, **89-18** (ed Nagra), Nagra, Baden, Switzerland, http://www.nagra.ch/data/documents/database/dokumente/$default/Default%20Folder/Publikationen/NTBs%201989-1990/e_ntb89-18.pdf accessed 06 May 2016.

McDonald MG, Harbaugh AW (1984) A modular three-dimensional finite-difference groundwater flow model. *U.S. Geological Survey Open-File Report*, **83–875**.

McGrail BP, Sullivan EC, Spane FA, Bacon DH, Hund G, Thome PD, Thompson CJ, Reidel SP, Colwell FS (2009) *Preliminary Hydrogeologic Characterization Results from the Wallula Basalt Pilot Study*. PNWD-4129, Battelle-Pacific Northwest Division, Richland, Washington.

McGuire KJ, McDonnell JJ, Weiler M, Kendall C, McGlynn BL, Welker JM, Seibert J (2005) The role of topography on catchment-scale water residence time. *Water Resources Research,* **41**, W05002, doi:10.1029/2004WR003657.

Mclnerney P, Guillen A, Courrioux G, Calcagno P, Lees T (2005) Building 3D geological models directly from the data? A new approach applied to Broken Hill, Australia, *U.S. Geological Survey Open-File Report*, **2005-1428**, http://pubs.usgs.gov/of/2005/1428/mcinerney/ accessed 06 May 2016.

McKenna JR, Blackwell DD, Richards MC (2005) Natural state modeling, structure, preliminary temperature and chemical synthesis of the Dixie Valley, Nevada Geothermal System. Proceedings Thirtieth Workshop on Geothermal Reservoir Engineering, Stanford University, Stanford, California, January 31-February 2, 2005, *Stanford Geothermal Program Technical Report*, **SGP-TR-176**.

McKenzie D (1984) The generation and compaction of partially molten rock. *Journal of Petrology*, **2**, 713–765.

McKenzie D (1987) The compaction of igneous and sedimentary rocks. *Journal of the Geological Society,* **144**, 299–307.

McKenzie JM, Voss CI (2013) Permafrost thaw in a nested groundwater-flow system. *Hydrogeology Journal*, **21**, 299–316.

McKiernan AW, Saffer DM (2006) Data report: Permeability and consolidation properties of subducting sediments off Costa Rica, ODP Leg 205. *Proceedings of the Ocean Drilling Program, Scientific Results,* **205**, 1–24.

McNeill LC, Ienaga M, Tobin H, Saito S, Goldberg D, Moore JC, Mikada H (2004) Deformation and in situ stress in the Nankai Accretionary prism from resistivity-at-bit images, ODP Leg 196. *Geophysical Research Letters*, **31**, L02602.

Medina R, Elkhoury J, Morris J, Prioul R, Desroches J, Detwiler R (2015) Flow of dense suspensions through fractures: significant in-plane velocity variations caused by small variations in solid concentration. *Geofluids*, **15**, 24–36.

Méheust Y, Schmittbuhl J (2003) Scale effects related to flow in rough fractures. *Pure and Applied Geophysics*, **160**, 1023–1050.

Menegon L, Fusseis F, Stunitz H, Xiao XH (2015) Creep cavitation bands control porosity and fluid flow in lower crustal shear zones. *Geology*, **43**, 227–230.

Menzies CD (2012) Fluid flow associated with the Alpine Fault, South Island, New Zealand. PhD thesis, University of Southampton.

Menzies CD, Teagle DAH, Craw D, Cox SC, Boyce AJ, Barrie D (2014) Incursion of meteoric waters into the ductile regime in an active orogen. *Earth and Planetary Science Letters*, **399**, 1–14.

Mesri G, Olson RE (1971) Mechanisms controlling the permeability of clays. *Clays and Clay Minerals,* **19**, 151–158.

Meyer H, Hetzel R, Fügenschuh B, Strauss H (2010) Determining the growth rate of topographic relief using in situ-produced ^{10}Be: a case study in the Black Forest, Germany. *Earth and Planetary Science Letters*, **290**, 391–402.

Michaels AS, Lin C (1954) Permeability of kaolinite. *Industrial and Engineering Chemistry*, **46**, 1239–1246.

Micklethwaite S (2008) Optimally oriented "fault-valve" thrusts: evidence for aftershock-related fluid pressure pulses? *Geochemistry, Geophysics, Geosystems*, **9**, doi:10.1029/2007GC001916.

Micklethwaite S, Cox SF (2006) Progressive fault triggering and fluid flow in aftershock domains: examples from mineralized Archaean fault systems. *Earth and Planetary Science Letters*, **250**, 318–330.

Micklethwaite S, Ford A, Witt W, Sheldon H (2015) The where and how of faults, fluids, and permeability – insights from fault stepovers, scaling properties, and gold mineralization. *Geofluids*, **15**, 240–251.

Micklethwaite S, Sheldon HA, Baker T (2010) Active fault and shear processes and their implications for mineral deposit formation and discovery. *Journal of Structural Geology*, **32**, 151–165.

Micucki EJ (1998) Hydrothermal transport and depositional processes in Archean lode-gold systems: a review. *Ore Geology Reviews*, **13**, 307–321.

Mikada H, Becker K, Moore JC, Klaus A, ODP Leg 196 Scientific Party (2002) *Proceedings of the Ocean Drilling Program, Initial Reports*, **196**, doi:10.2973/odp.proc.ir.196.2002.

Miller SA (2013) The role of fluids in tectonic and earthquake processes. *Advances in Geophysics*, **54**, 1–46.

Miller SA (2015) Modeling enhanced geothermal systems and the essential nature of large-scale changes in permeability at the onset of slip. *Geofluids,* **15**, 338–349.

Miller SA, Collettini C, Chiaraluce L, Cocco M, Barchi M, Kaus BJP (2004) Aftershocks driven by a high-pressure CO_2 source at depth. *Nature*, **427**, 724–727.

Miller SA, Nur A (2000) Permeability as a toggle switch in fluid-controlled crustal processes. *Earth and Planetary Science Letters*, **183**, 133–146.

Miller SA, Nur A, Olgaard DL (1996) Earthquakes as a coupled shear stress high pore pressure dynamical system. *Geophysical Research Letters,* **23**, 197–200.

Milliken KL, Esch WL, Reed RM, Zhang T (2012) Grain assemblages and strong diagenetic overprinting in siliceous mudrocks, Barnett Shale (Mississippian), Fort Worth Basin, Texas. *AAPG Bulletin*, **96**, 1553–1578.

Milliken KL, Reed RM (2010) Multiple causes of diagenetic fabric anisotropy in weakly consolidated mud, Nankai accretionary prism, IODP Expedition 316. *Journal of Structural Geology,* **32**, 1887–1898.

Milodowski AE, Gillespie MR, Naden J, Fortey NJ, Shepherd TJ, Pearce JM, Metcalfe R (1998) The petrology and paragenesis of fracture mineralization in the Sellafield area, west Cumbria. *Proceedings of the Yorkshire Geological Society*, **52**, 215–241.

Milord I, Sawyer EW, Brown M (2001) Formation of diatexite migmatite and granite magma during anatexis of semi-pelitic metasedimentary rocks: an example from St. Malo, France. *Journal of Petrology*, **42**, 487–505.

Milsch H, Heinrich W, Dreisen G (2003) Reaction-induced flow in synthetic quartz-bearing marbles. *Contributions to Mineralogy and Petrology*, **146**, 286–296.

Min K-B, Rutqvist J, Elsworth D (2009) Chemically and mechanically mediated influences on the transport and mechanical characteristics of rock fractures. *International Journal of Rock Mechanics and Mining Sciences*, **46**, 80–89.

Min K-B, Rutqvist J, Tsang C-F, Jing L (2004) Stress-dependent permeability of fractured rock masses: a numerical study. *International Journal of Rock Mechanics and Mining Sciences*, **41**, 1191–1210.

MINEDEX. Geological Survey of Western Australia, http://www.dmp.wa.gov.au/3970.aspx, accessed 2014.

Miyazawa M (2011) Propagation of an earthquake triggering front from the 2011 Tohoku-Oki earthquake. *Geophysical Research Letters*, **38**, L23307.

Moe H, McNeish JA, McCord JP, Andrews RW (1990) Interpretation of hydraulic testings at the Schafisheim borehole. In: *Nagra Technical Report*, **89-09** (ed Nagra), Nagra, Baden, Switzerland, http://www.nagra.ch/data/documents/database/dokumente/$default/Default%20Folder/Publikationen/NTBs%201989-1990/e_ntb89-09.pdf accessed 06 May 2016.

Mogi K, Mochizuki H, Kurokawa Y (1989) Temperature changes in an artesian spring at Usami in the Izu Peninsula (Japan) and their relation to earthquakes. *Tectonophysics*, **159**, 95–108.

Monaghan JJ (2012) Smoothed particle hydrodynamics and its diverse applications. *Annual Review of Fluid Mechanics*, **44**, 323–346.

Mondol NH, Bjorlykke K, Jahren J (2008) Experimental compaction of clays: relationship between permeability and petrophysical properties in mudstones. *Petroleum Geoscience*, **14**, 319–337.

Montgomery C (2013). Fracturing fluids. *Proceedings International Conference for Effective and Sustainable Hydraulic Fracturing (HF2013), Brisbane, Australia*, May 20–22, 2013, InTech, pp. 3–24.

Montgomery DR, Manga M (2003) Streamflow and water well responses to earthquakes. *Science*, **300**, 2047–2049.

Moore DE, Lockner DA, Byerlee JD (1994) Reduction of permeability in granite at elevated temperatures. *Science*, **265**, 1558–1561.

Moore DE, Morrow CA, Byerlee JD (1982) Use of swelling clays to reduce permeability and its potential application to nuclear waste repository sealing. *Geophysical Research Letters*, **9**, 1009–1012.

Moore DE, Morrow CA, Byerlee JD (1983) Chemical reactions accompanying fluid flow through granite held in a temperature gradient. *Geochimica et Cosmochimica Acta*, **47**, 445–453.

Moore GF, Taira A, Klaus A, ODP Leg 190 Scientific Party (2001) *Proceedings of the Ocean Drilling Program, Initial Reports*, **190**, doi:10.2973/odp.proc.ir.l90.2001.

Moore JC (1989) Tectonics and hydrogeology of accretionary prisms: role of the décollement zone. *Journal of Structural Geology*, **11**, 95–106.

Moore JC, Moore GF, Cochrane GR, Tobin HJ (1995) Negative-polarity seismic reflections along faults of the Oregon accretionary prism: indicators of overpressuring. *Journal of Geophysical Research*, **100**, 12895–12906.

Moore JC, ODP Leg 110 Scientific Party (1987) Expulsion of fluids from depth along a subduction-zone décollement horizon. *Nature*, **326**, 785–788.

Moore JC, Orange D, Kulm LD (1990) Interrelationship of fluid venting and structural evolution: *Alvin* observations from the frontal accretionary prism, Oregon. *Journal of Geophysical Research*, **95**, 8795–8808.

Moore JC, Saffer D (2001) Updip limit of the seismogenic zone beneath the accretionary prism of southwest Japan: an effect of diagenetic to low-grade metamorphic processes and increasing effective stress. *Geology*, **29**, 183–186.

Morad S, Ketzer JM, de Ros LF (2000) Spatial and temporal distribution of diagenetic alterations in siliciclastic rocks: implications for mass transfer in sedimentary basins. *Sedimentology,* **47**, 95–120.

Moran K, Gray WGD, Brown KM (1995) Permeability and stress history of sediment from the Cascadia margin. *Proceedings of the Ocean Drilling Program, Scientific Results,* **146-1**, 275–280.

Morgan JK, Ramsey EB, Ask MVS (2008) Deformation and mechanical strength of sediments at the Nankai subduction zone. In: *The Seismogenic Zone of Subduction Thrust Faults* (eds Dixon TH, Moore JC), pp. 210–256. Columbia University Press, New York.

Morgan P, Seager WR, Golombek MP (1986) Cenozoic thermal mechanical and tectonic evolution of the Rio Grande Rift. *Journal of Geophysical Research*, **91**, 6263–6276.

Morris BL, Lawrence ARL, Chilton PJC, Adams B, Calow RC, Klinck BA (2003a) Groundwater and its susceptibility to degradation: a global assessment of the problem and options for management. *United Nations Environment Programme (UNEP) Early Warning and Assessment Report Series*, **RS 03-3**.

Morris JD, Villinger HW, Klaus A, ODP Leg 205 Scientific Party (2003b) *Proceedings of the Ocean Drilling Program, Initial Reports*, **205**, doi:10.2973/odp.proc.ir.205.2003.

Morris JP, Monaghan JJ (1997) A switch to reduce SPH viscosity. *Journal of Computational Physics*, **136**, 41–50.

Morrow CA, Lockner DA (1997) Permeability and porosity of the Illinois UPH 3 drillhole granite and a comparison with other deep drillhole rocks. *Journal of Geophysical Research*, **102**, 3067–3075.

Morrow CA, Lockner DA, Moore DE, Byerlee JD (1981) Permeability of granite in a temperature gradient. *Journal of Geophysical Research*, **86**, 3002–3008.

Mortensen AK, Axelsson G (2013) Developing a Conceptual Model of a Geothermal System: presented at "Short Course on Conceptual Modelling of Geothermal Systems", Santa Tecla, El Salvador, February 24 - March 2, 2013, accessed at http://www.os.is/gogn/unu-gtp-sc/UNU-GTP-SC-16-29.pdf.

Mortimer N (1993) Jurassic tectonic history of the Otago schist, New Zealand. *Tectonics*, **12**, 237–244.

Mottl MJ, Wheat CG, Fryer P, Gharib J, Martin JB (2004) Chemistry of springs across the Mariana forearc shows progressive devolatilization of the subducting plate. *Geochimica et Cosmochimica Acta*, **68**, 4915–4933.

Muir-Wood R, King G (1993) Hydrological signatures of earthquake strain. *Journal of Geophysical Research*, **98**, 22035–22068.

Müller TM, Sahay PN (2011) Stochastic theory of dynamic permeability in poroelastic media. *Physical Review E*, **84**, 026329.

Munier R, Talbot CJ (1993) Segmentation, fragmentation and jostling of cratonic basement in and near Åspö, southeast Sweden. *Tectonics*, **12**, 713–727.

Muntean JL, Einaudi MT (2000) Porphyry gold deposits of the Refugio district, Maricunga belt, northern Chile. *Economic Geology*, **95**, 1445–1472.

Munz IA, Yardley BWD, Banks DA, Wayne D (1995) Deep penetration of sedimentary fluids into basement rocks from southern Norway: evidence from hydrocarbon and brine inclusions in quartz veins. *Geochimica et Cosmochimica Acta*, **59**, 239–254.

Munz IA, Yardley BWD, Gleeson SA (2002) Petroleum infiltration of high-grade basement, South Norway: pressure-temperature-time (P-T-t-X) constraints. *Geofluids*, **2**, 41–53.

Murdoch LC, Germanovich LN (2012) Storage change in a flat-lying fracture during well tests. *Water Resources Research*, **48**, W12528.

Murdoch LC, Richardson JR, Tan QF, Malin SC, Fairbanks C (2006) Forms and sand transport in shallow hydraulic fractures in residual soil. *Canadian Geotechnical Journal*, **43**, 1061–1073.

Nabelek PI (2002) Calc-silicate reactions and bedding-controlled isotopic exchange in the Notch Peak aureole, Utah: implications for differential fluid fluxes with metamorphic grade. *Journal of Metamorphic Geology*, **20**, 429–440.

Nabelek PI (2009) Numerical simulation of kinetically-controlled calc-silicate reactions and fluid flow with transient permeability around crystallizing plutons. *American Journal of Science,* **309**, 517–548.

Nagra (1985) Sondierbohrung Böttstein, Untersuchungsbericht. *Nagra Technischer Bericht (Technical Report of the Swiss National Cooperative for the Disposal of Radioactive Waste)*, **85–01**.

Nagra (1992) Sondierbohrung Schafisheim, Untersuchungsbericht. *Nagra Technischer Bericht (Technical Report of the Swiss National Cooperative for the Disposal of Radioactive Waste)*, **88-11**.

Najari M, Selvadurai APS (2014) Thermo-hydro-mechanical response of granite to temperature changes. *Environmental Earth Sciences*, **72**, 189–198.

Nakagawa M (1983) Geology and petrology of Moriyoshi volcano. *Journal of the Japanese Association of Mineralogy, Petrology and Economic Geology*, **78**, 197–210.

Nakajima J, Yoshida K, Hasegawa A (2013) An intraslab seismic sequence activated by the 2011 Tohoku-oki earthquake: evidence for fluid-related embrittlement. *Journal of Geophysical Research,* **118**, 3492–3505.

Nakazato H, Oba T, Itaya T (1996) The geology and K-Ar ages of the Gassan volcano, northeast Japan. *Journal the Japanese Association of Mineralogy, Petrology and Economic Geology*, **91**, 1–10.

National Research Council (1996) *Rock Fractures and Fluid Flow*. National Academies Press, Washington, DC.

National Research Council (2001) *Basic Research Opportunities in the Earth Sciences*. National Academies Press, Washington, DC.

Nazareth JJ, Hauksson E (2004) The seismogenic thickness of the southern California crust. *Bulletin of the Seismological Society of America*, **94**, 940–960.

Neglia S (1979) Migration of fluids in sedimentary basins. *American Association of Petroleum Geologists Bulletin*, **63**, 573–597.

Nehlig P, Juteau T (1988) Flow porosities, permeabilities and preliminary data on fluid inclusions and fossil thermal gradients in the crustal sequence of the Semail ophiolite (Oman). *Tectonophysics*, **151**, 199–221.

Nehlig P, Juteau T, Bendel V, Cotten J (1994) The root zones of oceanic hydrothermal systems – Constraints from the Samail Ophiolite (Oman). *Journal of Geophysical Research*, **99**, 4703–4713.

Nelson PH, Kibler JE (2001) A catalog of porosity and permeability from core plugs in siliciclastic tocks. *U.S. Geological Survey Open-File Report*, **03–420**.

Nemcok M, Henk A, Gayer RA, Vandycke S, Hathaway TM (2002) Strike-slip fault bridge fluid pumping mechanism: insights from field-based palaeostress analysis and numerical modelling. *Journal of Structural Geology*, **24**, 1885–1902.

Nemoto K, Watanabe N, Hirano N, Tsuchiya N (2009) Direct measurement of contact area and stress dependence of anisotropic flow through rock fracture with heterogeneous aperture distribution. *Earth and Planetary Science Letters,* **281**, 81–87.

Neuman SP (1994) Generalized scaling of permeabilities: validation and effect of support scale. *Geophysical Research Letters*, **21**, 349–352.

Neuman SP (2005) Trends, prospects and challenges in quantifying flow and transport through fractured rocks. *Hydrogeology Journal*, **13**, 124–147.

Neuzil C (1994) How permeable are clays and shales? *Water Resources Research*, **30**, 145–150.

Neuzil CE (1995) Abnormal pressures as hydrodynamic phenomena. *American Journal of Science,* **295**, 742–786.

Neuzil CE (2003) Hydromechanical coupling in geologic processes. *Hydrogeology Journal*, **11**, 41–83.

Newcomb RC (1959) Some preliminary notes on ground water in the Columbia River Basalt. *Northwest Science*, **33**, 1–18.

Nguyen TS, Börgesson L, Chijimatsu M, Hernelind J, Jing L, Kobayashi A, Fujita T, Jussila P, Rutqvist J, Jing L (2009) A case study on the influence of THM coupling on the near field safety of a spent fuel repository in sparsely fractured granite. *Environmental Geology*, **57**, 1239–1254.

Nguyen TS, Jing L (ed) (2008) *DECOVALEX-THMC Project, Task A, Influence of near field coupled THM phenomena on the performance of a spent fuel repository.* Report of Task *A2,* SKI Report, **44**.

Nguyen TS, Selvadurai APS (1995) Coupled thermal-mechanical-hydrological behaviour of sparsely fractured rock: implications for nuclear fuel waste disposal. *International Journal of Rock Mechanics and Mining Sciences*, **32**, 465–479.

Nguyen TS, Selvadurai APS (1998) A model for coupled mechanical and hydraulic behaviour of a rock joint. *International Journal for Numerical and Analytical Methods in Geomechanics*, **22**, 29–48.

Nielsen KA (2007) *Fractured Aquifers: Formation Evaluation by Well Testing*. Trafford Publishing, Victoria, BC.

Nishimoto S, Yoshida H (2010) Hydrothermal alteration of deep fractured granite: effects of dissolution and precipitation. *Lithos*, **115**, 153–162.

Noir J, Jacques E, Bekri S, Adler PM, Tapponnier P, King GCP (1997) Fluid flow triggered migration of events in the 1989 Dobi earthquake sequence of Central Afar. *Geophysical Research Letters*, **24**, 2335–2338.

Nolan TB, Anderson GH (1934) The geyser area near Beowawe, Eureka County, Nevada. *American Journal of Science*, **27**, 215–229.

Noorishad J, Tsang CF, Witherspoon PA (1984) Coupled thermo-hydraulic-mechanical phenomena in saturated fractured porous rocks: numerical approach. *Journal of Geophysical Research*, **89**, 10365–10373.

Nordgård Bolås HM, Hermanrud C, Schutter TA, Grimsmo Teige GM (2008) Is stress-insensitive chemical compaction responsible for high overpressures in deeply buried North Sea chalks? *Marine and Petroleum Geology*, **25**, 565–587.

Norris RJ, Cooper AF (2001) Late Quaternary slip rates and their significance for slip partitioning on the Alpine Fault, New Zealand. *Journal of Structural Geology*, **23**, 507–520.

Norton D, Knapp R (1977) Transport phenomena in hydrothermal systems – Nature of porosity. *American Journal of Science*, **277**, 913–936.

Norton D, Knight J (1977) Transport phenomena in hydrothermal systems: cooling plutons. *American Journal of Science*, **277**, 937–981.

Nunn JA, Deming D (1991) Thermal constraints on basin-scale flow systems. *Geophysical Research Letters*, **18**, 967–970.

Nye JF (1953) The flow law of ice from measurements in glacier tunnels, laboratory experiments and the Jungfraufirn borehole experiment. *Proceedings of the Royal Society of London, Series A, Mathematical and Physical Sciences*, **219A**, 477–489.

Oelkers EH, Schott J (2001) An experimental study of enstatite dissolution rates as a function of pH, temperature, and aqueous Mg and Si concentration, and the mechanism of pyroxene/pyroxenoid dissolution. *Geochimica et Cosmochimica Acta,* **65**, 1219–1231.

Ohzono M, Yabe Y, linuma T, Ohta Y, Miura S, Tachibana K, Sato T, Demachi T (2013) Strain anomalies induced by the 2011 Tohoku Earthquake (M_w9.0) as observed by a dense GPS network in northeastern Japan. *Earth, Planets and Space*, **64**, 1231–1238.

Okada T, Matsuzawa T, Umino N, Yoshida K, Hasegawa A, Takahashi H, Yamada T, Kosuga M, Takeda T, Kato A, Igarashi T, Obara K, Sakai S, Saiga A, Iidaka T, Iwasaki T, Hirata N, Tsumura N, Yamanaka Y, Terakawa T, Nakamichi H, Okuda T, Horikawa S, Katao H, Miura T, Kubo A, Matsushima T, Goto K, Miyamachi H (2015) Hypocenter migration and crustal seismic velocity distribution observed for the inland earthquake swarms induced by the 2011 Tohoku earthquake in NE Japan: implications for crustal fluid distribution and crustal permeability. *Geofluids*, **15**, 293–309.

Okada T, Umino N, Hasegawa A (2003) Rupture process of the July 2003 northern Miyagi earthquake sequence, NE Japan, estimated from double-difference hypocenter locations. *Earth, Planets, and Space*, **55**, 741–750.

Okada T, Umino N, Hasegawa A, Group for the aftershock observations of the Iwate-Miyagi Nairiku Earthquake in 2008 (2012) Hypocenter distribution and heterogeneous seismic velocity structure in and around the focal area of the 2008 Iwate-Miyagi Nairiku Earthquake, NE Japan—Possible seismological evidence for a fluid driven compressional inversion earthquake. *Earth, Planets, and Space*, **64**, 717–728.

Okada T, Yoshida K, Ueki S, Nakajima J, Uchida N, Matsuzawa T, Umino N, Hasegawa A, Group for the aftershock observations of the 2011 off the Pacific coast of Tohoku earthquake (2011) Shallow inland earthquakes in NE Japan possibly triggered by the 2011 off the Pacific coast of Tohoku Earthquake. *Earth, Planets and Space*, **63**, 749–754.

Okada Y (1992) Internal deformation due to shear and tensile faults in a half-space. *Bulletin of the Seismological Society of America*, **82**, 1018–1040.

Oliver NHS (1995) Hydrothermal history of the Mary Kathleen fold belt, Mt. Isa Block,Queensland. *Australian Journal of Earth Sciences*, **42**, 267–280.

Oliver NHS (1996) Review and classification of structural controls on fluid flow during regional metamorphism. *Journal of Metamorphic Geology*, **14**, 477–492.

Oliver NH, Butera KM, Rubenach MJ, Marshall LJ, Cleverley, JS, Mark G, Esser D (2008). The protracted hydrothermal evolution of the Mount Isa Eastern Succession: A review and tectonic implications. *Precambrian Research*, **163**, 108–130.

Olmsted FH, Rush FE (1987) Hydrogeologic reconnaissance of the Beowawe geysers geothermal area, Nevada. *Geothermics*, **16**, 27–46.

Olsen HW (1966) Darcy's law in saturated kaolinite. *Water Resources Research*, **2**, 287–295.

Olson P, Christensen U (1986) Solitary wave-propagation in a fluid conduit within a viscous matrix. *Journal of Geophysical Research*, **91**, 6367–6374.

Olsson R, Barton N (2001) An improved model for hydromechanical coupling during shearing of rock joints. *International Journal of Rock Mechanics and Mining Sciences*, **38**, 317–329.

Ordonez-Miranda J, Alvarado-Gil J (2011) On the stability of the exact solutions of the dual-phase lagging model of heat conduction. *Nanoscale Research Letters*, **6**, 327.

Ordonez-Miranda J, Alvarado-Gil JJ, Yang R (2012) Effective thermal conductivity of metal-dielectric composites at the non-dilute limit. *International Journal of Thermophysics*, **33**, 2118–2124.

Orense RP, Kiyota T, Yamada S, Cubrinovski M, Hosono Y, Okamura M, Yasuda S (2011) Comparison of liquefaction features observed during the 2010 and 2011 Canterbury earthquakes. *Seismological Research Letters*, **82**, 905–918.

Ortiz AER, Renner J, Jung R (2011) Hydromechanical analyses of the hydraulic stimulation of borehole Basel 1. *Geophysical Journal International*, **185**, 1266–1287.

Ostrowski LP, Kloska MB (1989) Final interpretation of hydraulic testing at the Siblingen borehole. In: *Nagra Technical Report*, **89-10** (ed Nagra), Nagra, Baden, Switzerland. http://www.timeride.ch/data/documents/database/dokumente/$default/Default%20Folder/Publikationen/NTBs%201989-1990/e_ntb89-10.pdf, accessed 06 May 2016.

Owens L (2013) Geochemical investigation of hydrothermal and volcanic systems in Iceland, New Mexico and Antarctica. PhD thesis, New Mexico Institute of Mining and Technology, http://www.ees.nmt.edu/outside/alumni/papers/2013d_owens_lb.pdf accessed 06 May 2016.

Ozisik MN, Tzou DY (1994) On the wave theory in heat conduction. *Journal of Heat Transfer*, **116**, 526–535.

Papadopulos SS, Bredehoeft JD, Cooper HH (1973) On the analysis of 'slug test' data. *Water Resources Research*, **9**, 1087–1089.

Parsons B, Sclater JG (1977) An analysis of the variation of ocean floor bathymetry and heat flow with age. *Journal of Geophysical Research*, **82**, 803–827.

Parsons T, Sliter R, Geist EL, Jachens RC, Jaffe BE, Foxgrover A, Hart PE, McCarthy J (2003) Structure and mechanics of the Hayward-Rodgers Creek Fault step-over, San Francisco Bay, California. *Bulletin of the Seismological Society of America*, **93**, 2187–2200.

Paschke SS, Banta ER, Dupree JA, Capesius JP, Litke DW (2011) Groundwater availability of the Denver Basin aquifer system, Colorado, *U.S. Geological Survey Professional Paper*, **1770**.

Patrinos GP, Cooper DN, van Mulligen E, Gkantouna V, Tzimas G, Tatum Z, Schultes E, Roos M, Barend M (2012) Microattribution and nanopublication as means to incentivize the placement of human genome variation data into the public domain. *Human Mutation*, **33**, 1503–1512.

Patton FD (1966) Multiple modes of shear failure in rock. *Proceedings 1st Congress of International Society of Rock Mechanics, Lisbon*, 509-13.

Pazdniakou A, Adler PM (2013) Dynamic permeability of porous media by the lattice Boltzmann method. *Advances in Water Resources*, **62B**, 292–302.

Pearce JA, Lippard SJ, Roberts S (1984) Characteristics and tectonic significance of supra-subduction zone ophiolites. *Geological Society of London Special Publications*, **16**, 77–94.

Peltzer G, Rosen P, Rogez F, Hudnut K (1996) Postseismic rebound in fault step-overs caused by pore fluid flow. *Science*, **273**, 1202–1204.

Pepin J, Person M, Phillips F, Kelley S, Timmons S, Owens L, Witcher J, Gable C (2015) Deep fluid circulation within crystalline basement rocks and the role of hydrologic windows in the formation of the Truth or Consequences, New Mexico low-temperature geothermal system. *Geofluids*, **15**, 139–160.

Person M, Banerjee A, Hofstra D, Sweetkind D, Gao Y (2008) Hydrologic models of modern and fossil geothermal systems within the Great Basin: implications for Carlin-type gold mineralization. *Geosphere*, **4**, 888–917.

Person M, Hofstra A, Sweetkind D, Stone W, Cohen D, Gable C, Banerjee A (2012) Analytical and numerical models of hydrothermal fluid flow at fault intersections. *Geofluids*, **12**, 312–326.

Person M, Taylor J, Dingman S (1998) Sharp interface models of salt water intrusion and wellhead delineation on Nantucket Island, Massachusetts. *Groundwater*, **36**, 731–742.

Pester NJ, Reeves EP, Rough ME, Ding K, Seewald JS, Seyfried WE (2012) Subseafloor phase equilibria in high-temperature hydrothermal fluids of the Lucky Strike Seamount (mid-Atlantic Ridge, 37°17'N). *Geochimica et Cosmochimica Acta*, **90**, 303–322.

Peters C (2008a) Accessibilities of reactive minerals in consolidated sedimentary rock: an imaging study of three sandstones. *Chemical Geology*, **265**, 198–208.

Peters EJ (2012) *Advanced Petrophysics, Volume 1, Geology, Porosity, Absolute Permeability, Heterogeneity, and Geostatistics*. Live Oak Book Company, Palo Alto, CA.

Peters SE (2005) Geologic constraints on the macroevolutionary history of marine animals. *Proceedings of the National Academy of Sciences USA*, **102**, 12326–12331.

Peters SE (2006) Macrostratigraphy of North America. *The Journal of Geology*, **114**, 391–412.

Peters SE (2008b) Environmental determinants of extinction selectivity in the fossil record. *Nature*, **454**, 626–629.

Peters SE, Kelly DC, Fraass A (2013) Oceanographic controls on the diversity and extinction of planktonic foraminifera. *Nature*, **4932**, 398–401.

Peters SE, Zhang C, Livny M, Ré C (2014) A machine-compiled macroevolutionary history of Phanerozoic life. ArXiv Preprint: 1406.2963.

Petrovitch CL, Nolte DD, Pyrak-Nolte LJ (2013) Scaling of fluid flow versus fracture stiffness. *Geophysical Research Letters*, **40**, 2076–2080.

Phillips OM (1991) *Flow and Reactions in Permeable Rocks*. Cambridge University Press, Cambridge.

Piggott AR, Elsworth D (1993), Laboratory assessment of the equivalent apertures of a rock fracture. *Geophysical Research Letters*, **20**, 1387–1390.

Pine RJ, Batchelor AS (1984) Downward migration of shearing in jointed rock during hydraulic injections. *International Journal of Rock Mechanics and Mining Sciences*, **21**, 249–263.

Platt JP, Leggett JK, Young J, Raza H, Alam S (1985) Large-scale sediment underplating in the Makran accretionary prism, southwest Pakistan. *Geology*, **13**, 507–511.

Plesha ME (1987) Constitutive models for rock discontinuities with dilatancy and surface degradation. *International Journal for Numerical and Analytical Methods in Geomechanics*, **11**, 345–362.

Plouraboué F, Kurowski P, Boffa JM, Hulin JP, Roux S (2000) Experimental study of the transport properties of rough self-affine fractures. *Journal of Contaminant Hydrology,* **46**, 295–318.

Plume RW, Carlton SM (1988) Hydrogeology of the Great Basin region of Nevada, Utah, and adjacent states. *U.S. Geological Survey Hydrologic Investigations Atlas*, **HA-694-A**, scale 1:100,000.

Plummer LN, Bexfield LM, Anderholm SK, Sanford WE, Eurybiades B (2004) Geochemical characterization of groundwater flow in the Santa Fe Group aquifer system, Middle Rio Grande Basin, New Mexico. *U.S. Geological Survey Water-Resources Investigations Report*, **03–4131**.

Poiseuille J-M (1844) *Recherches Expérimentales sur le Mouvement des Liquides Dans les Tubes de Très-petits Diamètres*. Imprimerie Royale, Paris.

Pokrovski GS, Borisova AY, Harrichoury JC (2008) The effect of sulfur on vapor-liquid fractionation of metals in hydrothermal systems. *Earth and Planetary Science Letters*, **266**, 345–362.

Polak A, Elsworth D, Yasuhara A, Grader AS, Halleck PM (2003) Permeability reduction of a natural fracture under net dissolution by hydrothermal fluids. *Geophysical Research Letters*, **30**, doi:10.1029/2003GL017575.

Pollack HN, Hurter SJ, Johnson JR (1993) Heat flow from the Earth's interior: analysis of the global data set. *Reviews of Geophysics*, **31**, 267–280.

Polski Y, Capuano L, Finger J, Huh M, Knudsen S, Chip Mansure A, Raymond D, Swanson R (2008) Enhanced Geothermal Systems (EGS) well construction technology evaluation report. *Sandia Report*, **SAND2008-7866**, Sandia National Laboratories, Albuquerque, New Mexico.

Porcello JJ, Tolan TL, Lindsey KA (2009) Groundwater level declines in the Columbia River Basalt Group and their relationship to mechanisms for groundwater recharge—A conceptual groundwater system model, Columbia Basin Ground Water Management Area of Adams, Franklin, Grant, and Lincoln Counties. Othello, Washington, prepared by the Columbia Basin Ground Water Management Area of Adams, Franklin, Grant, and Lincoln Counties, June 2009.

Porta G, Chaynikov S, Riva M, Guadagnini A (2013) Upscaling solute transport in porous media from the pore scale to dual-and multicontinuum formulations. *Water Resources Research*, **49**, 2025–2039.

Powell T, Cumming W (2010) Spreadsheets for geothermal water and gas geochemistry. *Proceedings of the 35th Workshop on Geothermal Reservoir Engineering, Stanford University*, **SGP-TR-188**.

Powell WC (1929) Report of an investigation of the Hot Springs artesian basin, Hot Springs, New Mexico. *Ninth Biennial Report of the State Engineer of New Mexico,* 1929–1930, **120-9**.

Power IM, Wilson SA, Dipple GM (2013) Serpentinite carbonation for CO_2 sequestration. *Elements*, **9**, 115–121.

Power WL, Durham WB (1997) Topography of natural and artificial fractures in granitic rocks: implications for studies of rock friction and fluid migration. *International Journal of Rock Mechanics and Mining Sciences,* **34**, 979–989.

Power WL, Tullis TE, Brown SR, Boitnott GN, Scholz CH (1987) Roughness of natural fault surfaces. *Geophysical Research Letters,* **14**, 29–32.

Pratt H, Swolfs H, Brace W, Black A (1977) Elastic and transport properties of in situ jointed granite. *International Journal of Rock Mechanics and Mining Sciences*, **14**, 35–45.

Preisig G, Cornaton FJ, Perrochet P (2012) Regional flow simulation in fractured aquifers using stress-dependent parameters. *Groundwater*, **50**, 376–385.

Preisig G, Eberhardt E, Gischig V, Roche V, van der Baan M, Valley B, Kaiser P, Duff D, Lowther R (2015) Development of connected rock mass permeability in massive crystalline rocks through hydraulic fracture propagation and shearing accompanying fluid injection. *Geofluids*, **15**, 321–337.

Pride SR, Tromeur E, Berryman JG (2002) Biot slow-wave effects in stratified rock. *Geophysics*, **67**, 271–281.

PRISM Climate Group (2004) *PRISM climate group: Oregon State University.* Accessed October 1, 2009, http://www.prismclimate.org.

Priyatkina N, Kullerud K, Bergh S, Armitage P, Ravna E (2011) CO_2 sequestration during interactions between fluid and mafic to intermediate intrusive rocks on Vannoya Island, West Troms Basement Complex, North Norway. *Proceedings 10th International Congress of Applied Mineralogy, Trondheim (ICAM)*, pp. 549–553.

Putnis A, John T (2010) Replacement processes in the Earth's crust. *Elements*, **6**, 159–164.

Pyrak-Nolte LJ, Cook NGW, Nolte DD (1988) Fluid percolation through single fractures, *Geophysical Research Letters*, **15**, 1247–1250.

Pyrak-Nolte LJ, Morris JP (2000) Single fractures under normal stress: the relation between fracture specific stiffness and fluid flow. *International Journal of Rock Mechanics and Mining Sciences*, **37**, 245–262.

Pyrak-Nolte LJ, Myer LR, Cook NGW, Witherspoon PA (1987) Hydraulic and mechanical properties of natural fractures in low permeability rock. *Proceedings International Congress on Rock Mechanics of ISRM*, Balkema, Rotterdam, 225–231.

Quigley M, Van DR, Litchfield NJ, Villamor P, Duffy B, Barrell DJA, Furlong K, Stahl T, Bilderback E, Noble D (2012) Surface rupture during the 2010 M_w7.1 Darfield (Canterbury) earthquake: implications for fault rupture dynamics and seismic-hazard analysis. *Geology*, **40**, 55–58.

Quigley M, Van DR, Villamor P, Litchfield NJ, Barrell DJA, Furlong K, Stahl T, Duffy B, Bilderback E, Noble D, Townsend DB, Begg JG, Jongens R, Ries W, Claridge J, Klahn A, Mackenzie H, Smith A, Hornblow S, Nicol R, Cox SC, Langridge RM, Pedley K (2010) Surface rupture of the Greendale Fault during the Darfield (Canterbury) Earthquake, New Zealand: initial findings. *Bulletin of the New Zealand Society for Earthquake Engineering*, **43**, 236–242.

Quon SH, Ehlers EG (1963) Rocks of the northern part of the mid-Atlantic Ridge. *Geological Society of America Bulletin*, **74**, 1–7.

Rabinowicz M, Ricard Y, Gregoire M (2002) Compaction in a mantle with a very small melt concentration: implications for the

generation of carbonatitic and carbonate-bearing high alkaline mafic melt impregnations. *Earth and Planetary Science Letters*, **203**, 205–220.

Rabinowicz M, Vigneresse JL (2004) Melt segregation under compaction and shear channeling: application to granitic magma segregation in a continental crust. *Journal of Geophysical Research*, **109**, B04407.

Raffensperger JP, Garven G (1995) The formation of unconformity-type uranium ore deposits, 1, Coupled groundwater flow and heat transport modeling. *American Journal of Science*, **295**, 581–636.

Ramm M (1992) Porosity-depth trends in reservoir sandstones: theoretical models related to Jurassic sandstones, offshore Norway. *Marine and Petroleum Geology*, **9**, 553–567.

Ramsay JG (1980) The crack-seal mechanism of rock deformation. *Nature*, **284**, 135–139.

Ranalli G (1995) *Rheology of the Earth*. Springer-Verlag, New York.

Ranero CR, Grevemeyer I, Sahling H, Barckhausen U, Hensen C, Wallmann K, Weinrebe W, Vannucchi P, von Huene R, McIntosh K (2008) Hydrological system of erosional convergent margins and its influence on tectonics and interpolate seismogenesis. *Geochemistry, Geophysics, Geosystems*, **9**, Q03S04.

Ranero CR, Morgan JP, McIntosh K, Reichert C (2003) Bending-related faulting and mantle serpentinization at the Middle America trench. *Nature*, **425**, 367–373.

Ranjram M, Gleeson T, Luijendijk E (2015) Is the permeability of crystalline rock in the shallow crust related to depth, lithology, or tectonic setting? *Geofluids*, **15**, 106–119.

Raven KG, Gale JE (1985) Water flow in a natural rock fracture as a function of stress and sample size. *International Journal of Rock Mechanics and Mining Sciences*, **22**, 251–261.

Redmond PB, Einaudi MT, Inan EE, Landtwing MR, Heinrich CA (2004) Copper deposition by fluid cooling in intrusion-centered systems: new insights from the Bingham porphyry ore deposit, Utah. *Geology*, **32**, 217–220.

Reece JS, Flemings PB, Germaine JT (2013) Data report: Permeability, compressibility, and microstructure of resedimented mudstone from IODP Expedition 322, Site C0011. In Saito S, Underwood MB, Kubo Y, and the Expedition 322 Scientists, *Proceedings of the Integrated Ocean Drilling Program*, **322**, 1–26.

Reidel SP (1983) Stratigraphy and petrogenesis of the Grande Ronde Basalt from the deep canyon country of Washington, Oregon, and Idaho. *Geological Society of America Bulletin*, **94**, 519–542.

Reidel SP, Camp VE, Tolan TL, Martin BS (2013) The Columbia River flood basalt province: stratigraphy, areal extent, volume, and physical volcanology. *Geological Society of America Special Paper*, **497**, 1–43.

Reidel SP, Johnson VG, Spane FA (2002) Natural gas storage in basalt aquifers of the Columbia Basin, Pacific Northwest USA—A guide to site characterization. Pacific Northwest National Laboratory, Richland, Washington, PNNL-13962, http://www.pnl.gov/main/publications/external/technical_reports/PNNL-13962.pdf, accessed 06 May 2016.

Reinecker J, Tingay M, Muller B, Heidbach O (2010) Present-day stress orientation in the Molasse Basin. *Tectonophysics*, **482**, 129–138.

Reiter M, Eggleston R, Broadwell B, Minier J (1986) Estimates of terrestrial heat flow from deep petroleum tests along the Rio Grande Rift in central and southern New Mexico. *Journal of Geophysical Research*, **91**, 6225–6245.

Rejeb A, Rouabhi A, Millard A, Maßmann J, Uehara S (2008) *DECOVALEX-THMC Project, Task C, Hydromechanical response of the Tournemire Argillite to the underground openings excavation: unsaturated zones and mine-by-test experiment*. Final Report, SKI Report, **44**.

Renard F, Brosse E, Gratier JP (2000a) The different processes involved in the mechanism of pressure-solution in quartz-rich rocks and their interactions. In: *Quartz Cementation of Sandstones* (eds Worden RH, Morad S). *International Association of Sedimentologists Special Publication*, **29**, pp. 67–78, IAS.

Renard F, Gratier JP, Jamtveit B (2000b) Kinetics of crack-sealing, intergranular pressure solution, and compaction around active faults. *Journal of Structural Geology*, **22**, 1395–1407.

Renner JL, White DE, Williams DL (1975) Hydrothermal convection systems. In: Assessment of geothermal resources of the United States 1975. *United States Geological Survey Circular*, **726**, 5–57.

Renshaw CE (1995) On the relationship between mechanical and hydraulic apertures in rough-walled fractures. *Journal of Geophysical Research*, **100**, 24629–24636.

Reuschle T (2011) Data report: Permeability measurements under confining pressure, Expeditions 315 and 316, Nankai Trough. In: Kinoshita M, Tobin H, Ashi J, Kimura G, Lallemant S, Screaton EJ, Curewitz D, Masago H, Moe KT, and the Expedition 314/315/316 Scientists, *Proceedings of the Integrated Ocean Drilling Program*, **314/315/316**, 1–17.

Revil A (2002) Mechanical compaction of sand/clay mixtures. *Journal of Geophysical Research*, **107**, doi:10.1029/2001JB000318.

Revil A, Cathles LM (1999) Permeability of shaly sands. *Water Resources Research*, **35**, 651–662.

Revil A, Cathles LM (2002) Fluid transport by solitary waves along growing faults – A field example from the South Eugene Island Basin, Gulf of Mexico. *Earth and Planetary Science Letters*, **202**, 321–335.

Revil A, Florsch N (2010) Determination of permeability from spectral induced polarization in granular media. *Geophysical Journal International*, **181**, 1480–1498.

Revil A, Leroy P, Titov K (2005) Characterization of transport properties of argillaceous sediments: application to the Callovo-Oxfordian argillite. *Journal of Geophysical Research*, **110**, B06202, doi:10.1029/2004JB003442.

Reyes AG, Christenson BW, Faure K (2010) Sources of solutes and heat in low-enthalpy mineral waters and their relation to tectonic setting, New Zealand. *Journal of Volcanology and Geothermal Research*, **192**, 117–141.

Reyners ME (2009) Large subduction thrust earthquake shakes southern New Zealand. *Eos Transactions American Geophysical Union*, **90**, 282.

Reyners ME (2011) Lessons from the destructive M_w6.3 Christchurch, New Zealand, earthquake. *Seismological Research Letters*, **82**, 371–372.

Rice JR (1992) Fault stress states, pore pressure distributions, and the weakness of the San Andreas fault. In: *Fault Mechanics*

and Transport Properties of Rocks (eds Evans B, Wong T-F), pp. 475–503. Academic Press, San Diego.

Richard GC, Kanjilal S, Schmeling H (2012) Solitary-waves in geophysical two-phase viscous media: a semi-analytical solution. *Physics of the Earth and Planetary Interiors,* **198**, 61–66.

Richards JP (2003) Tectono-magmatic precursors for porphyry Cu-(Mo-Au) deposit formation. *Economic Geology*, **98**, 1515–1533.

Richards JP (2013) Giant ore deposits formed by optimal alignments and combinations of geological processes. *Nature Geoscience*, **6**, 911–916.

Richardson CJ, Cann JR, Richards HG, Cowan JG (1987) Metal-depleted root zones of the Troodos ore-forming hydrothermal systems, Cyprus. *Earth and Planetary Science Letters,* **84**, 243–253.

Richter FM, McKenzie D (1984) Dynamical models for melt segregation from a deformable rock matrix. *Journal of Geology*, **92**, 729–740.

Rider MH (2002) *The Geological Interpretation of Well Logs*. Rider-French Consulting Ltd., Sutherland.

Rimstidt JD, Barnes HL (1980) The kinetics of silica-water reactions. *Geochimica et Cosmochimica Acta,* **44**, 1683–1699.

Rimstidt JD, Cole DR (1983) Geothermal mineralization, I, The mechanism of formation of the Beowawe, Nevada, siliceous sinter deposit. *American Journal of Science*, **283**, 861–875.

Rinaldi AP, Rutqvist J, Cappa F (2013) Geomechanical effects on CO_2 leakage through fault zones during large-scale underground injection. *International Journal of Greenhouse Gas Control*, **20**, 117–131.

Robert F, Boullier A-M, Firdaous K (1995) Gold-quartz veins in metamorphic terranes and their bearing on the role of fluids in faulting. *Journal of Geophysical Research*, **100**, 861–881.

Roberts SJ, Nunn JA, Cathles LM, Cipriani F-D (1996) Expulsion of abnormally pressured fluids along faults. *Journal of Geophysical Research*, **101**, 231–252.

Roeloffs EA (1988) Hydrologic precursors to earthquakes: a review. *Pure and Applied Geophysics*, **126**, 177–209.

Roeloffs EA (1996) Poroelastic techniques in the study of earthquake related hydrologic phenomena. *Advances in Geophysics*, **37**, 135–195.

Roeloffs EA (1998) Persistent water level changes in a well near Parkfield, California, due to local and distant earthquakes. *Journal of Geophysical Research*, **103**, 868–889.

Rogers PSZ, Pitzer KS (1982) Volumetric properties of aqueous sodium chloride solutions. *Journal of Physical and Chemical Reference Data*, **11**, 15–81.

Rojstaczer SA, Ingebritsen SE, Hayba DO (2008) Permeability of continental crust influenced by internal and external forcing. *Geofluids,* **8**, 128–139.

Rojstaczer SA, Wolf S (1992) Permeability changes associated with large earthquakes: an example from Loma Prieta, California. *Geology*, **20**, 211–214

Rojstaczer SA, Wolf S, Michel R (1995) Permeability enhancement in the shallow crust as a cause of earthquake-induced hydrological changes. *Nature*, **373**, 237–239.

Rolandone F, Bürgmann R, Nadeau RM (2004) The evolution of the seismic-aseismic transition during the earthquake cycle: constraints from the time-dependent depth distribution of aftershocks. *Geophysical Research Letters*, **31**, doi:10.1029/2004GL021379.

Rona PA, Hannington MD, Raman CV, Thompson G, Tivey MK, Humphris SE, Lalou C, Petersen S (1993) Active and relict sea-floor hydrothermal mineralization at the TAG hydrothermal field, mid-Atlantic Ridge. *Economic Geology*, **88**, 1989–2017.

Ronov AB (1978) The Earth's sedimentary shell. *International Geology Review,* **24**, 1313–1363.

Roselle GT, Baumgartner LP, Valley JW (1999) Stable isotope evidence of heterogeneous fluid infiltration at the Ubehebe Peak contact aureole, Death Valley National Park, California. *American Journal of Science*, **299**, 93–138.

Rowe CD, Meneghini F, Moore JC (2009) Fluid-rich damage zone of an ancient out-of-sequence thrust, Kodiak Islands, Alaska. *Tectonics*, **28**, TC1006.

Rowe K, Screaton EJ, Ge S (2012) Coupled fluid-flow and deformation modeling of the frontal thrust region of the Kumano Basin transect, Japan: implications for fluid pressures and decollement downstepping. *Geochemistry, Geophysics, Geosystems*, **13**, Q0AD23.

Rowe K, Screaton E, Guo J, Underwood MB (2011) Data report: Permeabilities of sediments from the Kumano Basin transect off Kii Peninsula, Japan. In: Kinoshita M, Tobin H, Ashi J, Kimura G, Lallemant S, Screaton EJ, Curewitz D, Masago H, Moe KT, and the Expedition 314/315/316 Scientists, *Proceedings of the Integrated Ocean Drilling Program*, **314/315/316**, 1–24.

Rowland JC, Manga M, Rose TP (2008) The influence of poorly interconnected fault zone flow paths on spring geochemistry. *Geofluids*, **8**, 93–101.

Rowland JV, Simmons SF (2012) Hydrologic, magmatic and tectonic controls on hydrothermal flow, Taupo Volcanic Zone, New Zealand: implications for the formation of epithermal vein deposits. *Economic Geology*, **107**, 427–457.

Rubenach M (2013) Structural controls of metasomatism on a regional scale. In: *Metasomatism and the Chemical Transformation of Rocks* (eds Harlov DE, Austrheim H), Springer-Verlag, Berlin, Heidelburg, 93–140.

Rutqvist J (1995) Determination of hydraulic normal stiffness of fractures in hard rock from hydraulic well testing. *International Journal of Rock Mechanics and Mining Sciences*, **32**, 513–523.

Rutqvist J (2004) *Drift Scale THM Model*. MDL-NBS-HS-000017 REV 0, Bechtel SAIC Company, Las Vegas, Nevada.

Rutqvist J (2011) Status of the TOUGH-FLAC simulator and recent applications related to coupled fluid flow and crustal deformations. *Computers and Geoscience*, **37**, 739–750.

Rutqvist J (2012) The geomechanics of CO_2 storage in deep sedimentary formations. *International Journal of Geotechnical and Geological Engineering*, **30**, 525–551.

Rutqvist J (2015) Fractured rock stress-permeability relationships from in situ data and effects of temperature and chemical-mechanical couplings. *Geofluids*, **15**, 48–66.

Rutqvist J, Barr D, Birkholzer JT, Fujisaki K, Kolditz O, Liu Q-S, Fujita T, Wang W, Zhang C-Y (2009a) A comparative simulation study of coupled THM processes and their effect on fractured rock permeability around nuclear waste repositories. *Environmental Geology*, **57**, 1347–1360.

Rutqvist J, Börgesson L, Chijimatsu M, Hernelind J, Jing L, Kobayashi A, Nguyen S (2009b) Modeling of damage, permeability changes and pressure responses during excavation of the TSX tunnel in granitic rock at URL, Canada. *Environmental Geology*, **57**, 1263–1274.

Rutqvist J, Chijimatsu M, Jing L, De Jonge J, Kohlmeier M, Millard A, Nguyen TS, Rejeb A, Souley M, Sugita Y, Tsang C-F (2005) Numerical study of the THM effects on the near-field safety of a hypothetical nuclear waste repository – BMT1 of the DECOVALEX III project, Part 3, Effects of THM coupling in fractured rock. *International Journal of Rock Mechanics and Mining Sciences*, **42**, 745–755.

Rutqvist J, Freifeld B, Min K-B, Elsworth D, Tsang Y (2008) Analysis of thermally induced changes in fractured rock permeability during eight years of heating and cooling at the Yucca Mountain Drift Scale Test. *International Journal of Rock Mechanics and Mining Sciences*, **45**, 1373–1389.

Rutqvist J, Leung C, Hoch A, Wang Y, Wang Z (2013a) Linked multicontinuum and crack tensor approach for modeling of coupled geomechanics, fluid flow and transport in fractured rock. *International Journal of Rock Mechanics and Geotechnical Engineering*, **5**, 18–31.

Rutqvist J, Rinaldi AP, Cappa F, Moridis GJ (2013b) Modeling of fault reactivation and induced seismicity during hydraulic fracturing of shale-gas reservoirs. *Journal of Petroleum Science and Technology*, **107**, 31–44.

Rutqvist J, Stephansson O (1996) A cyclic hydraulic jacking test to determine the in situ stress normal to a fracture. *International Journal of Rock Mechanics and Mining Sciences*, **33**, 695–711.

Rutqvist J, Stephansson O (2003) The role of hydromechanical coupling in fractured rock engineering. *Hydrogeology Journal*, **11**, 7–40.

Rutqvist J, Tsang C-F (2002) A study of caprock hydromechanical changes associated with CO_2 injection into a brine formation. *Environmental Geology*, **42**, 296–305.

Rutqvist J, Tsang C-F (2003) Analysis of thermal-hydrologic-mechanical behavior near an emplacement drift at Yucca Mountain. *Journal of Contaminant Hydrology*, **62–63**, 637–652.

Rutqvist J, Tsang C-F (2012) Multiphysics processes in partially saturated fractured rock: experiments and models from Yucca Mountain. *Reviews of Geophysics*, **50**, RG3006.

Rutqvist J, Tsang C-F, Ekman D, Stephansson O (1997) Evaluation of in situ hydromechanical properties of rock fractures at Laxemar in Sweden. *Proceedings of 1st Asian Rock Mechanics Symposium ARMS 97*, Seoul, South Korea, 619–624.

Rutqvist J, Wu Y-S, Tsang C-F, Bodvarsson G (2002) A modeling approach for analysis of coupled multiphase fluid flow, heat transfer, and deformation in fractured porous rock. *International Journal of Rock Mechanics and Mining Sciences*, **39**, 429–442.

Saar MO (2011) Geothermal heat as a tracer of large-scale groundwater flow and as a means to determine permeability fields. *Hydrogeology Journal*, **19**, 31–52.

Saar MO, Manga M (2004) Depth dependence of permeability in the Oregon Cascades inferred from hydrogeologic, thermal, seismic, and magmatic modeling constraints. *Journal of Geophysical Research*, **109**, B04204.

Sadalage PJ, Fowler M (2012) *NoSQL Distilled: A Brief Guide to the Emerging World of Polyglot Persistence*. Addison-Wesley, Upper Saddle River, NJ.

Saffer DM (2003) Pore pressure development and progressive dewatering in underthrust sediments at the Costa Rican subduction margin: comparison with Northern Barbados and Nankai. *Journal of Geophysical Research*, **108**, doi:10.1029/2002JB001787.

Saffer DM (2007) Pore pressure within underthrust sediments in subduction zones. In: *The Seismogenic Zone of Subduction Thrust Faults* (eds Dixon T, Moore JC), pp. 171–209. Columbia University Press, New York.

Saffer DM (2010) Hydrostratigraphy as a control on subduction zone mechanics through its effects on drainage: an example from the Nankai Margin, SW Japan. *Geofluids*, **10**, 114–131.

Saffer DM (2015) The permeability of active subduction plate boundary faults. *Geofluids*, **15**, 193–215.

Saffer DM, Bekins BA (1998a) Episodic fluid flow in the Nankai accretionary complex: timescale, geochemistry, flow rates, and fluid budget. *Journal of Geophysical Research*, **103**, 30351–30370.

Saffer D, Bekins BA (1998b) Fluid budgets and pore pressures in the shallow Subduction Zone: a comparison of the Nankai and Cascadia accretionary systems (abstract). *Eos Transactions American Geophysical Union*, **79**, Fall Meeting Supplement, F899.

Saffer DM, Bekins BA (1999) Fluid budgets at convergent plate margins: implications for the extent and duration of fault zone dilation. *Geology*, **27**, 1095–1098.

Saffer DM, Bekins BA (2002) Hydrologic controls on the morphology and mechanics of accretionary wedges. *Geology*, **30**, 271–274.

Saffer DM, Bekins BA (2006) An evaluation of factors influencing pore pressure in accretionary complexes: implications for taper angle and wedge mechanics. *Journal of Geophysical Research,* **111**, B04101.

Saffer DM, Guo J, Underwood MB, Likos W, Skarbek RM, Song I, Gildow M (2011) Data report: Consolidation, permeability, and fabric of sediments from the Nankai continental slope, IODP Sites C0001, C0008, and C0004. In: Kinoshita M, Tobin H, Ashi J, Kimura G, Lallemant S, Screaton EJ, Curewitz D, Masago H, Moe KT, and the Expedition 314/315/316 Scientists, *Proceedings of the Integrated Ocean Drilling Program*, **314/315/316**, 1–61.

Saffer DM, McKiernan AW (2009) Evaluation of in situ smectite dehydration as a pore-water freshening mechanism in the Nankai Trough, offshore southwest Japan. *Geochemistry, Geophysics, Geosystems*, **10**, Q02010.

Saffer DM, Screaton EJ (2003) Fluid flow pathways at the toe of convergent margins: interpretation of sharp geochemical gradients. *Earth and Planetary Science Letters*, **213**, 261–270.

Saffer DM, Silver EA, Fisher AT, Tobin H, Moran K (2000) Inferred pore pressures at the Costa Rica subduction zone: implications for dewatering processes. *Earth and Planetary Science Letters*, **177**, 193–207.

Saffer DM, Tobin H (2011) Hydrogeology and mechanics of subduction zone forearcs: fluid flow and pore pressure. *Annual Review of Earth and Planetary Sciences*, **39**, 157–186.

Sahling H, Masson DG, Ranero C, Huhnerbach V, Weinrebe W *et al.* (2008) Fluid seepage at the continental margin offshore Costa Rica and southern Nicaragua. *Geochemistry, Geophysics, Geosystems*, **9**, Q05S05.

Sample J (1996) Isotopic evidence from authigenic carbonates for rapid upward fluid flow in accretionary wedges. *Geology*, **24**, 897–900.

Sanematsu K, Watanabe K, Duncan RA, Izawa E (2006) The history of vein formation determined by $^{40}Ar/^{39}Ar$ dating of adularia in the Hosen-1 vein at the Hishikari epithermal deposit, Japan. *Economic Geology*, **101**, 685–698.

Sanford RM, Bowers RL, Combs J (1979) Rio Grande Rift geothermal exploration case history, Elephant Butte prospect, south-central New Mexico. *Transactions Geothermal Resources Council*, **3**, 609–612.

Sanford WE, Konikow LF (1989) Simulation of calcite dissolution and porosity changes in salt water mixing zones in coastal aquifers. *Water Resources Research*, **25**, 655–667.

Sangawa A (1987) Damage of the 1611 Aizu earthquake in relation to surface faulting. *Zisin (Journal of the Seismological Society of Japan 2nd series)*, **40**, 235–245.

Sanner B (2000) Baden-Baden, a famous thermal spa with a long history. *Geo-Heat Center Quarterly Bulletin*, **21**, 16–22.

Santagata M, Germaine JT (2002) Sampling disturbance effects in normally consolidated clays. *Journal of Geotechnical and Geoenvironmental Engineering*, **128**, 997–1006.

Santagata M, Germaine JT (2005) Effect of OCR on sampling disturbance of cohesive soils and evaluation of laboratory reconsolidation procedures. *Canadian Geotechnical Journal*, **42**, 459–474.

Santagata M, Kang YI (2007) Effects of geologic time on the initial stiffness of clays. *Engineering Geology*, **89**, 98–111.

Santamarina JC, Klein KA, Wang YH, Prencke E (2002) Specific surface: determination and relevance. *Canadian Geotechnical Journal*, **39**, 233–241.

Sardini, P. Ledésert, B., Touchard, G. (1997) Quantification of microscopic pore networks by image analysis and measurements of permeability in the Soultz-sous-Forêts granite (Alsace, France). In *Fluid Flow and Transport in Rocks* (eds Jamtveit B, Yardley BWD), pp. 171–189, Chapman & Hall, London.

Sass JH, Lachenbruch AH, Munroe RJ, Green GW, Moses TH Jr (1971) Heat flow in the western United States. *Journal of Geophysical Research*, **76**, 6356–6431.

Sassa K, He B, Miyagi T, Strasser M, Konagai K, Ostric M, Setiawan H, Takara K, Nagai O, Yamashiki Y, Tutumi S (2012) A hypothesis of the Senoumi submarine megaslide in Suruga Bay in Japan – based on the undrained dynamic-loading ring shear tests and computer simulation. *Landslides*, **9**, 439–455.

Sato H, Hirata N, Iwasaki T, Matsubara M, Ikawa T (2002) Deep seismic reflection profiling across the Ou Backbone range, northern Honshu Island, Japan. *Tectonophysics*, **355**, 41–52.

Sato H, Yoshida T, Iwasaki T, Sato T, Ikeda Y, Umino N (2004) Late Cenozoic tectonic development of the back arc region of central northern Honshu, Japan, revealed by recent deep seismic profiling. *Journal of the Japanese Association for Petroleum Technology*, **69**, 145–154.

Sato T, Sakai R, Furuya K, Kodama T (2000) Coseismic spring flow changes associated with the 1995 Kobe earthquake. *Geophysical Research Letters*, **27**, 1219–1222.

Sausse J, Genter A (2005) Types of permeable fractures in granite. *Geological Society of London Special Publication*, **240**, 1–14.

Sawyer AH, Flemings PB, Elsworth D, Kinoshita M (2008) Response of submarine hydrologic monitoring instruments to formation pressure changes: theory and application to Nankai advanced CORKs. *Journal of Geophysical Research*, **113**, B01102.

Sawyer EW (1998) Formation and evolution of granite magmas during crustal reworking: the significance of diatexites. *Journal of Petrology*, **39**, 1147–1167.

Schiffman P, Smith BM (1988) Petrology and oxygen isotope geochemistry of a fossil seawater hydrothermal system within the Solea graben, northern Troodos ophiolite, Cyprus. *Journal of Geophysical Research*, **93**, 4612–4624.

Schiffman P, Smith BM, Varga RJ, Moores EM (1987) Geometry, conditions and timing of off-axis hydrothermal metamorphism and ore-deposition in the Solea graben. *Nature*, **325**, 423–425.

Schlische RW, Young SS, Ackermann RV, Gupta A (1996) Geometry and scaling relations of a population of very small rift-related normal faults. *Geology*, **24**, 683–686.

Schloemer S, Krooss BM (1997) Experimental characterisation of the hydrocarbon sealing efficiency of cap rocks. *Marine and Petroleum Geology*, **14**, 565–580.

Schlumberger Limited (1981) *RFT – Essentials of Pressure Test Interpretation*. Schlumberger, Paris.

Schneider J, Flemings PB, Day-Stirrat RJ, Germaine JT (2011) Insights into pore-scale controls on mudstone permeability through resedimentation experiments. *Geology*, **39**, 1011–1014.

Schneider Reece J, Flemings PB, Dugan B, Long H, Germaine JT (2012) Permeability-porosity relationships of shallow mudstones in the Ursa Basin, northern deepwater Gulf of Mexico. *Journal of Geophysical Research*, **117**, B12102.

Scholz CH (1998) Earthquakes and friction laws. *Nature*, **391**, 37–42.

Schroder RA, Strait SR (1987) Fluid temperature data from selected boreholes on the Hanford site. Rockwell Hanford Operations BWIP Supporting Document, SD-BWI-DP-065, Rev. 0.

Schultz RA, Soliva R, Fossen H, Okubo CH, Reeves DM (2008) Dependence of displacement-length scaling relations for fractures and deformation bands on the volumetric changes across them. *Journal of Structural Geology*, **30**, 1405–1411.

Schweisinger T, Murdoch LC, Huey CO Jr (2007) Design of a removable borehole extensometer. *Geotechnical Testing Journal*, **30**, 202–211.

Schweisinger T, Svenson EJ, Murdoch LC (2009) Introduction to hydromechanical well tests in fractured rock aquifers. *Ground Water*, **47**, 69–79.

Schweisinger T, Svenson EJ, Murdoch LC (2011) Hydromechanical behavior during constant-rate pumping tests in fractured gneiss. *Hydrogeology Journal*, **19**, 963–980.

Scott DR, Stevenson DJ (1984) Magma solitons. *Geophysical Research Letters*, **11**, 1161–1164.

Scott DR, Stevenson DJ (1986) Magma ascent by porous flow. *Journal of Geophysical Research*, **91**, 9283–9296.

Scott DR, Stevenson DJ, Whitehead JA (1986) Observations of solitary waves in a viscously deformable pipe. *Nature*, **319**, 759–761.

Scott RB, Rona PA, McGregor BA, Scott MR (1974) The TAG hydrothermal field. *Nature*, **251**, 301–302.

Scott S, Driesner T, Weis P (2015) Geologic controls on supercritical geothermal resources above magmatic intrusions. *Nature Communications*, **6**, 7837, doi:10.1038/ncomms8837.

Screaton EJ (2010) Recent advances in subseafloor hydrogeology: focus on basement-sediment interactions, subduction zones, and continental slopes. *Hydrogeology Journal*, **18**, 1547–1570.

Screaton EJ, Carson B, Davis EE, Becker K (2000) Permeability of a décollement zone: results from a two-well experiment in the Barbados accretionary complex. *Journal of Geophysical Research*, **105**, 21403–21410.

Screaton EJ, Carson B, Lennon GP (1995) Hydrogeologic properties of a thrust fault within the Oregon accretionary prism. *Journal of Geophysical Research*, **100**, 20025–20035.

Screaton EJ, Fisher AT, Carson B, Becker K (1997) Barbados Ridge hydrogeologic tests: implications for fluid migration along an active décollement. *Geology*, **25**, 239–242.

Screaton EJ, Gamage K, James S (2014) Data report: Permeabilities of Expedition 320/321 sediments from the Pacific Equatorial Transect. *Proceedings of the Integrated Ocean Drilling Program*, **320/321.**

Screaton EJ, Ge S (2012) The impact of megasplay faulting and permeability contrasts on Nankai Trough subduction zone pore pressures. *Geophysical Research Letters*, **39**, L22301.

Screaton EJ, Hays T, Gamage K, Martin JM (2006) Data report: Permeabilities of Costa Rica subduction zone sediments. *Proceeding of the Ocean Drilling Program, Scientific Results*, **205**.

Screaton EJ, Rowe K, Sutton J, Atalan G (2013) Data report: Permeabilities of Expedition 322 and 333 sediments from offshore the Kii Peninsula, Japan. *Proceedings of the Integrated Ocean Drilling Program*, **322**.

Screaton EJ, Saffer DM (2005) Fluid expulsion and overpressure development during initial subduction at the Costa Rica convergent margin. *Earth and Planetary Science Letters*, **233**, 361–374.

Screaton EJ, Wuthrich DR, Dreiss SJ (1990) Permeabilities, fluid pressures, and flow rates in the Barbados Ridge complex. *Journal of Geophysical Research*, **95**, 8997–9007.

Seager WR, Mack GH (2003) Geology of the Caballo Mountains, New Mexico. *New Mexico Bureau of Geology and Mineral Resources Memoir*, **49**.

Seager WR, Morgan P (1979) Rio Grande Rift in southern New Mexico, west Texas, and northern Chihuahua. In: *Rio Grande Rift-Tectonics and Magmatism* (ed Riecker RE), pp. 87–106, American Geophysical Union, Washington, DC

Segall P, Rice JR (1995) Dilatancy, compaction, and slip instability of a fluid-infiltrated fault. *Journal of Geophysical Research*, **100**, 22155–22171.

Selvadurai APS (ed) (1996) *Mechanics of Poroelastic Media*. Kluwer Academic Publishers, Dordrecht, The Netherlands.

Selvadurai APS (2000) *Partial Differential Equations in Mechanics Vol. 1: Fundamentals, Laplace's Equation, the Diffusion Equation, the Wave Equation*. Springer-Verlag, Berlin.

Selvadurai APS (2004) Stationary damage modelling of poroelastic contact. *International Journal of Solids and Structures*, **41**, 2043–2064.

Selvadurai APS (2007) The analytical method in geomechanics. *Applied Mechanics Reviews*, **60**, 87–106.

Selvadurai APS (2009) Fragmentation of ice sheets during impact. *Computer Modeling in Engineering and Science*, **52**, 259–277.

Selvadurai APS (2015) Normal stress-induced permeability hysteresis of a fracture in a granite cylinder. *Geofluids*, **15**, 37–47.

Selvadurai APS, Boulon MJ (eds) (1995) *Mechanics of Geomaterial Interfaces*. Studies in Applied Mechanics, **42**, Elsevier, Amsterdam.

Selvadurai APS, Boulon MJ, Nguyen TS (2005) The permeability of an intact granite. *Pure and Applied Geophysics*, **162**, 373–407.

Selvadurai APS, Carnaffan P (1997) A transient pressure pulse technique for the measurement of permeability of a cement grout. *Canadian Journal of Civil Engineering*, **24**, 489–502.

Selvadurai APS, Glowacki A (2008) Evolution of permeability hysteresis of Indiana Limestone during isotropic compression. *Ground Water*, **46**, 113–119.

Selvadurai APS, Ichikawa Y (2013) Some aspects of air-entrainment on decay rates in hydraulic pulse tests. *Engineering Geology*, **165**, 38–45.

Selvadurai APS, Jenner L (2012) Radial flow permeability testing of an argillaceous limestone. *Ground Water*, **51**, 100–107.

Selvadurai APS, Letendre A, Hekimi B (2011) Axial flow hydraulic pulse testing of an argillaceous limestone. *Environmental Earth Sciences*, **64**, 2047–2058.

Selvadurai APS, Najari M (2013) On the interpretation of hydraulic pulse tests on rock specimens. *Advances in Water Resources*, **53**, 139–149.

Selvadurai APS, Najari M (2015) Laboratory-scale hydraulic pulse testing: influence of air fraction in the fluid-filled cavity in the estimation of permeability. *Geotechnique*, **65**, 124–134.

Selvadurai APS, Nguyen TS (1995) Computational modeling of isothermal consolidation of fractured porous media. *Computers and Geotechnics*, **17**, 39–73.

Selvadurai APS, Nguyen TS (1997) Scoping analyses of the coupled thermal-hydrological-mechanical behaviour of the rock mass around a nuclear fuel waste repository. *Engineering Geology*, **47**, 379–400.

Selvadurai APS, Selvadurai PA (2010) Surface permeability tests: experiments and modelling for estimating effective permeability. *Proceedings of the Royal Society, Mathematics and Physical Sciences Series A*, **466**, 2819–2846.

Selvadurai APS, Sepehr K (1999a) Discrete element modelling of fragmentable geomaterials with size dependent strength. *Engineering Geology*, **53**, 235–241.

Selvadurai APS, Sepehr K (1999b) Two dimensional discrete element simulation of ice-structure interaction. *International Journal of Solids and Structures*, **36**, 4919–4940.

Selvadurai APS, Shirazi A (2004) Mandel-Cryer effects in fluid inclusions in damage susceptible poroelastic media. *Computers and Geotechnics*, **37**, 285–300.

Selvadurai APS, Shirazi A (2005) An elliptical disc anchor in a damage-susceptible poroelastic medium. *International Journal of Numerical Methods in Engineering*, **16**, 2017–2039.

Selvadurai APS, Suvorov AP, Selvadurai PA (2015) Thermo-hydro-mechanical processes in fractured rock formations during glacial advance. *Geoscientific Model Development*, **8**, 2167–2185.

Selvadurai APS, Yu Q (2005) Mechanics of a discontinuity in a geomaterial. *Computers and Geotechnics*, **32**, 92–106.

Selvadurai APS, Yue ZQ (1994) On the indentation of a poroelastic layer. *International Journal of Numerical and Analytical Methods in Geomechanics*, **18**, 161–175.

Senger RK, Fogg GE (1990) Stream functions and equivalent freshwater heads for modeling regional flow of variable-density ground water, 2, Application and implications for modeling strategy. *Water Resources Research*, **26**, 2097–2106.

Serra O (1982) *Fundamentals of Well-log Interpretation, 1, The Acquisition of Logging Data*. Elsevier, Amsterdam.

Shand SJ (1949) Rocks of the mid-Atlantic ridge. *Journal of Geology,* **57**, 89–92.

Shao JF, Hoxha D, Bart M, Homand F, Duveau G, Souley M, Hoteit N (1999) Modelling of induced anisotropic damage in granites. *International Journal of Rock Mechanics and Mining Sciences*, **36**, 1001–1012.

Shapiro SA, Dinske C (2009a) Scaling of seismicity induced by nonlinear fluid-rock interaction. *Journal of Geophysical Research*, **114**, doi:10.1029/2008JB006145.

Shapiro SA, Dinske C (2009b) Fluid-induced seismicity: pressure diffusion and hydraulic fracturing. *Geophysical Prospecting*, **57**, 301–310.

Shapiro SA, Huenges E, Borm G (1997) Estimating the crust permeability from fluid-injection-induced seismic emission at the KTB site. *Geophysical Journal International*, **131**, F15–F18.

Shapiro SA, Patzig R, Rothert E, Rindschwentner J (2003) Triggering of seismicity by pore pressure perturbations: permeability signatures of the phenomenon. *Pure and Applied Geophysics*, **160**, 1051–1066.

Shapiro SA, Rothert E, Rath V, Rindschwentner J (2002) Characterization of fluid transport properties of reservoirs using induced microseismicity. *Geophysics*, **67**, 212–220.

Sharp JM Jr, Domenico PA (1976) Energy transport in thick sequences of compacting sediment. *Geological Society of America Bulletin*, **87**, 390–400.

Sheldon HA, Micklethwaite S (2007) Damage and permeability around faults: implications for mineralization. *Geology*, **34**, 903–906.

Shen Z, Sun J, Zhang P, Wan Y, Wang M, Biirgmann R (2009) Slip maxima at fault junctions and rupturing of barriers during the 2008 Wenchuan earthquake. *Nature Geoscience*, **2**, 718–724.

Sheng P, Zhou M-Y (1988) Dynamic permeability in porous media. *Physical Review Letters*, **61**, 1591–1594.

Sheppard SMF (1986) Characterization and isotopic variations in natural waters. In: *Stable Isotopes in High Temperature Geologic Processes* (eds Valley JW, Taylor HP, Jr, O'Neil JR). *Reviews of Mineralogy*, **16**, pp. 165–184, Mineralogical Society of America.

Sheppard SMF, Gilg HA (1996) Stable isotope geochemistry of clay minerals. *Clay Mineralogy*, **31**, 1–24.

Shi Y, Wang CY (1986) Pore pressure generation in sedimentary basins: overloading versus aquathermal. *Journal of Geophysical Research*, **91**, 2153–2162.

Shi YL, Wang CY (1988) Generation of high pore pressures in accretionary prisms – Inferences from the Barbados subduction complex. *Journal of Geophysical Research,* **93**, 8893–8910.

Shi Z, Wang G, Liu C (2013a) Advances in research on earthquake fluids hydrogeology in China: a review. *Earthquake Science*, **26**, 415–425.

Shi Z, Wang G, Liu C (2013b) Co-seismic groundwater level changes induced by the May 12, 2008 Wenchuan earthquake in the near field. *Pure and Applied Geophysics*, **170**, 1773–1783.

Shi Z, Wang G, Liu C, Mei J, Wang J, Fang H (2013c) Coseismic response of groundwater level in the Three Gorges well network and its relationship to aquifer parameters. *Chinese Science Bulletin*, **58**, 3080–3087.

Shi Z, Wang G, Manga M, Wang C-Y (2015) Continental-scale water-level response to a large earthquake. *Geofluids*, **15**, 310–320.

Shi Z, Wang G, Wang C-Y, Manga M, Liu C (2014) Comparison of hydrological responses to the Wenchuan and Lushan earthquakes. *Earth and Planetary Science Letters*, **391**, 193–200.

Shinohara H (2008) Excess degassing from volcanoes and its role on eruptive and intrusive activity. *Reviews of Geophysics*, **46**, RG4005.

Shipboard Scientific Party (1994) Site 892. In: *Proceedings of the Ocean Drilling Program, Initial Reports*, **146** (eds Carson B, Westbrook GK, Musgrave RJ, Suess E), 301–378.

Shipboard Scientific Party (1995a) Site 948. *Proceedings of the Ocean Drilling Program, Initial Reports*, **156**, 87–192.

Shipboard Scientific Party (1995b) Site 949. *Proceedings of the Ocean Drilling Program, Initial Reports*, **156**, 193–257.

Shiping L, Yushou L, Yi L, Zhenye W, Gang Z (1994) Permeability-strain equations corresponding to the complete stress-strain path of Yinzhuang Sandstone. *International Journal of Rock Mechanics and Mining Sciences*, **31**, 383–391.

Shipley TH, ODP Leg 156 Scientific Party (1994) Seismically inferred dilatancy distribution, northern Barbados Ridge décollement: implications for fluid migration and fault strength. *Geology*, **22**, 411–414.

Shipley TH, Ogawa Y, Blum P, ODP Leg 156 Scientific Party (1995) Proceedings of the Ocean Drilling Program, Initial Reports, **156**.

Shmonov VM, Vitiovtova VM, Zharikov AV, Grafchikov AA (2003) Permeability of the continental crust: implications of experimental data. *Journal of Geochemical Exploration*, **78–79**, 697–699.

Shrag D (2007) Preparing to capture carbon. *Science*, **315**, 812–813.

Sibson R (1981a) A brief description of natural neighbor interpolation. In: *Interpolating Multivariate Data* (ed Barnett V), pp. 21–36, John Wiley & Sons, New York.

Sibson RH (1981b) Fluid flow accompanying faulting: field evidence and models. In: *Earthquake Prediction: An International Review,* Maurice Ewing Ser., Vol. 4 (eds Simpon DW, Richards PG), pp. 593–603. American Geophysical Union, Washington, DC.

Sibson RH (1987) Earthquake rupturing as a mineralizing agent in hydrothermal systems. *Geology*, **15**, 701–704.

Sibson RH (1992) Fault-valve behavior and the hydrostatic lithostatic fluid pressure interface. *Earth-Science Reviews*, **32**, 141–144.

Sibson RH (1996) Structural permeability of fluid-driven fault-fracture meshes. *Journal of Structural Geology*, **18**, 1031–1042.

Sibson RH (2001) Seismogenic framework for hydrothermal transport and ore deposition. *Society of Economic Geologists Reviews*, **14**, 25–50.

Sibson RH (2007) An episode of fault-valve behavior during compressional inversion? The 2004 M6.8 Mid-Niigata Prefecture, Japan, earthquake sequence. *Earth and Planetary Science Letters*, **257**, 188–199.

Sibson RH (2013) Stress switching in subduction forearcs: implications for overpressure containment and strength cycling on megathrusts. *Tectonophysics*, **600**, 142–152.

Sibson RH, Moore JMM, Rankin AH (1975) Seismic pumping – A hydrothermal fluid transport mechanism. *Journal of the Geological Society of London*, **131**, 653–659.

Sibson RH, Robert F, Poulsen KH (1988) High-angle reverse faults, fluid-pressure cycling, and mesothermal gold-quartz deposits. *Geology*, **16**, 551–555.

Sibson RH, Rowland JV (2003) Stress, fluid pressure and structural permeability in seismogenic crust, North Island, New Zealand. *Geophysical Journal International*, **154**, 584–594.

Sil S, Freymueller JT (2006) Well water level changes in Fairbanks, Alaska, due to the great Sumatra-Andaman earthquake. *Earth, Planets, and Space*, **58**, 181–184.

Sillitoe RH (2010) Porphyry copper systems. *Economic Geology*, **105**, 3–41.

Silver EA, Kastner M, Fisher AT, Morris JD, McIntosh KD, Saffer DM (2000) Fluid flow paths in the crust of the Middle America Trench, Costa Rica margin. *Geology*, **28**, 679–682.

Simmons SF, Brown KL (2007) The flux of gold and related metals through a volcanic arc, Taupo Volcanic Zone, New Zealand. *Geology*, **35**, 1099–1102.

Simpson GDH (1998) Dehydration-related deformation during regional metamorphism, NW Sardinia, Italy. *Journal of Metamorphic Geology*, **16**, 457–472.

Skarbek RM, Saffer DM (2009) Pore pressure development beneath the decollement at the Nankai subduction zone: implications for plate boundary fault strength and sediment dewatering. *Journal of Geophysical Research,* **114**, B07401.

SKB (2008) Site description of Forsmark at completion of the site investigation phase. In: *SKB Technical Report*, **08-05** (ed SKB), SKB, Stockholm, Sweden, http://www.skb.se/upload/publications/pdf/TR-08-05.pdf accessed 06 May 2016.

Skelton ADL, Graham CM, Bickle, MJ (1995) Lithological and structural controls on regional 3-D fluid flow patterns during greenschist facies metamorphism of the Dalradian of the SW Scottish Highlands. *Journal of Petrology*, **36**, 563–586.

Skelton ADL, Valley JV, Graham CM, Bickle, MJ, Fallick AE (2000) The correlation of reaction and isotope fronts and the mechanism of metamorphic fluid flow. *Contributions to Mineralogy and Petrology*, **138**, 364–375.

Slack TZ, Murdoch LC, Germanovich LN, Hisz DB (2013) Reverse water-level change during interference slug tests in fractured rock. *Water Resources Research*, **49**, 1552–1567.

Sloan SW, Booker R (1986) Removal of singularities in Tresca and Mohr-Coulomb yield functions. *Communications in Applied Numerical Methods*, **2**, 173–179.

Smeulders DMJ, Eggels RLGM, Dongen MEHV (1992) Dynamic permeability: reformulation of theory and new experimental and numerical data. *Journal of Fluid Mechanics*, **245**, 211–227.

Smith C (1983) Thermal hydrology and heat flow of Beowawe geothermal area, Nevada. *Geophysics*, **48**, 618–626.

Smith GI, Friedman I, Veronda G, Johnson CA (2002) Stable isotope compositions of water in the Great Basin, United States, 3, Comparison of ground waters with modern precipitation. *Journal of Geophysical Research*, **107**, doi:10.1029/2001JD000567.

Smith L, Chapman DS (1983) On the thermal effects of groundwater flow, 1, Regional scale systems. *Journal of Geophysical Research*, **88**, 593–608.

Smith-Konter B, Sandwell D (2009) Stress evolution of the San Andreas fault system: recurrence interval versus locking depth. *Geophysical Research Letters*, **36**, doi:10.1029/2009GL037235.

Snow DT (1968a) Hydraulic character of fractured metamorphic rocks of the Front Range and implications to the Rocky Mountain Arsenal Well. *Quarterly of the Colorado School of Mines*, **63**, 167–200.

Snow DT (1968b) Rock fracture spacings, openings, and porosities. *Journal of the Soil Mechanics and Foundations Division, ASCE*, **94**, 73–91.

Snow DT (1970) The frequency and apertures of fractures in rock. *International Journal of Rock Mechanics and Mining Sciences*, **7**, 23–40.

Snyder DT, Haynes JV (2010) Groundwater conditions during 2009 and changes in groundwater levels from 1984 to 2009, Columbia Plateau Regional Aquifer System, Washington, Oregon, and Idaho. *U.S. Geological Survey Scientific Investigations Report*, **2010–5040**.

Sohn RA (2007) Stochastic analysis of exit fluid temperature records from the active TAG hydro thermal mound (Mid-Atlantic Ridge, 26°N), 1, Modes of variability and implications for subsurface flow. *Journal of Geophysical Research*, **112**, B07101, doi:10.1029/2006JB004435.

Soliva R, Benedicto A (2004) A linkage criterion for segmented normal faults. *Journal of Structural Geology*, **26**, 2251–2267.

Solomon EA, Kastner M, Wheat G, Jannasch HW, Robertson G Davis EE, Morris JD (2009) Long-term hydrogeochemical records in the oceanic basement and forearc prism at the Costa Rica subduction zone. *Earth and Planetary Science Letters*, **282**, 240–251.

Solum JG, van der Pluijm BA (2009) Quantification of fabrics in clay gouge from the Carboneras fault, Spain and implications for fault behavior. *Tectonophysics*, **475**, 554–562.

Song C, Ekinci MK, Underwood MB, Henry P (2015) Data report: Permeability and microfabric of mud (stone) samples from IODP Sites C0011 and C0012, NanTroSEIZE subduction inputs. In: Saito S, Underwood MB, Kubo Y, and the Expedition 322 Scientists, Proceedings of the Integrated Ocean Drilling Program, 322, doi:10.2204/iodp.proc.322.211.2015.

Sophocleous M (2010) Groundwater management practices, challenges, and innovations in the High Plains aquifer, USA—lessons and recommended actions. *Hydrogeology Journal*, **18**, 559–575.

Souley M, Homand F, Pepa S, Hoxha D (2001) Damage-induced permeability changes in granite: a case example at the URL in Canada. *International Journal of Rock Mechanics and Mining Sciences*, **38**, 297–310.

Spane FA (1982) Hydrologic studies within the Pasco Basin. Proceedings of the 1982 National Waste Terminal Storage Program Information Meeting, U.S. Department of Energy, DOE/NWTS-30, p. 23–8.

Spane FA (2013) *Preliminary Analysis of Grande Ronde Basalt Formation Flow Top Transmissivity as It Relates to Assessment and Site Selection Applications for Fluid/Energy Storage and Sequestration Projects*. Pacific Northwest National Laboratory, U.S. Department of Energy, PNNL-22436.

Spane FA, Bonneville A, McGrail BP, Thome PD (2012) *Hydrologic Characterization Results and Recommendations for the Wallula Basalt Pilot Well*. PNWD-4368, Battelle-Pacific Northwest Division, Richland, Washington.

Spencer DW (1963) The interpretation of grain size distribution curves of clastic sediments. *Journal of Sedimentary Petrology*, **33**, 180–190.

Spiegelman M (1993) Physics of melt extraction – Theory, implications and applications. *Philosophical Transactions of the Royal Society of London, Series A, Mathematical, Physical and Engineering Sciences,* **342**, 23–41.

Spinelli GA, Mozley PS, Tobin HJ, Underwood MB, Hoffman NW, Bellew GM (2007) Diagenesis, sediment strength, and pore collapse in sediment approaching the Nankai Trough subduction zone. *GSA Bulletin*, **119**, 377–390.

Spinelli GA, Saffer DM (2004) Along-strike variations in underthrust sediment dewatering on the Nicoya margin, Costa Rica related to the updip limit of seismicity. *Geophysical Research Letters,* **31**, L04613.

Spinelli G, Saffer DM, Underwood MB (2006) Effects of along-strike variability in temperature on the hydrogeology of the Nicoya margin subduction zone, Costa Rica. *Journal of Geophysical Research*, **111**, B04403.

Standards New Zealand (2004) NZS1170.5:2004, Structural Design Actions, Part 5, Earthquake Actions New Zealand.

Staude S, Bons PD, Markl G (2009) Hydrothermal vein formation by extension-driven dewatering of the middle crust: an example from SW Germany. *Earth and Planetary Science Letters,* **286**, 387–395.

Staudigel H, Gillis K, Duncan R (1986) K/Ar and Rb/Sr ages of celadonites from the Troodos ophiolite, Cyprus. *Geology*, **14**, 72–75.

Stauffer P, Bekins BA (2001) Modeling consolidation and dewatering near the toe of the northern Barbados accretionary complex. *Journal of Geophysical Research*, **106**, 6369–6383.

Steefel CI, Maher K (2009) Fluid-rock interaction: a reactive transport approach. In: *Thermodynamics and Kinetics of Water-Rock Interaction*, vol. **70** (eds Oelkers EH, Schott J), pp. 87–124, Mineralogical Society of America, Chantilly, VA.

Steele-Maclnnes M, Han L, Lowell RP, Rimstidt JD, Bodnar RJ (2012a) The role of fluid phase immiscibility in quartz dissolution and precipitation in sub-seafloor hydrothermal systems. *Earth Planetary Science Letters*, **321–322**, 139–151.

Steele-Maclnnes M, Han L, Lowell RP, Rimstidt JD, Bodnar RJ (2012b) Quartz precipitation and fluid inclusion characteristics in sub-seafloor hydrothermal systems associated with volcanogenic massive sulphide deposits. *Central European Journal of Geosciences*, **4**, 275–286.

Stenger R (1982) Petrology and geochemistry of the basement rocks of the research drilling project Urach 3. In: *The Urach Geothermal Project* (ed Haenel R), pp. 41–48, Schweizerbart'sche Verlagsbuchhandlung, Stuttgart.

Stephansson O (ed) (1985) *Proceedings of the International Symposium on Fundamentals of Rock Joints*. Björkliden, Norway.

Steurer JF, Underwood MB (2003) Data report: The relation between physical properties and grain-size variations in hemipelagic sediments from Nankai Trough. *Proceedings of the Ocean Drilling Program, Scientific Results*, **190/196**, 1–25.

Stevenson D (1989) Spontaneous small-scale melt segregation in partial melts undergoing deformation. *Geophysical Research Letters*, **16**, 1067–1070.

Stirling MW, McVerry GH, Berryman KR (2002) A new seismic hazard model for New Zealand. *Bulletin of the Seismological Society of America*, **92**, 1878–1903.

Stirling MW, McVerry GH, Gerstenberger MC, Litchfield NJ, Van DR, Berryman KR, Barnes P, Wallace LM, Villamor P, Langridge RM, Lamarche G, Nodder S, Reyners ME, Bradley B, Rhoades DA, Smith WD, Nicol A, Pettinga J, Clark KJ, Jacobs K (2012) National seismic hazard model for New Zealand: 2010 update. *Bulletin of the Seismological Society of America*, **102**, 1514–1542.

Stober I (1986) Strömungsverhalten in Festgesteinsaquiferen mit Hilfe von Pump- und Injektionsversuchen. *Geologisches Jahrbuch, Reihe C*, **42**, 204.

Stober I (1995) *Die Wasserführung des kristallinen Grundgebirges [Water in the Crystalline Basement]*. Ferdinand Enke Verlag, Stuttgart.

Stober I (1996) Researchers study conductivity of crystalline rock in proposed radioactive waste site. *Eos, Transactions American Geophysical Union*, **77**, 93–94.

Stober I (2011) Depth- and pressure-dependent permeability in the upper continental crust: data from the Urach 3 geothermal borehole, southwest Germany. *Hydrogeology Journal*, **19**, 685–699.

Stober I, Bucher K (2004) Fluid sinks within the Earth's crust. *Geofluids,* **4**, 143–151.

Stober I, Bucher K (2005a) The upper continental crust, an aquifer and its fluid: hydraulic and chemical data from 4 km depth in fractured crystalline basement rocks at the KTB test site. *Geofluids,* **5**, 8–19.

Stober I, Bucher K (2005b) Deep-fluids: Neptune meets Pluto. In: *The Future of Hydrogeology* (ed Voss C), *Hydrogeology Journal*, **13**, 112–115.

Stober I, Bucher K (2007a) Hydraulic properties of the crystalline basement. *Hydrogeology Journal*, **15**, 213–224.

Stober I, Bucher K (2007b) Erratum to: hydraulic properties of the crystalline basement. *Hydrogeology Journal*, **15**, 1643.

Stober I, Bucher K (2015) Hydraulic conductivity of fractured upper crust: insights from hydraulic tests in boreholes and fluid-rock interaction in crystalline basement rocks. *Geofluids*, **15**, 161–178.

Stober I, Richter A, Brost E, Bucher K (1999) The Ohlsbach Plume: natural release of deep saline water from the crystalline basement of the black forest. *Hydrogeology Journal*, **7**, 273–283.

Strasser M, Henry P, Kanamatsu T, Moe KT, Moore GF, IODP Expedition 333 Scientists (2012) Scientific drilling of masstransport deposits in the Nankai accretionary wedge: first results from IODP Expedition 333. In: *Submarine Mass Movements and Their Consequences* (eds Yamada Y, Kawamura K, Ikehara K, Ogawa Y, Urgeles R, Mosher D, Chaytor J, Strasser M), pp. 671–681. Springer, Dordrecht.

Struhsacker EM (1980) The geology of the Beowawe geothermal system, Eureka and Lander Counties, Nevada. *University of Utah Research Institute Report*, **ESL-37**.

Stuyfzand PJ (1989) An accurate, relatively simple calculation of the saturation index of calcite for fresh to salt water. *Journal of Hydrology*, **105**, 95–107.

Suetnova EI, Carbonell R, Smithson SB (1994) Bright seismic reflections and fluid movement by porous flow in the lower crust. *Earth and Planetary Science Letters,* **126**, 161–169.

Sumita I, Yoshida S, Kumazawa M, Hamano Y (1996) A model for sedimentary compaction of a viscous medium and its application to inner-core growth. *Geophysical Journal International*, **124**, 502–524.

Summers WK (1976) Catalog of thermal waters in New Mexico. *New Mexico Bureau of Mines and Mineral Resources Hydrologic Report*, **4**.

Sun H, Feistel R, Koch M, Markoe A (2008) New equations for density, entropy, heat capacity and potential temperature of a saline thermal fluid. *Deep-Sea Research, Part I, Oceanographic Research Papers*, **55**, 1304–1310

Sundaram PN, Watkins DJ, Ralph WE (1987) Laboratory investigation of coupled stress-deformation-hydraulic flow in a natural rock fracture. *Proceedings of the 28th U.S. Symposium on Rock Mechanics*, University of Arizona, Tuscon, 29 June-1 July, 1987, 593–600.

Sussman M, Smereka P, Osher S (1994) A level set approach for computing solutions to incompressible 2-phase flow. *Journal of Computational Physics*, **114**, 146–159.

Sutherland R, Berryman KR, Norris R (2006) Quaternary slip rate and geomorphology of the Alpine Fault: implications for kinematics and seismic hazard in southwest New Zealand. *Geological Society of America Bulletin*, **118**, 464–474.

Sutherland R, Eberhart-Phillips D, Harris RA, Stern TA, Beavan RJ, Ellis SM, Henrys SA, Cox SC, Norris RJ, Berryman KR, Townend J, Bannister SC, Pettinga J, Leitner B, Wallace LM, Little TA, Cooper AF, Yetton M, Stirling MW (2007) Do great earthquakes occur on the Alpine Fault in central South Island, New Zealand? In: *A Continental Plate Boundary: Tectonics at South Island, New Zealand* (eds Okaya DA, Stern TA, Davey FJ). *American Geophysical Union Geophysical Monograph*, **175**, pp. 235–251, AGU.

Sutherland R, Toy VG, Townend J, Cox SC, Eccles JD, Faulkner DR, Prior DJ, Norris RJ, Mariani E, Boulton C, Carpenter BM, Menzies CD, Little TA, Hastings M, De PG, Langridge RM, Scott HR, Lindroos ZR, Fleming B, Kopf AJ (2012) Drilling reveals fluid control on architecture and rupture of the Alpine fault, New Zealand. *Geology*, **40**, 1143–1146.

Svenson E, Schweisinger T, Murdoch LC (2008) Field evaluation of the hydromechanical behavior of flat-lying fractures during slug tests. *Journal of Hydrology*, **359**, 30–45.

Swanberg CA, Walkey WC, Combs J (1988) Core hole drilling and the "rain curtain" phenomenon at Newberry Volcano, Oregon. *Journal of Geophysical Research*, **93**, 10163–10173.

Tada R, Siever R (1989) Pressure solution during diagenesis. *Annual Reviews of Earth and Planetary Science*, **17**, 89–118.

Tadokoro K, Ando M (2002) Evidence for rapid fault healing derived from temporal changes in S wave splitting. *Geophysical Research Letters*, **29**, doi:10.1029/2001GL013644.

Taira A, Hill I, Firth J, Berner U, Brückmann W, Byrne T, Chabernaud T, Fisher A, Foucher JP, Gamo T, Gieskes J, Hyndman R, Karig D, Kastner M, Kato Y, Lallemant S, Lu R, Maltman A, Moore G, Moran K, Olaffson G, Owens W, Pickering K, Siena F, Taylor E, Underwood M, Wilkinson C, Yamano M, Zhang J (1992) Sediment deformation and hydrogeology of the Nankai Trough accretionary prism: synthesis of shipboard results of ODP Leg 131. *Earth and Planetary Science Letters*, **109**, 431–450.

Taira T, Silver PG, Niu F, Nadeau RM (2009) Remote triggering of fault-strength changes on the San Andreas fault at Parkfield. *Nature*, **461**, 636–677.

Tait A, Henderson R, Turner R, Zheng X (2006) Thin plate smoothing spline interpolation of daily rainfall for New Zealand using a climatological rainfall surface. *International Journal of Climatology*, **26**, 2097–2115.

Takahashi M, Hirata A, Koide H (1990) Effect on confining pressure and pore pressure on permeability of Inada granite. *Journal of the Japan Society of Engineering Geology,* **31**, 105–114 (in Japanese with English abstract).

Tanaka A, Ishikawa Y (2005) Crustal thermal regime inferred from magnetic anomaly data and its relationship to seismogenic layer thickness. *Physics of the Earth and Planetary Interiors*, **152**, 257–266.

Tanikawa W, Hirose T, Mukoyoshi H, Tadai O, Lin W (2013) Fluid transport properties in sediments and their role in large slip near the surface of the plate boundary fault in the Japan Trench. *Earth and Planetary Science Letters*, **382**, 150–160.

Tanikawa W, Tadai O, Mukoyoshi H (2014) Permeability changes in simulated granite faults during and after frictional sliding. *Geofluids*, **14**, 481–494.

Tanner WF (1964) Modification of sediment size distributions. *Journal of Sedimentary Research*, **34**, 156–164.

Taron J, Elsworth D (2009) Thermal-hydrologic-mechanical-chemical processes in the evolution of engineered geothermal reservoirs. *International Journal of Rock Mechanics and Mining Sciences,* **46**, 855–864.

Taron J, Elsworth D (2010a) Coupled mechanical and chemical processes in engineered geothermal reservoirs with dynamic permeability. *International Journal of Rock Mechanics and Mining Sciences,* **47**, 1339–1348.

Taron J, Elsworth D (2010b) Constraints on the compaction rate and equilibrium in the pressure solution creep of quartz aggregates and fractures: controls of aqueous concentration. *Journal of Geophysical Research*, **115**, B07211, doi:10.1029/2009JB007118.

Taron J, Elsworth D, Min K-B (2009) Numerical simulation of thermal-hydrologic-mechanical-chemical processes

in deformable, fractured porous media. *International Journal of Rock Mechanics and Mining Sciences*, **46**, 842–854.

Taron J, Hickman S, Ingebritsen SE, Williams C (2014) Using a fully coupled, open-source THM simulator to examine the role of thermal stresses in shear stimulation of enhanced geothermal systems. 48th US Rock Mechanics/Geomechanics Symposium, Minneapolis, Minnesota, 1–4 June 2014.

Tavenas F, Jean P, Leblond P, Leroueil S (1983) The permeability of natural soft clays, Part II, Permeability characteristics. *Canadian Geotechnical Journal*, **20**, 645–660.

Taylor B, Zellmer K, Martinez F, Goodliffe Andrew (1996) Sea-floor spreading in the Lau back-arc basin. *Earth and Planetary Science Letters*, **144**, 35–40.

Taylor DW (1948) *Fundamentals of Soil Mechanics*. John Wiley and Sons, New York.

Taylor E, Leonard J (1990) Sediment consolidation and permeability at the Barbados forearc. *Proceedings of the Ocean Drilling Program, Scientific Results,* **110**, 289–308.

Teagle DAH, Alt JC, Halliday AN (1998) Tracing the evolution of hydrothermal fluids in the upper oceanic crust: Sr-isotopic constraints from DSDP/ODP Holes 504B and 896A. In: *Modern Ocean-Floor Processes and the Geological Record*, **148** (eds Mills RA, Harrison K), pp. 81–97. Geological Society of London, London.

Teichert BMA, Torres ME, Bohrmann G, Eisenhauer A (2005) Fluid sources, fluid pathways and diagenetic reactions across an accretionary prism revealed by Sr and B geochemistry. *Earth and Planetary Science Letters*, **239**, 106–121.

Tenthorey E, Cox SF (2006) Cohesive strengthening of fault zones during the interseismic period: an experimental study. *Journal of Geophysical Research*, **11**, B09202.

Tenthorey E, Fitz Gerald J (2006) Feedbacks between deformation, hydrothermal reaction and permeability evolution in the crust: experimental insights. *Earth and Planetary Science Letters*, **247**, 117–129.

Terakawa T, Hashimoto C, Matsu'ura M (2013) Changes in seismic activity following the 2011 Tohoku-oki earthquake: effects of pore fluid pressure. *Earth and Planetary Science Letters*, **365**, 17–24.

Terakawa T, Miller SA, Deichmann N (2012) High fluid pressure and triggered earthquakes in the enhanced geothermal system in Basel, Switzerland. *Journal of Geophysical Research*, **117**, doi:10.1029/2011JB008980.

Terzaghi C (1925) Principles of soil mechanics. *Engineering News-Record*, **95**, 19–27.

Tester JW (2006) *The Future of Geothermal Energy, Part 1, Summary and Part 2, Full Report*. Massachusetts Institute of Technology, Cambridge, MA.

Theis CV (1963) Estimating the transmissivity of a water-table aquifer from the specific capacity of a well. *U.S. Geological Survey Water Supply Paper*, **1536-1**, 332–336.

Theis CV, Taylor GC, Murray CR (1941) Thermal waters of the Hot Springs artesian basin, Sierra County, New Mexico. *Fourteenth and Fifteenth Biennial Reports of the State Engineer of New Mexico*, 419–492.

Thielicke W, Stamhuis E (2012) PIVLab - Time-resolved digital particle image velocimetry tool for MATLAB. Ver. 1.32.

Thompson TB, Teal L, Meeuwig RO (2002) Gold deposits of the North Carlin Trend. *Nevada Bureau of Mines and Geology Bulletin*, **111**.

Thorpe RK, Watkins DJ, Ralph WE, Hsu R, Flexser R (1982) Strength and permeability test on ultra-large Stripa Granite core. *Lawrence Berkeley Laboratory, Berkeley, California, Report*, **LBL-11203**.

Thorwart M, Dzierma Y, Rabbel W, Hensen C (2013) Seismic swarms, fluid flow and hydraulic conductivity in the forearc offshore North Costa Rica and Nicaragua. *International Journal of Earth Sciences*, **103**, 1789–1799.

Tian M, Ague JJ (2014) The impact of porosity waves on crustal reaction progress and CO_2 mass transfer. *Earth and Planetary Science Letters*, **390**, 80–92.

Timar-Geng Z, Fügenschuh B, Wetzel A, Dresmann H (2006) Low-temperature thermochronology of the flanks of the southern Upper Rhine Graben. *International Journal of Earth Sciences*, **95**, 685–702.

Tivey MK, Humphris SE, Thompson G, Hannington MD, Rona P (1995) Deducing patterns of fluid flow and mixing within the TAG active hydrothermal mound using mineralogical and geochemical data. *Journal of Geophysical Research*, **100**, 12527–12555.

Tobin HJ, Kinoshita M (2006) NanTroSEIZE: the IODP Nankai Trough seismogenic zone experiment. *Scientific Drilling*, **2**, 23–27.

Tobin HJ, Moore JC, Moore GF (1994) Fluid pressure in the frontal thrust of the Oregon accretionary prism: experimental constraints. *Geology*, **22**, 979–982.

Tobin HJ, Saffer DM (2009) Elevated fluid pressure and extreme mechanical weakness of a plate boundary thrust, Nankai Trough subduction zone. *Geology,* **37**, 679–682.

Tobin HJ, Vannucchi P, Meschede M (2001) Structure, inferred mechanical properties, and implications for fluid transport in the décollement zone, Costa Rica convergent margin. *Geology*, **29**, 907–910.

Toda S, Stein RS, Lin J (2011) Widespread seismicity excitation throughout central Japan following the 2011 M = 9.0 Tohoku earthquake and its interpretation by Coulomb stress transfer. *Geophysical Research Letters,* **38**, doi:10.1029/2011GL047834.

Toda S, Stein RS, Richards-Dinger K, Bozkurt SB (2005) Forecasting the evolution of seismicity in southern California: animations built on earthquake stress transfer. *Journal of Geophysical Research,* **110**, B05S16.

Tolan TL, Reidel SP, Beeson MH, Anderson JL, Fecht KR, Swanson DA (1989) Revisions to the estimates of the areal extent and volume of the Columbia River Basalt Group. In: *Volcanism and Tectonism in the Columbia River Flood-Basalt Province* (eds Reidel SP, Hooper PR) *Geological Society of America Special Paper*, **239**, pp. 1–20, Geological Society of America.

Tokunaga T, Hosoya S, Tosaka H, Kojima K (1998) An estimation of the intrinsic permeability of argillaceous rocks and the effects on long-term fluid migration. *Geological Society of London Special Publication*, **141**, 83–94.

Tong P, Zhao D, Yang D (2012) Tomography of the 2011 Iwaki earthquake (M 7.0) and Fukushima nuclear power plant area. *Solid Earth*, **3**, 43–51.

Töth J (1962) A theory of groundwater motion in small drainage basins in central Alberta, Canada. *Journal of Geophysical Research*, **67**, 4375–4388.

Töth J (1978) Gravity-induced cross-formational flow of formation fluids, Red Earth region, Alberta, Canada: analysis, patterns, and evolution. *Water Resources Research*, **14**, 805–843.

Townend J, Sherburn S, Arnold R, Boese C, Woods L (2012) Three-dimensional variations in present-day tectonic stress along the Australia-Pacific plate boundary in New Zealand. *Earth and Planetary Science Letters*, **353–354**, 47–59.

Townend J, Zoback MD (2000) How faulting keeps the crust strong. *Geology*, **28**, 399–402.

Truesdell AH (1976) Summary of section III: geochemical techniques in exploration. *Proceedings of the 2nd U.N. Symposium on the Development and Use of Geothermal Resources, San Francisco 1975*. Vol. I, pp. liii–lxxx. U.S. Government Printing Office, Washington, DC.

Tsang C-F (1991) Coupled thermomechanical hydrochemical processes in rock fractures. *Reviews of Geophysics*, **29**, 537–551.

Tsang C-F (1999) Linking thermal, hydrological and mechanical processes in fractured rocks. *Annual Review of Earth and Planetary Sciences*, **27**, 359–384.

Tsang C-F, Bernier F, Davies C (2005) Geohydromechanical processes in the excavation damaged zone in crystalline rock, rock salt, and indurated and plastic clays – in the context of radioactive waste disposal. *International Journal of Rock Mechanics and Mining Sciences*, **42**, 109–125.

Tsang C-F, Neretnieks I (1998) Flow channeling in heterogeneous fractured rocks. *Reviews of Geophysics,* **36**, 275–298.

Tsang YW, Birkholzer JT, Muldiopadhyay S (2009) Modeling of thermally driven hydrological processes in partially saturated fractured rock. *Reviews of Geophysics,* **47**, RG3004.

Tsang YW, Witherspoon P (1981) Hydromechanical behaviour of a deformable rock fracture subject to normal stress. *Journal of Geophysical Research*, **86**, 9287–9298.

Tsuji T, Kawamura K, Kanamatsu T, Kasaya T, Fujikura K, Ito Y, Tsuru T, Kinoshita M (2013) Extension of continental crust by anelastic deformation during the 2011 Tohoku-oki earthquake: the role of extensional faulting in the generation of a great tsunami. *Earth and Planetary Science Letters*, **364**, 44–58.

Tumarkina E, Misra S, Burlini L, Connolly JAD (2011) An experimental study of the role of shear deformation on partial melting of a synthetic metapelite. *Tectonophysics*, **503**, 92–99.

Uehara SI, Shimamoto T (2004) Gas permeability evolution of cataclasite and fault gouge in triaxial compression and implications for changes in fault-zone permeability structure through the earthquake cycle. *Tectonophysics*, **378**, 183–195.

Ujiie K, Hisamitsu T, Taira A (2003) Deformation and fluid pressure variation during initiation and evolution of the plate boundary décollement zone in the Nankai accretionary prism. *Journal of Geophysical Research*, **108**, doi:10.1029/2002JB002314.

Ulven OI, Jamtveit B, Malthe-Sorenssen A (2014) Reaction-driven fracturing of porous rock. *Journal of Geophysical Research*, **119**, 7473–7486, doi:10.1002/2014JB011102.

Umino N, Okada T, Hasegawa A (2002) Foreshock and aftershock sequence of the 1998 M 5.0 Sendai, northeastern Japan, earthquake and its implications for earthquake nucleation. *Bulletin of the Seismological Society of America*, **92**, 2465–2477.

Underwood MB (2007) Sediment inputs to subduction zones: why lithostratigraphy and clay mineralogy matter. In: *The Seismogenic Zone of Subduction Thrusts* (eds Dixon TH, Moore JC), pp. 42–85. Columbia University Press, New York.

Upton P, Sutherland R (2014) High permeability and low temperature correlates with proximity to brittle failure within mountains at an active tectonic boundary, Manapouri tunnel, Fiordland, New Zealand. *Earth and Planetary Science Letters*, **389**, 176–187.

Valley B, Evans KF (2009) Stress orientation to 5 km depth in the basement below Basel (Switzerland) from borehole failure analysis. *Swiss Journal of Geosciences*, **102**, 467–480.

Valsami E, Cann JR (1992) Mobility of rare earth elements in zones of intense hydro- thermal alteration in the *Pindos ophiolite,* Greece. In: *Ophiolites and Their Modern Oceanic Analogues*, vol. **60** (ed Parson LM), pp. 219–232, Geological Society of London, London.

Van Ark E, Detrick RS, Canales JP, Carbotte SM, Harding AJ, Kent GM, Nedimovic MR, Wilcock WSD, Diebold JB, Babcock J (2007) Seismic structure of the Endeavour segment, Juan de Fuca Ridge: correlations with seismicity and hydrothermal activity. *Journal of Geophysical Research*, **112**, B02401.

Vannucchi P, Leoni L (2007) Structural characterization of the Costa Rica décollement: evidence for seismically induced fluid pulsing. *Earth and Planetary Science Letters*, **262**, 413–428.

Varga RJ, Gee JS, Bettison-Varga L, Anderson RS, Johnson CE (1999) Early establishment of hydrothermal systems during structural extension; palaeomagnetic evidence from the Troodos ophiolite, Cyprus. *Earth and Planetary Science Letters*, **171**, 221–235.

Vasseur G, Djeran-Maigre I, Grunberger D, Rousset G, Tessier D, Velde B (1995) Evolution of structural and physical parameters of clays during experimental compaction. *Marine and Petroleum Geology,* **12**, 941–954.

Vermilye JM, Scholz CH (1995) Relation between vein length and aperture. *Journal of Structural Geology,* **17**, 423–434.

Vernotte P (1958) Les paradoxes de la theorie continue de l'equation de la chaleur. *Comptes Rendus*, **246**, 3154–3155.

Vidale JE, Li Y-G (2003) Damage to the shallow Landers Fault from the nearby Hector Mine earthquake. *Nature*, **421**, 524–526.

Vigneresse JL, Barbey P, Cuney M (1996) Rheological transitions during partial melting and crystallization with application to felsic magma segregation and transfer. *Journal of Petrology*, **37**, 1579–1600.

Vila M, Fernandez M, Jiminez-Munt I (2010) Radiogenic heat production variability of some common lithological groups and its significance to lithospheric thermal modeling. *Tectonophysics,* **490**, 152–164.

Vincent M (2013) Five things you didn't want to know about hydraulic fractures. In: *Effective and Sustainable Hydraulic Fracturing* (eds Bunger A, McLennan J, Jeffrey R), pp. 81–93, InTech, Rijeka, Croatia.

Viola G, Venvik Ganerød G, Wahlgren CH (2009) Unraveling 1.5 Ga of brittle deformation history in the Laxemar-Simpevarp area, southeast Sweden: a contribution to the Swedish site investigation study for the disposal of highly radioactive nuclear waste. *Tectonics*, **28**, TC5007.

Von Damm K (1995) Controls on the chemistry and temporal variability of seafloor hydrothermal fluids. In: *Seafloor Hydrothermal Systems*, vol. **91** (eds Humphris SE, Zierenberg RA, Mullineaux LS, Thomson RE), pp. 222–247, American Geophysical Union, Washington, DC.

Von Damm KL, Bischoff JL, Rosenbauer RJ (1991) Quartz solubility in hydrothermal seawater; an experimental study and equation describing quartz solubility for up to 0.5 M NaCl solutions. *American Journal of Science*, **291**, 977–1007.

von Huene R, Lee H (1982) The possible significance of pore fluid pressures in subduction zones. In: *Studies in Continental Margin Geology* (eds Watkins JS, Drake CL), *American Association of Petroleum Geologists Memoir,* **34**, pp. 781–791, American Association of Petroleum Geologists.

von Quadt A, Erni M, Martinek K, Moll M, Peytcheva I, Heinrich CA (2011) Zircon crystallization and the lifetimes of ore-forming magmatic-hydrothermal systems. *Geology*, **39**, 731–734.

Voss CI, Provost AM (2002) *S*UTRA, A model for saturated-unsaturated variable-density ground-water flow with solute or energy transport. *U.S. Geological Survey Water-Resources Investigations Report*, **02-4231**.

Vrolijk P, Fisher AT, Gieskes J (1991) Geochemical and thermal evidence for fluid migration in the Barbados accretionary prism (ODP Leg 110). *Geophysical Research Letters*, **18**, 947–950.

Vrolijk P, Sheppard SMF (1987) Syntectonic veins from the Barbados accretionary prism (ODP Leg 110): record of paleohydrology. *Sedimentology*, **38**, 671–690.

Wagner GA, Reimer GM (1972) Fission track tectonics: the tectonic interpretation of fission track apatite ages. *Earth and Planetary Science Letters*, **14**, 263–268.

Wagner W, Kretschmar H-J (2008) *International Steam Tables, Properties of Water and Steam,* 2nd edn Springer-Verlag, Berlin, Heidelberg.

Wakita H (1975) Water wells as possible indicators of tectonic strain. *Science*, **189**, 553–555.

Walder J, Nur A (1984) Porosity reduction and crustal pore pressure development. *Journal of Geophysical Research*, **89**, 1539–1548.

Walderhaug O, Eliassen A, Aase NE (2012) Prediction of permeability in quartz-rich sandstones: examples from the Norwegian continental shelf and the Fontainebleau Sandstone. *Journal of Sedimentary Research*, **82**, 899–912.

Waldhauser F, Ellsworth B (2000) A double-difference earthquake location algorithm: method and application to the northern Hayward Fault, California. *Bulletin of the Seismological Society of America*, **90**, 1353–1368.

Waldhauser F, Schaff DP, Diehl T, Engdahl ER (2012) Splay faults imaged by fluid-driven aftershocks of the 2004 M_w9.2 Sumatra-Andaman earthquake. *Geology*, **40**, 243–246.

Walker CT (1975) Geochemistry of boron. *Benchmark Papers in Geology*, **23**.

Walker D, Rhen I, Gurban I (1997) Summary of hydrogeologic conditions at Aberg, Bebergy and Ceberg. In: *SKB Technical Report*, **97-23** (ed SKB), SKB, Stockholm, Sweden, http://www.skb.se/upload/publications/pdf/TR97-23webb.pdf, accessed 07 May 2016.

Walker JD, Kirby E, Andrew JE (2005) Strain transfer and partitioning between the Panamint Valley, Searles Valley, and Ash Hill fault zones, California. *Geosphere*, **1**, 111–118.

Wallace LM, Beavan RJ, McCaffrey R, Berryman KR, Denys P (2007) Balancing the plate motion budget in the South Island, New Zealand using GPS, geological and seismological data. *Geophysical Journal International*, **168**, 332–352.

Walsh JJ, Bailey WR, Childs C, Nicol A, Bonson CG (2003) Formation of segmented normal faults: a 3-D perspective. *Journal of Structural Geology*, **25**, 1251–1262.

Wang C (1985) Ground-water studies for earthquake prediction in China. *Pure and Applied Geophysics*, **122**, 215–217.

Wang C-Y (2001) Coseismic hydrologic response of an alluvial fan to the 1999 Chi-Chi earthquake, Taiwan. *Geology*, **29**, 831–834.

Wang C-Y, Chia Y (2008) Mechanism of water level changes during earthquakes: near field versus intermediate field. *Geophysical Research Letters*, **35**, L12402.

Wang C-Y, Chia Y, Wang P-L, Dreger D (2009) Role of S waves and Love waves in coseismic permeability enhancement. *Geophysical Research Letters*, **36**, L09404.

Wang C-Y, Dreger DS, Wang CH, Mayeri D, Berryman JG (2003) Field relations among coseismic ground motion, water level change and liquefaction for the 1999 Chi-Chi ($M_w = 7.5$) earthquake, Taiwan. *Geophysical Research Letters*, **30**, doi:10.1029/2003GL017601.

Wang C-Y, Manga M (2010a) *Earthquakes and Water* (Lecture Notes in Earth Sciences, **114**). Springer-Verlag, Berlin, Heidelberg.

Wang C-Y, Manga M (2010b) Hydrologic responses to earthquakes and a general metric. *Geofluids*, **10**, 210–216.

Wang C-Y, Wang CH, Kuo CH (2004a) Temporal change in groundwater level following the 1999 ($M_w = 7.5$) Chi-Chi earthquake, Taiwan. *Geofluids*, **4**, 210–220.

Wang C-Y, Wang CH, Manga M (2004b) Coseismic release of water from mountains: evidence from the 1999 ($M_w = 7.5$) Chi-Chi, Taiwan, earthquake. *Geology*, **32**, 769–772.

Wang C-Y, Wang LP, Manga M, Wang CH, Chen CH (2013) Basin-scale transport of heat and fluid induced by earthquakes. *Geophysical Research Letters*, **40**, 3893–3897, doi:10.1002/grl.50738

Wang H (2000) *Theory of Linear Poroelasticity with Applications to Geomechanics and Hydrogeology*. Princeton University Press, Princeton, NJ.

Wang J, Cook P, Trautz R, Flexser S, Hu Q, Salve R, Hudson D, Conrad M, Tsang Y, Williams K, Soll W, Turin J (2001) *In-Situ Field Testing of Processes*. ANL-NBS-HS-000005 REV01, Bechtel SAIC Company, Las Vegas, Nevada.

Wang K (1994) Kinematic models of dewatering accretionary prisms. *Journal of Geophysical Research*, **99**, 4429–4438.

Wang K, Davis EE (1996) Theory for the propagation of tidally induced pore pressure variations in layered subseafloor formations. *Journal of Geophysical Research*, **101**, 11483–11495.

Wark DA, Watson EB (2006) TitaniQ: a titanium-in-quartz geothermometer. *Contributions to Mineralogy and Petrology*, **152**, 743–754.

Warren JE, Price HS (1961) Flow in heterogeneous porous media. *SPE Journal*, **1**, 153–169.

Watanabe N, Hirano N, Tsuchiya N (2008) Determination of aperture structure and fluid flow in a rock fracture by high-resolution numerical modeling on the basis of a flow-through experiment under confining pressure. *Water Resources Research,* **44**, W06412, doi:10.1029/2006WR005411.

Watanabe N, Hirano N, Tsuchiya N (2009) Diversity of channeling flow in heterogeneous aperture distribution inferred from integrated experimental-numerical analysis on flow through shear fracture in granite. *Journal of Geophysical Research,* **114**, B04208, doi:10.1029/2008JB005959.

Watanabe N, Ishibashi T, Hirano N, Tsuchiya N, Ohsaki Y, Tamagawa T, Tsuchiya Y, Okabe H (2011a) Precise 3D numerical modeling of fracture flow coupled with X-ray Computed tomography for reservoir core samples. *SPE Journal,* **16**, 683–691.

Watanabe N, Ishibashi T, Ohsaki Y, Tsuchiya NY, Tamagawa T, Hirano N, Okabe H, Tsuchiya N (2011b) X-ray CT based numerical analysis of fracture flow for core samples under various confining pressure. *Engineering Geology*, **123**, 338–346.

Watanabe N, Ishibashi T, Tsuchiya N, Ohsaki Y, Tamagawa T, Tsuchiya Y, Okabe H, Ito H (2012) Geologic core holder with CFR PEEK body for the X-ray CT based numerical analysis of fracture flow under confining pressure. *Rock Mechanics and Rock Engineering,* **46**, 413–418.

Watt JT, Glen JMG, John D, Ponce DA (2007) Three-dimensional geologic model of the northern Nevada rift and the Beowawe geothermal system, north-central Nevada. *Geosphere*, **3**, 667–682.

Wei ZQ, Hudson JA (1988) Permeability of jointed rock masses. In: *Rock Mechanics and Power Plants* (ed Romana M), pp. 613–626. Balkema, Rotterdam.

Weinberg RF, Hodkiewicz PF, Groves DI (2004) What controls gold distribution in Archean terranes? *Geology*, **32**, 545–548.

Weingarten M, Ge S, Godt JW, Bekins BA, Rubinstein JL (2015) High-rate injection is associated with the increase in U.S. mid-continent seismicity. *Science*, **348**, 1336–1340.

Weis P (2014) The physical hydrology of ore-forming magmatic-hydrothermal systems. *Society of Economic Geologists Special Publication*, **18**, 59–75.

Weis P (2015) The dynamic interplay between saline fluid flow and rock permeability in magmatic -hydrothermal systems. *Geofluids,* **15**, 350–371.

Weis P, Driesner T (2013) The interplay of non-static permeability and fluid flow as a pre-requisite for supercritical geothermal resources. *Energy Procedia*, **40**, 102–106.

Weis P, Driesner T, Coumou D, Geiger S (2014) Hydrothermal, multi-phase convection of H_2O-NaCl fluids from ambient to magmatic temperatures: a new numerical scheme and benchmarks for code comparison. *Geofluids*, **14**, 347–371.

Weis P, Driesner T, Heinrich CA (2012) Porphyry-copper ore shells form at stable pressure-temperature fronts within dynamic fluid plumes. *Science*, **338**, 1613–1616.

Weisenberger T, Bucher K (2010) Zeolites in fissures of granites and gneisses of the central Alps. *Journal of Metamorphic Geology*, **28**, 825–847.

Weisenberger T, Bucher K (2011) Mass transfer and porosity evolution during low temperature water-rock interaction in gneisses of the Simano nappe: Arvigo, Val Calanca, Swiss Alps. *Contributions to Mineralogy and Petrology*, **162**, 61–81.

Weiss E (1982) A computer program for calculating relative-transmissivity input arrays to aid model calibration. *U.S. Geological Survey Open-File Report*, **82–447**.

Weissmann GS, Zhang Y, LaBolle EM, Fogg GE (2002) Dispersion of groundwater age in an alluvial aquifer system. *Water Resources Research*, **38**, doi:10.1029/2001WR000907.

Welch AH, Bright DJ, Knochenmus LA (2007) Water resources of the Basin and Range carbonate-rock aquifer system in White Pine County, Nevada, and adjacent areas in Nevada and Utah. *U.S. Geological Survey Scientific Investigations Report*, **2007–5261**.

Welhan JA, Poredai RJ, Rison W, Craig H (1988) Helium isotopes in geothermal and volcanic gases of the western United States, I, Regional variability and magmatic origin. *Journal of Volcanology and Geothermal Research*, **34**, 185–199.

Wells A, Yetton MD, Duncan RP, Stewart GH (1999) Prehistoric dates of the most recent Alpine fault earthquakes, New Zealand. *Geology*, **27**, 995–998.

Wells DL, Coppersmith KJ (1994) New empirical relationships among magnitude, rupture length, rupture width, rupture area, and surface displacement. *Bulletin of the Seismological Society of America*, **84**, 974–1002.

Wells JT, Ghiorso MS (1991) Coupled fluid flow and reaction in mid-ocean ridge hydrothermal systems; the behavior of silica. *Geochimica et Cosmochimica Acta*, **55**, 2467–2481.

Wells NS, Clough TJ, Condron LM, Baisden WT, Harding JS, Dong Y, Lewis GD, Lear G (2013) Biogeochemistry and community ecology in a spring-fed urban river following a major earthquake. *Environmental Pollution*, **182**, 190–200.

Wells SG, Granzow H (1981) Hydrogeology of the thermal aquifer near Truth or Consequences, New Mexico. In: State-Coupled Low-Temperature Geothermal Resource Assessment Program, Fiscal Year 1980, 3–5 to 3–51.

Weltje GJ, Prins MA (2003) Muddled or mixed? Inferring palaeoclimate from size distributions of deep-sea elastics. *Sedimentary Geology*, **162**, 39–62.

Wesnousky SG, Barron AD, Briggs RW, Caskey SJ, Kumar S, Owen L (2005) Paleoseismic transect across the northern Great Basin. *Journal of Geophysical Research*, **110**, doi:10.1029/2004JB003283.

West AJ (2012) Thickness of the chemical weathering zone and implications for erosional and climatic drivers of weathering and for carbon-cycle feedbacks. *Geology*, **40**, 811–814.

Westbrook GK, Carson B, Musgrave RJ, ODP Leg 146 Scientific Party (1994) *Proceedings of the Ocean Drilling Program, Initial Reports*, **146** (Pt. 1).

Westergaard HM (1952) *Theory of Elasticity and Plasticity*. Harvard University Press, Cambridge.

White DE (1998) The Beowawe geysers, Nevada, before geothermal development. *United States Geological Survey Bulletin*, **1998**.

White R, Spinelli GA, Mozley PS, Dunbar NW (2010) Importance of volcanic glass alteration to sediment stabilization: offshore Japan. *Sedimentology*, **58**, 1138–1154.

Wiggins C, Spiegelman M (1995) Magma migration and magmatic solitary waves in 3-D. *Geophysical Research Letters*, **22**, 1289–1292.

Wilkinson BH, McElroy BJ, Kesler SE, Peters SE, Rothman ED (2009) Global geologic maps are tectonic speedometers – rates

of rock cycling from area-age frequencies. *Geological Society of America Bulletin*, **121**, 760–779.

Wilkinson DS, Ashby MF (1975) Pressure sintering by power law creep. *Acta Metallurgica*, **23**, 1277–1285.

Wilkinson JJ (2013) Triggers for the formation of porphyry ore deposits in magmatic arcs. *Nature Geoscience*, **6**, 917–925.

Wilkinson WB, Shipley EL (1972) Vertical and horizontal laboratory measurements in clay soils. *Developments in Soil Science*, **2**, 285–298.

Willemse EJM (1997) Segmented normal faults: correspondence between three-dimensional mechanical models and field data. *Journal of Geophysical Research*, **102**, 675–692.

Williams CF, DeAngelo J (2008) Mapping geothermal potential in the western United States. *Transactions of the Geothermal Resources Council*, **32**, 181–188.

Williams CF, DeAngelo J (2011) Evaluation of approaches and associated uncertainties in the estimation of temperatures in the upper crust of the Western United States. *Transactions of the Geothermal Resources Council*, **35**, 1599–1605.

Williams GP, Troutman BM (1987) Algebraic manipulation of equations for best-fit straight lines. In: *Use and Abuse of Statistical Methods in the Earth Sciences* (ed Size WB), pp. 129–141. Oxford University Press, Oxford.

Wilson AM, Huettel M, Klein S (2008) Grain size and depositional environment as predictors of permeability in coastal marine sands. *Estuarine, Coastal and Shelf Science*, **80**, 193–199.

Wilson RAM (1959) The geology of the Xeros-Troodos area. *Geological Survey Department Memoir*, **1**, Geological Survey Department, Nicosia, Cyprus.

Winograd IJ (1971) Hydrogeology of ash-flow tuff: a preliminary statement. *Water Resources Research*, **7**, 994–1006.

Winograd IJ, Thordarson W (1975) Hydrogeologic and hydrochemical framework, south-central Great Basin, Nevada-California, with special reference to the Nevada Test Site. *U.S. Geological Survey Professional Paper*, **712-C**.

Winter TC, Harvey JW, Franke OL, Alley WA (1998) Ground water and surface water: a single resource. *U.S. Geological Survey Circular,* **1139**.

Wissa AEZ, Christian JT, Davis EH, Heiberg S (1971) Consolidation at a constant rate of strain. *Journal of the Soil Mechanics and Foundations Division ASCE*, **97**, 1393–1413.

Witcher JC (1988) Geothermal resources of southwestern New Mexico and southeastern Arizona. *New Mexico Geological Society Guidebook*, **39**, 191–198.

Witherspoon PA, Amick C, Gale J, Iwai K (1979) Observation of a potential size effect in experimental determination of the hydraulic properties of fractures. *Water Resources Research*, **15**, 1142–1146.

Witherspoon PA, Wang JSY, Iwai K, Gale JE (1980) Validity of cubic law for fluid-flow in a deformable rock fracture. *Water Resources Research*, **16**, 1016–1024.

Witt WK, Ford A, Hanrahan B, Mamuse A (2013) Regional-scale targeting for gold in the Yilgarn Craton: part 1 of the Yilgarn Gold Exploration Targeting Atlas. *Western Australia Geological Survey Report*, **125**.

Wittwer C (1986) Probenahmen und chemische analysen von grundwassern aus den Sondierbohrungen. In: *Nagra Technical Report*, **85–49** (ed Nagra), Nagra, Baden, Switzerland, http://www.nagra.cn/data/documents/database/dokumente/%24default/Default%20Folder/Publikationen/NTBs%201985-1986/d_ntb85-49.pdf, accessed 07 May 2016.

Wladis D, Jönsson P, Wallroth T (1997) Regional characterization of hydraulic properties or rock using well test data. *Swedish Nuclear Fuel Waste Management Company (SKB) Technical Report,* **SKB-TR- 97-2** (ed SKB), SKB, Stockholm, Sweden.

Wolf-Gladrow D (2000) *Lattice-Gas Cellular Automata and Lattice Boltzmann Models – An Introduction*. Springer, Berlin.

Wong A, Wang C-Y (2007) Field relations between the spectral composition of ground motion and hydrological effects during the 1999 Chi-Chi (Taiwan) earthquake. *Journal of Geophysical Research*, **112**, B10305.

Worthington M, Lubbe R (2007) The scaling of fracture compliance. *Geological Society London Special Publication*, **270**, 73–82.

Xu X, Wen X, Yu G, Chen G, Klinger Y, Hubbard J, Shaw J (2009) Coseismic reverse-and oblique-slip surface faulting generated by the 2008 M_w7.9 Wenchuan earthquake, China. *Geology*, **37**, 515–518.

Xue L, Li H-B, Brodsky EE, Xu Z-Q, Kano Y, Wang H, Mori JJ, Si J-L, Pei J-L, Zhang W, Yang G, Sun Z-M, Huang Y (2013) Continuous permeability measurements record healing inside the Wenchuan earthquake fault zone. *Science*, **340**, 1555–1559.

Yadav SK, Chakrapani GJ (2006) Dissolution kinetics of rock-water interactions and its implications. *Current Science*, **90**, 932–937.

Yamamoto K, Yoshida H, Akagawa F, Nishimoto S, Metcalfe R (2013) Redox front penetration in the fractured Toki Granite, central Japan: an analogue for redox buffering in fractured crystalline host rocks for repositories of long-lived radioactive waste. *Applied Geochemistry*, **35**, 75–87.

Yang Y, Aplin AC (1998) Influence of lithology and compaction on the pore size distribution and modelled permeability of some mudstones from the Norwegian margin. *Marine and Petroleum Geology*, **15**, 163–175.

Yang Y, Aplin AC (2007) Permeability and petrophysical properties of 30 natural mudstones. *Journal of Geophysical Research*, **112**, B03206.

Yang Y, Aplin AC (2010) A permeability-porosity relationship for mudstones. *Marine and Petroleum Geology*, **27**, 1692–1697.

Yang Z, Peng X-F, Lee D-J, Chen M-Y (2009) An image-based method for obtaining pore-size distribution of porous media. *Environmental Science & Technology*, **43**, 3248–3253.

Yardley BWD (1981) The effect of cooling on the water content and mechanical properties of metamorphosed rocks. *Geology*, **9**, 405–408.

Yardley BWD (1986) Fluid migration and veining in the Connemara Schists. In: *Fluid-Rock Reactions During Metamorphism, Advances in Physical Geochemistry*, Vol. 5 (eds Walther JV, Wood BJ), pp. 109–131. Springer-Verlag, New York.

Yardley BWD (2009) The role of water in the evolution of the continental crust. *Journal of the Geological Society*, **166**, 585–600.

Yardley BWD (2013) The chemical composition of metamorphic fluids in the crust. In: *Metasomatism and the Chemical Transformation of Rock* (eds Harlov DE, Austrheim H), Springer-Verlag, Berlin, Heidelberg, 17–51.

Yardley BWD, Baumgartner LP (2007) Fluid processes in deep crustal fault zones. In: *Tectonic Faults–Agents of Change on a*